

Right ventricular failure  
in pulmonary arterial hypertension:  
*squaring the circle*

Eva Lilian Peters

The work presented in this thesis was performed at the departments of pulmonology and physiology of the Amsterdam UMC, location VUmc, Amsterdam Cardiovascular Research Institute, Amsterdam, The Netherlands.

The research in this thesis was supported by grants from the Netherlands CardioVascular Research Initiative (CVON-2021-08 PHAEDRA, CVON-2018-29 PHAEDRA-IMPACT, CVON-2017-10 Dolphin-Genesis) and from the Netherlands Organization for Scientific Research (NWO VICI 918.16.610 and VIDI 917.18.338).

Financial support by de Hartstichting for printing this thesis is gratefully acknowledged.

Cover design and Layout:	Publiss   <a href="http://www.publiss.nl">www.publiss.nl</a>
Printing:	Ridderprint   <a href="http://www.ridderprint.nl">www.ridderprint.nl</a>
ISBN:	978-94-6416-769-6

Copyright © 2021 by E.L. Peters. All rights reserved. No part of this work may be reproduced or transmitted in any form or by any means without the written permission of the author. The rights of published chapters belong to the publishers of the respective journals.

VRIJE UNIVERSITEIT

Right ventricular failure in pulmonary arterial  
hypertension: *squaring the circle*

ACADEMISCH PROEFSCHRIFT

ter verkrijging van de graad Doctor aan  
de Vrije Universiteit Amsterdam,  
op gezag van de rector magnificus  
prof.dr. C.M. van Praag,  
in het openbaar te verdedigen  
ten overstaan van de promotiecommissie  
van de Faculteit der Geneeskunde  
op donderdag 9 december 2021 om 9.45 uur  
in de aula van de universiteit,  
De Boelelaan 1105

door

**Eva Lilian Peters**  
geboren te Krommenie

**promotor:** prof.dr. A. Vonk Noordegraaf

**copromotoren:** prof.dr. H.J. Bogaard  
dr. F.S. de Handoko-Man

**promotiecommissie:** prof.dr. J. van der Velden  
prof.dr. C.P. Allaart  
dr. P.I. Bonta  
prof.dr. F. Di Lisa  
dr. M. Nabben

*kon je met een liedje maar  
godswonderen verrichten  
de lammen laten lopen  
de blinden laten zien*

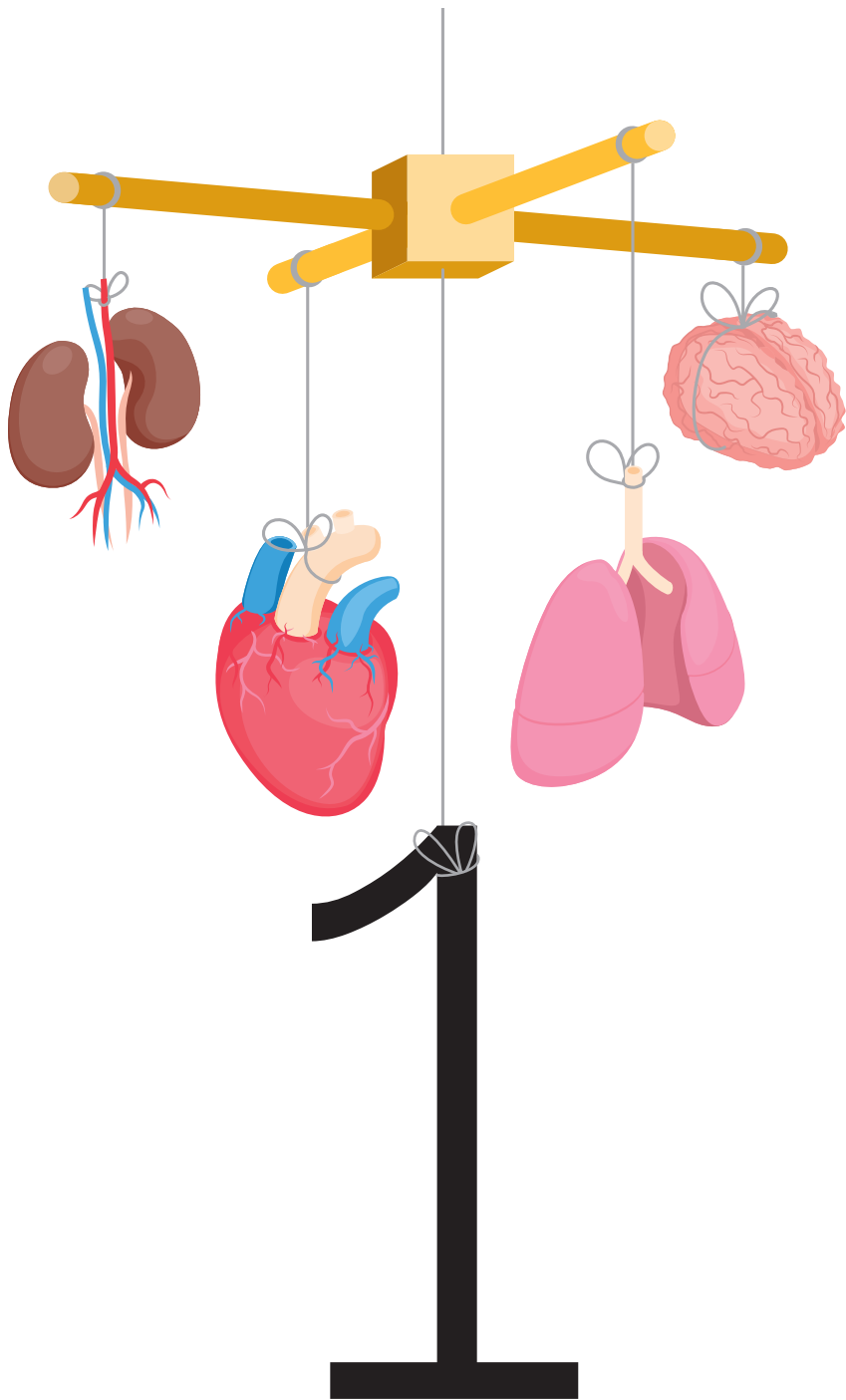
*dat zou mooi zijn  
dat zou mooi zijn  
dat werd een prachtig lied  
met een pracht couplet  
en een pracht refrein  
maar zo mooi maak ik ze niet*

*- De Dijk*

## Table of contents

<b>Chapter 1</b>	Introduction and thesis outline	9
<b>Chapter 2</b>	Regulation of myoglobin in hypertrophied rat cardiomyocytes in experimental pulmonary hypertension <i>Pflugers Arch, 2016</i>	23
<b>Chapter 3</b>	IGF-1 attenuates hypoxia-induced atrophy but inhibits myoglobin expression in C2C12 skeletal muscle myotubes <i>Int. J. Mol. Sci., 2017</i>	49
<b>Chapter 4</b>	Meijer and Vloedman's histochemical demonstration of mitochondrial coupling obeys Lambert-Beer's law in the myocardium <i>Histochem. Cell. Biol., 2018</i>	71
<b>Chapter 5</b>	Increased MAO-A activity promotes progression of pulmonary arterial hypertension <i>Am. J. Res. Cell. Mol. Biol., 2021</i>	85
<b>Chapter 6</b>	Bisoprolol and/or hyperoxic breathing do not reduce hyperventilation in pulmonary arterial hypertension patients <i>Submitted to Pulm. Circ. 2021</i>	115
<b>Chapter 7</b>	Neurohormonal modulation in pulmonary arterial hypertension <i>Eur. Res. J. 2021</i>	123
<b>Chapter 8</b>	Discussion and future perspectives	155
<b>Appendix</b>	Nederlandse samenvatting	170
	List of publications	174
	Dankwoord	175
	Squaring the circle	182





# INTRODUCTION AND THESIS OUTLINE

---

## CHAPTER 1

Idiopathic pulmonary arterial hypertension (iPAH) is a progressive lung disease, with a poor prognosis. Remodelling of the pulmonary vascular bed causes obstruction and narrowing of the lumen, ultimately leading to increased mean pulmonary artery pressure (mPAP). iPAH is diagnosed when right heart catheterization shows a mPAP greater than 20 mmHg, accompanied by pulmonary wedge pressure below 15 mmHg and pulmonary vascular resistance higher than 3 wood units, in absence of a known condition that can lead to pulmonary hypertension [1]. The cut-off value for mPAP was recently lowered from 25 to 21 mmHg, as a normal mPAP rarely exceeds 14 mmHg and a mPAP of 20 mmHg is associated with reduced survival [2–4]. Despite advances in treatment, prognosis remains poor. Estimated 5-year survival is 60–65% at best, on optimal therapy, but is often worse depending on the presence of risk factors [5].

Although iPAH is a pulmonary vascular disease, patients eventually die from right ventricular (RV) failure. Insight in the mechanisms underlying RV failure in iPAH is therefore important to develop novel treatments. Due to the increase in pulmonary vascular resistance and mPAP, the load on the RV is up to five times greater. The RV, normally a low-pressure pump, converts into a high-pressure pump. To sustain this increase in pressure, the thin-walled RV initially responds by cardiomyocyte hypertrophy. However, adaptation mechanisms eventually become insufficient and the RV enters a vicious circle of tissue hypoxia, altered metabolism, neurohormonal activation and further RV failure (Fig. 1), ultimately leading to death of the patient [6, 7]. When this vicious circle can be slowed down, RV failure may be deferred. Possible solutions for slowing the vicious circle of RV failure include, but are not limited to: 1) improvement of oxygen supply, 2) reduction of oxygen demand and 3) restoration of the neurohormonal balance.

### Oxygen supply

Oxygen supply from the outside air to a cell depends on oxygen uptake in the lungs, blood flow towards the tissue, and oxygen extraction by the cell [8] (Fig. 2). Upon inhalation, oxygen-rich air enters the lungs into the smallest units of the lungs: the alveoli. Alveoli are surrounded by a vast network of capillaries, creating a major surface for gas exchange (Fig. 2A). Due to the difference in partial pressure of oxygen between the alveoli and the blood, oxygen enters the blood by diffusion. Once it enters the blood, the oxygen is bound to haemoglobin (Hb). The rate at which Hb binds oxygen depends on the partial pressures of oxygen and carbon dioxide, temperature and pH. This system of oxygen transport provides maximal oxygen uptake at the lungs and at the same time maximal oxygen unloading at tissues where it is needed (e.g., the working heart). Oxygen-rich blood from the lungs then enters the left ventricle of the heart, where it is pumped throughout the systemic circulation (Fig. 2B). When oxygenated blood reaches tissues, oxygen diffuses from Hb into the cell.

In cardiac and skeletal muscle, oxygen is further transported throughout the cell by myoglobin (Mb), a molecule structurally and functionally related to Hb (Fig. 2C). Finally, oxygen-poor blood returns to the RV, where it is pumped to the lungs to be provided with oxygen again.

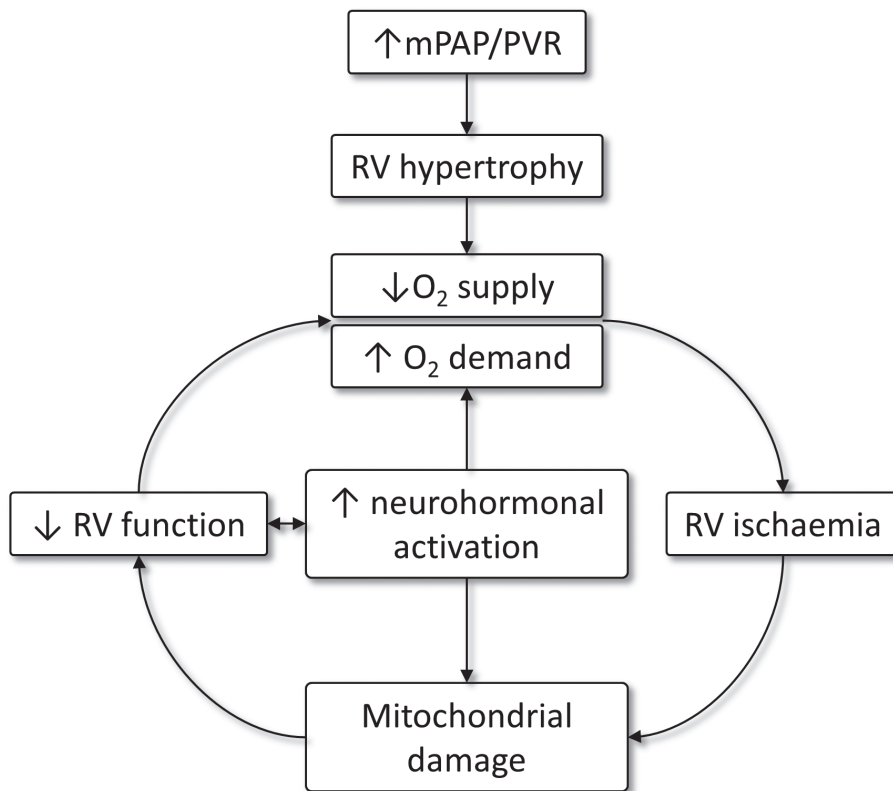


Figure 1 – **Vicious circle of right ventricular failure in pulmonary arterial hypertension.** Increased pulmonary artery pressure and resistance pose an increased load on the RV. Initially, the RV adapts by hypertrophy. If the overload persists, eventually the RV enters a vicious circle of reduced oxygen supply and increased oxygen demand leading to RV ischaemia and mitochondrial damage. Deterioration of RV function causes activation of neurohormonal systems and contributes to further oxygen supply/demand mismatch. mPAP = mean pulmonary artery pressure; PVR = pulmonary vascular resistance; RV = right ventricular

In iPAH, poor RV function and therefore decreased cardiac output (CO) causes reduced perfusion of all organs, including the heart itself, thereby limiting oxygen supply. In addition, the high RV pressure impedes coronary artery blood flow during systole causing reduced mean total coronary blood flow to the RV [9]. At

the cellular and molecular level, oxygen supply to the RV is impaired in at least three ways: First, iron deficiency is common among iPAH patients [10]. As iron is an important co-factor to bind oxygen to Hb and Mb, this impacts oxygen supply and limits exercise capacity [11]. Second, when the increased cross-sectional area of hypertrophied RV cardiomyocytes is not accompanied by a similar increase in the number of capillaries per cardiomyocyte, capillary density is decreased [12]. Oxygen needs to travel further from the cell membrane to the core of the cell, and hypoxia may develop. Third, Mb expression and concentration are reduced in the RV, further impairing oxygen supply within the cell [12]. The significance of these changes became apparent in a rat model of pulmonary hypertension (PH) which showed that not the degree of hypertrophy per se, but rather the insufficiency of oxygen supply, causes progressive RV failure [12]. Likewise, in PAH patients the degree of RV hypertrophy does not necessarily relate to RV function [13]. The mismatch in oxygen supply and demand is relevant not only to the RV but also to the skeletal muscles, including respiratory muscles, where reduced capillary density causes reduced oxygen supply as well [14].

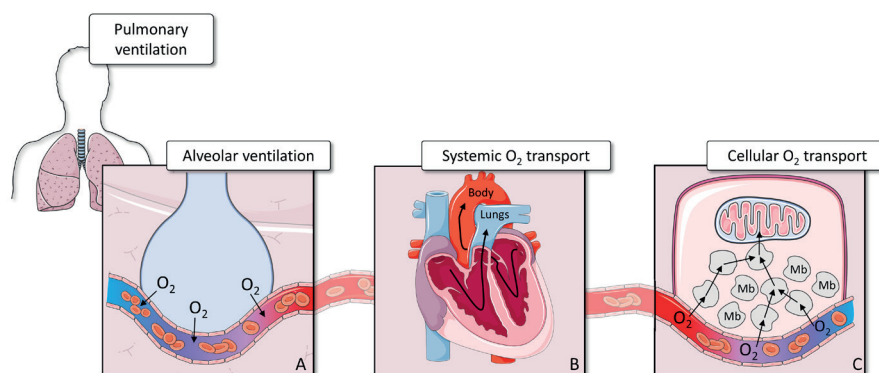


Figure 2 – **Oxygen transport from outside air into the cell.** Upon inhalation, oxygen enters the alveoli and diffuses into the blood, where it binds to haemoglobin in red blood cells. Oxygenated blood from the lungs enters the left atrium and subsequently the left ventricle of the heart, from where it is pumped throughout the body. Finally, when oxygen reaches a tissue, it is released and further transported inside the cell by Mb. Mb = myoglobin

## Oxygen demand

Now that we discussed the importance of oxygen supply and the changes herein in iPAH, we will take a closer look on what (cardiac) cells use this oxygen for, and what determines their demand for oxygen.

By far the largest part of oxygen is used for energy production, which takes place in the mitochondria (Fig. 3). The adult heart uses predominantly fatty acid oxidation

(FAO) for energy production (60-90%), with an additional contribution of glucose metabolism (10-40%) [6]. However, direct combustion of one gram of glucose yields enough energy to heat one litre of water by 3.7 °C. Therefore, release of energy in the cell needs to be done stepwise. First, fatty acids or glucose are metabolised into Acetyl CoA, which is fed into the Krebs cycle. Through this cycle, energy stored in phosphate bonds is transferred to NAD<sup>+</sup> and FADH which are reduced to NADH and FADH<sub>2</sub>, respectively. The Krebs cycle itself yields very little energy. Yet, the energy stored in NADH and FADH<sub>2</sub> is subsequently used in the electron transport chain (ETC) in a process called oxidative phosphorylation.

The ETC consists of five complexes (complex I-V), within the inner mitochondrial membrane. NADH and FADH<sub>2</sub>, formed in the Krebs cycle, carry one electron and one proton (H<sup>+</sup>). NADH releases the electron and proton at complex I, while FADH<sub>2</sub> releases them at complex II. As the electrons are passed through the ETC, complex I, III and IV use the energy from these electrons to pump protons into the intermembrane space, between the inner and outer mitochondrial membrane (IMM and OMM, respectively). Finally, at complex IV the electrons are passed on to oxygen, and water is formed. Protons cannot pass the lipid bilayer of the membrane and as such, a proton gradient builds up across the IMM. At complex V, the kinetic energy of these protons flowing down the gradient is used to generate adenosine triphosphate (ATP). ATP provides energy to virtually all processes in a cell. Without oxygen available, electrons cannot be passed on from complex IV. When this reaction stops, the whole ETC will come to halt, and oxidative phosphorylation can no longer take place. No ATP will be formed, and cells quickly die because of energy starvation [8]. Therefore, oxygen is essential to ATP generation and thus to life.

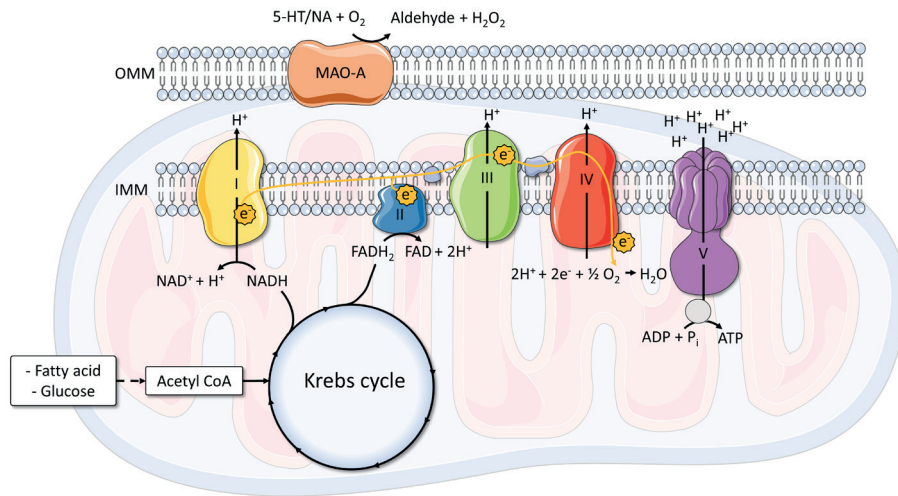


Figure 3 – **Oxygen consumption at the mitochondria.** Oxygen is used mainly at the mitochondria, where it functions as an electron acceptor in the electron transport chain and is therefore highly required during energy production. Monoamine oxidase A, located at the outer mitochondrial membrane, uses oxygen for the oxidative deamination of serotonin and noradrenaline. OMM = outer mitochondrial membrane; IMM = inner mitochondrial membrane; MAO-A = monoamine oxidase A; 5-HT = serotonin; NA = noradrenaline; Acetyl CoA = acetyl co-enzyme A; NAD = nicotinamide-adenine-dinucleotide; FAD = flavine-adenine-dinucleotide; ADP = adenosine diphosphate; ATP = adenosine triphosphate; P<sub>i</sub> = free phosphate.

Mechanical efficiency is defined as the amount of work that is produced from a certain amount of energy. Given that energy is produced using oxygen, mechanical efficiency of a muscle can be defined as the amount of work delivered, divided by oxygen consumption of that muscle. In the conversion from oxygen to ATP to work, inefficiency can be introduced at several places, including inefficient ATP production in the mitochondria, inefficient use of ATP at the sarcomeres, or by the use of oxygen for processes other than energy generation. In iPAH patients, mechanical efficiency of the RV, defined as power output/oxygen consumption, is decreased in patients with more progressive heart failure, due to increased oxygen consumption [15]. In rats, this degree of inefficiency is related to RV cross-sectional area, indicating reduced efficiency at the cardiomyocyte level [15]. The RV has reduced numbers of mitochondria, with abnormal size and shape [16]. This could be an adaptation aimed to reduce oxygen consumption. However, oxygen consumption by mitochondria seems to be reduced already, at least in rat models [16, 17]. This indicates mitochondrial dysfunction and may contribute to increased production of reactive oxygen species (ROS) [17].

ROS are formed when  $O_2$  solely accepts an electron, but no proton, and are a natural by-product of aerobic metabolism, although they are also formed in other places in the cell. In small amounts, ROS have important signalling functions. However, ROS are extremely unstable and oxidize any molecule they meet within the cell. Therefore, large amounts of ROS inevitably cause mitochondrial and cellular damage. Major sources of ROS are monoamine oxidases (MAOs), a class of enzymes located on the OMM (Fig. 3). In the human heart, MAO-A and MAO-B are both present, but MAO-A is the predominant form. MAO-A sequentially hydrolyses serotonin and noradrenaline, amongst others, to aldehydes and ROS, a process that is dependent on oxygen. Therefore, MAO-A may consume large amounts of oxygen that can no longer be used to generate energy [18]. In addition, the large amounts of ROS and aldehydes that are formed in this process are toxic to cells.

The role of MAO-A in iPAH has not been investigated. However, studies in left ventricular (LV) failure indicate a role of MAO-A in the development of heart failure. MAO-A generated ROS contribute to myocyte hypertrophy, whereas lack of MAO-A reduces oxidative stress, LV remodelling and apoptosis in animal models of heart failure. Overexpression occurs in the aging heart, and following volume overload, pressure overload or myocardial infarction [18]. In addition, cardiac upregulation of MAO-A is accompanied by ultrastructural defects of mitochondria, ATP depletion, necrosis and eventually heart failure [19]. In fact, increased MAO-A activity may consume so much oxygen, that complex V of the ETC starts to work in reverse mode, which uses ATP rather than generating it [18]. Data on MAO-A in the RV is scarce. It was shown that MAO-A and MAO-B are upregulated in human ischemic RV versus non failing RV, and importantly that MAO-A activity is positively correlated to mPAP [20]. MAO-A activity is also increased in the RV in a monocrotaline rat model of PH [21]. In this model, MAO-A inhibition led to reduced basal oxygen consumption, underlining the possible substantial contribution of MAO-A to oxygen consumption in iPAH [21].

## The neurohormonal system

Cardiovascular homeostasis, or the maintenance of steady internal physiological conditions, is maintained due to strict regulation of blood pressure, cardiac output and peripheral resistance in blood vessels. In this way, blood is directed to places where it is needed most to deliver oxygen and remove carbon dioxide ( $CO_2$ ) (i.e., the most metabolically active tissues). Baroreceptors and chemoreceptors continuously monitor blood pressure and composition, and peripheral blood flow. In case homeostasis is disturbed, several mechanisms are activated to restore the balance. The primary, and fastest mechanism is autoregulation. Increased levels of  $CO_2$  or reduced pH indicate increased tissue activity and cause local vasodilation to increase blood flow and restore homeostasis. When autoregulation

is insufficient, the neurohormonal system takes over.

Two pillars of the neurohormonal system are the autonomic nervous system (ANS) and the renin-angiotensin-aldosterone (RAAS) system (Fig. 4). The ANS is particularly sensitive to changes in blood pressure and composition and can respond quickly by increasing heart rate and peripheral resistance to restore blood pressure, and by increasing ventilation and gas exchange in the lungs to restore oxygen and CO<sub>2</sub> levels in the blood. The RAAS ensures long-term homeostasis and is sensitive to changes in blood volume rather than pressure or composition. Both within the ANS and the RAAS, opposing pathways determine the net activation of these systems.

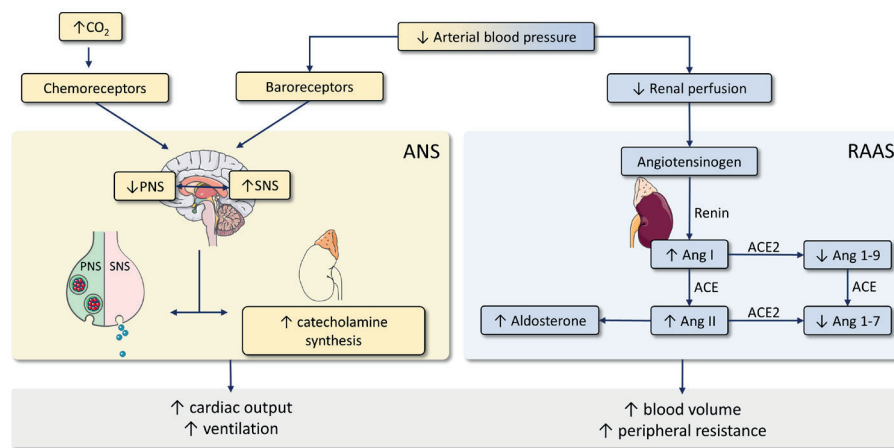


Figure 4 – **Neurohormonal regulation of cardiovascular homeostasis.** A drop in blood pressure or increase in blood CO<sub>2</sub> levels change the balance within the autonomic nervous system and renin-angiotensin aldosterone system so, that cardiac output and ventilation are increased, and cardiovascular homeostasis is restored. Adapted from Peters, EL; Eur. Res. J. 2021. ANS = autonomic nervous system; PNS = parasympathetic nervous system; SNS = sympathetic nervous system; RAAS = renin-angiotensin aldosterone system; Ang = angiotensin

Although both systems are highly required to maintain cardiovascular homeostasis, it is believed that chronic activation of the neurohormonal system eventually becomes maladaptive. In iPAH, imbalances both in the ANS and RAAS have been described at systemic as well as cellular levels. Plasma levels of noradrenaline, Angiotensin (Ang) II and aldosterone are increased, while parasympathetic (PNS) activity and plasma levels of Ang1-7 and Ang1-9 are reduced. This causes imbalances towards predominant sympathetic nervous system (SNS) and Ang II activity. At the cellular level, these imbalances are reflected in downregulation of beta-adrenergic receptors in the heart, and increased formation of Ang II as well as increased Ang II-receptor expression in the lungs [22, 23]. The changes in neu-

rohormonal activation, both at systemic and cellular levels, are associated with faster disease progression, poor survival and cardiac and vascular remodelling. In addition, chronically increased SNS activity is thought to underlie hyperventilation, a phenomenon commonly observed in iPAH patients [24] and adding to the disease burden.

## Aim and outline

The aim of this thesis is to slow down the vicious circle of RV deterioration and eventually failure in iPAH. To this end, we investigated if and how oxygen supply can be improved, oxygen demand can be reduced and the neurohormonal balance can be restored.

In **chapter 2**, we investigated how Mb expression, and thus intracellular oxygen transport, is regulated in a rat model of PH, specifically in the hypertrophied RV. We studied Mb gene- and protein expression while taking into account cell size, to determine why the rate of hypertrophy diverges from the possible increase in oxygen supply. Subsequently, in **chapter 3**, we aimed to increase Mb expression and cell size concurrently in cultured C<sub>2</sub>C<sub>12</sub> mouse skeletal muscle myotubes. Previous studies suggested a benefit of combining hypoxia and fatty acid supplementation. Therefore, we applied a combination of anabolic stimulation, hypoxia and fatty acid supplementation.

Second, we focussed on oxygen demand. In **chapter 4**, we estimated mitochondrial efficiency *ex vivo*, and from small amounts of tissue, by quantifying a histochemical determination that has been described before [25]. In addition, we related mitochondrial efficiency to the fatty acid composition, and thereby membrane integrity, of the IMM.

In **chapter 5**, we used clorgyline to specifically inhibit ROS production by MAO-A in two rat models of PH. Thereby, we were able to investigate its effects on vascular remodelling and secondary effects on the heart, as well as direct effects on cardiac remodelling and cardiac function. Moreover, we applied the method described in chapter 4 to study the effect of clorgyline on mitochondrial efficiency in the RV.

Lastly, we studied interventions on the neurohormonal system in iPAH. In **chapter 6**, we investigated whether interventions that lower SNS activity can reduce hyperventilation in iPAH patients. Therefore, we compared ventilation both at rest and during exercise while patients were on long-term beta-blocker or placebo treatment. In addition, patients underwent hyperoxic breathing with 40% oxygen at rest, to acutely reduce SNS activity and improve hypoxaemia, while we examined ventilation.

## CHAPTER 1

In **chapter 7**, we discussed in detail the changes in the neurohormonal system that have been described in iPAH, and reviewed the interventions on the neurohormonal system that have been tested pre-clinically and/or clinically. We discussed what is needed to improve translation of neurohormonal modulation strategies from the lab to the clinic.

Our findings and future perspectives are discussed in **Chapter 8**.

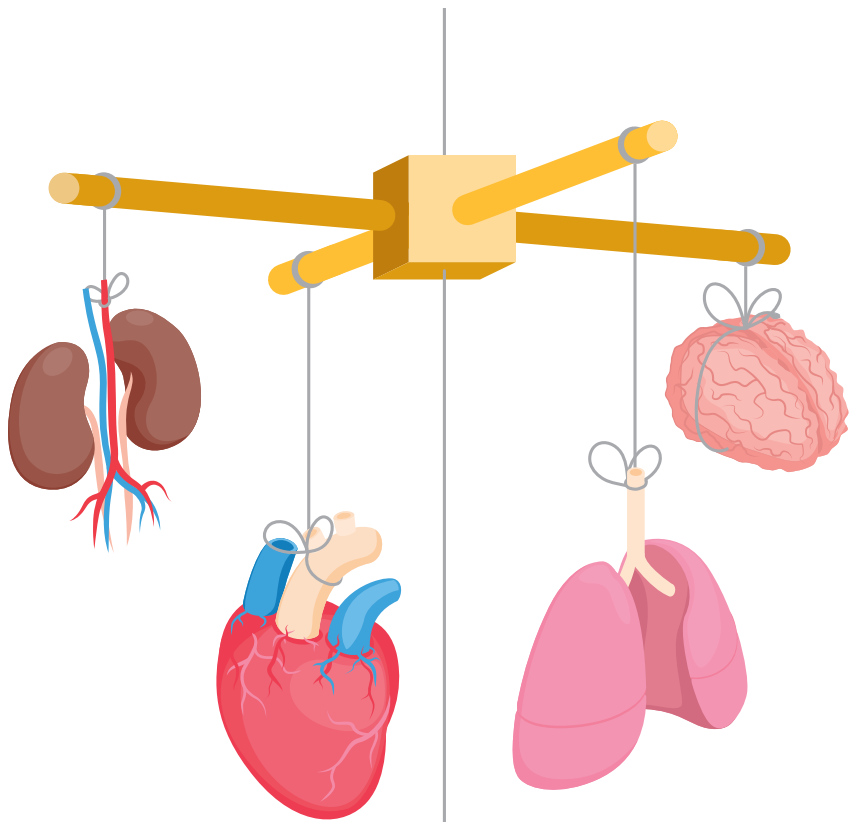
## References

1. Galiè N, Humbert M, Vachiery J-L, Gibbs S, Lang I, Torbicki A, Simonneau G, Peacock A, Vonk Noordegraaf A, Beghetti M, Ghofrani A, Sanchez MAG, Hansmann G, Klepetko W, Lancellotti P, Matucci M, McDonagh T, Pierard LA, Trindade PT, Zompatorie M, Hoeper M. 2015 ESC/EAS Guidelines for the diagnosis and treatment of pulmonary hypertension. *Ration. Pharmacother. Cardiol.* 2016; 12: 79–86.
2. Simonneau G, Montani D, Celermajer DS, Denton CP, Gatzoulis MA, Krowka M, Williams PG, Souza R. Haemodynamic definitions and updated clinical classification of pulmonary hypertension. *Eur. Respir. J.* 2019;53.
3. Hoeper MM, Humbert M. The new haemodynamic definition of pulmonary hypertension: Evidence prevails, finally! *Eur. Respir. J.* 2019;53.
4. Simon J, Gibbs R, Torbicki A. Proposed new pulmonary hypertension definition: Is 4 mm(Hg) worth re-writing medical textbooks? *Eur. Respir. J.* 2019;53.
5. Farber HW, Miller DP, Poms AD, Badesch DB, Frost AE, Muros-Le Rouzic E, Romero AJ, Benton WW, Elliott CG, McGoon MD, Benza RL. Five-year outcomes of patients enrolled in the REVEAL registry. *Chest* 2015; 148: 1043–1054.
6. Ryan JJ, Archer SL. The right ventricle in pulmonary arterial hypertension: Disorders of metabolism, angiogenesis and adrenergic signaling in right ventricular failure. *Circ. Res.* 2014; 115: 176–188.
7. Vonk-Noordegraaf A, Haddad F, Chin KM, Forfia PR, Kawut SM, Lumens J, Naeije R, Newman J, Oudiz RJ, Provencher S, Torbicki A, Voelkel NF, Hassoun PM. Right heart adaptation to pulmonary arterial hypertension: Physiology and pathobiology. *J. Am. Coll. Cardiol.* 2013; 62.
8. Martini FH, Nath JL. Fundamentals of anatomy and physiology. 8th ed. 2009.
9. Van Wolferen SA, Marcus JT, Westerhof N, Spreeuwenberg MD, Marques KMJ, Bronzwaer JGF, Henkens IR, Gan CTJ, Boonstra A, Postmus PE, Vonk-Noordegraaf A. Right coronary artery flow impairment in patients with pulmonary hypertension. *Eur. Heart J.* 2008; 29: 120–127.
10. Ruiter G, Lankhorst S, Boonstra A, Postmus PE, Zweegman S, Westerhof N, Van Der Laarse WJ, Vonk-Noordegraaf A. Iron deficiency is common in idiopathic pulmonary arterial hypertension. *Eur. Respir. J.* 2011; 37: 1386–1391.
11. Ruiter G, Manders E, Happé CM, Schalij I, Groepenhoff H, Howard LS, Wilkins MR, Bogaard HJ, Westerhof N, van der Laarse WJ, de Man FS, Vonk-Noordegraaf A. Intravenous iron therapy in patients with idiopathic pulmonary arterial hypertension and iron deficiency. *Pulm. Circ.* 2015; 5: 466–472.
12. Ruiter G, Wong YY, de Man FS, Handoko ML, Jaspers RT, Postmus PE, Westerhof N, Niessen HWM, van der Laarse WJ, Vonk-Noordegraaf A. Right ventricular oxygen supply parameters are decreased in human and experimental pulmonary hypertension. *HEALUN* 2013; 32: 231–240.
13. Van Der Bruggen CEE, Tedford RJ, Handoko ML, Van Der Velden J, De Man FS. RV pressure overload: From hypertrophy to failure. *Cardiovasc. Res.* 2017;113 p. 1423–1432.
14. Riou M, Pizzimenti M, Enache I, Charloux A, Canuet M, Andres E, Talha S, Meyer A, Geny B. Skeletal and Respiratory Muscle Dysfunctions in Pulmonary Arterial Hypertension. *J. Clin. Med.* 2020; 9: 410.

## CHAPTER 1

15. Wong YY, Handoko ML, Mouchaers KTB, de Man FS, Vonk-Noordegraaf A, Van der Laarse WJ, Man FS de, Vonk Noordegraaf A, Van der Laarse WJ. Reduced mechanical efficiency of rat papillary muscle related to degree of hypertrophy of cardiomyocytes. *Am. J. Physiol. Heart Circ. Physiol.* 2010; 298: H1190-7.
16. Balestra GM, Mik EG, Eerbeek O, Specht PAC, van der Laarse WJ, Zuurbier CJ. Increased in vivo mitochondrial oxygenation with right ventricular failure induced by pulmonary arterial hypertension: Mitochondrial inhibition as driver of cardiac failure? *Respir. Res.* 2015; 16.
17. Gomez-Arroyo J, Mizuno S, Szczepanek K, Van Tassel B, Natarajan R, Dos Remedios CG, Drake JI, Farkas L, Kraskauskas D, Wijesinghe DS, Chalfant CE, Bigbee J, Abbate A, Lesnefsky EJ, Bogaard HJ, Voelkel NF. Metabolic gene remodeling and mitochondrial dysfunction in failing right ventricular hypertrophy secondary to pulmonary arterial hypertension. *Circ. Hear. Fail.* 2013; 6: 136-144.
18. Kaludercic N, Mialet-Perez J, Paolocci N, Parini A, Di Lisa F. Monoamine oxidases as sources of oxidants in the heart. *J. Mol. Cell. Cardiol.* 2014; 73: 34-42.
19. Villeneuve C, Guilbeau-Frugier C, Sicard P, Lairez O, Ordener C, Duparc T, De Paulis D, Couderc B, Spreux-Varoquaux O, Tortosa F, Garnier A, Knauf C, Valet P, Borchi E, Nediani C, Gharib A, Ovize M, Delisle M-B, Parini A, Mialet-Perez J. p53-PGC-1 $\alpha$  Pathway Mediates Oxidative Mitochondrial Damage and Cardiomyocyte Necrosis Induced by Monoamine Oxidase-A Upregulation: Role in Chronic Left Ventricular Dysfunction in Mice. *Antioxid. Redox Signal.* 2013; 18: 5-18.
20. Manni ME, Rigacci S, Borchi E, Bargelli V, Miceli C, Giordano C, Raimondi L, Nediani C. Monoamine oxidase is overactivated in left and right ventricles from ischemic hearts: An intriguing therapeutic target. *Oxid. Med. Cell. Longev.* 2016; 2016: 1-10.
21. Van Eif VWW, Bogaards SJP, Van der Laarse WJ. Intrinsic cardiac adrenergic (ICA) cell density and MAO-A activity in failing rat hearts. *J. Muscle Res. Cell Motil.* 2014; 35: 47-53.
22. Maron BA, Leopold JA. Emerging concepts in the molecular basis of pulmonary arterial hypertension: Part II: Neurohormonal signaling contributes to the pulmonary vascular and right ventricular pathophenotype of pulmonary arterial hypertension. *Circulation* 2015; 131: 2079-2091.
23. Maron BA, Leopold JA, Hemnes AR. Metabolic syndrome, neurohumoral modulation, and pulmonary arterial hypertension. *Br. J. Pharmacol.* 2019; 177: 1457-1471.
24. Naeije R, van de Borne P. Clinical relevance of autonomic nervous system disturbances in pulmonary arterial hypertension. *Eur. Respir. J.* 2009; 34: 792-794.
25. Meijer AEFH, Vloedman AHT. The Histochemical Characterization of the Coupling State of Skeletal Muscle Mitochondria. *Histochemistry* 1980; 69: 217-232.





2

# REGULATION OF MYOGLOBIN IN HYPERTROPHIED RAT CARDIOMYOCYTES IN EXPERIMENTAL PULMONARY HYPERTENSION

---

**Eva L. Peters**, Carla Offringa, Dorien Kos, Willem J. van der Laarse,  
Richard T. Jaspers

*Pflügers Archiv – European Journal of Physiology*, 2016. 468, p:1697-1707

## Abstract

A major problem in chronic heart failure is the inability of hypertrophied cardiomyocytes to maintain the required power output. A Hill-type oxygen diffusion model predicts that oxygen supply is limiting in hypertrophied cardiomyocytes at maximal rates of oxygen consumption and that this limitation can be reduced by increasing the myoglobin (Mb) concentration. We explored how cardiac hypertrophy, oxidative capacity, and Mb expression in right ventricular cardiomyocytes are regulated at the transcriptional and translational levels in an early stage of experimental pulmonary hypertension, in order to identify targets to improve the oxygen supply/demand ratio. Male Wistar rats were injected with monocrotaline to induce pulmonary hypertension (PH) and right ventricular heart failure. The messenger RNA (mRNA) expression levels per nucleus of growth factors insulin-like growth factor-1Ea (IGF-1Ea) and mechano growth factor (MGF) were higher in PH than in healthy controls, consistent with a doubling in cardiomyocyte cross-sectional area (CSA). Succinate dehydrogenase (SDH) activity was unaltered, indicating that oxidative capacity per cell increased. Although the Mb protein concentration was unchanged, Mb mRNA concentration was reduced. However, total RNA per nucleus was about threefold higher in PH rats versus controls, and Mb mRNA content expressed per nucleus was similar in the two groups. The increase in oxidative capacity without an increase in oxygen supply via Mb-facilitated diffusion caused a doubling of the critical extracellular oxygen tension required to prevent hypoxia ( $PO_{2crit}$ ). We conclude that Mb mRNA expression is not increased during pressure overload-induced right ventricular hypertrophy and that the increase in myoglobin content per myocyte is likely due to increased translation. We conclude that increasing Mb mRNA expression may be beneficial in the treatment of experimental PH.

## Introduction

Myoglobin is an oxygen buffer and transporter and substantially contributes to mitochondrial oxygen supply, particularly at low intracellular oxygen tension (<10 mmHg) [63]. The myoglobin content is decreased in several models of chronic heart failure (CHF), including dog, turkey, and chicken models, which correlates with biochemical and physiological markers of myocardial performance [33]. A decrease in myoglobin (Mb) concentration has also been reported in rat models of pulmonary hypertension (PH) with progressive heart failure (HF) [22, 40, 53] but not with stable HF [31, 40]. Furthermore, a reduction of Mb was observed in necropsies of the right-sided myocardium of pulmonary hypertensive patients [40]. These studies suggest that Mb deficiency may be a determinant of the progression of CHF due to chronic pressure overload.

Apart from oxygen transport and buffering, Mb also facilitates intracellular fatty acid transport and regulates fatty acid metabolism [50]. This is emphasized by the observation that heart muscle in mice lacking Mb (*myo*<sup>-/-</sup>) switches towards glycolytic metabolism [10]. Mb also regulates oxygen supply and consumption by generation and/or scavenging of nitric oxide (NO) [64], which enables vasodilation [11] or reduces mitochondrial oxygen consumption via inhibition of complex I and/or complex IV [4]. This can protect the heart from oxidative stress in hypoxia [11]. In addition, Mb has suicidal-peroxidase activity [9] and serves as an iron store [5]. A substantial proportion of CHF patients is iron deficient [52]. Also, mice lacking Mb (*myo*<sup>-/-</sup>) showed differential gene expression patterns upon induction of isoproterenol-induced heart failure, suggesting a role for Mb in adaptation to overload [30].

Chronic pressure overload induces extensive myocardial hypertrophy [6, 22, 40, 53], which reduces wall stress but also decreases mechanical efficiency in hypertrophied rat papillary muscle [65]. Especially when cardiomyocyte cross-sectional area (CSA) becomes larger than approximately 400–500  $\mu\text{m}^2$  [65]. Thus, the oxygen demand of hypertrophied myocytes increases several folds, and the extracellular oxygen tension required to prevent hypoxic cores when mitochondria are maximally activated ( $\text{PO}_{2\text{crit}}$ ) may become limiting [6, 40, 53, 54], also because capillary density is reduced [40, 51, 60]. Hence, a mismatch between oxygen demand and supply arises and either cardiomyocyte hypoxia develops [6, 49, 54] or metabolism must be inhibited [2], which in either case results in reduced energy for contraction and cardiac output.

CSA and oxidative capacity of a muscle are normally under tight control and show a strong inverse relationship that closely fits the Hill-type diffusion model [59]. It is therefore likely that the potential to increase CSA and  $\text{VO}_{2\text{max}}$  simultaneously is limited by oxygen diffusion. Thus, cardiomyocytes can likely sustain greater cell

## CHAPTER 2

size, increased oxidative capacity and higher workload only when Mb concentration and/or number of capillaries per myocyte increases [6, 53, 59]. The latter does not occur within 4 weeks in our model of experimental PH [6, 40, 51], but we have previously found that a monocrotaline dose of 40 mg/kg was lethal in rats with a low myoglobin concentration in right-sided cardiomyocytes ( $\approx 0.25$  mM [6]) whereas compensated hypertrophy developed when the concentration of myoglobin was high ( $\approx 0.6$  mM [31, 40]). The reason why myoglobin concentrations differed between these studies is not known, but could be related to food composition or housing conditions [46]. Increasing the myoglobin concentration in skeletal muscle by iron therapy in iron-deficient PH patients has some beneficial effects [39].

The mechanisms underlying the regulation of Mb during hypoxia and increased contractile activity are not yet fully understood [21]. Contractile activity increases  $Ca^{2+}$  levels and thereby activates the calcineurin (CN)-nuclear factor of activated T cells (NFAT)/myocyte enhancer factor 2 (MEF2) pathway, which is known to stimulate Mb expression [20] as well as pathological hypertrophy [29]. Also, a progressive increase in Mb messenger RNA (mRNA) and protein has been demonstrated in rats following thyroid hormone  $T_3$  treatment, where Mb levels exceeded euthyroid levels [14]. Type 3 deiodinase (D3) is an inhibitor of  $T_3$  activity and is expressed locally in the hypertrophied heart by a hypoxia-inducible factor (HIF)-1 $\alpha$ -dependent pathway [49]. The outcome of these signalling pathways with respect to the Mb concentration in progressive experimental PH is a heterogeneous reduction of the myoglobin concentration in right ventricular myocytes [49].

There are several possibilities why the Mb concentration lags behind the rate of cardiomyocyte hypertrophy. First, the capacity of transcription could be the limiting factor in hypertrophied cardiomyocytes, because the volume of cytoplasm per nucleus increases twofold in 2 weeks [6]. However, Ruiters et al. [40] showed that myoglobin mRNA per nucleus increased by a similar factor in stable PH 40 days after the monocrotaline injection but not in progressive PH 35 days after the monocrotaline injection (at a similar degree of hypertrophy), causing a reduced Mb mRNA concentration in progressive PH at the time of sacrifice. Furthermore, it may be that the translation of Mb mRNA is slow or inefficient in progressive PH. It is also possible that increasing ROS production causes Mb degradation. These data suggest that Mb mRNA expression is inadequate in progressive HF but also indicate that it can be upregulated in overloaded heart muscle. Hence, the aim of this study was to explore how the Mb concentration and the oxidative capacity are regulated at an early stage of progressive PH in concordance with cell size.

We hypothesized that Mb mRNA expression does increase at an early stage of the development of progressive myocardial hypertrophy. We focused on transcriptional (mRNAs: Mb, peroxisome proliferator-activated receptor gamma

coactivator 1-alpha [PGC-1 $\alpha$ ], succinate dehydrogenase [SDH], cytochrome c oxidase [COX], and vascular endothelial growth factor [VEGF] and translational control of protein synthesis (ribosomal RNA [rRNA], insulin-like growth factor-1Ea [IGF-1Ea], and mechano growth factor [MGF]) and protein degradation (muscle RING-finger protein-1 [MuRF1], muscle atrophy F-box [Mafbx], BCL2/adenovirus E1B 19 kDa interacting protein 3 [BNIP3]) and glycolytic metabolism (glyceraldehyde 3-phosphate dehydrogenase [GAPDH]).

## Methods

### Animals and preparations

The study was approved by the Animal Experimental Committee of the Vrije Universiteit Amsterdam (Amsterdam, The Netherlands) and conformed to the guide of the Dutch Research Council for care and use of laboratory animals. Male Wistar rats ( $n = 13$ ) obtained from Harlan (Horst, The Netherlands) were injected subcutaneously with 60 mg/kg monocrotaline (MCT) at 170–190 g body mass to induce progressive right ventricular HF. This protocol causes a reduction of cardiac output of 25 to 30% after 3.5 to 4 weeks [16, 65]. Untreated rats ( $n = 10$ ) were used as controls. All animals received water and standard rat chow (Teklad 2016, Envigo, UK) ad libitum. Three weeks after MCT treatment, rats were anesthetized with halothane and the hearts were rapidly excised and perfused with Tyrode solution (120 mM NaCl, 5 mM KCl, 1.2 mM  $MgSO_4$ , 2.0 mM  $Na_2HPO_4$ , 27 mM  $NaHCO_3$ , 1 mM  $CaCl_2$ , 10 mM glucose and 20 mM 2,3-butanedione monoxime, equilibrated with 95 %/5 %  $O_2/CO_2$  at pH 7.6 and 10 °C) to prevent contraction and to remove blood. Biopsies of the right ventricular wall were embedded in 15% (w/v) gelatine in Tyrode, pH 7.5, and then frozen in liquid nitrogen. Sections of 5  $\mu m$  thickness were cut and either air dried for 15 min prior to the determination of SDH activity (see below) or stored at  $-80$  °C for later analysis of the Mb concentration.

### Succinate dehydrogenase histochemistry and determination of cross-sectional area of cardiomyocytes

SDH activity was measured in the incubation medium (37.5 mM sodium phosphate buffer, pH 7.6, 75 mM sodium succinate, 5 mM sodium azide, and 0.4 mM tetranitro blue tetrazolium) as previously described [34]. Briefly, sections were incubated in the dark for 7 min at 37 °C [6]. The spatially averaged absorbance of individual cells in each section was measured at 660 nm using a calibrated microdensitometer [22] and is expressed as the rate of staining in absorbance units per micrometre section thickness and per second incubation time ( $\Delta A_{660} \cdot \mu m^{-1} \cdot s^{-1}$ ). SDH activity is proportional to  $VO_{2max}$  under hyperoxic conditions in vitro [6, 56]. The measurement included the determination of the CSA of the cell. Absorbance was measured in 20 myocytes, so that a reliable estimate of the mean value was obtained. NIH Image and Image J (<http://rsbweb.nih.gov/ij/>) were used for analysis, taking the pixel-to-aspect ratio into account.

### Myoglobin concentration

For the determination of Mb concentration, sections were first fixed in paraformaldehyde vapor and subsequently in 2.5 % glutaraldehyde solution for 10 min [53]. Sections were then incubated for 1 h in 59 ml of 50 mM TRIS/80 mM

KCl buffer, pH 8.0 which contained 25 mg ortho-tolidine dissolved in 2 ml 96% ethanol at 50 °C and 1.43 ml of 70% tertiary-butyl-hydroperoxide (Fluka Chemie, Switzerland) [22, 53]. Absorbance was measured at 436 nm and converted to Mb concentration using gelatine sections containing known equine Mb (Sigma, The Netherlands) concentrations.

### Calculation of PO<sub>2</sub> crit

An estimate of the minimal extracellular oxygen tension required to prevent hypoxic cell cores when mitochondria are maximally active (PO<sub>2crit</sub>) of the cardiomyocytes can be calculated as follows [17, 32]:

$$PO_{2crit} = (VO_{2max} \cdot R^2 - 4D_{Mb} \cdot MbO_{2R}) / 4\alpha_M \cdot D_{O_2} \quad (1)$$

where VO<sub>2</sub> is the rate of oxygen consumption (mM·s<sup>-1</sup>), R is the radius of the cell, D<sub>Mb</sub> is the diffusion coefficient for Mb in the sarcoplasm, α<sub>M</sub> is the solubility of oxygen in the muscle, and D<sub>O<sub>2</sub></sub> is the diffusion coefficient for oxygen in muscle tissue. Furthermore, MbO<sub>2R</sub> depends on PO<sub>2crit</sub>, the concentration of oxygenated and deoxygenated Mb (Mb<sub>tot</sub>), and the half-saturation pressure of Mb (P<sub>50</sub>) as follows:

$$MbO_{2R} = PO_{2crit} \cdot Mb_{tot} / (PO_{2crit} + P_{50}) \quad (2)$$

Substitution of the latter into the first equation allowed the calculation of PO<sub>2crit</sub> as a function of parameters that were measured or estimated using calibrated histochemistry [53] or obtained from literature (see below).

To estimate PO<sub>2crit</sub> at VO<sub>2max</sub>, VO<sub>2max</sub> was estimated from measured SDH values based on previous observations that showed SDH activity to be proportional to VO<sub>2max</sub> with a staining rate of 1·10<sup>-4</sup> ΔA·660·μm<sup>-1</sup>·s<sup>-1</sup> corresponding to a VO<sub>2max</sub> of 0.6 mM·s<sup>-1</sup> [6, 56]. The concentration of Mb was determined from the heart sections as described above. All other values were obtained from literature: D<sub>Mb</sub> = 0.27·10<sup>-4</sup> mm<sup>2</sup>·s<sup>-1</sup> [3], α<sub>M</sub>·DO<sub>2</sub> = 2 nM·mm<sup>-2</sup>·s<sup>-1</sup>·mmHg<sup>-1</sup> [55], and P<sub>50</sub> = 6.5 mmHg [8, 13, 45]. Note that this calculation provides an underestimation of PO<sub>2crit</sub> because zero-order kinetics for mitochondrial oxygen consumption and equilibrium of the reaction of myoglobin with oxygen are assumed (see [41] and [7], respectively, for discussion).

### Quantitative polymerase chain reaction (qPCR)

Parts (mean mass 68.8 ± 8.24 mg) of the right ventricular free wall were weighed while frozen. Total RNA was extracted using a RiboPure kit (Applied Biosystems, Carlsbad, CA) according to the manufacturer's instructions. Real-time PCR was performed using a StepOne Real-Time PCR system (Applied Biosystems) to

## CHAPTER 2

determine mRNA expression levels. From each muscle, 500 ng total RNA was reverse transcribed using an RNA-to-cDNA kit (Applied Biosystems). For each gene target, 5  $\mu$ l of the reverse transcribed reaction product was amplified using Fast SYBR Green Mastermix (Applied Biosystems). The primers used are listed in Table 1. Mean cycle thresholds were converted to relative expressions by subtracting the 18S rRNA cycle threshold and determining  $2^{-\Delta Ct}$ . Expressions relative to 18S rRNA were multiplied by total RNA per milligram of heart tissue to obtain mRNA concentrations. By multiplying the concentration by the mean CSA of the cardiomyocytes, expression levels of the genes per nucleus were determined. This normalization is based on the observations that the number of myocyte nuclei does not change during the development of hypertrophy [54] and that myocyte length does not change [57]. In this case, the volume of cytoplasm per nucleus is proportional to myocyte CSA and thus normalization for CSA reflects changes in gene expression per nucleus. It should be noted that the expression per nucleus is therefore not an absolute value but rather a relative measure.

Table 1 – **Primers used for qPCR analyses.** *BNIP3* = *BCL2/adenovirus E1B 19 kDa interacting protein 3*, *COX* = *cytochrome c oxidase*, *GAPDH* = *glyceraldehyde 3-phosphate dehydrogenase*, *IGF* = *insulin-like growth factor*, *Mafbx* = *muscle atrophy F-box*, *MGF* = *mechano growth factor*, *MuRF1* = *muscle RING-finger protein-1*, *PGC-1 $\alpha$*  = *peroxisome proliferator-activated receptor gamma coactivator 1-alpha*, *SDH* = *succinate dehydrogenase*, *VEGF* = *vascular endothelial growth factor*

<b>Gene</b>	<b>Forward (5-3)</b>	<b>Reverse (3-5)</b>
<i>18S</i>	CGAACGTCTGCCTATCAACTT	ACCCGTGGTCACCATGGTA
<i>Myoglobin</i>	CCGGTCAAGTACCTGGAGTTTA	TCCCCGGAATATCTCTTCTTC
<i>VEGF</i>	CTGCTGTGGACTTGAGTTGG	AAGACCACACCGGAGTCTTT
<i>IGF-1Ea</i>	AAGCCTACAAAGTCAGCTCG	TCAAGTGTACTTCCTTCTGAGTC
<i>MGF</i>	CAAGACTCAGAAGTCCCAGC	AAGTGTACTTCCTTCTCTCTC
<i>MuRF1</i>	TGCCCCCTTACAAAGCATCTT	CAGCATGGAGATGCAATTGC
<i>Mafbx</i>	TGAAGACCGGCTACTGTGGAA	CGGATCTGCCGCTCTGA
<i>BNIP3</i>	GTCACCTCCCAGGCCTGTCGC	TACCCAGGAGCCCTGCAGTTCT
<i>GAPDH</i>	TGGCCTCCAAGGAGTAAGAAAC	GGCCTCTCTTTGCTCTCAGTATC
<i>PGC-1<math>\alpha</math></i>	ATGAGAAGCGGGAGTCTGAA	GCGCTCTTCAATTGCTTTCT
<i>SDH</i>	CAGAGAAGGGATCTGTGGCT	TGTTGCCTCCGTTGATGTTT
<i>COX1</i>	TGCCAGTATTAGCAGCAGGT	GAATTGGGTCTCCACCTCCA
<i>COX4</i>	AGTCCAATTGTACCGCATCC	ACTCATTGGTGCCCTTGTTT

## Statistical analysis

Independent t-tests were used to compare measurements from MCT-treated animals with those of the control animals. Equality of variance was tested using Levene's test and corrected if significant. Normality was tested using the Shapiro-Wilk test. For data with a non-normal distribution, the Mann-Whitney U test was used. Values are given as mean  $\pm$  standard error of the mean (SEM) unless stated otherwise;  $p < 0.05$  was considered statistically significant.

## Results and discussion

### Effects of MCT on cardiomyocyte phenotype

Figure 1 shows lung mass and RV myocyte CSA against body mass, CSA against lung mass, and CSA, SDH activity, and Mb concentration both for PH rats and controls. Lung mass and CSA were higher in MCT-treated rats although body mass was lower (Fig. 1a–c) illustrating the detrimental effects of the MCT injection after 21 days.

Cardiomyocyte CSA of MCT rats thus increased 1.8-fold compared to that of controls ( $p < 0.001$ ; Fig. 1d–f), confirming hypertrophy. Based on the hyperbolic inverse relationship between muscle fiber size and oxidative capacity [56, 59], we expected to see a decrease in oxidative capacity during hypertrophy. However, SDH activity was similar in PH rats and controls ( $p = 0.34$ ; Fig. 1d, e, and g), indicating that oxidative capacity per unit volume of cytoplasm was retained after MCT injection. Since CSA was increased, the total oxidative capacity per cardiomyocyte increased. As this is accompanied by higher oxygen consumption per cardiomyocyte, these hypertrophied cells would require increased Mb concentrations to prevent hypoxia. However, Mb concentrations in PH and control samples were not statistically different ( $p = 0.11$ ; Fig. 1h–j).

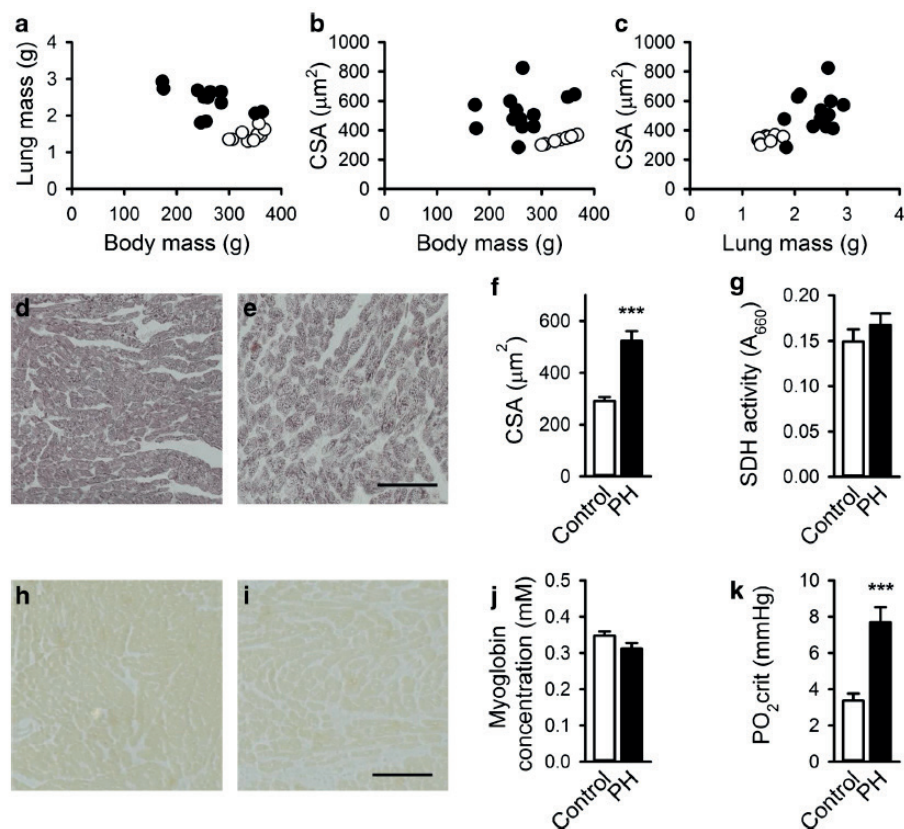


Figure 1 – Effects of monocrotaline-induced pulmonary hypertension on phenotypic characteristics of the rats and cardiomyocytes in rat right ventricle. Lung mass (a) and myocyte CSA (b) are plotted against body mass, and myocyte CSA is plotted against lung mass (c). Representative examples of control and PH right ventricular cardiomyocytes stained for succinate dehydrogenase (SDH) activity (d, e) and myoglobin (h, i) are shown. MCT-induced heart failure caused hypertrophy of cardiomyocytes, as illustrated by an increase in cellular cross-sectional area (CSA) (f). Nevertheless, SDH activity (g) and myoglobin protein concentration (h–j) both remained constant. Therefore,  $PO_{2crit}$  was increased in PH (k). \*\*\* $p < 0.001$ . White bars/circles: control group, black bars/circles: PH. Scale bar indicates 100  $\mu m$

The increase in absolute oxidative capacity without a concomitant increase in Mb protein concentration led to a  $PO_{2crit}$  in PH (7.7 mmHg) that was over twofold greater than the  $PO_{2crit}$  (3.4 mmHg) in controls ( $p < 0.001$ ; Fig. 1k). The increase in  $PO_{2crit}$  and the decrease in the capillary density [40, 51, 60] are likely to cause core hypoxia in cardiomyocytes at the maximum heart rate [54].

The Mb concentrations in the present study are different from those previously reported [6, 22, 53]. This variation indicates that Mb regulation in MCT-induced PH is complicated. The Mb concentration was previously shown to be decreased in experimental PH [40] after 4 weeks, suggesting that the decrease occurs during the fourth week, when the cardiomyocytes no longer increase in size [6].

### Effects of MCT on total RNA content in the right ventricle

The volume of cytoplasm each nucleus had to maintain (i.e., the myonuclear domain) increased with CSA. Thus, to maintain SDH activity and Mb concentration, either the rate of transcription/translation or both should have been enhanced and/or the half-life of Mb should have increased. Because 80–85% of all RNA within muscle cells consists of rRNA [28], we first assessed total RNA content per milligram heart tissue, as a measure of translational capacity.

Total RNA was proportional to wet weight (Fig. 2a;  $p < 0.001$ ). However, the relationship differed between PH rats and controls, indicating that rats with PH had 32 % higher total RNA levels per milligram muscle tissue ( $p = 0.001$ ). Total RNA per nucleus was 2.7 times higher in PH rats compared to controls ( $p < 0.001$ ; Fig. 2b). Expression levels of 18S rRNA relative to total RNA were similar ( $p = 0.96$ ; Fig. 2c). Based on these results, we conclude that rRNA content was proportional to the increase in total RNA, reflecting a higher overall translational capacity in PH cardiomyocytes. Hence, it is unlikely that a limitation in the translational capacity impaired the increase in Mb protein expression.

The increase in total RNA and the absolute increase of 18S rRNA expression levels in PH rats also indicate that mRNA expression levels normalized to 18S rRNA lead to an underestimation of the mRNA expression levels in PH rats compared to controls. Therefore, we normalized subsequent mRNA expression levels both as cardiac tissue mRNA concentration and as amount per nucleus.

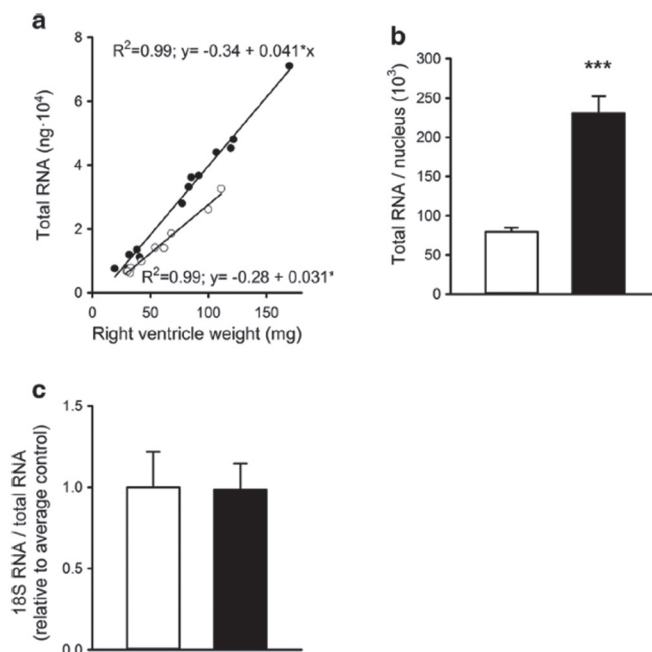


Figure 2 – **Effects of monocrotaline-induced pulmonary hypertension on total RNA content and 18S rRNA in rat right ventricle.** The amount of total RNA was proportional to the weight of the right ventricle, although the relationship is different for PH rats versus controls (a). The mean amount of total RNA per nucleus was more than twofold greater for the PH group compared to controls (b). Nevertheless, the expression of 18S rRNA relative to total RNA was similar in both groups (c). \*\*\* $p < 0.001$ , \*\* $p < 0.01$ . White bars/circles: control, black bars/circles: PH

## Effects of MCT on transcription of regulators of protein synthesis and degradation

We studied mRNA expression levels of several factors related to protein synthesis and degradation as shown in Fig. 3. In order to explain the lack of increase in Mb concentrations, we considered IGF-1Ea and its splice variant MGF, which are known to activate both the rate of transcription and translation [15] and repress several mediators of degradation [43]. In response to exercise or overload, IGF-1 acts as an autocrine/paracrine factor to induce hypertrophy in left ventricular myocardium of rats [42] and humans [47]. It has been shown that physiologic and pathologic cardiac hypertrophy are mediated by different pathways whereby IGF-1 is essential for physiologic hypertrophy and acts via the phosphatidylinositol 3-kinase (PI3K)-Akt-mammalian target of rapamycin (mTOR) pathway whereas pathologic hypertrophy is mediated by the Ca<sup>2+</sup>-CN-NFAT pathway (see [61] for review).

Relative to 18S rRNA expression levels and expressed as concentration (i.e., per milligram tissue), IGF-1Ea expression levels did not differ significantly between the two groups ( $p = 0.41$ ,  $p = 0.07$ ; Fig. 3a, b). However, expression levels of mRNA per nucleus increased 3.5-fold in PH rats compared to controls ( $p < 0.01$ ; Fig. 3c). MGF expression levels were also increased, irrespective of whether they were expressed relative to 18S ( $p < 0.001$ ), concentration ( $p < 0.01$ ), or per nucleus ( $p < 0.001$ ; Fig. 3a–c). In addition to the activation of mRNA transcription and translation, MGF has been shown to preserve cardiac function by inhibiting apoptotic pathways in the myocardium and preventing pathologic cardiac hypertrophy [27].

As expression of IGF-1Ea and MGF mRNA per nucleus were both increased, it is conceivable that the rates of transcription and translation were increased. To investigate this further, we assessed several markers of protein degradation. MuRF1 and Mafbx are known to regulate contractile protein degradation, thereby preventing massive hypertrophy in skeletal and cardiac muscle cells [25, 62]. Furthermore, BNIP3 induces mitochondrial dysfunction and autophagy [36] and apoptosis under hypoxic conditions [38]. Since SDH protein expression was unexpectedly increased, we also studied BNIP3 mRNA expression levels.

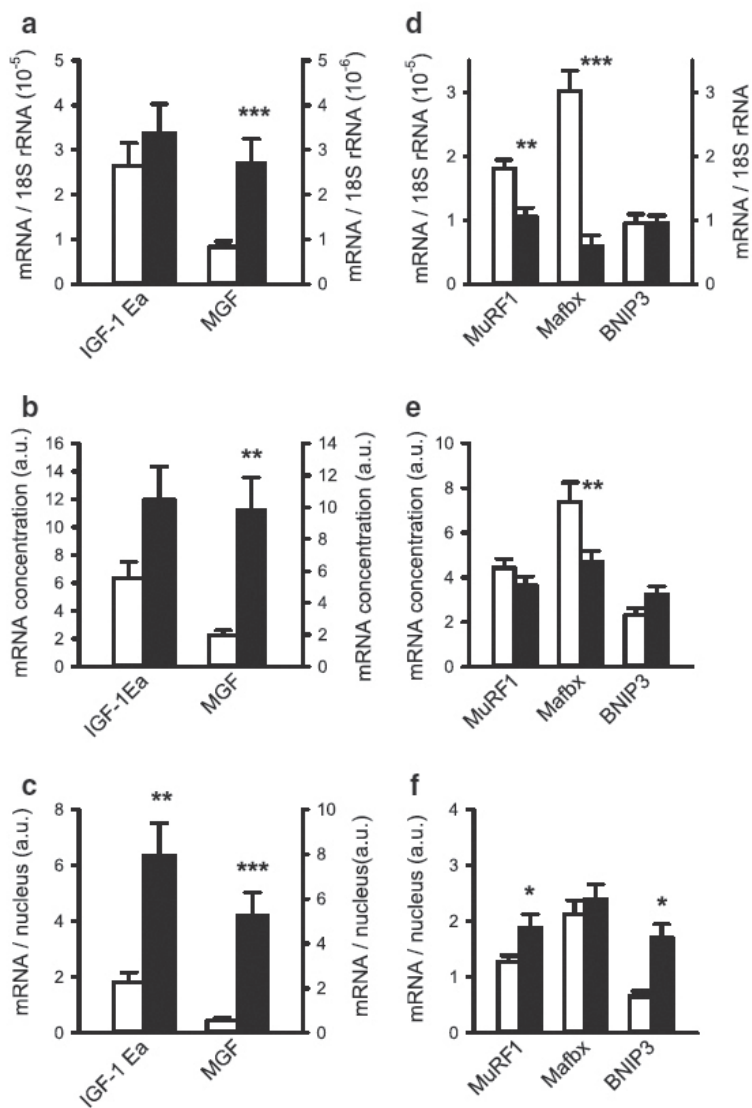


Figure 3 - Effects of monocrotaline-induced pulmonary hypertension in rat on expression of regulators of protein synthesis and degradation in the right ventricle. Expression levels of insulin-like growth factor (IGF)-1Ea and mechano growth factor (MGF) mRNA are presented relative to 18S (a), as concentration per milligram heart tissue (b) or per nucleus (c). Expression levels of muscle RING-finger protein-1 (MuRF1), muscle atrophy F-box (Mafbx), and BCL2/adenovirus E1B 19 kDa interacting protein 3 (BNIP3) were analyzed as markers of degradation and shown relative to 18S (d), as concentration (e) and per nucleus (f). Note that the right axis in d applies only to BNIP3 expression levels. \*\*\* $p < 0.001$ , \*\* $p < 0.01$ , \* $p < 0.05$ . White bars: control, black bars: PH

The expression levels of MuRF1, Mafbx, and BNIP3 were lower or unaltered in PH rats versus controls when expressed relative to 18S rRNA ( $p < 0.01$ ,  $p < 0.001$ , and  $p = 0.99$ , respectively; Fig. 3d), whereas an increase was shown in the expression per nucleus for MuRF1 and BNIP3 (both  $p < 0.05$ ) by 1.5- and 2.6-fold, respectively (Fig. 3f). This appeared to be sufficient to keep the concentration constant, whereas the concentration of Mafbx was rather decreased ( $p < 0.01$ ) due to the constant expression per nucleus (Fig. 3e). Together, these results show a clear elevation in the mRNA concentration of growth factors involved in protein synthesis. By contrast, the concentration of E3 ligases was lower or remained constant. The increase in translational machinery and signalling was apparently sufficient to maintain but not to increase the Mb concentration.

### Effects of MCT on transcriptional expression of metabolic enzymes

GAPDH catalyses the conversion of glyceraldehyde 3-phosphate to D-glycerate 1,3-bisphosphate and is a marker of glycolytic metabolism. Expression levels of GAPDH did not differ between the two groups when expressed relative to 18S rRNA or as mRNA concentration (Fig. 4a, b). When considered per nucleus, GAPDH mRNA expression levels were 2.5-fold higher in PH rats compared to control ( $p < 0.05$ ; Fig. 4c). Because the mRNA concentration does not decrease and the rRNA increases, this result suggests an increase of the glycolytic capacity in MCT-induced PH. A shift towards glycolytic metabolism was also observed in *myo*<sup>-/-</sup> mice suggesting compensation for the lack of Mb [10]. However, Mb concentrations in the present study remained constant and thus do not explain the supposed increase in glycolytic capacity. Alternatively, a shift towards glycolytic metabolism that was associated with a transition towards a decompensated state in PH [51] may have accounted for the increased glycolytic capacity as shown here. Regardless of the underlying mechanism, this shift may reflect one way to lower oxygen utilization of the cardiac myocytes.

We investigated whether SDH mRNA expression levels were increased. Expressed relative to 18S rRNA, we observed a decrease in PH rats compared to controls ( $p < 0.05$ ; Fig. 4a) while mRNA concentration remained constant (Fig. 4b). By contrast, the expression per nucleus was almost twice as high in PH rats versus controls ( $p < 0.01$ ; Fig. 4c). Because cardiomyocyte CSA and SDH activity both increased almost twofold in PH rats versus controls, it can be concluded that SDH mRNA expression was sufficient and in line with the increase in SDH activity per myocyte.

SDH and COX activities have been shown to be proportional during the development of MCT-induced PH [31]. To confirm that SDH activity reflected the oxidative capacity, we also measured mRNA expression levels of both COX1 and

## CHAPTER 2

COX4, subunits of cytochrome c oxidase. Although expression levels of both were decreased relative to 18S ( $p < 0.05$ ; Fig. 4a), the mRNA concentrations remained constant (Fig. 4b). The expression of COX4 mRNA per nucleus was increased almost twofold, in line with the SDH activity (Fig. 4c). Expression per nucleus is not shown for COX1 because this subunit is encoded by the mitochondrial DNA [12]. However, the observed increase in COX4 expression per nucleus, together with the constant COX1 mRNA concentration despite the increase in cell size, indicates that expression levels of both subunits were proportional to SDH activity and were not limiting the increased oxidative capacity. Therefore, SDH activity seems an appropriate estimate of  $VO_{2max}$  used to estimate  $PO_{2crit}$ .

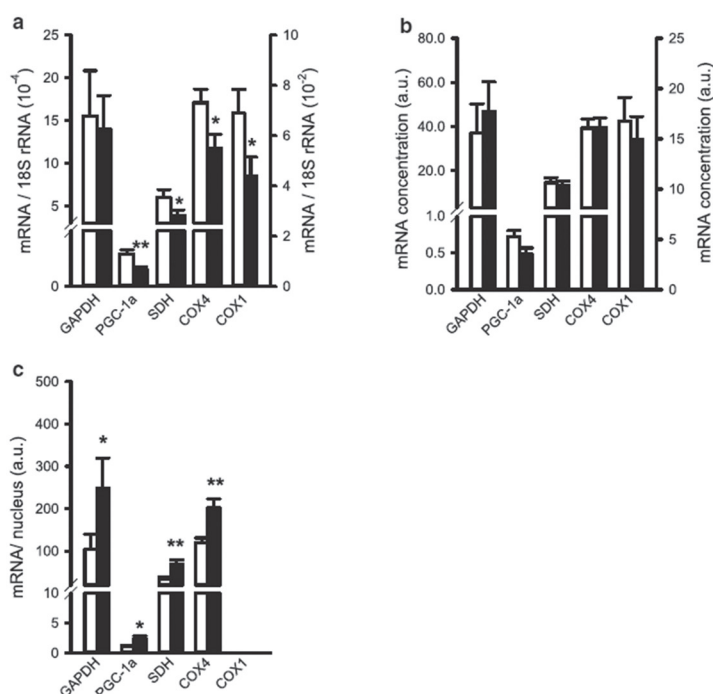


Figure 4 – **Effects of monocrotaline-induced pulmonary hypertension on expression of metabolic markers in rat right ventricle.** Expression levels of glyceraldehyde 3-phosphate dehydrogenase (GAPDH), peroxisome proliferator-activated receptor gamma coactivator 1-alpha (PGC-1α), succinate dehydrogenase (SDH), cytochrome c oxidase (COX) 4, and COX1 are shown relative to 18S (a), as concentration (b) and per nucleus (c). Note that the right axis in a and b only applies to COX1. COX1 expression levels per nucleus are not presented because this subunit is encoded by the mitochondrial DNA. \*\*\* $p < 0.001$ , \*\* $p < 0.01$ , \* $p < 0.05$ . White bars: control, black bars: PH

We also investigated how SDH activity was maintained despite substantial hypertrophy. PGC-1 $\alpha$  is known to be the master regulator of mitochondrial biosynthesis [23, 35]. Following hypoxia, its expression is increased or PGC-1 $\alpha$  is activated because of an increase in ROS production, p38 mitogen-activated protein kinase (MAPK) and AMP-activated protein kinase (AMPK) levels [18, 48]. However, although we show that expression levels relative to that of 18S rRNA were lower ( $p < 0.01$ ; Fig. 4a), the expression per nucleus was over twofold higher in PH rats versus controls (Fig. 4c), and there was no difference in PGC-1 $\alpha$  mRNA concentrations between the two groups (Fig. 4c).

We conclude that the upregulation of PGC-1 $\alpha$  per nucleus is probably the reason why the oxidative capacity was maintained. We observed that cardiomyocyte hypertrophy with maintained SDH activity requires an increase in interstitial  $PO_{2crit}$ . This implies that in order to make use of all mitochondrial enzyme activity, oxygen supply to the cardiomyocytes needs to be increased.

### **Effects of MCT on transcriptional regulation of proteins involved in oxygen supply or the regulation thereof**

To explain the lack of increase in Mb concentration, we assessed both Mb and VEGF mRNA expression levels, as these are indicative of changes in oxygen supply. In addition to its role in angiogenesis [24], it is suggested that VEGF can directly stimulate Mb mRNA transcription via a currently unknown mechanism [58]. An increase of VEGF expression could be either the result of enhanced expression or activation of PGC-1 $\alpha$  [1] or resulting from stabilization of HIF-1 $\alpha$  [48]. It is known that HIF-1 $\alpha$  promotes VEGF-induced angiogenesis under hypoxic conditions [44]. Although we did not measure HIF-1 $\alpha$ , it is reported to accumulate consistently in PH [6, 37, 49, 51, 54]. No differences in VEGF mRNA expression levels relative to 18S rRNA were observed (Fig. 5a), and although the expression levels per nucleus were increased in PH rats compared to controls ( $p < 0.001$ ; Fig. 5c), there was no difference between the groups in the VEGF mRNA concentration (Fig. 5b). These findings are consistent with previous reports that VEGF protein expression remains constant both in stable and progressive HF in rats after 3 weeks of right ventricular overload [40].

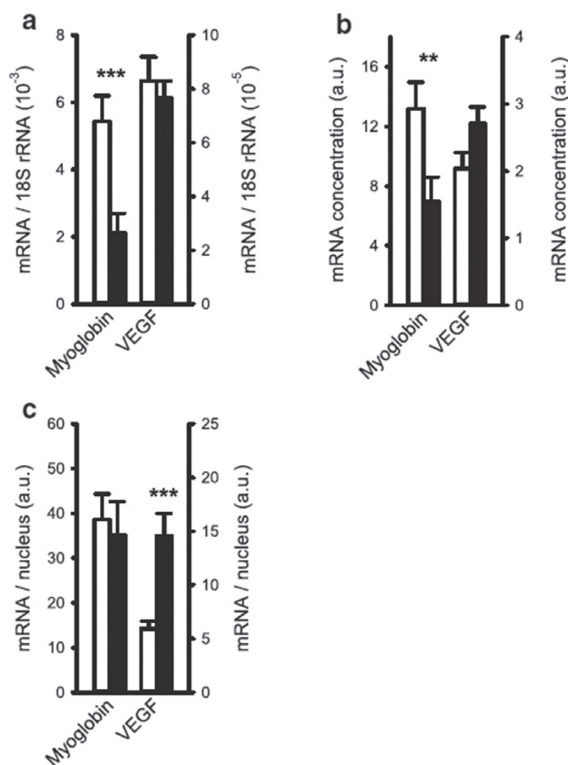


Figure 5 – **Effects of monocrotaline-induced pulmonary hypertension on mRNA expression levels of myoglobin and vascular endothelial growth factor in rat right ventricle.** Expression levels of myoglobin (Mb) and vascular endothelial growth factor (VEGF) are presented for both the PH group and controls relative to 18S (a), as concentration (b) or per nucleus (c). \*\*\* $p < 0.001$ , \*\* $p < 0.01$ , \* $p < 0.05$ . White bars: control, black bars: PH

Although a decrease was seen in the expression relative to 18S RNA ( $p < 0.001$ ) and mRNA concentration ( $p < 0.01$ ; Fig. 5a, b), the expression of Mb mRNA per nucleus remained constant in PH rats (Fig. 5c). In order to retain a stable Mb protein concentration with the increased cell size, we had expected to find a higher expression of Mb mRNA per nucleus. Our data suggest that the Mb protein concentration was maintained due to an increase in the rate of translation, rather than by an increased rate of transcription. It should be noted that we did not correct for an increase in interstitial space from 11% in controls to 1% in PH rats [40]. However, such a correction would only slightly increase the calculated concentration of Mb mRNA per milligram right ventricle tissue by 12–21%, but expression levels per nucleus would remain unaltered. This extends results of Ruiter et al. [40] who showed that myoglobin mRNA was also not upregulated at later stages of progressive PH, whereas it was upregulated in compensated

PH. Furthermore, after 2 weeks of isoproterenol-induced cardiac hypertrophy, Mb mRNA expression was shown to be constant [30]. However, this was expressed relative to a certain amount of RNA. Since we have shown here that total RNA increased in MCT-induced cardiac hypertrophy, this may also be the case for isoproterenol-induced cardiac hypertrophy and would increase Mb mRNA concentrations in diseased mice. Further research is needed to reveal whether Mb mRNA is only upregulated at even earlier onset of heart failure or whether Mb mRNA expression levels are differentially altered in the different models. Thus, our hypothesis is rejected, and the question remains why Mb mRNA expression was not upregulated at an early stage of progressive PH. One explanation for this surprising result is that oxidative metabolism was inhibited in progressive PH [2], thereby preventing the hypoxia stimulus required for myoglobin expression, while myocytes can adapt to hypoxia by increasing myoglobin expression in compensated PH.

Previous studies have demonstrated regulation of Mb via  $\text{Ca}^{2+}$ -CN-NFAT/MEF2 pathways [29] indicating that contractile activity may contribute to the regulation of Mb expression. Furthermore, it has been demonstrated that hypoxia in combination with contractile activity enhances Mb expression in C2C12 myotubes, mouse skeletal [20] and heart [26] muscle, and zebrafish high oxidative muscles [19]. However, this was not the case in our MCT-induced overload of the cardiomyocytes of the right ventricle, despite the fact that increased power output and reduced oxygen tension (judging from increased HIF-1 $\alpha$  expression [6, 37, 49, 51, 54]) were likely present. However, Mb expression was increased following lipid supplementation in hypoxic C2C12 cells and rat soleus muscle, independent of CN signalling, suggesting that other pathways for Mb expression do exist [46]. Furthermore, as mentioned before, iron supplementation [39] and treatment with thyroid hormone [14, 22] both successfully increased Mb expression in PH patients and rat, respectively, and thus may serve as required additional stimuli. In conclusion, this study shows that Mb mRNA expression was not sufficient to increase Mb protein concentrations even at an early stage of progressive PH. Upregulating Mb mRNA expression, e.g., by supplementation of iron [39] and fatty acid [46] and/or stimulation of the thyroid hormone receptor [14], is therefore a promising therapeutic strategy. Further research should reveal the optimal combination of hypoxia, load, and dietary status to increase Mb mRNA and protein levels in chronic heart failure.

## References

1. Arany Z, Foo SY, Ma Y, Ruas JL, Bommi-Reddy A, Girnun G, Cooper M, Laznik D, Chinsomboon J, Rangwala SM, Baek KH, Rosenzweig A, Spiegelman BM (2008) HIF-independent regulation of VEGF and angiogenesis by the transcriptional coactivator PGC-1 $\alpha$ . *Nature* 451:1008–1012. doi:10.1038/nature06613
2. Balestra GM, Mik EG, Eerbeek O, Specht P, van der Laarse WJ, Zuurbier CJ (2015) Increased in vivo mitochondrial oxygenation with right ventricular failure induced by pulmonary arterial hypertension: mitochondrial inhibition as driver of cardiac failure? *Respir Res* 16:6. doi:10.1186/s12931-015-0178-6
3. Baylor SM, Pape PC (1988) Measurement of myoglobin diffusivity in the myoplasm of frog skeletal muscle fibres. *J Physiol* 406:247–275. doi:10.1113/jphysiol.1988.sp017379
4. Clementi E, Brown GC, Feelisch M, Moncada S (1998) Persistent inhibition of cell respiration by nitric oxide: crucial role of S-nitrosylation of mitochondrial complex I and protective action of glutathione. *Proc Natl Acad Sci U S A* 95:7631–7636
5. Dallman PR, Schwartz HC (1965) Distribution of cytochrome C and myoglobin in rats with dietary iron deficiency. *Pediatrics* 35:677–686. doi:10.1172/JCI105269
6. des Tombe AL, van Beek-Harmsen BJ, Lee-de Groot MBE, Van der Laarse WJ (2002) Calibrated histochemistry applied to oxygen supply and demand in hypertrophied rat myocardium. *Microsc Res Tech* 58:412–420. doi:10.1002/jemt.10153
7. Endeward V (2012) The rate of the deoxygenation reaction limits myoglobin- and hemoglobin-facilitated O<sub>2</sub> diffusion in cells. *J Appl Physiol* 112:1466–1473. doi:10.1152/jappphysiol.00835.2011
8. Enoki Y, Matsumura K, Ohga Y, Kohzaki H, Hattori M (1995) Oxygen affinities (P<sub>50</sub>) of myoglobins from four vertebrate species (*Canis familiaris*, *Rattus norvegicus*, *Mus musculus* and *Gallus domesticus*) as determined by a kinetic and an equilibrium method. *Comp Biochem Physiol B Biochem Mol Biol* 110:193–199. doi:10.1016/0305-0491(94)00119-F
9. Flögel U, Godecke A, Klotz LO, Schrader J (2004) Role of myoglobin in the antioxidant defense of the heart. *FASEB* 18:1156–1158. doi:10.1096/fj.03-1382fje
10. Flögel U, Laussmann T, Godecke A, Abanador N, Schafers M, Fingas CD, Metzger S, Levkau B, Jacoby C, Schrader J (2005) Lack of myoglobin causes a switch in cardiac substrate selection. *Circ Res* 96:e68–e75. doi:10.1161/01.RES.0000165481.36288.d2
11. Flögel U, Merx MW, Godecke A, Decking UK, Schrader J (2001) Myoglobin: a scavenger of bioactive NO. *Proc Natl Acad Sci U S A* 98:735–740. doi:10.1073/pnas.011460298
12. Garnier A, Fortin D, Deloménie C, Momken I, Veksler V, Ventura-Clapier R (2003) Depressed mitochondrial transcription factors and oxidative capacity in rat failing cardiac and skeletal muscles. *J Physiol* 551:491–501. doi:10.1113/jphysiol.2003.045104
13. Gayeski TE, Honig CR (1991) Intracellular PO<sub>2</sub> in individual cardiac myocytes in dogs, cats, rabbits, ferrets, and rats. *Am J Phys* 260:H522–H531
14. Giannocco G, DosSantos RA, Nunes MT (2004) Thyroid hormone stimulates myoglobin gene expression in rat cardiac muscle. *Mol Cell Endocrinol* 226:19–26. doi:10.1016/j.mce.2004.07.007
15. Goldspink G, Yang SY (2004) The splicing of the IGF-I gene to yield different muscle growth factors. In: *Advances in Genetics*. Academic Press, San Diego, p 23–49

16. Handoko ML, de Man FS, Happé CM, Schali J, Musters RJ, Westerhof N, Postmus PE, Paulus WJ, van der Laarse WJ, Vonk-Noordegraaf A (2009) Opposite effects of training in rats with stable and progressive pulmonary hypertension. *Circulation* 120:42–49. doi:10.1161/circulationaha.108.829713
17. Hill AV (1965) *Trials and trails in physiology*. Edward Arnold, London
18. Jager S, Handschin C, St-Pierre J, Spiegelman BM (2007) AMP-activated protein kinase (AMPK) action in skeletal muscle via direct phosphorylation of PGC-1 $\alpha$ . *Proc Natl Acad Sci U S A* 104:12017–12022. doi:10.1073/pnas.0705070104
19. Jaspers RT, Testerink J, Della Gaspera B, Chanoine C, Bagowski CP, van der Laarse WJ (2014) Increased oxidative metabolism and myoglobin expression in zebrafish muscle during chronic hypoxia. *Biology open* 3:718–727. doi:10.1242/bio.20149167
20. Kanatous SB, Mammen PP, Rosenberg PB, Martin CM, White MD, Dimaio JM, Huang G, Muallem S, Garry DJ (2009) Hypoxia reprograms calcium signaling and regulates myoglobin expression. *Am J Physiol Cell Physiol* 296:C393–C402. doi:10.1152/ajpcell.00428.2008
21. Kanatous SB, Mammen PPA (2010) Regulation of myoglobin expression. *J Exp Biol* 213:2741–2747. doi:10.1242/jeb.041442
22. Lee-de Groot MBE, des Tombe AL, Van der Laarse WJ (1998) Calibrated histochemistry of myoglobin concentration in cardiomyocytes. *J Histochem Cytochem* 46:1077–1084. doi:10.1177/002215549804600912
23. Lehman JJ, Barger PM, Kovacs A, Saffitz JE, Medeiros DM, Kelly DP (2000) Peroxisome proliferator-activated receptor gamma coactivator-1 promotes cardiac mitochondrial biogenesis. *J Clin Invest* 106:847–856. doi:10.1172/JCI10268
24. Leung DW, Cachianes G, Kuang WJ, Goeddel DV, Ferrara N (1989) Vascular endothelial growth factor is a secreted angiogenic mitogen. *Science* 246:1306–1309. doi:10.1126/science.2479986
25. Li H-H, Kedar V, Zhang C, McDonough H, Arya R, Wang D-Z, Patterson C (2004) Atrogin-1/ muscle atrophy F-box inhibits calcineurin-dependent cardiac hypertrophy by participating in an SCF ubiquitin ligase complex. *J Clin Invest* 114:1058–1071. doi:10.1172/JCI22220
26. Mammen PP, Kanatous SB, Yuhanna IS, Shaul PW, Garry MW, Balaban RS, Garry DJ (2003) Hypoxia-induced left ventricular dysfunction in myoglobin-deficient mice. *Am J Physiol Heart Circ Physiol* 285:2132–2142. doi:10.1152/ajpheart.00147.2003
27. Mavrommatis E, Shioura KM, Los T, Goldspink PH (2013) The E-domain region of mechano-growth factor inhibits cellular apoptosis and preserves cardiac function during myocardial infarction. *Mol Cell Biochem* 381:69–83. doi:10.1007/s11010-013-1689-4
28. Millward DJ, Garlick PJ, James WP, Nnanyelugo DO, Ryatt JS (1973) Relationship between protein synthesis and RNA content in skeletal muscle. *Nature* 241:204–205. doi:10.1038/241204a0
29. Molkenkin JD, LU JR, Antos CL, Markham B, Richardson JA, Robbins J, Grant SR, Olson EN (1998) A calcineurin-dependent transcriptional pathway for cardiac hypertrophy. *Cell* 93:215–228. doi:10.1016/S0092-8674(00)81573-1
30. Molojavyi A, Lindecke A, Raupach A, Moellendorf S, Kohrer K, Godecke A (2010) Myoglobin-deficient mice activate a distinct cardiac gene expression program in response to isoproterenol-induced hypertrophy. *Physiol Genomics* 41:137–145. doi:10.1152/physiolgenomics.90297.2008

## CHAPTER 2

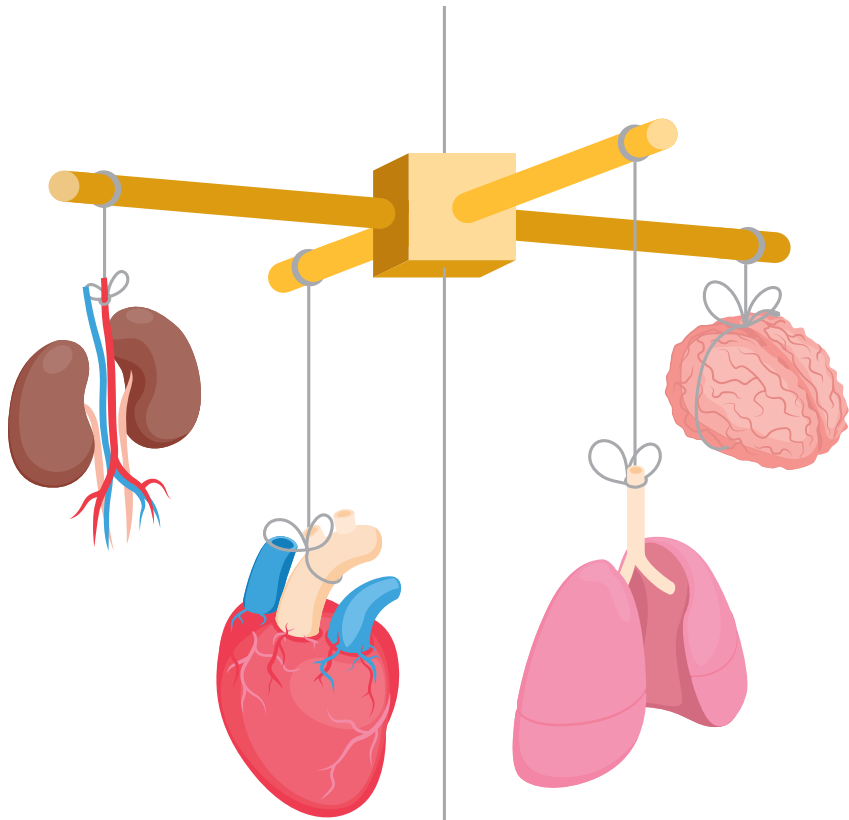
31. Mouchaers KT, Schalij I, Versteilen AM, Hadi AM, van Nieuw Amerongen GP, van Hinsbergh VW, Postmus PE, van der Laarse WJ, Vonk-Noordegraaf A (2009) Endothelin receptor blockade combined with phosphodiesterase-5 inhibition increases right ventricular mitochondrial capacity in pulmonary arterial hypertension. *Am J Physiol Heart Circ Physiol* 297:200–207. doi:10.1152/ajpheart.00893.2008
32. Murray JD (1974) On the role of myoglobin in muscle respiration. *J Theor Biol* 47:115–126. doi:10.1016/0022-5193(74)90102-7
33. O'Brien PJ, O'Grady M, McCutcheon LJ, Shen H, Nowack L, Horne RD, Mirsalimi SM, Julian RJ, Grima EA, Moe GW, Armstrong PW (1992) Myocardial myoglobin deficiency in various animal models of congestive heart failure. *J Mol Cell Cardiol* 24:721–730. doi:10.1016/0022-2828(92)93386-X
34. Pool CW, Scholten G, Diegenbach PC (1979) Quantitative succinate dehydrogenase histochemistry I. A methodological study on mammalian and fish muscle. *Histochemistry* 64:251–262. doi:10.1007/BF00495025
35. Puigserver P, Wu Z, Park CW, Graves R, Wright M, Spiegelman BM (1998) A cold-inducible coactivator of nuclear receptors linked to adaptive thermogenesis. *Cell* 92:829–839. doi:10.1016/S0092-8674(00)81410-5
36. Quinsay MN, Thomas RL, Lee Y, Gustafsson AB (2010) Bnip3-mediated mitochondrial autophagy is independent of the mitochondrial permeability transition pore. *Autophagy* 6:855–862. doi:10.4161/auto.6.7.13005
37. Redout EM, Wagner MJ, Zuidwijk MJ, Boer C, Musters RJ, van Hardevelde C, Paulus WJ, Simonides WS (2007) Right-ventricular failure is associated with increased mitochondrial complex II activity and production of reactive oxygen species. *Cardiovasc Res* 75:770–781. doi:10.1016/j.cardiores.2007.05.012
38. Regula KM (2002) Inducible expression of BNIP3 provokes mitochondrial defects and hypoxia-mediated cell death of ventricular myocytes. *Circ Res* 91:226–231. doi:10.1161/01.res.0000029232.42227.16
39. Ruiter G, Manders E, Happé CM, Schalij I, Groepenhoff H, Howard LS, Wilkins MR, Bogaard HJ, Westerhof N, van der Laarse WJ, de Man FS, Vonk-Noordegraaf A (2015) Intravenous iron therapy in patients with idiopathic pulmonary arterial hypertension and iron deficiency. *Pulm Circ* 5:466–472. doi:10.1086/682217
40. Ruiter G, Wong YY, de Man FS, Handoko LM, Jaspers RT, Postmus PE, Westerhof N, Niessen HWM, van der Laarse WJ, Vonk-Noordegraaf A (2013) Right ventricular oxygen supply parameters are decreased in human and experimental pulmonary hypertension. *J Heart Lung Transplant* 32:231–240. doi:10.1016/j.healun.2012.09.025
41. Rumsey WL, Schlosser C, Nuutinen EM, Robiolio M, Wilson DF (1990) Cellular energetics and the oxygen dependence of respiration in cardiac myocytes isolated from adult rat. *J Biol Chem* 265:15392–15402
42. Ruwhof C, Van Der Laarse A (2000) Mechanical stress-induced cardiac hypertrophy: mechanisms and signal transduction pathways. *Cardiovasc Res* 47:23–37. doi:10.1016/S0008-6363(00)00076-6
43. Sacheck JM, Ohtsuka A, McLary SC, Goldberg AL (2004) IGF-I stimulates muscle growth by suppressing protein breakdown and expression of atrophy-related ubiquitin ligases, atrogin-1 and MuRF1. *Am J Physiol Endocrinol Metab* 287:591–601. doi:10.1152/ajpendo.00073.2004

44. Sano M, Minamino T, Toko H, Miyauchi H, Orimo M, Qin Y, Akazawa H, Tateno K, Kayama Y, Harada M, Shimizu I, Asahara T, Hamada H, Tomita S, Molkentin JD, Zou Y, Komuro I (2007) p53-induced inhibition of Hif-1 causes cardiac dysfunction during pressure overload. *Nature* 446:444–448. doi:10.1038/nature05602
45. Schenkman KA, Marble DR, Burns DH, Feigl EO (1997) Myoglobin oxygen dissociation by multiwavelength spectroscopy. *J Appl Physiol* 82:86–92
46. Schlater AE, De Miranda MA, Frye MA, Trumble SJ, Kanatous SB (2014) Changing the paradigm for myoglobin: a novel link between lipids and myoglobin. *J Appl Physiol* 117:307–315. doi:10.1152/jappphysiol.00973.2013
47. Sernerl GG, Modesti PA, Boddi M, Cecioni I, Paniccia R, Coppo M, Galanti G, Simonetti I, Vanni S, Papa L, Bandinelli B, Migliorini A, Modesti A, Maccherini M, Sani G, Toscano M (1999) Cardiac growth factors in human hypertrophy. Relations with myocardial contractility and wall stress. *Circ Res* 85:57–67. doi:10.1161/01.RES.85.157
48. Shoag J, Arany Z (2010) Regulation of hypoxia-inducible genes by PGC-1 alpha. *Arterioscler Thromb Vasc Biol* 30:662–666. doi:10.1161/ATVBAHA.108.181636
49. Simonides WS, Mulcahey MA, Redout EM, Muller A, Zuidwijk MJ, Visser TJ, Wassen FW, Crescenzi A, da-Silva WS, Harney J, Engel FB, Obregon MJ, Larsen PR, Bianco AC, Huang SA (2008) Hypoxia-inducible factor induces local thyroid hormone inactivation during hypoxic-ischemic disease in rats. *J Clin Invest* 118:975–983. doi:10.1172/JCI32824
50. Sriram R, Kreutzer U, Shih L, Jue T (2008) Interaction of fatty acid with myoglobin. *FEBS Lett* 582:3643–3649. doi:10.1016/j.febslet.2008.09.047
51. Sutendra G, Dromparis P, Paulin R, Zervopoulos S, Haromy A, Nagendran J, Michelakis ED (2013) A metabolic remodeling in right ventricular hypertrophy is associated with decreased angiogenesis and a transition from a compensated to a decompensated state in pulmonary hypertension. *J Mol Med* 91:1315–1327. doi:10.1007/s00109-013-1059-4
52. Tang YD, Katz SD (2006) Anemia in chronic heart failure: prevalence, etiology, clinical correlates, and treatment options. *Circulation* 113:2454–2461. doi:10.1161/circulationaha.105.583666
53. van Beek-Harmsen BJ, Bekedam MA, Feenstra HM, Visser FC, van der Laarse WJ (2004) Determination of myoglobin concentration and oxidative capacity in cryostat sections of human and rat skeletal muscle fibres and rat cardiomyocytes. *Histochem Cell Biol* 121:335–342. doi:10.1007/s00418-004-0641-9
54. van Beek-Harmsen BJ, Feenstra HM, van der Laarse WJ (2011) Inadequate myocardial oxygen supply/demand in experimental pulmonary hypertension. In: Sulica R, Prestion I (eds) *Pulmonary hypertension—from bench research to clinical challenges*. InTechEurope, Rijeka, Croatia, pp. 151–166
55. van der Laarse WJ, des Tombe AL, van Beek-Harmsen BJ, Lee-de Groot MBE, Jaspers RT (2005) Krogh's diffusion coefficient for oxygen in isolated *Xenopus* skeletal muscle fibers and rat myocardial trabeculae at maximum rates of oxygen consumption. *J Appl Physiol* 99:2173–2180. doi:10.1152/jappphysiol.00470.2005
56. van der Laarse WJ, Diegenbach PC, Elzinga G (1989) Maximum rate of oxygen consumption and quantitative histochemistry of succinate dehydrogenase in single muscle fibres of *Xenopus laevis*. *J Muscle Res Cell Motil* 10:221–228
57. van Eif VW, Bogaards SJ, van der Laarse WJ (2014) Intrinsic cardiac adrenergic (ICA) cell density and MAO-A activity in failing rat hearts. *J Muscle Res Cell Motil* 35:47–53. doi:10.1007/s10974-013-9373-6

## CHAPTER 2

58. van Weel V, Deckers MM, Grimbergen JM, van Leuven KJ, Lardenoye JH, Schlingemann RO, van Nieuw Amerongen GP, van Bockel JH, van Hinsbergh VW, Quax PH (2004) Vascular endothelial growth factor overexpression in ischemic skeletal muscle enhances myoglobin expression in vivo. *Circ Res* 95:58–66. doi:10.1161/01.RES.0000133247.69803.c3
59. van Wessel T, de Haan A, van der Laarse WJ, Jaspers RT (2010) The muscle fiber type-fiber size paradox: hypertrophy or oxidative metabolism? *Eur J Appl Physiol* 110:665–694. doi:10.1007/s00421-010-1545-0
60. Vonk-Noordegraaf A, Haddad F, Chin KM, Forfia PR, Kawut SM, Lumens J, Naeije R, Newman J, Oudiz RJ, Provencher S, Torbicki A, Voelkel NF, Hassoun PM (2013) Right heart adaptation to pulmonary arterial hypertension. *J Am Coll Cardiol* 62:22–33. doi:10.1016/j.jacc.2013.10.027
61. Weeks KL, McMullen JR (2011) The Athlete's heart vs. the failing heart: can signaling explain the two distinct outcomes? *Physiology* 26:97–105. doi:10.1152/physiol.00043.2010
62. Witt CC, Witt SH, Lerche S, Labeit D, Back W, Labeit S (2008) Cooperative control of striated muscle mass and metabolism by MuRF1 and MuRF2. *EMBO J* 27:350–360. doi:10.1038/sj.emboj.7601952
63. Wittenberg BA, Wittenberg JB, Caldwell PR (1975) Role of myoglobin in the oxygen supply to red skeletal muscle. *J Biol Chem* 250:9038–9043
64. Wittenberg JB (2003) Myoglobin function reassessed. *J Exp Biol* 206:2011–2020. doi:10.1242/jeb.00243
65. Wong YY, Handoko ML, Mouchaers KT, de Man FS, Vonk-Noordegraaf A, van der Laarse WJ (2010) Reduced mechanical efficiency of rat papillary muscle related to degree of hypertrophy of cardiomyocytes. *Am J Physiol Heart Circ Physiol* 298:H1190–H1197. doi:10.1152/ajpheart.00773.2009





3

# **IGF-1 ATTENUATES HYPOXIA-INDUCED ATROPHY BUT INHIBITS MYOGLOBIN EXPRESSION IN C2C12 SKELETAL MUSCLE MYOTUBES**

---

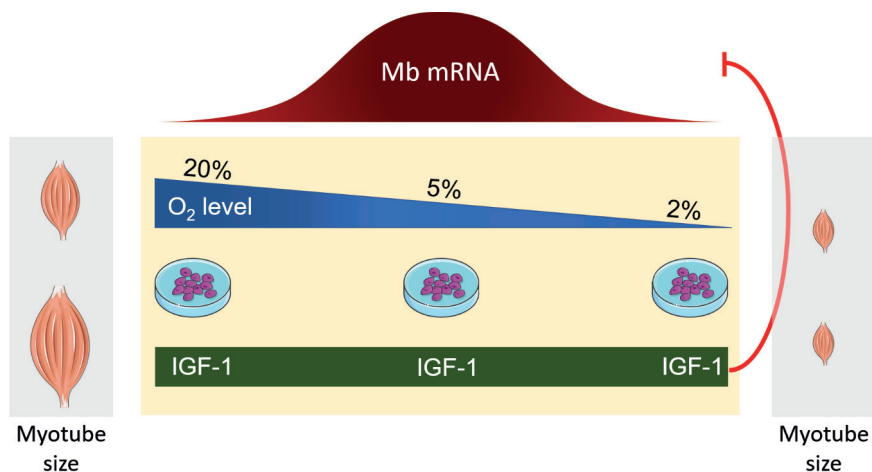
**Eva L. Peters**, Sandra M. van der Linde, Ilse S.P. Vogel, Mohammad Haroon, Carla Offringa, Gerard M.J. de Wit, Pieter Koolwijk, Willem J. van der Laarse, Richard T. Jaspers

*International Journal of Molecular Sciences*, 2017, 18 (9), p:1889

## Abstract

Chronic hypoxia is associated with muscle wasting and decreased oxidative capacity. By contrast, training under hypoxia may enhance hypertrophy and increase oxidative capacity as well as oxygen transport to the mitochondria, by increasing myoglobin (Mb) expression. The latter may be a feasible strategy to prevent atrophy under hypoxia and enhance an eventual hypertrophic response to anabolic stimulation. Mb expression may be further enhanced by lipid supplementation. We investigated individual and combined effects of hypoxia, insulin-like growth factor (IGF)-1 and lipids, in mouse skeletal muscle C2C12 myotubes. Differentiated C2C12 myotubes were cultured for 24h under 20%, 5% and 2% oxygen with or without IGF-1 and/or lipid treatment.

In culture under 20% oxygen, IGF-1 induced 51% hypertrophy. Hypertrophy was only 32% under 5% and abrogated under 2% oxygen. This was not explained by changes in expression of genes involved in contractile protein synthesis or degradation, suggesting a reduced rate of translation rather than of transcription. Myoglobin mRNA expression increased by 75% under 5% O<sub>2</sub> but decreased by 50% upon IGF-1 treatment under 20% O<sub>2</sub>, compared to control. Inhibition of mammalian target of rapamycin (mTOR) activation using rapamycin restored Mb mRNA expression to control levels. Lipid supplementation had no effect on Mb gene expression. Thus, IGF-1-induced anabolic signalling can be a strategy to improve muscle size under mild hypoxia, but lowers Mb gene expression.



## Introduction

Chronic diseases and aging are conditions associated with a loss in muscle mass and increased fatigability [1]. One of the contributing factors to the deterioration of skeletal muscle may be hypoxia and the chronic disease-associated effects resemble those that have been reported in humans after experimental exposure to chronic hypoxia [2-5]. Humans show decreased muscle fibre cross-sectional area, and constant or lower mitochondrial volume, the latter being indicative for a lower oxidative capacity [3, 6, 7]. Similar effects were observed in C2C12 mouse skeletal myotubes, engineered skeletal muscle tissue, and in rodents where exposure to hypoxia also reduced time to fatigue during treadmill running [8-15].

One potent way to increase muscle strength is resistance exercise. However, studies on resistance exercise under hypoxia showed contradictory effects. Whereas some showed a blunted hypertrophic response to training under hypoxia [12, 16, 17], others suggested that training under hypoxia may prevent atrophy and can even enhance hypertrophy and oxidative metabolism [2, 18-24]. Insulin-like growth factor (IGF)-1 is well known for its anabolic effects by activation of mammalian target of rapamycin (mTOR) and its downstream effector p70S6K [25], although it is currently unknown whether IGF-1 treatment can oppose hypoxia-induced skeletal muscle atrophy [26-28].

With hypertrophy, the diffusion distance for oxygen to the core of the cell increases and thereby imposes a size constraint on the muscle fibre [29-31]. Myoglobin (Mb) facilitates oxygen diffusion within the cell and serves as an oxygen buffer [32, 33]. In hypertrophied muscle fibres and cardiac myocytes working at  $VO_{2max}$ , increased intracellular oxygen transport via Mb is required to prevent hypoxic cell cores [30, 34]. Therefore, inadequate oxygen supply or hypoxia limits hypertrophy. Increasing Mb expression may thus serve as a strategy to prevent atrophy under hypoxia and enhance an eventual hypertrophic response to IGF-1 [5].

When hypoxia is combined with exercise, calcium activates calcineurin (CN) [35]. CN then dephosphorylates myocyte enhancer factor 2 (MEF2) and nuclear factor of activated T-cells (NFAT) to induce translocation of these transcription factors to the nucleus, and subsequent Mb gene transcription [36]. Indeed, the combination of hypoxia and exercise increased Mb expression in different animal models as well as in human [5, 35, 37, 38]. Activation of the Akt-mTOR pathway causes hyperphosphorylation of NFAT in C2C12 myotubes, which prevented nuclear entry of NFAT and blunted NFAT-c1 activation upon calcium ionophore treatment [26]. It is unclear, however, whether IGF-1-induced mTOR activation also prevents NFAT-induced Mb transcription.

## CHAPTER 3

A possible way to enhance Mb expression in a CN-NFAT independent manner could be lipid supplementation [39]. Indeed, supplementation of poly-unsaturated fatty acids (PUFA's) in patients with chronic obstructive pulmonary disease (COPD) and healthy rats showed marked improvements in exercise capacity [40-43]. In addition, lipid supplementation previously showed effects on genes involved in protein breakdown and mitochondrial biogenesis [44, 45]. Yet, no experimental studies were undertaken to investigate whether increased Mb expression via a CN-NFAT independent pathway, combined with a hypertrophic stimulus, has synergistic effects on muscle hypertrophy and oxidative capacity under hypoxia.

The aims of this study were therefore to investigate whether: 1) IGF-1 can attenuate hypoxia-induced atrophy, 2) IGF-1 inhibits Mb gene expression by hyperphosphorylation of NFAT and 3) increased Mb expression via a CN-NFAT independent pathway combined with IGF-1 treatment and hypoxia, has synergistic effects on myotube hypertrophy and its regulation. We hypothesized that IGF-1 antagonizes the atrophic effects of hypoxia in C2C12 myotubes but inhibits Mb gene transcription via mTOR-induced hyperphosphorylation of NFAT. Further, we expect that a CN-NFAT independent increase in Mb, induced by lipid supplementation, enhances the hypertrophic effects of IGF-1.

## Results

### Effects of hypoxia, IGF-1 and lipids on myotube size

Culturing for 24h under hypoxia caused a decrease in mean myotube diameter ( $p < 0.01$ ; Figures 1a, b) by 24% under 5%  $O_2$  and by 40% under 2%  $O_2$  compared to 20%  $O_2$ . Under 20%  $O_2$ , supplementation of IGF-1 increased myotube diameter by 51%. This increase was 32% under 5%  $O_2$  and hypertrophy was absent under 2%  $O_2$ , indicating that at lower oxygen tensions the hypertrophic response was attenuated and eventually blunted. Lipid supplementation had an overall hypertrophic effect ( $p = 0.04$ ) but did not enhance IGF-1-induced hypertrophy.

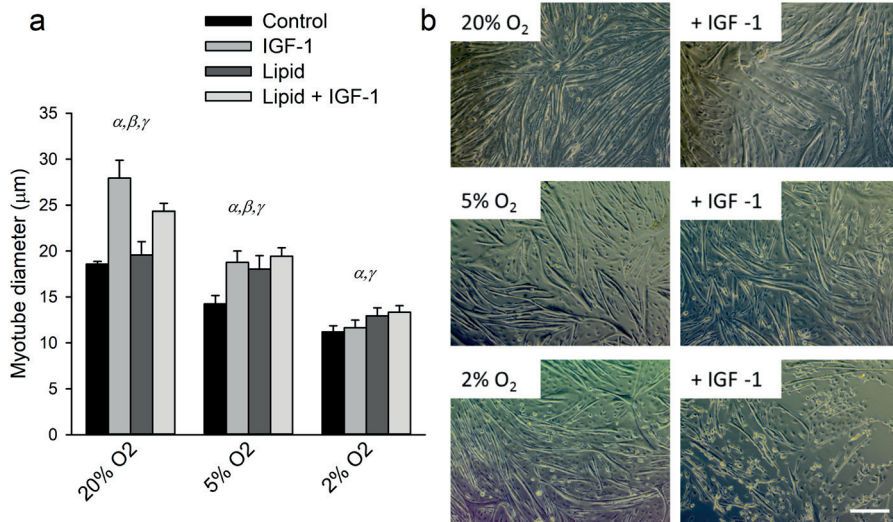


Figure 1 – **IGF-1 - induced hypertrophy is abrogated under hypoxia.** (a) Fibre diameter of myotubes cultured the last 24h of differentiation under different oxygen tensions, with and without supplementation of IGF-1 and lipid. (b) Representative photographs of control- and IGF-1 supplemented cells in all three oxygen tensions.  $\alpha$  = significant effect of oxygen tension compared to other O<sub>2</sub> tensions;  $\beta$  = significant effect of IGF-1 treatment within that specific oxygen tension;  $\gamma$  = significant overall effect of lipid supplementation. Values are given as mean  $\pm$  SEM, n=6. Scale bar represents 250  $\mu$ m

### Effects of hypoxia, IGF-1 and lipids on regulators of protein synthesis and degradation

Next, we looked further into the underlying mechanisms of hypoxia-induced atrophy and the blunted hypertrophic response to IGF-1. Surprisingly,  $\alpha$ -actin mRNA expression levels increased in hypoxia ( $p < 0.01$ ; Figure 2a), whereas IGF-1 had no effect on  $\alpha$ -actin mRNA expression ( $p = 0.37$ ). To explain this increase in  $\alpha$ -actin expression, we investigated mRNA expression levels of MyoD and myogenin, both involved in the regulation of contractile protein gene expression and activation of satellite cells. Both genes had lower expression levels following IGF-1 treatment in all three oxygen conditions ( $p < 0.01$  for both; Figures 2b,c). Also, oxygen had a significant main effect on MyoD and myogenin expression levels ( $p < 0.01$  for both) with expression levels of both being lower under 2% O<sub>2</sub> than those under 20% ( $p < 0.01$  and  $p < 0.05$ , respectively) and under 5% O<sub>2</sub> ( $p < 0.05$  and  $p < 0.01$ , respectively).

Muscle RING finger 1 (MuRF1) and Muscle atrophy F-box (MAFbx) expression levels decreased following IGF-1 treatment under all three oxygen conditions ( $p < 0.01$  and  $p < 0.05$ , respectively; Figures 2d,e), while neither MuRF1 nor MAFbx

expression levels were changed by lipid supplementation ( $p=0.24$  and  $p=0.64$  respectively). The interaction effect between IGF-1 supplementation and oxygen conditions ( $p<0.01$ ) revealed that, in absence of IGF-1, MAFbx mRNA expression levels increased under 5% compared to those under 20% O<sub>2</sub>, whereas they decreased under 2% O<sub>2</sub> when IGF-1 was added. In presence of IGF-1, MuRF1 mRNA expression levels under 5% and 2% O<sub>2</sub> were lower than those under 20% O<sub>2</sub> whereas this was not the case in the absence of IGF-1. These results suggest that protein degradation is at most slightly increased under hypoxia and strongly decreased upon IGF-1 supplementation.

### Effects of hypoxia, IGF-1 and lipids on regulators of metabolism

Figure 3 shows mRNA expression levels of genes related to oxidative- or glycolytic metabolism and myosin heavy chain types. Oxidative enzyme capacity as reflected by SDH mRNA expression was decreased under hypoxia in a dose dependent manner ( $p<0.001$ ; Figure 3a) whereas neither lipid supplementation ( $p=0.51$ ) nor IGF-1 treatment ( $p=0.50$ ) affected SDH mRNA expression levels.

Peroxisome proliferator-activated receptor-gamma coactivator (PGC)-1 $\alpha$  was also negatively affected by hypoxia ( $p<0.001$ ; Figure 3b). IGF-1 treatment caused a decrease in PGC-1 $\alpha$  mRNA expression levels in all three oxygen conditions ( $p<0.001$ ) whereas lipid supplementation had no effect on PGC-1 $\alpha$  mRNA expression levels ( $p=0.26$ ). Glyceraldehyde-3-phosphate dehydrogenase (GAPDH) was measured as a marker of glycolytic metabolism and was increased by lowering oxygen concentrations to 5% only ( $p<0.001$ ; Figure 3c). Both IGF-1 and lipid supplementation did not alter GAPDH mRNA expression levels ( $p=0.73$  and  $p=0.53$  respectively).

We further investigated whether these metabolic alterations coincided with myosin heavy chain (MHC) type switching. Compared to 20% O<sub>2</sub>, mRNA expression levels of slow, oxidative MHC type I increased almost four-fold under 5% O<sub>2</sub> ( $p<0.001$ ; Figure 3d) but decreased upon IGF-1 treatment and lipid supplementation ( $p<0.001$  for both). By contrast, mRNA expression levels of the fast, glycolytic MHC type IIB were increased by IGF-1 treatment ( $p<0.001$ ; Figure 3e). Relative to 20% O<sub>2</sub> MHC IIB mRNA expression levels were higher under 5% O<sub>2</sub> than under 2% O<sub>2</sub> ( $p<0.01$ ). In addition, lipid supplementation lowered MHC IIB expression ( $p<0.05$ ). These results indicate that lowering oxygen levels caused a reduction in oxidative metabolism and that IGF-1 likely favoured a shift towards glycolytic metabolism and expression of the fast MHC type IIB.

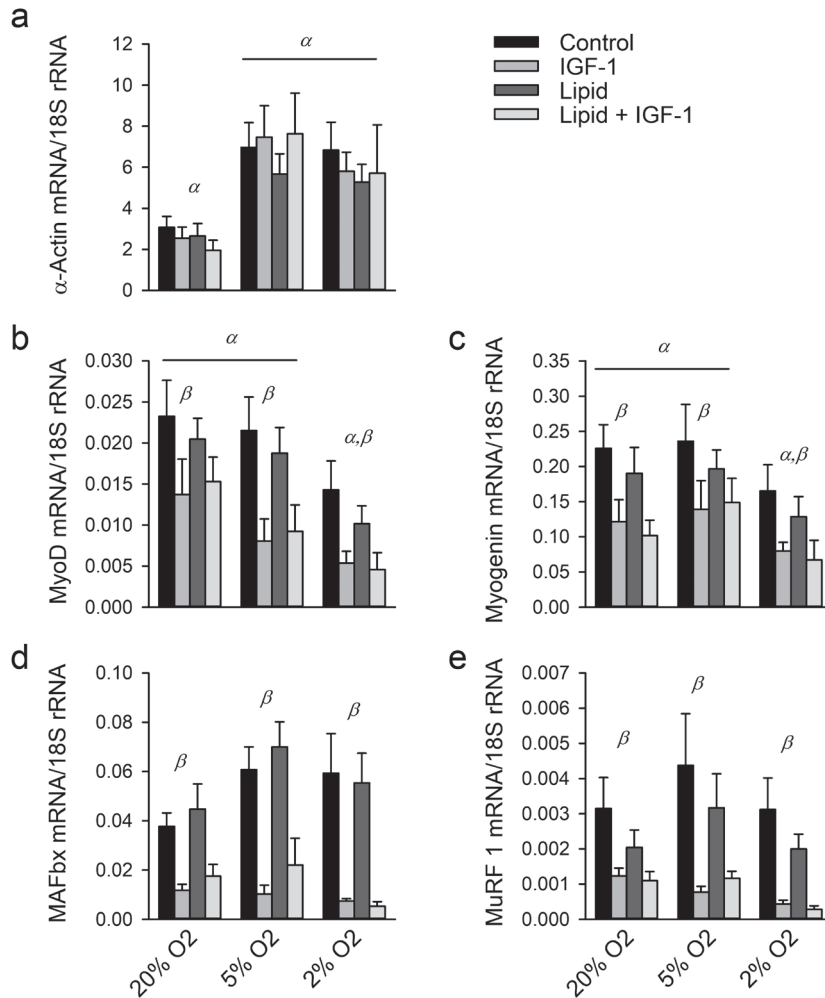


Figure 2 – **Regulators of protein synthesis are decreased under hypoxia and following IGF-1 supplementation whereas regulators of protein synthesis are only slightly increased under hypoxia.** (a) mRNA expression levels of  $\alpha$ -actin under different oxygen tensions, with and without 24h supplementation of IGF-1 and lipid. (b,c) mRNA expression levels of differentiation markers MyoD and myogenin. (d,e) mRNA expression levels of protein degradation markers MAFbx and MuRF1. Please note that the interaction for IGF-1 treatment with oxygen tension is not depicted.  $\alpha$  = significant effect of oxygen tension compared to other O<sub>2</sub> tensions denoted with  $\alpha$ ;  $\beta$  = significant overall effect of IGF-1 treatment;  $\gamma$  = significant overall effect of lipid supplementation. Although  $\beta$  and  $\gamma$  designate overall effects, symbols are placed above each oxygen tension for clarity. Values are given as mean  $\pm$  SEM, n=6.

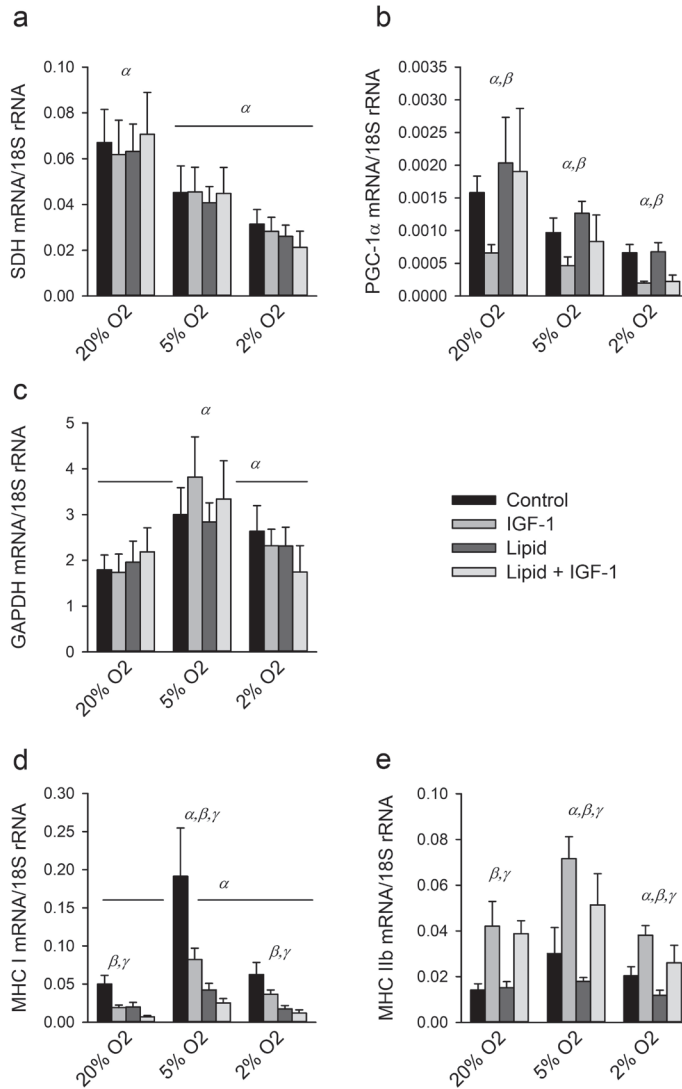


Figure 3 – Hypoxia likely causes a reduction in oxidative metabolism and a shift to more glycolytic metabolism. (a,b) mRNA expression levels of SDH and PGC-1 $\alpha$  for myotubes cultured the last 24h of differentiation under different oxygen tensions, with and without IGF-1 and lipid as markers of oxidative metabolism. (c) mRNA expression levels of GAPDH as marker of glycolytic metabolism. (d,e) mRNA expression levels of MHC I and -IIb were measured as markers for fibre type switching.  $\alpha$  = significant effect of oxygen tension compared to other O<sub>2</sub> tensions denoted with  $\alpha$ ;  $\beta$  = significant overall effect of IGF-1 treatment;  $\gamma$  = significant overall effect of lipid supplementation. Although  $\beta$  and  $\gamma$  designate overall effects, symbols are placed above each oxygen tension for clarity. Values are given as mean  $\pm$  SEM, n=6.

## Effects of hypoxia, IGF-1 and lipids on markers of oxygen transport

To investigate the effects of hypoxia, IGF-1 treatment and lipid supplementation on the regulation of oxygen supply to the cells, we investigated mRNA expression levels of vascular endothelial growth factor (VEGF) and Mb, as well as Mb protein expression as is shown in figure 4. VEGF expression levels increased under hypoxia ( $p < 0.001$ ; Figure 4a). IGF-1 treatment did not show any effect on VEGF expression levels ( $p = 0.19$ ) whereas lipid supplementation decreased VEGF expression levels ( $p < 0.001$ ).

Oxygen tension had a significant main effect on Mb mRNA expression levels ( $p < 0.001$ ; Figure 4b) which were increased under 5% O<sub>2</sub> compared to 20% ( $p < 0.001$ ). However, under 2% O<sub>2</sub>, expression levels of Mb mRNA did not significantly differ from those in 20% O<sub>2</sub> ( $p = 1.00$ ). Furthermore, upon IGF-1 treatment, Mb mRNA expression levels decreased in all three oxygen conditions ( $p < 0.001$ ). Lipid supplementation itself did not significantly increase Mb mRNA expression levels ( $p = 0.1$ ) and the absence of any significant interaction with IGF-1 indicates that lipid supplementation also could not prevent the IGF-1-induced decrease in Mb mRNA expression.

The Mb content was measured as absorbance using a calibrated histochemical method based on peroxidase activity [46]. Since absorbance measurements depend on the path length, we verified whether IGF-1-induced hypertrophy occurs equally in all radial directions. The increase in width did not differ from the increase in height ( $p = 0.34$ ). On average, upon IGF-1 treatment myotube width and height increased by 25% and 33%, respectively ( $p < 0.001$  for both; Figures 4 c,d). This suggests that IGF-1 induced myotube hypertrophy occurred uniformly in radial directions. Since absorbance due to Mb peroxidase activity is proportional to path length up to at least 16  $\mu\text{m}$ , Mb absorbance normalized by myotube diameter is taken as a measure of Mb concentration because Lambert-Beer's law applies [46].

Despite an increase in Mb mRNA expression levels in 5% O<sub>2</sub>, Mb content per myotube did not change in any of the oxygen conditions, nor due to IGF-1 treatment or lipid supplementation (results not shown,  $p = 0.33$ ,  $p = 0.35$  and  $p = 0.38$ , respectively). However, Mb concentration was higher under 2% O<sub>2</sub> compared to 5% and 20% O<sub>2</sub> ( $p < 0.01$ ) whereas IGF-1 and lipid supplementation showed no effects ( $p = 0.19$  and  $p = 0.93$ , respectively, Figure 4e).

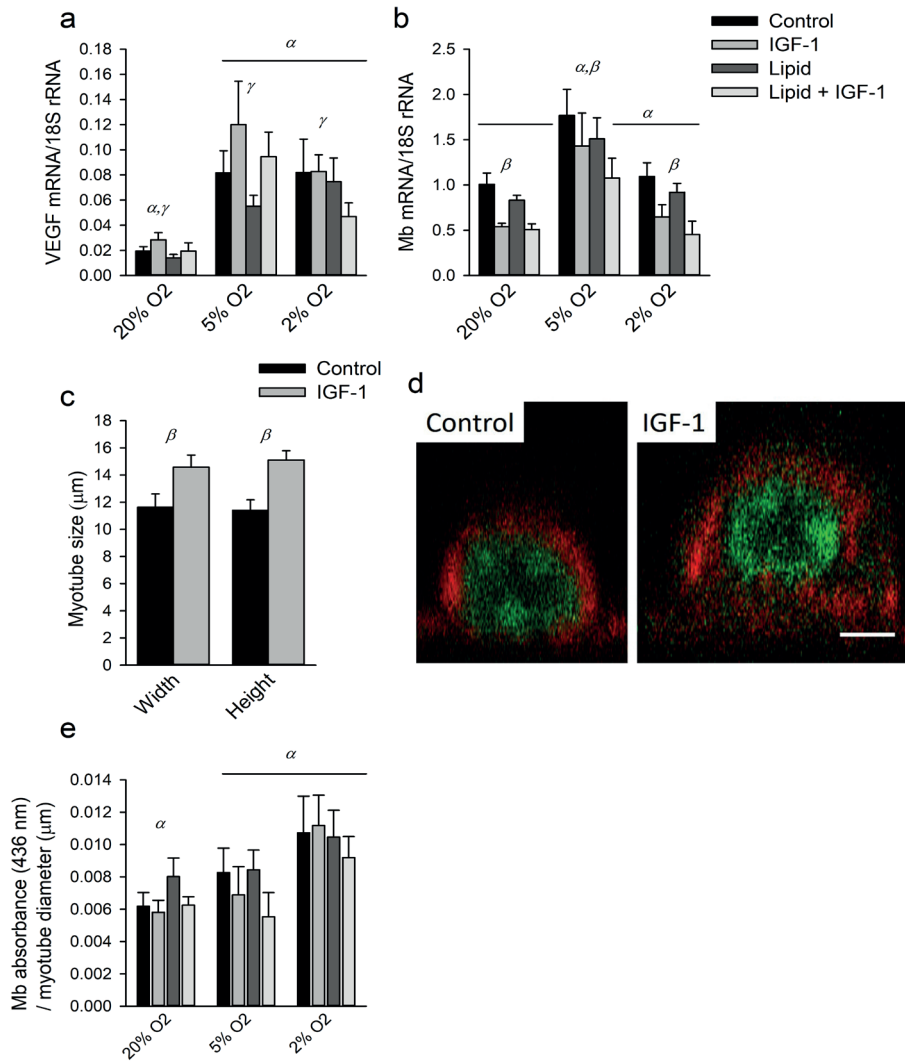


Figure 4 – IGF-1 lowers Mb mRNA expression but not Mb protein concentration in the cells. (a,b) mRNA expression levels of VEGF and Mb for myotubes cultured the last 24h of differentiation under different oxygen tensions, with and without IGF-1 and lipid. (c) In a separate experiment, height and width of myotubes was measured. n=20 myotubes. (d) Representative examples of cross-sections of individual myocytes live stained in red for F-actin and in green for DNA. Scale bar represents 5 µm. (e) Absorbance due to myoglobin peroxidase activity normalized by myotube diameter as a measure of concentration.  $\alpha$  = significant effect of oxygen tension compared to other O<sub>2</sub> tensions denoted with  $\alpha$ ;  $\beta$  = significant overall effect of IGF-1 treatment;  $\gamma$  = significant overall effect of lipid supplementation. Although  $\beta$  and  $\gamma$  designate an overall effect, for clarity symbols are placed above every oxygen tension. Values are given as mean  $\pm$  SEM, n=6.

### IGF-1 inhibits myoglobin mRNA expression via mTOR activation

To investigate whether the inhibition of Mb expression by IGF-1 was indeed caused by hyperphosphorylation of NFAT via mTOR, we inhibited IGF-1-induced mTOR signalling by rapamycin. Mb mRNA expression levels relative to control levels are shown in Figure 5. Both IGF-1 and rapamycin showed a significant main effect on Mb mRNA expression levels ( $p < 0.05$  for both). An interaction for IGF-1\*rapamycin ( $p < 0.05$ ) was present, indicative of the opposite effects of both treatments.

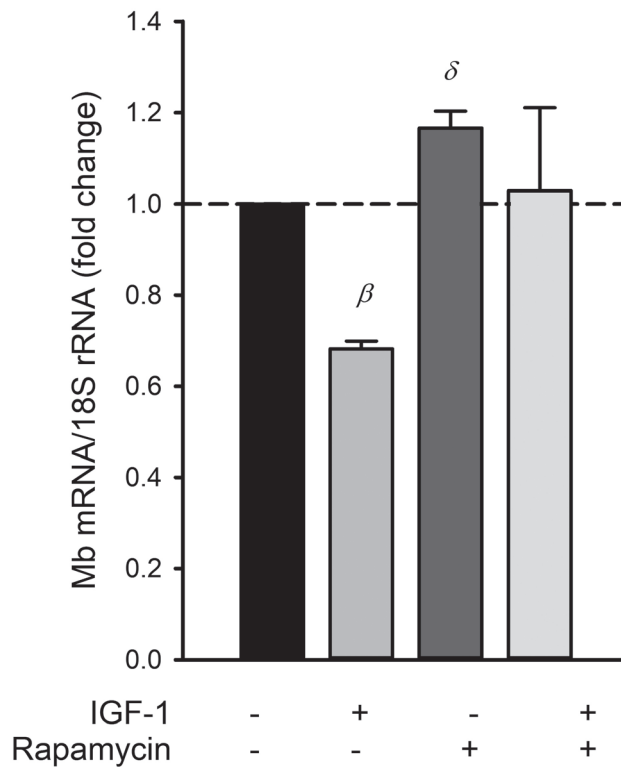


Figure 5 – **IGF-1 inhibits Mb mRNA expression, which can be restored by inhibition of mTOR.** Mb mRNA expression levels relative to control myotubes for myotubes treated for 24h with IGF-1, myotubes treated with rapamycin or a combination. Myotubes were cultured under 20% O<sub>2</sub>.  $\beta$  = significant effect of IGF-1 treatment,  $\gamma$  = significant effect of rapamycin treatment. Values are given as mean  $\pm$  SEM, n= 4.

## Discussion

As expected, myotube diameter decreased under hypoxia, as well as mRNA expression levels of SDH and its regulator PGC-1 $\alpha$ . Surprisingly, the decrease in diameter was accompanied by increased, rather than decreased,  $\alpha$ -actin mRNA expression levels. MyoD and myogenin are myogenic factors and mRNA expression of myogenin is related to  $\alpha$ -actin promoter activity [47]. We determined therefore mRNA expression levels of MyoD and myogenin to investigate regulation of protein synthesis at the transcriptional level, and showed a decrease under 2% but not under 5% O<sub>2</sub>, consistent with literature [48-50]. On the other hand, MAFbx mRNA expression levels increased only under 5% O<sub>2</sub> whereas MuRF1 mRNA expression levels remained unaltered, suggesting only a minor -if any- increase in protein degradation. Thus, mRNA expression levels of our markers for protein synthesis and degradation cannot explain why  $\alpha$ -actin mRNA expression levels were increased concomitant with the decrease in myotube diameter.

Alternatively, mRNA translation may be impaired under hypoxia. In vivo both in rat and human, contradictory results regarding the phosphorylation of Akt, mTOR and p70S6K have been reported [12, 51-53]. However, C2C12 myoblasts cultured under hypoxia showed reduced basal Akt-mTOR activation, as well as blunted IGF-1-induced Akt-mTOR activation [50]. Also, C2C12 myotubes cultured under 2% O<sub>2</sub> for 48 h showed lower IGF-1-induced phosphorylation of Akt, mTOR and p70S6K after 60 and 180 min of IGF-1 stimulation compared to normoxic controls. In addition, in engineered skeletal muscle constructs a reduction in p70S6K phosphorylation following 24h culture under 1% O<sub>2</sub> was shown recently [15]. These results indicate that the rate of translation is indeed inhibited by hypoxia [53, 54].

## IGF-1 induced hypertrophy is limited by hypoxia

We investigated whether IGF-1 can prevent hypoxia-induced atrophy. Although IGF-1 induced hypertrophy in myotubes cultured under 20% and 5% O<sub>2</sub>, the amount of hypertrophy under 5% O<sub>2</sub> was 80% of that under 20% O<sub>2</sub> and thereby only opposed the hypoxia-induced atrophy. In culture under 2% O<sub>2</sub>, atrophy was not prevented by IGF-1.

IGF-1 treatment markedly decreased MuRF1 and MAFbx mRNA expression levels under all three oxygen conditions, indicating that protein degradation was indeed decreased. Surprisingly, MyoD and myogenin mRNA expression levels also decreased following IGF-1 treatment whereas  $\alpha$ -actin mRNA expression levels remained unaffected by IGF-1. Although generally associated with myogenesis [55, 56], doses of IGF-1 similar to the present dose (13 nM) previously diminished myogenic protein expression in C2C12 myoblasts to almost undetectable levels 24h after plating from suspension whereas expression increased above control

72h after plating, also dependent on cell density [57]. Thus, the response of MyoD and myogenin to IGF-1 treatment may depend on timing and duration of the treatment and/or on local  $PO_2$ . Future investigations should reveal whether prolonged anabolic signalling in hypoxia can eventually induce hypertrophy.

### **IGF-1 inhibits myoglobin gene expression via activation of mTOR**

In C2C12 myotubes, IGF-1 has been shown to cause hyperphosphorylation of NFAT-c1 by mTOR and thereby IGF-1 prevented calcium ionophore-induced activation of NFAT-c1 [26]. Here, we show that IGF-1 treatment also lowers Mb mRNA expression levels. This is likely due to the hyperphosphorylation of NFAT by mTOR, since inhibition of mTOR by rapamycin increased Mb mRNA expression levels.

Despite decreased Mb mRNA expression levels following IGF-1 treatment, the Mb absorbance due to peroxidase activity was similar for all conditions. However, myotube diameter decreased under hypoxia. Assuming that myotube atrophy also occurred uniformly in all radial directions, we conclude that the concentration of Mb was increased under 2%  $O_2$ , as reflected by a higher Mb absorbance/diameter ratio. Thus, despite an increase in Mb mRNA expression under hypoxia the total content of Mb per unit of myotube length did not increase and the increase in concentration was only due to myotube atrophy.

### **Lipid supplementation does not increase myoglobin gene expression**

We hypothesized that Mb expression can be increased by lipid supplementation [39]. We found that lipid supplementation had no effect on either Mb mRNA or protein expression. Differences in timing and duration of the exposure may explain the discrepancy between present and previous results [39, 58]. Particularly in the study by Schlater et al. myotubes were cultured with lipid during 7 days of differentiation, whereas in our study lipids were present only for the last 24h of differentiation. Possibly, lipid supplementation primes skeletal muscle to enhance Mb expression, which would agree with previous findings in primary myotubes from Weddel seal [58]. In rats fed high-fat diets for 32 weeks, starting at 6 weeks of age, a positive effect on Mb expression was also observed indicating that lipid supplementation exerts its effect on Mb expression not only during myogenesis. It may be that the longer duration of supplementation explains the difference in results of the present study and of previous research [39, 58]. We conclude that one day of supplementation is not sufficient. However, lipid supplementation reduced VEGF mRNA expression. Since VEGF may induce Mb expression [59], lipid supplementation can have inhibited, rather than stimulated Mb expression via VEGF signalling.

## CHAPTER 3

It should be noted that some studies used albumin as a carrier for the uptake of fatty acids which could also explain the absence of lipid-induced Mb expression [44, 60]. However, the increase in Mb expression previously reported by Schlater et al. was found without addition of albumin to the culture medium. Also, we show an effect of lipid supplementation on myotube diameter and mRNA expression levels of VEGF and both MHC types, indicating that supplementation affected gene expression. It remains elusive whether lipid supplementation can induce fibre type switching and explain the effects of lipid supplementation in vivo.

We conclude that the hypertrophic response to IGF-1 is blunted under hypoxia. Although IGF-1 can attenuate hypoxia-induced atrophy of myotubes to a limited extent, it inhibits Mb mRNA expression. This cannot be circumvented following 24h of lipid supplementation.

## Materials and methods

### Cell culture and myotube analyses

C2C12 myotubes were grown for four days in Dulbecco's Modified Eagle's Media (DMEM, Life Technologies), supplemented with 10% foetal bovine serum (FBS, Thermo Scientific), 1% Penicillin/Streptomycin (PS, Life Technologies), and 0.5% fungizone (Life Technologies) and kept in a humidified incubator at 37°C, 5% CO<sub>2</sub>. Differentiation was induced at 60-70% confluency by changing the media to DMEM, supplemented with 2% horse serum (HS, GE Healthcare Life Sciences), 1% PS and 0.5% fungizone (Life Technologies), for four days. After 3 days of differentiation, myotubes were cultured for 24 hours under different oxygen tensions (20%, 5% or 2% O<sub>2</sub>) using a custom designed hypoxia workstation as described before [61]. Myotubes were cultured in either differentiation medium, or in medium supplemented with IGF-1 (100 ng/ml, Peprotech), a mixture of lipids (5% lipid-supplemented media [2 µg/ml arachidonic acid, 10 µg/ml each of linoleic, linolenic, myristic, oleic, palmitic and stearic fatty acids], Sigma), or a combination thereof. Rapamycin (2 ng/ml, Bioaustralis) was added one hour prior to IGF-1 treatment and in 20% oxygen conditions only.

Four photographs of each well were taken at 10x magnification after the 24h treatment. Diameters were measured in 20 myotubes (5 in each image) at 5 equidistant locations along the length of the cell using ImageJ (<http://rsbweb.nih.gov/ij/>) and taking into account the pixel-to-aspect ratio.

### Live cell imaging

To assess whether IGF-1-induced hypertrophy was equal in all radial directions C2C12 myotubes were cultured in 8-wells Ibidi-treated plates (Ibidi) as described above and either or not treated with IGF-1 for 24h. Myotubes were stained in red for F-actin filaments using Sir-Actin (0.62-2.5  $\mu$ M, Cytoskeleton, Inc.) and in green for the nucleus using Syto-9 (200nM, Thermo Scientific). Both stains were incubated for 4 hours. Verapamil (10  $\mu$ M, Cytoskeleton, Inc.) was added to prevent excretion of the staining by the myotubes. Images were captured using a SP8 STED microscope (Leica microsystems GmbH). 3D reconstructions were created from Z-stacks with 0.3  $\mu$ m spacing. Height and width of the cells were measured in about 20 myotubes in each condition using The Medical Imaging Interaction Toolkit (MITK, <http://www.mitk.org>) at 5 equidistant locations along the length of the myotubes.

### Myoglobin concentration

After culture, while remaining adhered to culture discs, myotubes were fixed for 10 minutes using glutaraldehyde (Sigma) [62] and subsequently incubated for 60 minutes in a buffer with O-tolidine (Sigma) and T-butylhydroperoxide (Fluka Chemie) [62]. Images were taken at 5x magnification (Leica DMRB). Absorbance was measured at 436 nm. The method was validated using gelatine sections containing known concentrations of horse myoglobin [46]. For each condition 20 myotubes were measured as described above.

### Quantitative polymerase chain reaction (qPCR)

Cells were harvested for RNA isolation in TRIreagent (Life Technologies) and stored at -80 °C. RNA was isolated using RiboPureTMkit (Applied Biosystems) and converted to cDNA with high-capacity RNA to cDNA master mix (Applied Biosystems). cDNA was diluted 10x and stored at -20 °C until further use. For each gene target 5  $\mu$ l of cDNA was amplified in duplicate using Fast SYBR Green Mastermix (Applied Biosystems) on a StepOne Real-Time PCR system (Applied Biosystems). Primers are listed in table 1. Mean cycle thresholds were converted to relative expressions by subtraction of the 18S rRNA cycle threshold and determination of  $2^{-\Delta C_t}$  [63].

### Statistical analysis

Three-way ANOVA was performed with factors oxygen tension, IGF-1 and lipid supplementation. Normality of the data was checked using Shapiro-Wilk tests. In case of non-normality ANOVA was performed on logarithmic transformed data. Equality of variances was verified using Levene's test. Significant main effects were

## CHAPTER 3

further investigated using Bonferroni multiple comparisons. Significant interaction effects were followed-up by one-way ANOVA using Bonferroni correction. Values are given as mean  $\pm$  standard error of the mean (SEM);  $p < 0.05$  was considered statistically significant. Unless stated otherwise  $n = 6$ .

## Acknowledgements

Mohammad Haroon was funded by the European Commission through MOVE-AGE, an Erasmus Mundus Joint Doctorate Program (2011-0015). The authors would like to thank Jeroen Kole and René J.P. Musters for excellent help with live cell imaging.

Table 1 – **Primers used for PCR analysis.** *GAPDH* = glyceraldehyde-3-phosphate dehydrogenase, *MAFbx* = muscle atrophy F-box, *Mb* = Myoglobin, *MHC* = Myosin Heavy Chain, *MuRF1* = muscle RING finger 1, *PGC-1 $\alpha$*  = peroxisome proliferator-activated-gamma coactivator - 1 $\alpha$ , *SDH* = succinate dehydrogenase; *VEGF* = vascular endothelial growth factor.

Target mRNA	Forward	Reverse
18S	GTAACCCGTTGAACCCCAT	CCATCCAATCGGTAGTAGCG
GAPDH	TGAAGCAGGCATCTGAGGG	CGAAGGTGGAAGAGTGGGAG
MAFbx	AGACTGGACTTCTCGACTGC	TCAGCTCCAACAGCCTTACT
Mb	GGAAGTCCTCATCGGTCTGT	GCCCTTCATATCTTCCTCTGA
MHC I	AGATCCGAAAGCAACTGGAG	CTGCCTTGATCTGTTGAAC
MHC IIB	CAACTGAGTGAAGTGAAGACC	AGCTGAGAAACCATAGCGTC
MuRF1	GGGCTACCTTCTCTCAAGTGC	CGTCCAGAGCGTGTCTCACTC
MyoD	AGCACTACAGTGGCGACTCA	GCTCCACTATGCTGGACAGG
Myogenin	CCCAACCCAGGAGATCATT	GTCTGGGAAGGCAACAGACA
PGC-1 $\alpha$	ACACAACCCGAGTCGCAACA	GGGAACCCCTTGGGGTCAATTTGG
SDH	GTCAGGAGCCAAAATGGCG	CGACAGGCCTGAACTGC
$\alpha$ -Actin	GGCCAGAGTCAGAGCAGCAGAAAC	CACCAGGCCAGAGCCGTTGT
VEGF	CTGTAACGATGAAGCCCTGGAGTG	GGTGAGGTTTGATCCGCATGATCT

## Supplementary materials

Supplementary materials can be found at [www.mdpi.com/1422-0067/18/9/1889/s1](http://www.mdpi.com/1422-0067/18/9/1889/s1)

## References

1. Moylan, J. S.; Reid, M. B., Oxidative stress, chronic disease, and muscle wasting. *Muscle Nerve* **2007**, 35, (4), 411-429, 10.1002/mus.20743.
2. Bigard, A. X.; Brunet, A.; Guezennec, C. Y.; Monod, H., Skeletal muscle changes after endurance training at high altitude. *J Appl Physiol* **1991**, 71, (6), 2114-2121.
3. Hoppeler, H.; Kleinert, E.; Schlegel, C.; Claassen, H.; Howald, H.; Kayar, S. R.; Cerretelli, P., Morphological adaptations of human skeletal muscle to chronic hypoxia. *Int J Sports Med* **1990**, 11 Suppl 1, S3-9, 10.1055/s-2007-1024846.
4. Green, H. J.; Sutton, J. R.; Cymerman, A.; Young, P. M.; Houston, C. S., Operation Everest II: adaptations in human skeletal muscle. *J Appl Physiol (1985)* **1989**, 66, (5), 2454-61.
5. Jaspers, R. T.; Testerink, J.; Della Gaspera, B.; Chanoine, C.; Bagowski, C. P.; van der Laarse, W. J., Increased oxidative metabolism and myoglobin expression in zebrafish muscle during chronic hypoxia. *Biol Open* **2014**, 3, (8), 718-727, 10.1242/bio.20149167.
6. MacDougall, J. D.; Green, H. J.; Sutton, J. R.; Coates, G.; Cymerman, A.; Young, P.; Houston, C. S., Operation Everest II: structural adaptations in skeletal muscle in response to extreme simulated altitude. *Acta Physiol Scand* **1991**, 142, (3), 421-427, 10.1111/j.1748-1716.1991.tb09176.x.
7. Howald, H.; Pette, D.; Simoneau, J. A.; Uber, A.; Hoppeler, H.; Cerretelli, P., Effect of chronic hypoxia on muscle enzyme activities. *Int J Sports Med* **1990**, 11 Suppl 1, S10-4, 10.1055/s-2007-1024847.
8. Elliott, B. The role of acute ambient hypoxia in the regulation of myostatin. Doctoral thesis, University of Westminster, 2015.
9. Slot, I. G.; Schols, A. M.; Vosse, B. A.; Kelders, M. C.; Gosker, H. R., Hypoxia differentially regulates muscle oxidative fiber type and metabolism in a HIF-1alpha-dependent manner. *Cell Signal* **2014**, 26, (9), 1837-1845, 10.1016/j.cellsig.2014.04.016.
10. Li, W.; Hu, Z. F.; Chen, B.; Ni, G. X., Response of C2C12 myoblasts to hypoxia: the relative roles of glucose and oxygen in adaptive cellular metabolism. *Biomed Res Int* **2013**, 2013, 326346, 10.1155/2013/326346.
11. Wüst, R. C.; Jaspers, R. T.; van Heijst, A. F.; Hopman, M. T.; Hoofd, L. J.; van der Laarse, W. J.; Degens, H., Region-specific adaptations in determinants of rat skeletal muscle oxygenation to chronic hypoxia. *Am J Physiol Heart Circ Physiol* **2009**, 297, (1), H364-74, 10.1152/ajpheart.00272.2009.
12. Chaillou, T.; Koulmann, N.; Simler, N.; Meunier, A.; Serrurier, B.; Chapot, R.; Peinnequin, A.; Beaudry, M.; Bigard, X., Hypoxia transiently affects skeletal muscle hypertrophy in a functional overload model. *Am J Physiol Regul Integr Comp Physiol* **2012**, 302, (5), R643-54, 10.1152/ajpregu.00262.2011.
13. Chaudhary, P.; Suryakumar, G.; Prasad, R.; Singh, S. N.; Ali, S.; Ilavazhagan, G., Chronic hypobaric hypoxia mediated skeletal muscle atrophy: role of ubiquitin-proteasome pathway and calpains. *Mol Cell Biochem* **2012**, 364, (1-2), 101-113, 10.1007/s11010-011-1210-x.
14. Abdelmalki, A.; Fimbel, S.; Mayet-Sornay, M. H.; Sempore, B.; Favier, R., Aerobic capacity and skeletal muscle properties of normoxic and hypoxic rats in response to training. *Pflügers Archiv* **1996**, 431, (5), 671-679, 10.1007/bf02253829.
15. Martin, N. R. W.; Aguilar-Agon, K.; Robinson, G. P.; Player, D. J.; Turner, M. C.; Myers, S. D.; Lewis, M. P., Hypoxia Impairs Muscle Function and Reduces Myotube Size in Tissue Engineered Skeletal Muscle. *Journal of Cellular Biochemistry* **2017**, n/a-n/a, 10.1002/jcb.25982.

## CHAPTER 3

16. Etheridge, T.; Atherton, P. J.; Wilkinson, D.; Selby, A.; Rankin, D.; Webborn, N.; Smith, K.; Watt, P. W., Effects of hypoxia on muscle protein synthesis and anabolic signaling at rest and in response to acute resistance exercise. *Am J Physiol Endocrinol Metab* **2011**, 301, (4), E697-702, 10.1152/ajpendo.00276.2011.
17. Narici, M. V.; Kayser, B., Hypertrophic response of human skeletal muscle to strength training in hypoxia and normoxia. *Eur J Appl Physiol Occup Physiol* **1995**, 70, (3), 213-219, 10.1007/BF00238566.
18. Desplanches, D.; Hoppeler, H.; Linossier, M. T.; Denis, C.; Claassen, H.; Dormois, D.; Lacour, J. R.; Geyssant, A., Effects of training in normoxia and normobaric hypoxia on human muscle ultrastructure. *Pflügers Archiv* **1993**, 425, (3-4), 263-267, 10.1007/bf00374176.
19. Dufour, S. P.; Ponsot, E.; Zoll, J.; Doutreleau, S.; Lonsdorfer-Wolf, E.; Geny, B.; Lampert, E.; Flück, M.; Hoppeler, H.; Billat, V.; Mettaufer, B.; Richard, R.; Lonsdorfer, J., Exercise training in normobaric hypoxia in endurance runners. I. Improvement in aerobic performance capacity. *J Appl Physiol* **2006**, 100, (4), 1238-1248, 10.1152/jappphysiol.00742.2005.
20. Zoll, J.; Ponsot, E.; Dufour, S.; Doutreleau, S.; Ventura-Clapier, R.; Vogt, M.; Hoppeler, H.; Richard, R.; Fluck, M., Exercise training in normobaric hypoxia in endurance runners. III. Muscular adjustments of selected gene transcripts. *J Appl Physiol* **2006**, 100, (4), 1258-1266, 10.1152/jappphysiol.00359.2005.
21. Scott, B. R.; Slattery, K. M.; Sculley, D. V.; Dascombe, B. J., Hypoxia and resistance exercise: a comparison of localized and systemic methods. *Sports Med* **2014**, 44, (8), 1037-1054, 10.1007/s40279-014-0177-7.
22. Scott, B. R.; Loenneke, J. P.; Slattery, K. M.; Dascombe, B. J., Blood flow restricted exercise for athletes: A review of available evidence. *J Sci Med Sport* **2016**, 19, (5), 360-367, 10.1016/j.jsams.2015.04.014.
23. Abe, T.; Kearns, C. F.; Sato, Y., Muscle size and strength are increased following walk training with restricted venous blood flow from the leg muscle, Kaatsu-walk training. *J Appl Physiol* **2006**, 100, (5), 1460-1466, 10.1152/jappphysiol.01267.2005.
24. Fujita, S.; Abe, T.; Drummond, M. J.; Cadenas, J. G.; Dreyer, H. C.; Sato, Y.; Volpi, E.; Rasmussen, B. B., Blood flow restriction during low-intensity resistance exercise increases S6K1 phosphorylation and muscle protein synthesis. *J Appl Physiol* **2007**, 103, (3), 903-910, 10.1152/jappphysiol.00195.2007.
25. Burnett, P. E.; Barrow, R. K.; Cohen, N. A.; Snyder, S. H.; Sabatini, D. M., RAFT1 phosphorylation of the translational regulators p70 S6 kinase and 4E-BP1. *Proc Natl Acad Sci U S A* **1998**, 95, (4), 1432-7.
26. Rommel, C.; Bodine, S. C.; Clarke, B. A.; Rossman, R.; Nunez, L.; Stitt, T. N.; Yancopoulos, G. D.; Glass, D. J., Mediation of IGF-1-induced skeletal myotube hypertrophy by PI(3)K/Akt/mTOR and PI(3)K/Akt/GSK3 pathways. *Nat Cell Biol* **2001**, 3, (11), 1009-1013, 10.1038/ncb1101-1009.
27. Glass, D. J., Skeletal muscle hypertrophy and atrophy signaling pathways. *Int J Biochem Cell Biol* **2005**, 37, (10), 1974-1984, <http://dx.doi.org/10.1016/j.biocel.2005.04.018>.
28. Bodine, S. C.; Stitt, T. N.; Gonzalez, M.; Kline, W. O.; Stover, G. L.; Bauerlein, R.; Zlotchenko, E.; Scrimgeour, A.; Lawrence, J. C.; Glass, D. J.; Yancopoulos, G. D., Akt/mTOR pathway is a crucial regulator of skeletal muscle hypertrophy and can prevent muscle atrophy in vivo. *Nat Cell Biol* **2001**, 3, (11), 1014-1019, 10.1038/ncb1101-1014.
29. van der Laarse, W. J.; des Tombe, A. L.; Lee-de Groot, M. B. E.; Diegenbach, P. C., Size principle of striated muscle cells. *Neth J Zool* **1998**, 48, (3), 213-223, 10.1163/156854298X00075.

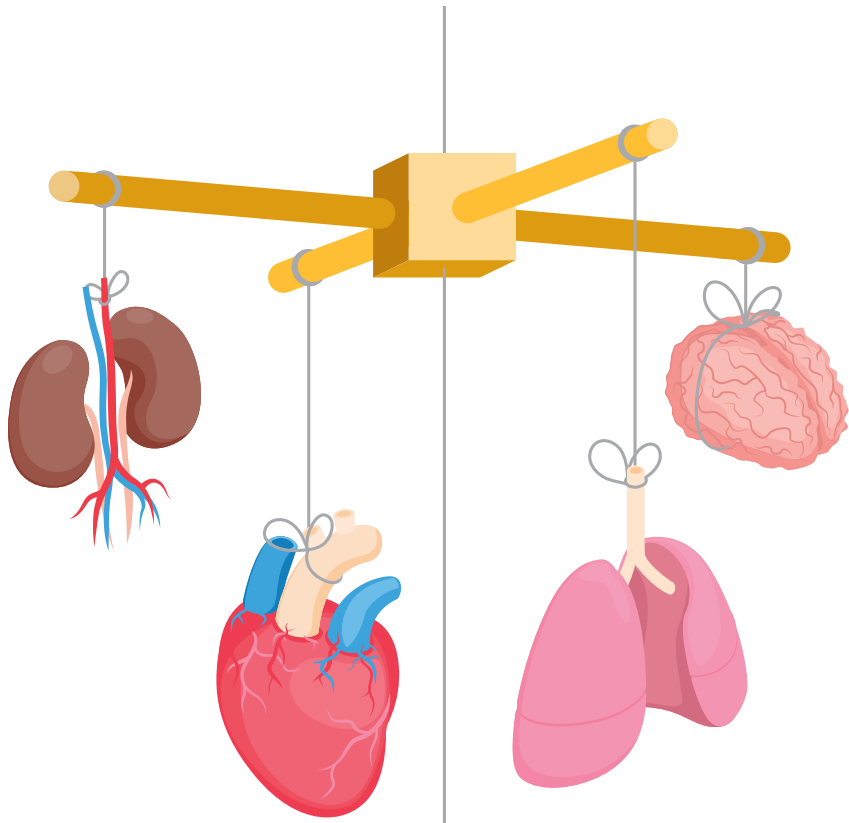
30. van Wessel, T.; de Haan, A.; van der Laarse, W. J.; Jaspers, R. T., The muscle fiber type-fiber size paradox: hypertrophy or oxidative metabolism? *Eur J Appl Physiol* **2010**, 110, (4), 665-694, 10.1007/s00421-010-1545-0.
31. Van der Laarse, W. J.; Diegenbach, P. C.; Elzinga, G., Maximum rate of oxygen consumption and quantitative histochemistry of succinate-dehydrogenase in single muscle fibers of *Xenopus Laevis*. *Journal of Muscle Research and Cell Motility* **1989**, 10, (3), 221-228, 10.1007/BF01739812.
32. Wittenberg, B. A.; Wittenberg, J. B., Myoglobin-mediated oxygen delivery to mitochondria of isolated cardiac myocytes. *Proc Natl Acad Sci USA* **1987**, 84, (21), 7503-7507.
33. Wittenberg, B. A.; Wittenberg, J. B.; Caldwell, P. R., Role of myoglobin in the oxygen supply to red skeletal muscle. *J Biol Chem* **1975**, 250, (23), 9038-9043.
34. Peters, E. L.; Offringa, C.; Kos, D.; Van der Laarse, W. J.; Jaspers, R. T., Regulation of myoglobin in hypertrophied rat cardiomyocytes in experimental pulmonary hypertension. *Pflugers Arch* **2016**, 468, (10), 1697-1707, 10.1007/s00424-016-1865-y.
35. Kanatous, S. B.; Mammen, P. P. A.; Rosenberg, P. B.; Martin, C. M.; White, M. D.; DiMaio, J. M.; Huang, G.; Muallem, S.; Garry, D. J., Hypoxia reprograms calcium signaling and regulates myoglobin expression. *Am J Physiol Cell Physiol* **2008**, 296, (3), C393-C402, 10.1152/ajpcell.00428.2008.
36. Kanatous, S. B.; Mammen, P. P. A., Regulation of myoglobin expression. *J Exp Biol* **2010**, 213, (16), 2741-2747, 10.1242/jeb.041442.
37. Vogt, M.; A., P.; Geiser, J.; Zuleger, C.; Billeter, R.; Hoppeler, H., Molecular adaptations in human skeletal muscle to endurance training under simulated hypoxic conditions. *J Appl Physiol* **2001**, 91, 173-182.
38. Terrados, N.; Jansson, E.; Sylven, C.; Kaijser, L., Is hypoxia a stimulus for synthesis of oxidative enzymes and myoglobin? *J Appl Physiol* **1990**, 68, (6), 2369-2372.
39. Schlater, A. E.; De Miranda, M. A.; Frye, M. A.; Trumble, S. J.; Kanatous, S. B., Changing the paradigm for myoglobin: a novel link between lipids and myoglobin. *J Appl Physiol* **2014**, 117, (3), 307-315, 10.1152/jappphysiol.00973.2013.
40. Broekhuizen, R.; Wouters, E. F.; Creutzberg, E. C.; Weling-Scheepers, C. A.; Schols, A. M., Polyunsaturated fatty acids improve exercise capacity in chronic obstructive pulmonary disease. *Thorax* **2005**, 60, (5), 376-382, 10.1136/thx.2004.030858.
41. Peoples, G. E.; McLennan, P. L., Dietary fish oil reduces skeletal muscle oxygen consumption, provides fatigue resistance and improves contractile recovery in the rat in vivo hindlimb. *Br J Nutr* **2010**, 104, (12), 1771-1779, doi:10.1017/S0007114510002928.
42. Peoples, G. E.; McLennan, P. L., Long-chain n-3 DHA reduces the extent of skeletal muscle fatigue in the rat in vivo hindlimb model. *Br J Nutr* **2014**, 111, (6), 996-1003, 10.1017/S0007114513003449.
43. Henry, R.; Peoples, G. E.; McLennan, P. L., Muscle fatigue resistance in the rat hindlimb in vivo from low dietary intakes of tuna fish oil that selectively increase phospholipid n-3 docosahexaenoic acid according to muscle fibre type. *Br J Nutr* **2015**, 114, (6), 873-884, 10.1017/S0007114515002512.
44. Huang, F.; Wei, H.; Luo, H.; Jiang, S.; Peng, J., EPA inhibits the inhibitor of kappaB alpha/NF-kappaB/muscle RING finger 1 pathway in C2C12 myotubes in a PPARgamma-dependent manner. *Br J Nutr* **2011**, 105, (3), 348-356, 10.1017/s0007114510003703.

## CHAPTER 3

45. Garcia-Roves, P.; Huss, J. M.; Han, D.-H.; Hancock, C. R.; Iglesias-Gutierrez, E.; Chen, M.; Holloszy, J. O., Raising plasma fatty acid concentration induces increased biogenesis of mitochondria in skeletal muscle. *Proc Natl Acad Sci U S A* **2007**, 104, (25), 10709-10713, 10.1073/pnas.0704024104.
46. Lee-de Groot, M. B. E.; des Tombe, A. L.; van der Laarse, W. J., Calibrated histochemistry of myoglobin concentration in cardiomyocytes. *Journal of Histochemistry & Cytochemistry* **1998**, 46, (9), 1077-1084, <https://doi.org/10.1177/002215549804600912>.
47. Marsh, D. R.; Carson, J. A.; Stewart, L. N.; Booth, F. W., Activation of the skeletal alpha-actin promoter during muscle regeneration. *J Muscle Res Cell Motil* **1998**, 19, (8), 897-907.
48. Di Carlo, A.; De Mori, R.; Martelli, F.; Pompilio, G.; Capogrossi, M. C.; Germani, A., Hypoxia inhibits myogenic differentiation through accelerated MyoD degradation. *J Biol Chem* **2004**, 279, (16), 16332-16338, 10.1074/jbc.M313931200.
49. Yun, Z.; Lin, Q.; Giaccia, A. J., Adaptive myogenesis under hypoxia. *Mol Cell Biol* **2005**, 25, (8), 3040-3055, 10.1128/mcb.25.8.3040-3055.2005.
50. Ren, H.; Accili, D.; Duan, C., Hypoxia converts the myogenic action of insulin-like growth factors into mitogenic action by differentially regulating multiple signaling pathways. *Proc Natl Acad Sci USA* **2010**, 107, (13), 5857-5862, 10.1073/pnas.0909570107.
51. de Theije, C. C.; Langen, R. C.; Lamers, W. H.; Schols, A. M.; Kohler, S. E., Distinct responses of protein turnover regulatory pathways in hypoxia- and semistarvation-induced muscle atrophy. *Am J Physiol Lung Cell Mol Physiol* **2013**, 305, (1), L82-91, 10.1152/ajplung.00354.2012.
52. Favier, F. B.; Costes, F.; Defour, A.; Bonnefoy, R.; Lefai, E.; Bauge, S.; Peinnequin, A.; Benoit, H.; Freyssenet, D., Downregulation of Akt/mammalian target of rapamycin pathway in skeletal muscle is associated with increased REDD1 expression in response to chronic hypoxia. *Am J Physiol Regul Integr Comp Physiol* **2010**, 298, (6), R1659-66, 10.1152/ajpregu.00550.2009.
53. Costes, F.; Gosker, H.; Feasson, L.; Desgeorges, M.; Kelders, M.; Castells, J.; Schols, A.; Freyssenet, D., Impaired exercise training-induced muscle fiber hypertrophy and Akt/mTOR pathway activation in hypoxemic patients with COPD. *J Appl Physiol (1985)* **2015**, 118, (8), 1040-9, 10.1152/jappphysiol.00557.2014.
54. Arthur, P. G.; Giles, J. J.; Wakeford, C. M., Protein synthesis during oxygen conformance and severe hypoxia in the mouse muscle cell line C2C12. *Biochim Biophys Acta* **2000**, 1475, (1), 83-89.
55. Rosenthal, S. M.; Cheng, Z. Q., Opposing early and late effects of insulin-like growth factor I on differentiation and the cell cycle regulatory retinoblastoma protein in skeletal myoblasts. *Proc Natl Acad Sci USA* **1995**, 92, (22), 10307-11.
56. Miyake, M.; Hayashi, S.; Sato, T.; Taketa, Y.; Watanabe, K.; Hayashi, S.; Tanaka, S.; Ohwada, S.; Aso, H.; Yamaguchi, T., Myostatin and MyoD family expression in skeletal muscle of IGF-1 knockout mice. *Cell Biol Int* **2007**, 31, (10), 1274-1279, <http://dx.doi.org/10.1016/j.cellbi.2007.05.007>.
57. Layne, M. D.; Farmer, S. R., Tumor necrosis factor-alpha and basic fibroblast growth factor differentially inhibit the insulin-like growth factor-I induced expression of myogenin in C2C12 myoblasts. *Exp Cell Res* **1999**, 249, (1), 177-187, 10.1006/excr.1999.4465.
58. De Miranda, M. A., Jr.; Schlater, A. E.; Green, T. L.; Kanatous, S. B., In the face of hypoxia: myoglobin increases in response to hypoxic conditions and lipid supplementation in cultured Weddell seal skeletal muscle cells. *J Exp Biol* **2012**, 215, (Pt 5), 806-813, 10.1242/jeb.060681.

### IGF-1 attenuates hypoxia-induced atrophy but inhibits myoglobin expression

59. van Weel, V.; Deckers, M. M.; Grimbergen, J. M.; van Leuven, K. J.; Lardenoye, J. H.; Schlingemann, R. O.; van Nieuw Amerongen, G. P.; van Bockel, J. H.; van Hinsbergh, V. W.; Quax, P. H., Vascular endothelial growth factor overexpression in ischemic skeletal muscle enhances myoglobin expression in vivo. *Circ Res* **2004**, *95*, (1), 58-66, 10.1161/01.RES.0000133247.69803.c3.
60. van der Vusse, G. J., Albumin as fatty acid transporter. *Drug Metab Pharmacokinet* **2009**, *24*, (4), 300-307, <http://doi.org/10.2133/dmpk.24.300>.
61. Nauta, T. D.; Duyndam, M. C. A.; Weijers, E. M.; van Hinsbergh, V. M. W.; Koolwijk, P., HIF-2 $\alpha$  Expression Regulates Sprout Formation into 3D Fibrin Matrices in Prolonged Hypoxia in Human Microvascular Endothelial Cells. *PLoS One* **2016**, *11*, (8), e0160700, 10.1371/journal.pone.0160700.
62. van Beek-Harmsen, B. J.; Bekedam, M. A.; Feenstra, H. M.; Visser, F. C.; van der Laarse, W. J., Determination of myoglobin concentration and oxidative capacity in cryostat sections of human and rat skeletal muscle fibres and rat cardiomyocytes. *Histochem Cell Biol* **2004**, *121*, (4), 335-342, 10.1007/s00418-004-0641-9.
63. Nagelkerke, A.; Mujcic, H.; Wouters, B.; Span, P. N., 18S is an appropriate housekeeping gene for in vitro hypoxia experiments. *British Journal of Cancer* **2010**, *103*, (4), 590-590, 10.1038/sj.bjc.6605754.



4

# MEIJER AND VLOEDMAN'S HISTOCHEMICAL DEMONSTRATION OF MITOCHONDRIAL COUPLING OBEYS LAMBERT-BEER'S LAW IN THE MYOCARDIUM

---

**Eva L. Peters**, David Comerford, Frédéric M. Vaz, Willem J. van der Laarse  
*Histochemistry and Cell Biology*, 2018, 151 (1), p:85-90

## Abstract

Uncoupling of mitochondrial proton pumping and adenosine triphosphate (ATP) production lowers mitochondrial efficiency. Current methods to determine mitochondrial efficiency require substantial amounts of tissue and permeabilization or isolation procedures. A simple histochemical method has been described by Meijer and Vloedman (1980) but this was not quantitative. We found linear correlations between 1) absorbance and sections thickness and 2) absorbance and incubation time. Because the method obeys Lambert-Beer's law, we can estimate ATP/O<sub>2</sub> ratios for healthy and overloaded right-sided rat myocardium. We related mitochondrial efficiency to the ratio between cardiolipin and its precursor phosphatidylglycerol. We found a non-linear relationship between mitochondrial efficiency and this ratio, indicating that lower mitochondrial efficiency as found in experimental pulmonary hypertension may be due to altered composition of the mitochondrial inner membrane. We conclude that the histochemical method of Meijer and Vloedman can be applied to quantify mitochondrial efficiency.

## Introduction

Mitochondrial uncoupling of oxygen consumption and adenosine triphosphate (ATP) resynthesis may play a role in various pathologies. Increased  $Mg^{2+}$ -stimulated ATPase activity and thus loosely coupled mitochondria, was shown to be a feature of some neuromuscular diseases (Meijer and Vloedman 1980). Also, in cardiomyopathy, mitochondrial dysfunction may play a critical role (Murphy et al. 2016). Decreased right-sided myocardial efficiency of pulmonary hypertensive patients and myocardial preparations of rats (Wong et al. 2010, 2011; Pham et al. 2018) may also be due to uncoupling and a concomitant decrease in the efficiency of mitochondria.

Mitochondrial efficiency measured in intact muscle preparations is 70-80% (corresponding to  $ATP/O_2 = 5$ ), indicating that at most 20-30% of the available energy of substrate oxidation is spent on futile ion pumping and heat generation (Lou et al. 2000; Barclay and Widen 2010). The flux of protons crossing the inner membrane without generating ATP by  $F_1F_o$  ATPase dissipates part of the chemiosmotic proton potential generated by the electron transport chain. Proton permeability of the inner membrane is regulated by uncoupling proteins and hormones and depends on the fatty acid composition of cardiolipin (Hoch 1998). When the futile flux of protons across the mitochondrial inner membrane increases, e.g., due to radical damage to the inner membrane, ATP generation by  $F_1F_o$  ATPase is disturbed.

Unfortunately, it is often impossible to determine the coupling state of mitochondria in intact preparations because this requires measurements of heat production and/or oxygen consumption and corrections for glycolytic ATP production. Current methods use permeabilized biopsies or isolated mitochondria to determine the coupling state biochemically. The latter methods require relatively large amounts of tissue (50 mg or more). It is also usually unknown how permeabilization or isolation procedures affect the coupling state (Picard et al. 2011). This is especially important because the isolation and permeabilization procedures often need to be optimized differently for test and control tissue.

We studied the possibility to determine the coupling state of mitochondria quantitatively in cryosections of rat myocardial tissue, using the histochemical method as described by Meijer and Vloedman (1980). The method is based on determination of MgATPase activity of  $F_1F_o$  ATPase operating in the reverse mode, i.e., pumping protons out of the mitochondrial matrix using energy from ATP hydrolysis. We investigated whether this histochemical method obeys Lambert-Beer's law with respect to the relationship between absorbance and incubation time and the relationship between absorbance and section thickness.

Furthermore, we applied the quantification to right ventricular myocardial tissue from control and pulmonary hypertensive rats, and related proton permeability to a marker of cardiolipin metabolism.

## Methods

### Animals

The study was approved by the Animal Experimental Committee of the Vrije Universiteit Amsterdam (Amsterdam, Netherlands). All procedures performed involving animals were in accordance with the guide of the Dutch Research Council for care and use of laboratory animals.

To investigate whether the method obeys Lambert-Beer's law, four male Wistar rats (body weight ranging from 262-341 g at time of experiment, Envigo, The Netherlands) were used. Rats were anesthetized with isoflurane, and hearts were excised and perfused with HEPES-buffered, oxygenated Tyrode (in mM: NaCl 140, KCl, 4.7, MgSO<sub>4</sub>·7H<sub>2</sub>O 1.2, NaH<sub>2</sub>PO<sub>4</sub>·H<sub>2</sub>O 2, 2,3-Butanedione monoxime (BDM) 20, CaCl<sub>2</sub> 1, HEPES 5, glucose 10, pH = 7.4, 10-15 °C). To investigate the effect of right ventricular overload on the coupling state of mitochondria in pulmonary hypertensive rats, another four healthy animals were compared with 11 monocrotaline (MCT) treated animals. Tissue was obtained 23 days after subcutaneous MCT injection (60 mg/kg) as described elsewhere (Van Eif et al. 2014). In both cases, the apex and right ventricular free wall were isolated and frozen in liquid nitrogen. F<sub>1</sub>F<sub>o</sub>ATPase was determined within one week after collection of the tissue. Tissue was stored at -80 °C for further analyses.

### Determination of F<sub>1</sub>F<sub>o</sub>ATPase activity

Meijer & Vloedman's method for complex V activity is based on the determination of F<sub>1</sub>F<sub>o</sub>ATPase activity in a Wachstein-Meissel medium (Meijer and Vloedman 1980). Maximum activity was obtained in the presence of 2,4-dinitrophenol (DNP, Fluka Chemie, Switzerland) which carries protons across the mitochondrial inner membrane. Background activity was measured after inhibition of F<sub>1</sub>F<sub>o</sub>ATPase by oligomycin (Sigma, The Netherlands). Sections were cut in a Leica CM 1950 cryostat (Nussloch, Germany). For determination of the absorbance as a function of incubation time, sections of 5 μm thickness were incubated for 30 seconds, 5, 10 or 15 minutes. To determine the absorbance at different section thicknesses, sections of 2 to 8 μm thick were cut and incubated for 10 minutes. The sections were fixed for 2 minutes on ice in Macrodex (0.9% NaCl, 1% CaCl<sub>2</sub>, 3.6% formalin, 7.7mM dextran-70) and subsequently washed 4 times in 0.9% NaCl + 1% CaCl<sub>2</sub>. Sections were then incubated at 37 °C.

The different incubation media were prepared from stock solutions of 0.2 M Tris maleate (pH 7.2), 60mM  $\text{Pb}(\text{NO}_3)_2$ , and 50mM  $\text{MgCl}_2$ . ATP- and oligomycin solutions were freshly made. ATP disodium salt (Sigma, The Netherlands) was dissolved in water and kept on ice until use. Oligomycin was dissolved in ethanol (1 mg/40  $\mu\text{l}$ ). Final concentrations were 80 mM Tris maleate, 3.6 mM  $\text{Pb}(\text{NO}_3)_2$ , 5 mM  $\text{MgCl}_2$ , 1 mM  $\text{Na}_2\text{ATP}$ , and 25 $\mu\text{M}$  oligomycin and/or 1 mM DNP. The pH was adjusted to 7.2 using 1N NaOH. To test whether oligomycin inhibition was time-dependent, we pre-incubated sections for 30 minutes at 37°C in medium with oligomycin but without lead nitrate and subsequently incubated in the medium containing both oligomycin and lead nitrate. To determine non-specific binding of lead, sections were incubated without ATP. After the incubation, sections were washed quickly in 4 changes of water and developed in 1%  $\text{Na}_2\text{S}$ , pH 7.5 at room temperature for 1-2 minutes. Finally, sections were washed again and mounted in glycerine-gelatine.

### Microdensitometry

Images of the sections were captured using NIH image and analysed using ImageJ (version 1.51u, <http://rbs.info.nih.gov>) as described previously (Lee-de Groot et al. 1998). None of the images have been manipulated. The absorbance of the final PbS precipitate in the sections was determined at 550 nm in individual myocytes. The absorbances of 10 myocytes, cut perpendicularly to the longitudinal axis, were measured in the centre of the cell (excluding nuclei). The extinction coefficient of the PbS precipitate at 450 nm is 3788 SD 797  $\text{M}^{-1}\cdot\text{cm}^{-1}$  (Van Noorden and Jonges 1992). At this wavelength, the absorbance is high at 10 minutes incubation time in 5  $\mu\text{m}$  thick myocardial sections (> 1 in positive controls), therefore we prefer absorbance measurements at 550 nm. The absorbance of PbS decreases continuously with increasing wavelength > 420 nm (Laborde et al. 1990). The ratio of absorbances at 550nm over 450 nm measured in myocardial sections was constant up to  $A_{450\text{nm}} = 0.6$  and equalled  $0.54 \pm 0.02$  (mean  $\pm$  S.D., n = 4; confirming results of Laborde et al. (1990)), indicating that the molar extinction coefficient of PbS at 550 nm equals  $2046 \text{ M}^{-1}\cdot\text{cm}^{-1}$ . We assume that the extinction coefficient at 550 nm with respect to phosphate equals  $3069 \text{ M}^{-1}\cdot\text{cm}^{-1}$  since the solubility product of  $\text{Pb}_3(\text{PO}_4)_2$  is reached before the solubility product of  $\text{PbHPO}_4$  is reached at pH 7.2. A similar value has been reported by Blanco & Sieck (1992).

### Coupling state of mitochondria: quantitative estimate of proton permeability and corresponding ATP/O<sub>2</sub>

It is assumed that F<sub>1</sub>F<sub>o</sub>ATPase activity is negligible in the presence of 25 μM oligomycin (IC<sub>50</sub> = 0.092 μM, Nesci et al. 2014) and that proton permeability is maximal in the presence of 1 mM 2,4-dinitrophenol (Heytler and Prichard 1962). The estimate of P/O<sub>2</sub> based on energy dissipation due to proton permeability of the inner membrane is calculated assuming the F<sub>1</sub>F<sub>o</sub>ATPase activity is proportional to the proton flux across the inner membrane into the matrix:

$$P/O_2 = 6.3[1 - (F_1F_o\text{ATPase activity} / F_1F_o\text{ATPase activity with DNP})]$$

where 6.3 is the theoretical maximum P/O<sub>2</sub> (Kushmerick 1983; Scheffler 2007).

### Cardiolipin and phosphatidylglycerol

Cardiolipin is an essential phospholipid component of the mitochondrial inner membrane. Markers of cardiolipin metabolism were determined in the right-sided myocardium by high performance liquid chromatography-mass spectrometry (Houtkooper et al. 2009). The ratio of the most abundant phosphatidylglycerol (PG (34:1), a precursor of cardiolipin) and cardiolipin (CL (72:8), containing four linoleic acid fatty acid side-chains) was used as indicator of cardiolipin metabolism. This ratio (PG/CL) is expressed relative to the mean ratio in controls (mean PG/CL is set to 1).

### Statistics

Statistical analyses were performed using GraphPad Prism 7.0 (GraphPad Software, La Jolla, CA, USA). Linear regression lines were fitted through the data and slopes and intercepts were compared using ANOVA. 95% confidence intervals (95%CI) were calculated for the slopes and y-intercept. Values are mean ± S.D. if not indicated otherwise.

## Results and discussion

Pilot experiments indicated that the original fixation time (10 minutes) was critical in heart muscle. Two minutes fixation was sufficient to prevent precipitate covering the section, while maintaining maximal ATPase activity. We did not observe a precipitate covering the section after 2 minutes of fixation nor the formation of precipitate in the incubation medium, indicating that all phosphate produced in the section precipitated close to the site of formation.

### Absorbance increases linearly with incubation time and section thickness

Figs. 1a and b show the increase in absorbance over time and the images used to measure the absorbance. In all conditions except incubation without ATP, the increase in absorbance was linear with incubation time and significantly different from zero ( $p < 0.0001$  for Test, DNP, Oligomycin and Oligomycin + preincubation,  $p = 0.17$  for no ATP). However, we observed a y-intercept for all conditions ( $A_{550} = 0.094 \pm 0.01$  on average). The regression lines of the oligomycin incubations with and without preincubation were similar, indicating that oligomycin binding to  $F_1F_0$  ATPase is fast, and that preincubation is not required. However, part of the ATPase activity is insensitive to oligomycin.

The increase in absorbance with increasing section thickness and corresponding images are shown in Figs. 1c and d. In all conditions, the increase in absorbance was linear over the measured interval and significantly different from zero ( $p < 0.0001$  for all, including no ATP). A Y-intercept was again present in all conditions ( $0.099 \pm 0.02$  on average,  $0.066$  for no ATP alone). Note that blank absorbance is set just outside the section, indicating that the intercept absorbance in Fig. 1d is due to the interaction of light with the unstained section itself, e.g., due to diffuse light scattering at the cut surfaces of the section. Were it due to PbS absorbance, a proportional relationship was expected in incubations without ATP. The absorbance increase with section thickness of unstained sections is relatively small:  $0.0032$  absorbance units/mm section thickness. Again, the relationships for oligomycin incubations with and without preincubation are similar, excluding diffusion effects on oligomycin binding.

## CHAPTER 4

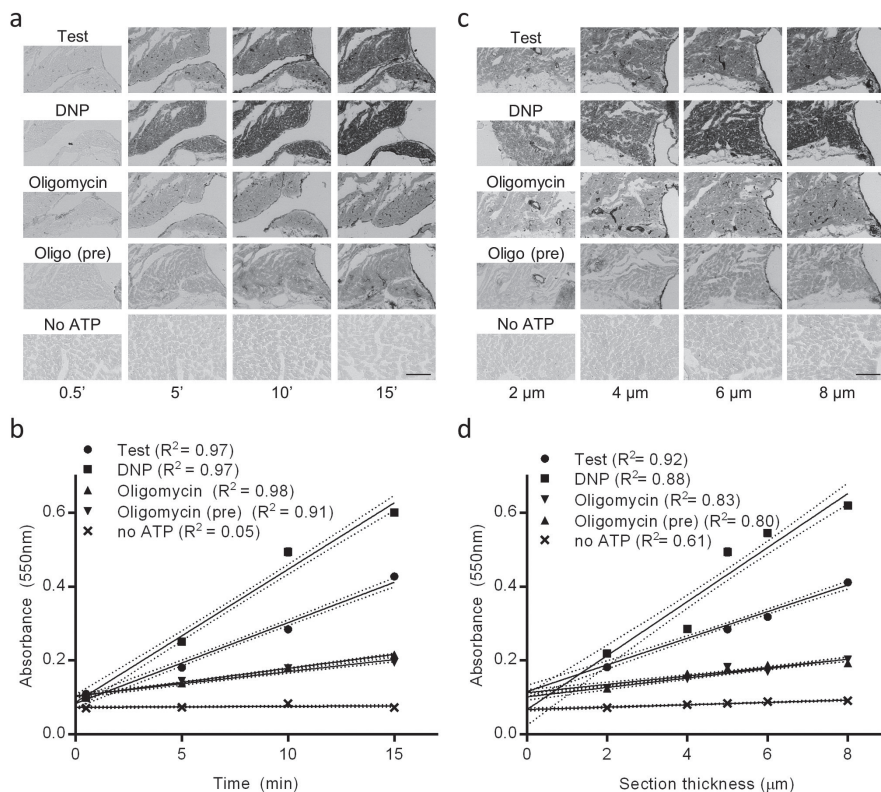


Figure 1 – **Quantification of time- and section thickness series.** (a) Representative images of serial sections that were incubated for 0.5, 5, 10 or 15 minutes. (b) the absorbance values of the sections shown in (a) were measured and plotted against incubation time. (c) Representative images of serial sections with different thickness, all incubated for 10 minutes. (d) the absorbance values of the sections shown in (c) were measured and plotted against sections thickness. Data at 5  $\mu$ m from (b), serial sections shown in (a) and (c) are both from the same heart.  $R^2$  values are given in (b) and (d) for the linear regression lines of absorbance with time or sections thickness, respectively. Dotted lines around the regression lines represent 95% confidence intervals. Scale bars represent 100  $\mu$ m. DNP = 2,4-dinitrophenol.

### Specificity of the reaction

A PbS precipitate is formed even in preparations incubated with oligomycin, indicating that the precipitate is not entirely due to mitochondrial  $F_1F_0$ ATPase or that oligomycin does not completely inhibit  $F_1F_0$ ATPase instantaneously. Since oligomycin is present in excess (20 times  $IC_{50}$ , Nesci *et al.*, 2014) and addition of DNP to oligomycin containing media did not increase the final absorbance after 10 minutes incubation (result not shown), it is likely that that oligomycin inhibition was complete. Also, both validations (for time and section thickness) showed no differences in the slope or intercept of incubations with oligomycin with or without preincubation. It is thus likely that the time needed for inhibition of  $F_1F_0$ ATPase is negligible compared to the incubation time. Therefore, we conclude that oligomycin-insensitive ATPases in cardiomyocytes contribute to the absorbance, as discussed by Meijer and Vloedman (1980).

4

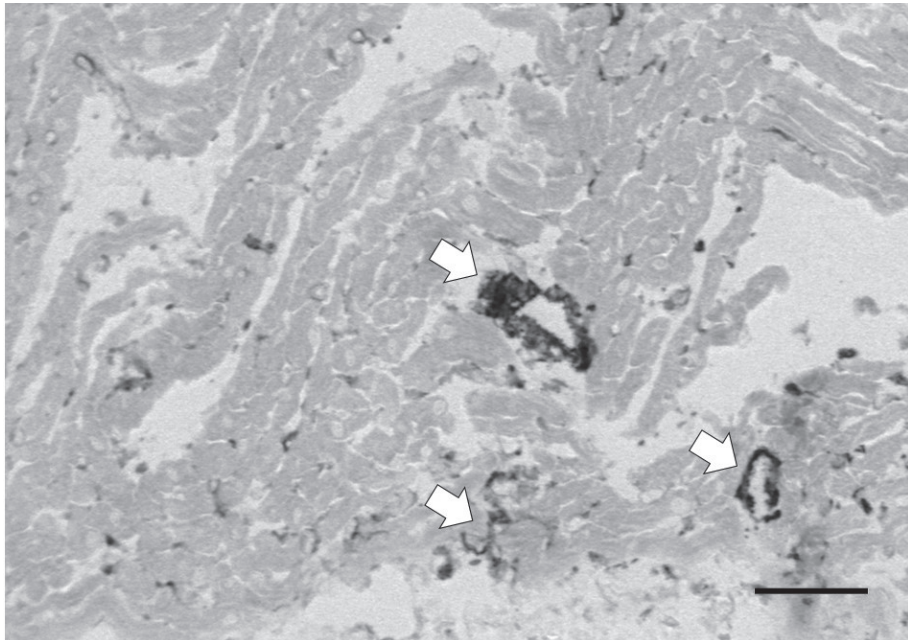


Figure 2 - **Enlargement of the incubation with oligomycin for 10 minutes, in a section of 5  $\mu$ m, as shown in Fig. 1a.** White arrows indicate cells with high ATPase activity in vessel walls. Also, larger spots with high ATPase activity are seen, possibly smaller vessels and capillaries. Scale bar represents 50  $\mu$ m.

In addition, these could be myosin ATPase, T-tubular MgATPase (Hidalgo *et al.* 1983) or ecto-ATPase (Zinchuk *et al.* 2002). Quantification of these ATPases is beyond the scope of the present study. Ecto-ATPase is mainly located on the outside of the cardiomyocyte sarcolemma and endothelial cells, but has also

## CHAPTER 4

been detected in T-tubules (Zinchuk et al. 2002). Myosin ATPase does contribute since treatment of sections with 10 mM blebbistatin for 10 minutes after fixation reduced the absorbance after oligomycin incubation from  $0.18 \pm 0.02$  to  $0.14 \pm 0.01$  (after subtraction of intercept absorbance: from  $0.09 \pm 0.02$  to  $0.05 \pm 0.01$ ), suggesting that about half of oligomycin-insensitive ATPase activity is myosin ATPase (result not shown). Triton X-100 partly deactivates T-tubular MgATPase (Ebus and Stienen 1996) but cannot be used as inhibitor in the present assay because it solubilizes mitochondrial membranes (Gurtubay et al. 1980). Also, high ATPase activity in vessel walls and endothelial cells is obvious, as is shown in Fig 2. Activity from sarcolemmal ecto-ATPases can easily be excluded from the absorbance measurements, by only measuring the absorbance in the centre of the cells. Thus, accurate determinations of the coupling state using Meijer and Vloedman's method require a correction for background ATPase activity by subtracting absorbance measured after incubation with oligomycin. Because the intercept is also present in the sections incubated in the presence of oligomycin, subtraction of the absorbance obtained after oligomycin incubation also provides this intercept correction.

Meijer and Vloedman (1980) demonstrated that addition of  $Pb^{2+}$  ions to the biochemical assay decreased  $F_1F_o$  ATPase activity. The inhibition decreased with the amount of tissue in the assay: from 88% inhibition at 2mg tissue/ml to 23% inhibition at 50mg tissue/ml homogenization medium, suggesting that inhibition is negligible beyond 200mg tissue/ml. We conclude that inhibition of the enzyme in the section by  $Pb^{2+}$  is negligible in the present study, because tissue density is 1050 mg/ml and because the free  $Pb^{2+}$  concentration near the enzyme must be lower than 3.6 mM to maintain the constant flux of lead ions into the section and because  $Pb^{2+}$  will at least partly precipitate with phosphate before it reaches the enzyme. It can be calculated using Lambert-Beer's law that the rate of phosphate precipitation in the section corresponds to 0.34 mM/s in the presence of DNP (Fig. 1b).

## ATP/O<sub>2</sub> ratios in myocardial control and pulmonary hypertensive rats

After correction, the absorbance data in test and positive controls obey Lambert-Beer's law and thus, it is possible to estimate the effect of proton permeability on ATP/O<sub>2</sub>. The result is shown in Fig. 3 where the relationship between the ATP/O<sub>2</sub> ratio calculated from proton permeability is plotted against a marker of cardiolipin metabolism, the PG/CL ratio. Paired determinations in the right ventricular free walls of healthy and pulmonary hypertensive rats show a normal ATP/O<sub>2</sub> = 5 in healthy hearts but a non-linearly decreasing coupling ratio with increasing PG/CL ratio. Low ATP/O<sub>2</sub> ratios of around 2 have severe energetic consequences. These results suggest that mitochondrial proton leak could be an important contributor to reduced myocardial efficiency in chronic heart failure. The mechanism behind the relationship in Fig 3. requires further study. The present histochemical method can be applied to myocardial samples smaller than a milligram, allowing for diagnostic tests of mitochondrial function in myocardial biopsies.

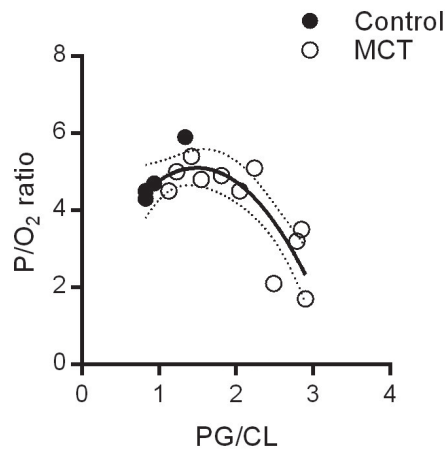


Figure 3 – ATP/O<sub>2</sub> ratios calculated from measures absorbance values, both in control and MCT-induced pulmonary hypertensive rats. A second order polynomial was fitted through the data (best fit curve  $ATP/O_2 = -1.4(PG/CL)^2 + 4.18(PG/CL) + 1.99$ ,  $R^2 = 0.69$ . PG = phosphatidylglycerol, CL = cardiolipin

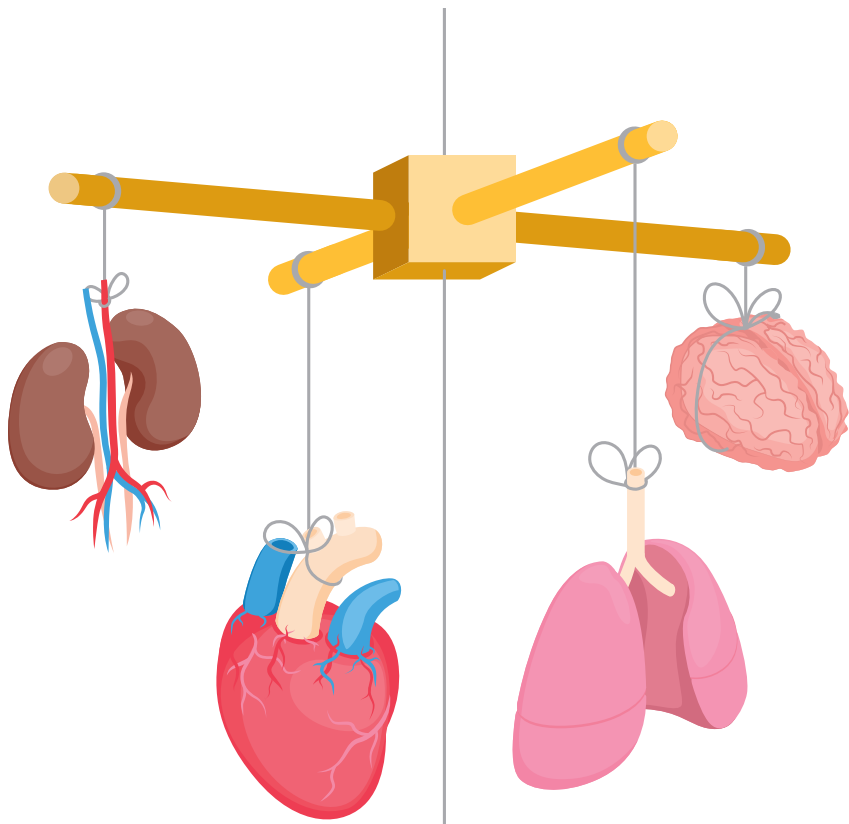
## Acknowledgements

Eva L. Peters was funded through a VICI grant (2002406) by the Dutch Organization for Scientific Research (NWO).

## References

1. Barclay CJ, Widen C (2010) Efficiency of cross-bridges and mitochondria in mouse cardiac muscle. *Adv Exp Med Biol* 682:267–278. doi: 10.1007/978-1-4419-6366-6\_15
2. Blanco CE, Sieck GC (1992) Quantitative determination of calcium-activated myosin adenosine triphosphatase activity in rat skeletal muscle fibres. *Histochem J* 24:431–444. doi: 10.1007/BF01089105
3. Ebus JP, Stienen GJM (1996) Origin of concurrent ATPase activities in skinned cardiac trabeculae from rat. *J Physiol* 492:675–687. doi: 10.1113/jphysiol.1996.sp021337
4. Gurtubay JI, Goñi FM, Gómez-Fernández JC, et al (1980) Triton X-100 solubilization of mitochondrial inner and outer membranes. *J Bioenerg Biomembr* 12:47–70. doi: 10.1007/BF00745012
5. Heytler PG, Prichard WW (1962) A new class of uncoupling agents - Carbonyl cyanide phenylhydrazones. *Biochem Biophys Res Commun* 7:272–275. doi: 10.1016/0006-291X(62)90189-4
6. Hidalgo C, Gonzalez ME, Lagos R (1983) Characterization of the Ca<sup>2+</sup>- or Mg<sup>2+</sup>-ATPase of transverse tubule membranes isolated from rabbit skeletal muscle. *J Biol Chem* 258:13937–13945
7. Hoch FL (1998) Cardiolipins and mitochondrial proton-selective leakage. *J Bioenerg Biomembr* 30:511–532. doi: 10.1023/A:1020576315771
8. Houtkooper RH, Rodenburg RJ, Thiels C, et al (2009) Cardiolipin and monolysocardiolipin analysis in fibroblasts, lymphocytes, and tissues using high-performance liquid chromatography-mass spectrometry as a diagnostic test for Barth syndrome. *Anal Biochem* 387:230–237. doi: 10.1016/j.ab.2009.01.032
9. Kushmerick JM (1983) Energetics of muscle contraction. In: *Handbook of Physiology*. Am Physiol Soc. Bethesda MD, pp 189–236
10. Laborde K, Bussières L, De Smet A, et al (1990) Quantification of renal NaKATPase activity by image analysing system. *Cytometry* 11:859–868. doi: 10.1002/cyto.990110802
11. Lee-de Groot MBE, Des Tombe AL, Van der Laarse WJ (1998) Calibrated Histochemistry of Myoglobin Concentration in Cardiomyocytes. *J Histochem Cytochem* 46:1077–1084. doi: 10.1177/002215549804600912
12. Lou F, Van der Laarse WJ, Curtin NA, Woledge RC (2000) Heat production and oxygen consumption during metabolic recovery of white muscle fibres from the dogfish scyloiorhinus canicula. *J Exp Biol* 203:1201–1210
13. Meijer AEFH, Vloedman AHT (1980) The Histochemical Characterization of the Coupling State of Skeletal Muscle Mitochondria. *Histochemistry* 69:217–232. doi: <https://doi.org/10.1007/BF00489769>
14. Murphy E, Ardehali H, Balaban RS, et al (2016) Mitochondrial Function, Biology, and Role in Disease: A Scientific Statement from the American Heart Association. *Circ Res* 118:1960–1991. doi: 10.1161/RES.000000000000104
15. Nesci S, Ventrella V, Trombetti F, et al (2014) Thiol oxidation is crucial in the desensitization of the mitochondrial F1FO-ATPase to oligomycin and other macrolide antibiotics. *Biochim Biophys Acta - Gen Subj* 1840:1882–1891. doi: 10.1016/j.bbagen.2014.01.008

16. Pham T, Nisbet L, Taberner A, et al (2018) Pulmonary arterial hypertension reduces energy efficiency of right, but not left, rat ventricular trabeculae. *J Physiol* 596:1153–1166. doi: 10.1113/JP275578
17. Picard M, Taivassalo T, Gouspillou G, Hepple RT (2011) Mitochondria: isolation, structure and function. *J Physiol* 589:4413–4421. doi: 10.1113/jphysiol.2011.212712
18. Scheffler IE (2007) *Mitochondria: Second Edition*. John Wiley & Sons, Inc., Hoboken, NJ
19. Van Eif VWW, Bogaards SJP, Van der Laarse WJ (2014) Intrinsic cardiac adrenergic (ICA) cell density and MAO-A activity in failing rat hearts. *J Muscle Res Cell Motil* 35:47–53. doi: 10.1007/s10974-013-9373-6
20. Van Noorden CJF, Jonges GN (1992) Molecular extinction coefficients of lead sulfide and polymerized diaminobenzidine as final reaction products of histochemical phosphatase reactions. *Cytometry* 13:644–648. doi: 10.1002/cyto.990130613
21. Wong YY, Handoko ML, Mouchaers KTB, et al (2010) Reduced mechanical efficiency of rat papillary muscle related to degree of hypertrophy of cardiomyocytes. *Am J Physiol Heart Circ Physiol* 298:H1190–7. doi: 10.1152/ajpheart.00773.2009
22. Wong YY, Ruiters G, Lubberink M, et al (2011) Right Ventricular Failure in Idiopathic Pulmonary Arterial Hypertension Is Associated With Inefficient Myocardial Oxygen Utilization. *Circ Heart Fail* 4:700–706. doi: 10.1161/CIRCHEARTFAILURE.111.962381
23. Zinchuk VS, Okada T, Seguchi H (2002) Combined biochemistry and histochemistry as a tool to investigate ecto-ATPase in the cardiac muscle. *Microsc Res Tech* 58:427–431. doi: 10.1002/jemt.10157



5

# INCREASED MAO-A ACTIVITY PROMOTES PROGRESSION OF PULMONARY ARTERIAL HYPERTENSION

---

**Eva L. Peters\***, Xiao-Qing Sun\*, Ingrid Schalij, Julie Birkmose Axelsen, Stine Andersen, Kondababu Kurakula, Maria Cataline Gomez-Puerto, Robert Szulcek, Xiaoke Pan, Denielli da Silva Goncalves Bos, Roy E.J. Schiepers, Asger Andersen, Marie-José Goumans, Anton Vonk Noordegraaf, Willem J. van der Laarse, Frances S. de Man, Harm Jan Bogaard

\* First authors contributed equally

*American Journal of Respiratory Cell and Molecular Biology, 2021. 64 (3), p:331-343*

## Abstract

**RATIONALE:** Monoamine oxidases (MAO), a class of enzymes bound to the outer mitochondrial membrane, are important sources of reactive oxygen species. Increased MAO-A activity in endothelial cells and cardiomyocytes contributes to vascular dysfunction and progression of left heart failure. **OBJECTIVES:** We hypothesized that inhibition of MAO-A can be used to treat pulmonary arterial hypertension (PAH) and right ventricular (RV) failure. **METHODS:** MAO-A level in PAH patient lung and RV samples was compared to non-PAH donors. Experimental PAH was induced in male Sprague-Dawley rats by Sugen 5416 and hypoxia (SuHx), and RV failure was induced in male Wistar rats by pulmonary trunk banding (PTB). Animals were randomized to receive either saline or MAO-A inhibitor clorgyline 10 mg/kg. Echocardiography and RV catheterization was performed, heart and lung tissues were collected for further analysis. **MEASUREMENTS AND MAIN RESULTS:** We found increased MAO-A expression in the pulmonary vasculature of PAH patients and in experimental PH induced by SuHx. Cardiac MAO-A expression and activity was increased in SuHx- and PTB-induced RV failure. Clorgyline treatment reduced RV afterload and pulmonary vascular remodelling in SuHx rats, through reduced pulmonary vascular proliferation and oxidative stress. Moreover, clorgyline improved RV stiffness, relaxation and reversed RV hypertrophy in SuHx rats. In PTB rats, clorgyline had no direct effect on the RV. Our study reveals the role of MAO-A in the progression of PAH. **CONCLUSIONS:** Collectively, these findings indicated that MAO-A may be involved in pulmonary vascular remodelling and consecutive RV failure.

## Introduction

Pulmonary arterial hypertension (PAH) is a fatal disease characterized by pulmonary vascular remodelling, increased right ventricular (RV) afterload and ultimately RV failure. Despite advances in treatment, current therapies are ineffective in stopping the disease progression (2). Therefore, new treatments are urgently needed. Reactive oxygen species (ROS)-mediated oxidative damage plays an important role in pulmonary vascular dysfunction and RV failure, and therefore therapies targeting the major ROS sources have been propagated (3).

ROS can be produced from multiple intracellular sources, and some have been identified to play important roles in PAH (3). Recently, an additional mitochondrial enzyme, monoamine oxidase (MAO), was found to be a major ROS source, with pathophysiological relevance in multiple cardiovascular diseases (4, 5). On the contrary to other ROS sources, MAO inhibitors are available and used in the clinic for the treatment of mood disorders, Parkinson's disease, and Alzheimer's disease (6). MAOs are flavoenzymes bound to the outer membrane of mitochondria, which oxidize neurotransmitters and biogenic amines, thereby producing  $H_2O_2$  and aldehyde. MAOs have two isoforms, MAO-A and MAO-B, which have different distributions, structures, inhibitor sensitivities and substrate affinities (6). While MAO-A and MAO-B are equally present in the lungs, MAO-A is the predominant isoform in cardiomyocytes of human and rodents (7, 8).

MAO-A catalyses preferentially serotonin (5-HT) and norepinephrine (NE), two monoamines with widely recognized roles in PAH (4, 9). Both plasma and lung endothelial cell (EC) derived 5-HT are increased in PAH patients, thus increasing substrate availability for MAO-A (10, 11). 5-HT is mostly metabolized by MAO-A in hepatic and lung ECs and induces ROS production (9). However, a role of MAO-A in lung ECs in PAH can be speculated. MAO-A activity was found to contribute to impaired vascular relaxation in ECs and increased proliferation in smooth muscle cells (SMCs) in different vascular diseases (12, 13), but its role remains unknown in the pulmonary vasculature in PAH. Apart from 5-HT, increased plasma NE was found in PAH patients with end-stage heart failure, contributing to increased activity of the sympathetic nervous system (SNS) (14). In cardiomyocytes, NE can induce a rise in MAO-A with markedly increased ROS and trigger hypertrophy (15). In various experimental models of heart failure, MAO-A inhibition was found to be beneficial, including those based on ischemia/reperfusion injury (16, 17), left ventricular (LV) pressure overload (15, 18) and diabetes (19, 20). However, the role of MAO-A in the RV is unknown.

## CHAPTER 5

Here we investigated the involvement of MAO-A and its impact on PAH and RV failure. Our results show that MAO-A expression is increased in the media and intima layers, but not in whole lung lysates of PAH patients and that MAO-A inhibitor has significant therapeutic effects in experimental PAH. Collectively, our findings suggest that MAO-A inhibition may be involved in pulmonary vascular remodelling.

## Methods

### Human samples, Cell cultures, and siRNA transfections

Human sample collection was approved by the local ethics committees at Amsterdam UMC (Amsterdam, the Netherlands) and written informed consent was obtained. Details are in the online supplement.

### Sugen 5416 and hypoxia rat model of PAH

SuHx rats was induced as described previously (21). Animals were randomized to receive clorgyline (started with 10 mg/kg, followed by 2 mg/kg, Sigma-Aldrich) or saline by intraperitoneal injection four times from week 8 to week 10. The study was approved by an independent local animal ethic committee at Amsterdam UMC (Amsterdam, the Netherlands, study number VU-FYS13-01A4), and were carried out in compliance with guidelines issued by the Dutch government. Details are in the online supplement.

### Pulmonary trunk banding rat model of RV failure

PTB rats was induced as described previously (22). PTB animals were randomized to receive clorgyline (started with 10 mg/kg, followed by 2 mg/kg, Sigma-Aldrich) or saline by intraperitoneal injection 3 times per week from week 2 to week 7. All experiments with PTB rats were in accordance with the Danish law for animal research (Danish Ministry of Justice, authorization number 2016-15-0201-01040) and approved by the Institutional Ethics Review Board. Details are in the online supplement.

### Echocardiography and RV catheterization

All animals underwent echocardiographic assessments and RV catheterization as published previously (21, 22). See the online supplement for details.

### Histology, Western Blot, MAO-A, and ATPase activity

See the online supplement for details.

## Statistics

Statistical analyses were performed using Prism for Windows (GraphPad 8 Software).  $p < 0.05$  was considered significant. All statistical tests used two-sided tests of significance. Data are presented as mean  $\pm$  SEM. Details are in the online supplement.

## Results

### MAO-A is increased in the pulmonary vasculature of patients with PAH

To investigate the expression pattern of MAO-A in human PAH lungs, we performed immunofluorescence staining on paraffin sections of patients with end-stage PAH. We found that MAO-A was expressed in several cell types in the lungs, including ECs, SMCs, fibroblasts and epithelial cells (Fig. 1A, Supplement Fig. E1). To determine the expression of MAO-A, we performed fluorescence quantification. We found that MAO-A expression in the pulmonary vasculatures of PAH patients was increased in the intima as well as in the media layer (Fig. 1B, C, Supplement Fig. E1). However, we did not observe increased MAO-A expression in human whole lung lysates (Fig. 1D, E).

Moreover, we did not observe differences in MAO-A expression in primary cultures of microvascular ECs (MVECs) or PAECs derived from PAH patients and controls (Supplement: Fig. E2A, B).

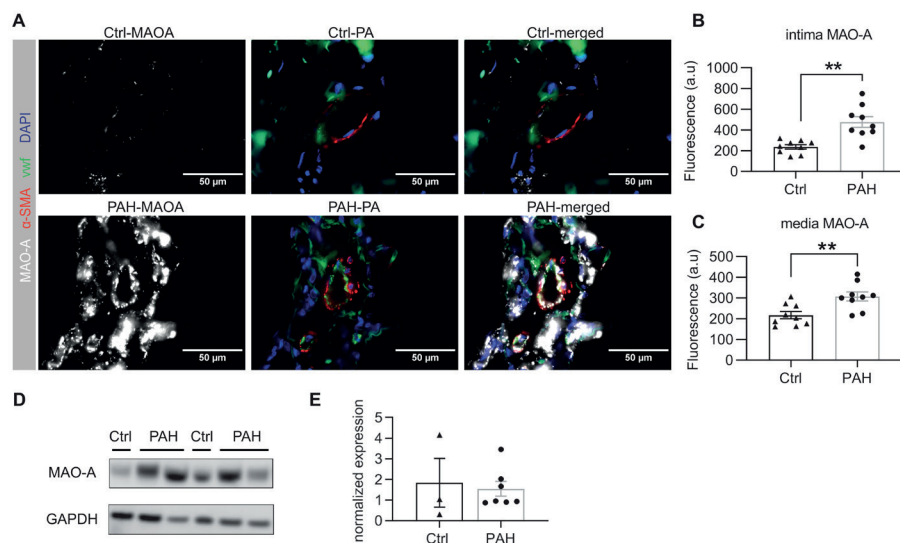


Figure 1 – **MAO-A expression is increased in the pulmonary vasculatures of PAH patients.** (A) Representative lung immunofluorescence staining for MAO-A of ctrl donors and end stage PAH patients.  $\alpha$ -SM (red), vWF (green) and DAPI (blue) were co-stained with MAO-A (white). Scale bar 50  $\mu$ m. (B, C) Quantification of fluorescence reveals increased MAO-A expression in the intima and media layers of the pulmonary vasculatures of PAH patients.  $n = 9$ . (D) Representative images of western blot on human lung homogenates for MAO-A, with GAPDH as loading control. (E) Quantification of western blot shows that MAO-A expression in whole lung homogenates has no difference between ctrl donors and end stage PAH patients. All data are presented as mean  $\pm$  SEM; Unpaired t-test. \*\* $p < 0.01$ . PA = pulmonary artery

## MAO-A is increased in the pulmonary vasculature in the rat model of SuHx-induced PAH

Consistent with the findings in the tissues from PAH patients, MAO-A expression was increased in the intima and media layers of the pulmonary vasculature of SuHx-PAH rats at 10 weeks into the disease (Fig. 2A-C). Moreover, as shown by histochemistry on lung cryosections, MAO-A activity was increased in the pulmonary vasculatures of SuHx rats at week 10 (Fig. 2D). However, MAO-A protein expression was unaltered in whole lung tissue (Fig. 2E, Supplement: Fig. E3A, B).

Increased MAO-A activity promotes progression of pulmonary arterial hypertension

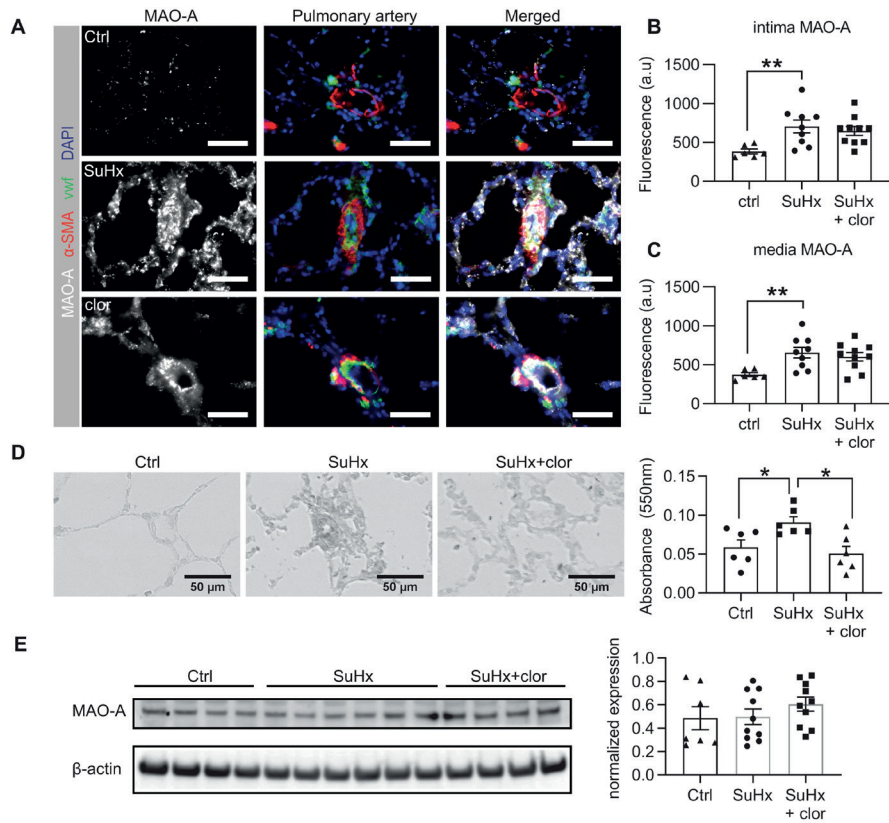


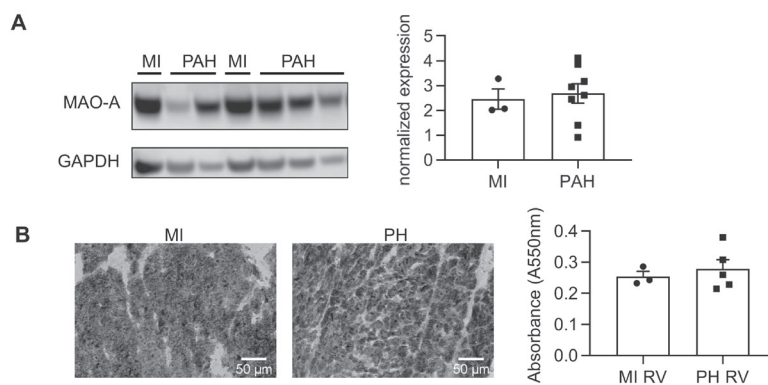
Figure 2 - **MAO-A is increased in the pulmonary vasculatures of SuHx rats.** (A) Representative lung immunofluorescence staining for MAO-A from ctrl, SuHx and SuHx+clorglyline groups. Scale bar 50  $\mu$ m. (B, C) Quantification of fluorescence shows increased MAO-A expression in the intima and media layers of the pulmonary vasculatures of SuHx rats. No difference in MAO-A expression was observed by clorglyline treatment. Ctrl: n = 6, SuHx: n = 9, SuHx+clor: n = 10. (D) Lung histochemistry staining shows increased MAO-A activity in the lungs from SuHx rats and reduced after clorglyline treatment. Scale bar 50  $\mu$ m. Incubation time: 4 hours. Ctrl: n = 6, SuHx: n = 6, SuHx+clor: n = 6. (E) Western blot on lung lysates shows unaltered MAO-A expression between ctrl, SuHx and clorglyline treated rats, with  $\beta$ -actin as loading control. ctrl: n = 7, SuHx: n = 10, SuHx+clor: n = 10. All data are presented as mean  $\pm$  SEM; One-way ANOVA followed by Bonferroni posthoc comparison between ctrl and SuHx, SuHx and SuHx+clor. \* $p$ <0.05, \*\* $p$ <0.01.

## RV MAO-A is increased in experimental models but not in patients with PAH

To investigate the expression and activity of MAO-A in the RV of PAH patients, we performed western blots on homogenates of the RV from patients with end-stage PAH and from controls (patients with myocardial infarction outside the RV). MAO-A expression was not increased in the RV of PH patients compared to control (Fig. 3A). In addition, enzyme histochemistry revealed no differences in MAO-A activity (Fig. 3B). MAO-A activity and expression were markedly increased in the RV of SuHx-PAH rats (Fig. 3C, D), as well as in the RV of PTB rats (Fig. 3E, F).

## Clorgyline treatment reduces RV afterload by reversing pulmonary vascular remodelling in rats with SuHx-induced PAH

To assess the therapeutic effect of MAO-A inhibition, we chose the irreversible MAO-A inhibitor clorgyline. Two weeks treatment with clorgyline reduced MAO-A activity in the PAH lungs (Fig. 2D), and left MAO-A protein expression unaltered (Fig. 2A-C,E). As shown by pressure-volume analysis, clorgyline reduced RV systolic pressure (RVSP) and arterial elastance (Ea) in SuHx rats (Fig. 4A). Consistently, as revealed by echocardiography analysis, clorgyline reduced total pulmonary resistance (TPR) (Fig. 4B). To further elucidate the origin of the reduced RV afterload, we measured pulmonary vascular remodelling (Fig. 4C). Clorgyline increased the percentage of open vessels, and reduced the remodelled and occluded vessels (Fig. 4D). Further quantification on the thickness of the pulmonary vascular layers revealed that clorgyline reversed vascular remodelling in the intima layer, but not the media layer (Fig. 4E, F). Consistently, as shown by PCNA immunofluorescence, clorgyline reduced proliferation in the intima layer, without affecting the proliferation of medial PSMCs (Fig. 4G-I). Cleaved caspase-3 western blots of whole lung lysates revealed no differences in apoptotic rates after clorgyline treatment (Fig. 4J).



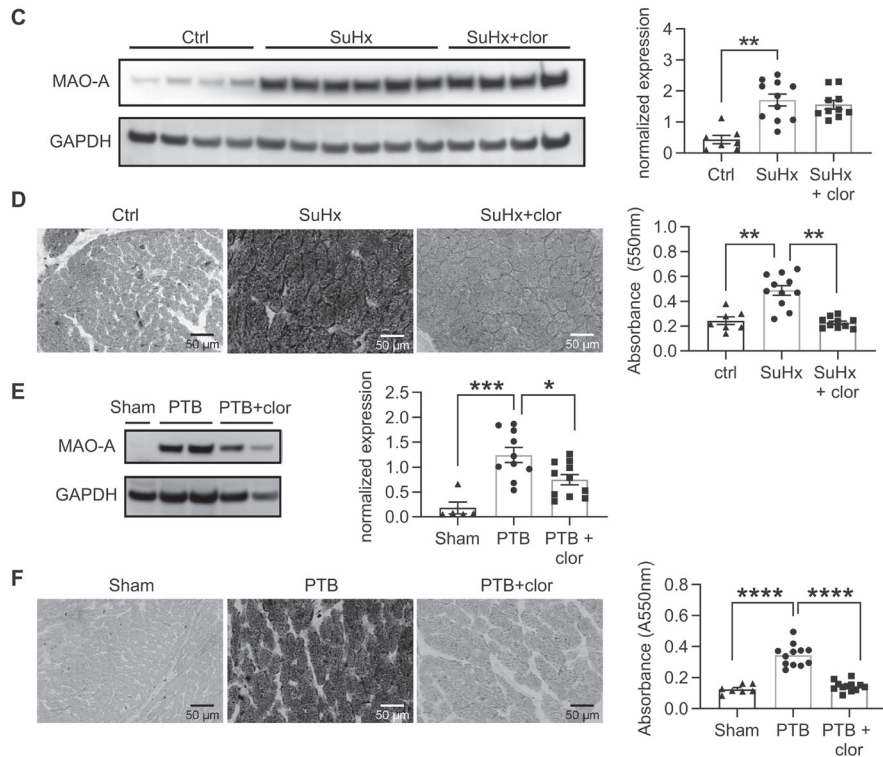


Figure 3 – MAO-A is increased in the RV from experimental PAH. (A) Western blot analysis reveals that MAO-A expression has no difference in the RVs between end stage PAH patients and MI patients. MI: n = 3; PH: n = 8. (B) Histochemistry staining reveals no difference in MAO-A activity between the RVs from PAH patients and MI patients. Scale bar 50  $\mu$ m. Incubation time: 90 minutes. MI: n = 3; PH: n = 5. (C) MAO-A expression was increased in the RV from SuHx rats, and it was not affected by clorgyline treatment. ctrl: n = 7, SuHx: n = 11, SuHx+clor: n = 10. (D) MAO-A activity was increased in SuHx RV compared to ctrl RV, and it was normalized by clorgyline treatment. Scale bar 50  $\mu$ m. Incubation time: 90 minutes. ctrl: n = 7, SuHx: n = 11, SuHx+clor: n = 10. (E) MAO-A expression was increased in the RV from PTB rats. Sham: n = 5, PTB: n = 10, PTB+clor: n = 11. (F) MAO-A activity was increased in the RV from PTB rats, and it was normalized after clorgyline treatment. Scale bar 50  $\mu$ m. Incubation time: 60 minutes. Sham: n = 7, PTB: n = 12, PTB+clor: n = 12. All data are presented as mean  $\pm$  SEM; One-way ANOVA followed by Bonferroni posthoc comparison between ctrl and SuHx, SuHx and SuHx+clor. \* $p$ <0.05, \*\* $p$ <0.01, \*\*\* $p$ <0.001, \*\*\*\* $p$ <0.0001. MI = myocardial infarction.

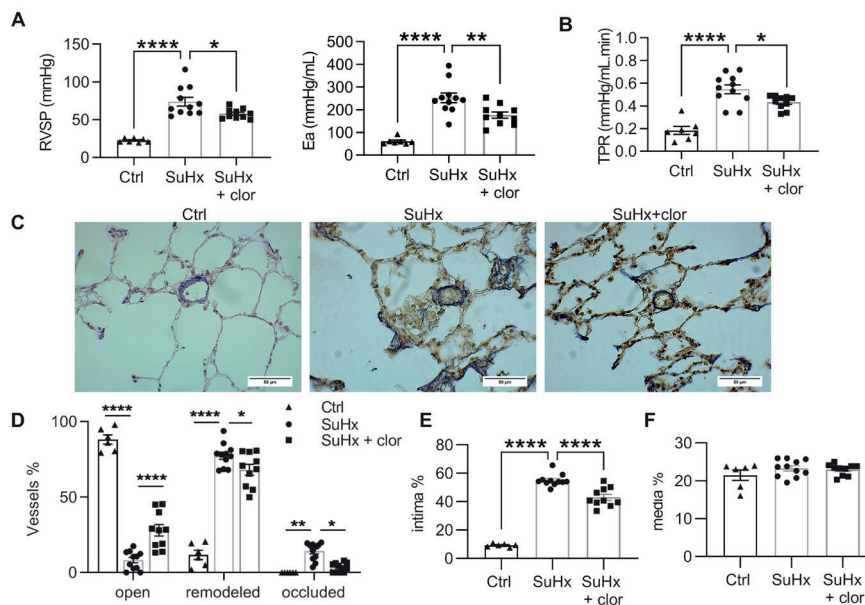
### Clorgyline treatment reduces oxidative stress in the pulmonary vasculature of rats with SuHx-induced PAH

Since MAO-A is an important ROS source (4, 5), we examined the effect of clorgyline on oxidative stress. Immunofluorescence staining with anti-8-Oxo-2'-deoxyguanosine (8-OHdG) revealed increased oxidative stress in the lungs and

pulmonary vasculatures of SuHx rats, and clorgyline normalized oxidative stress in the pulmonary vasculatures (Fig. 5A, B). However, no differences in 8-OHdG or nitrotyrosine levels in whole lung tissues were found after clorgyline treatment (Fig. 5C, D).

### Clorgyline treatment improves RV stiffness, relaxation, and RV hypertrophy in rats with SuHx-induced PAH

Consistent with the findings in the lungs, clorgyline normalized MAO-A activity in the RV of SuHx rats, while MAO-A protein expression was unaffected (Fig. 3C, D). Clorgyline improved RV stiffness and relaxation, as shown by reduced end diastolic elastance (Eed) and dP/dt(min), respectively (Fig. 6A). While dP/dt(max) was reduced by clorgyline, no difference was observed in load-independent RV contractility, as shown by end systolic elastance (Ees) (Supplement: Fig. E4A, Fig. 6A). Further echocardiography analysis showed no differences in tricuspid annular plane systolic excursion (TAPSE), RV end diastolic diameter (RVEDD), stroke volume (SV) (Fig. 6B), heart rate (HR) or cardiac output (CO) (data not shown). Clorgyline reversed RV hypertrophy as shown by reduced Fulton index and RV myocardial cross-sectional area (CSA) (Fig. 6C-E). By contrast, clorgyline had no effect on RV fibrosis, apoptosis or inflammation (Fig. 6F, G, Supplement: Fig. E4B, C).



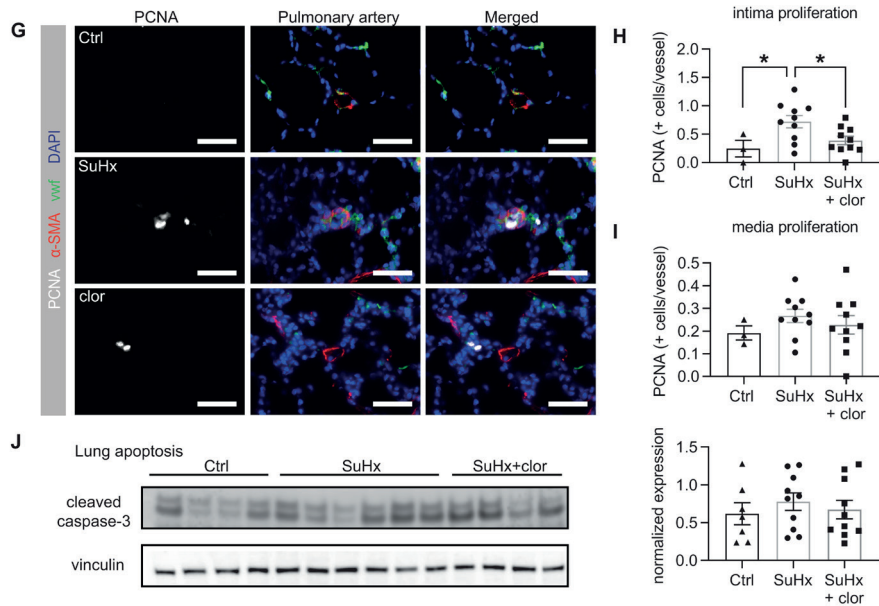
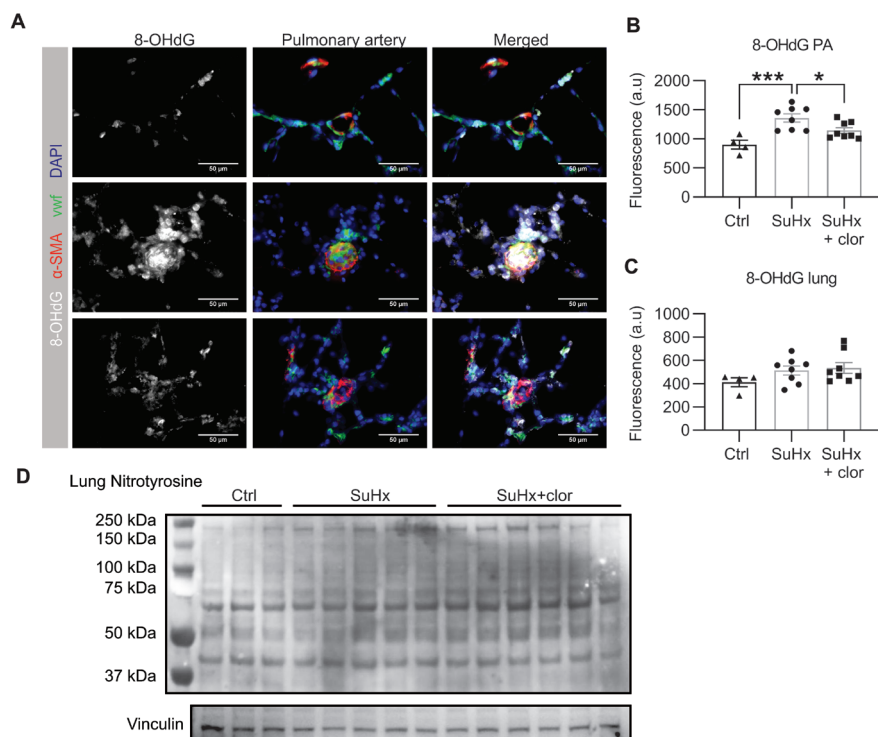


Figure 4 – **Clorgyline treatment reduced RV afterload in SuHx rats by reversing pulmonary vascular remodeling and proliferation.** (A) Pressure-volume loop analysis reveals decreased RVSP and RV afterload (Ea) after clorgyline treatment. ctrl: n = 7, SuHx: n = 11, SuHx+clor: n = 10. (B) Echocardiography analysis reveals reduced TPR after clorgyline treatment. ctrl: n = 7, SuHx: n = 11, SuHx+clor: n = 10. (C) Representative images of pulmonary vasculatures by elastic van Gieson staining. Scale bar 50  $\mu$ m. (D-F) Quantification of the histology images shows increased open vessels, reduced remodeled and occluded vessels in the lungs (D), reduced intima layer thickness (E), and unchanged media layer thickness (F) after clorgyline treatment. ctrl: n = 6, SuHx: n = 11, SuHx+clor: n = 10. (G) Representative lung immunofluorescence staining for proliferation with PCNA.  $\alpha$ -SM (red), vwf (green) and DAPI (blue) were co-stained with PCNA (white). Scale bar 50  $\mu$ m. (H, I) Quantification of PCNA positive cells shows reduced proliferation in intima layer of pulmonary vasculatures after clorgyline treatment, but not in the media layer. ctrl: n = 3, SuHx: n = 10, SuHx+clor: n = 10. (J) Western blot analysis on whole lung homogenates shows no difference in apoptotic rates between the groups. ctrl: n = 7, SuHx: n = 10, SuHx+clor: n = 10. All data are presented as mean  $\pm$  SEM; One-way ANOVA followed by Bonferroni posthoc comparison between ctrl and SuHx, SuHx and SuHx+clor. \* $p$ <0.05, \*\* $p$ <0.01, \*\*\*\* $p$ <0.0001.



**Figure 5. Clorgyline treatment reduced pulmonary vascular oxidative stress in SuHx rats.** (A) Representative lung immunofluorescence staining for oxidative stress with 8-OHdG.  $\alpha$ -SM (red), vwF (green) and DAPI (blue) were co-stained with 8-OHdG (white). Scale bar 50  $\mu$ m. (B) Quantification of fluorescence within the pulmonary vasculatures shows increased 8-OHdG in SuHx group compared to ctrl, and it was reduced by clorgyline. ctrl: n = 4, SuHx: n = 8, SuHx+clor: n = 8. (C) Quantification of 8-OHdG fluorescence shows no difference in the whole lung area between the groups. ctrl: n = 4, SuHx: n = 8, SuHx+clor: n = 8. (D) Western blot for oxidative stress with nitrotyrosine on whole lung homogenates did not reveal any difference between ctrl and SuHx rats, or between SuHx rats and SuHx rats treated with clorgyline. All data are presented as mean  $\pm$  SEM; One-way ANOVA followed by Bonferroni posthoc comparison between ctrl and SuHx, SuHx and SuHx+clor. \* $p$ <0.05, \*\*\* $p$ <0.001.

### **Clorgyline treatment has no direct effects on RV dysfunction induced by PTB**

To investigate the direct effects of MAO-A inhibitor on the RV, we treated PTB rats with clorgyline. Clorgyline decreased not only MAO-A activity, but also expression (Fig. 3E, F, Supplement: Fig. E5A). As expected, pressure-volume loop analysis showed increased RVSP and RV afterload in PTB rats (Supplement: Fig. E5B). Body weight at the end of the study was lower in clorgyline treated rats (data not shown), therefore we used body surface area (BSA) to index all hemodynamic parameters where applicable (23). Signs of RV dysfunction in PTB rats were confirmed by decreased TAPSE and RV relaxation (dP/dt min), while RV stiffness (Eed index), contractility (Ees index) and SV index (SVI) were preserved (Fig. 7 A, B), as well as HR and the resulting CO (data not shown). No difference was observed in RV function due to clorgyline treatment (Fig. 7A, B, Supplement: Fig. E5B).

Further measurement of RV remodelling revealed that clorgyline did not delay the progression of RV dilation, as shown by unaltered RVEDD index (RVEDDI) and RV end systolic diameter index (RVESDI) over time (Fig. 7A). RV hypertrophy was confirmed in PTB rats as shown by increased Fulton index and RV myocardial CSA, and no difference was found after clorgyline treatment (Fig. 7C-E). RV fibrosis and RV apoptosis were not significantly increased in PTB rats, and were not affected by clorgyline (Fig. 7E-G). Since MAO-A is bound to the outer mitochondrial membrane, produced ROS has its effects on the mitochondria (24). No differences in mitochondrial efficiency were found between the groups (Supplement: Fig. E5C). Collectively, we found that clorgyline had neither a beneficial nor detrimental effect on the RV in PTB rats.

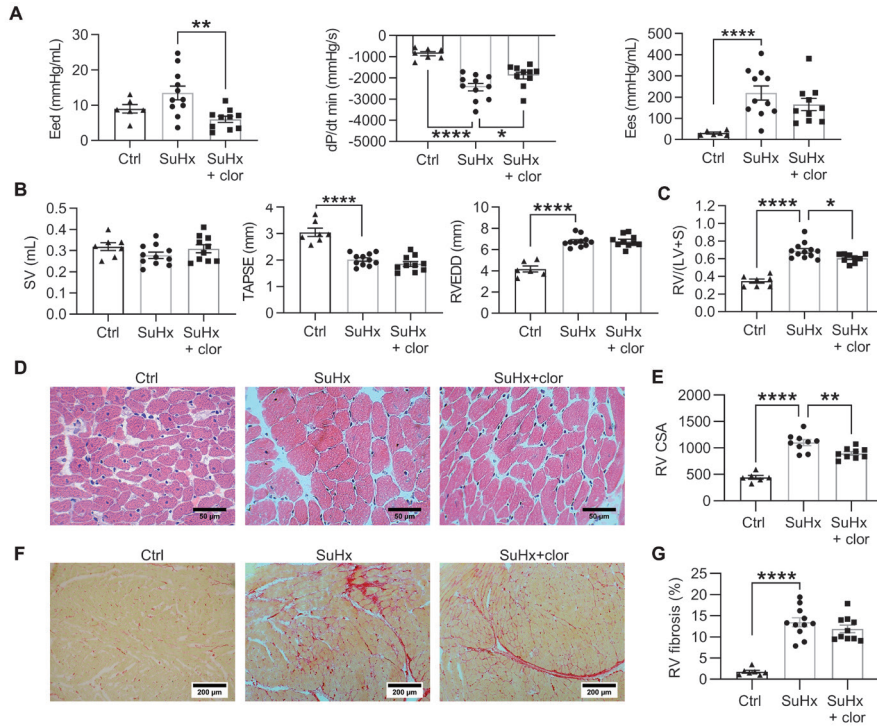
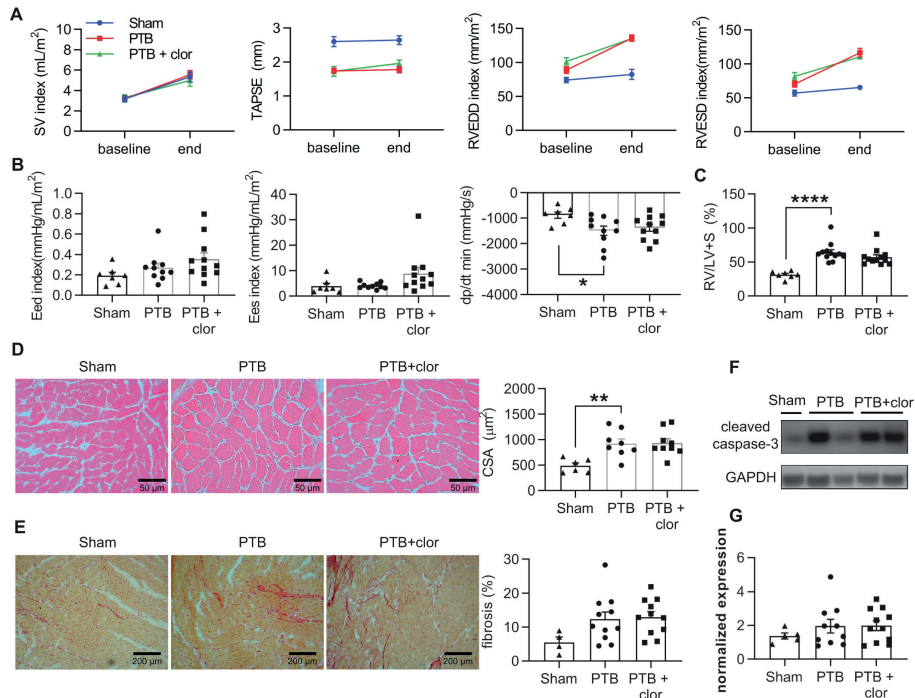


Figure 6 – Clorgyline treatment improved RV stiffness, relaxation and RV hypertrophy in SuHx rats.

(A) Pressure-volume loop analysis reveals that clorgyline reduced RV stiffness (Eed) and improved RV relaxation (dp/dt min). No difference was observed in RV contractility (Ees). Eed and Ees, ctrl: n = 6, SuHx: n = 11, SuHx+clor: n = 10. dp/dt min, ctrl: n = 7, SuHx: n = 11, SuHx+clor: n = 10. (B) No difference was observed in SV, TAPSE and RVEDD after clorgyline treatment by echocardiography analysis. ctrl: n = 7, SuHx: n = 11, SuHx+clor: n = 10. (C) Clorgyline treatment reduced Fulton index. ctrl: n = 7, SuHx: n = 12, SuHx+clor: n = 9. (D) Representative images of RV cardiomyocytes by H&E staining. Scale bar 50  $\mu$ m. (E) Clorgyline reduced RV hypertrophy as shown by reduced RV myocardial CSA. ctrl: n = 6, SuHx: n = 9, SuHx+clor: n = 9. (F) Representative images of RV fibrosis by picrosirius red staining. Scale bar 200  $\mu$ m. (G) No difference was observed by RV fibrosis quantification. ctrl: n = 7, SuHx: n = 11, SuHx+clor: n = 10. All data are presented as mean  $\pm$  SEM; One-way ANOVA followed by Bonferroni posthoc comparison between ctrl and SuHx, SuHx and SuHx+clor. \* $p$ <0.05, \*\* $p$ <0.01.

## Increased MAO-A activity promotes progression of pulmonary arterial hypertension



**Figure 7 – Clorgyline treatment has no detrimental effect on PTB induced RVF rats.** (A) Echocardiography reveals unaltered RV function as shown by SV index and TAPSE (Sham: n = 7, PTB: n = 12, PTB+clor: n = 12), and unaltered RV remodeling as shown by RVEDD index and RVESD index (Sham: n = 7, PTB: n = 11, PTB+clor: n = 12). (B) No difference was observed by clorgyline treatment in RV stiffness (Eed index), RV contractility (Ees index) and RV relaxation (dp/dt min), as shown by pressure-volume loop analysis. Sham: n = 7, PTB: n = 10, PTB+clor: n = 11. (C) Clorgyline did not affect Fulton index. Sham: n = 7, PTB: n = 12, PTB+clor: n = 12. (D) Representative images of RV cardiomyocytes by H&E staining. Scale bar 50 μm. RV hypertrophy was observed in PTB rats by quantification of RV myocardial CSA, and it was not affected by clorgyline treatment. Sham: n = 6, PTB: n = 8, PTB+clor: n = 9. (E) Representative images of RV fibrosis by picrosirius red staining. Scale bar 200 μm. No difference was observed in RV fibrosis between the groups. Sham: n = 6, PTB: n = 12, PTB+clor: n = 12. (F) Representative images of cleaved caspase-3 western blot on RV homogenates, with GAPDH as loading control. (G) Quantification of cleaved caspase-3 reveals that RV apoptosis has no difference between the groups. All data are presented as mean ± SEM; One-way ANOVA followed by Bonferroni posthoc comparison between ctrl and PTB, PTB and PTB+clor. Kruskal-Wallis test followed by Dunn's multiple comparison test was used for data that was not normally distributed. Two-way ANOVA for repeated measurements followed by Sidak's posthoc was used for repeated data of echocardiography analysis. \*p<0.05, \*\*p<0.01, \*\*\*\*p<0.0001.

## Discussion

In the present study, we demonstrated for the first time that MAO-A is increased in the pulmonary vasculature of PAH patients. Moreover, our data indicate that increased pulmonary vascular MAO-A activity is involved in the progression of PAH, and that MAO-A inhibition may help to reverse pulmonary vascular remodelling, thereby benefiting the RV.

### MAO-A up-regulation in the pulmonary vasculature in PAH

Previous studies have demonstrated that MAOs can be detected in several tissues, including the human and rodent lungs and heart (7, 8, 12). Consistent with these findings, we found that MAO-A was widely present in human and rat lungs and expressed within all layers of the vascular wall.

Increased vascular MAO-A activity has been implicated in different vascular diseases, including experimentally induced hypertension, inflammation and diabetes (12, 25-27). 5-HT, one of the main substrates of MAO-A is increased in PAH patients and experimentally induced PH, and plays a crucial role (10, 28). 5-HT is mostly metabolized into 5-Hydroxyindoleacetic acid (5-HIAA) by MAO-A in hepatic and lung ECs. A previous study suggested a normal or increased 5-HT metabolism in PAH patients, as plasma 5-HIAA remained elevated in PAH patients before and during epoprostenol treatment, which was expected to reduce platelet release of 5-HT (10). Consistently, here we show for the first time that MAO-A expression is up-regulated in the intima and media layers of the pulmonary vasculature of PAH patients, as well as in rats with experimentally induced PAH. Consistent with a previous study (8), we found that MAO-A is expressed in several other, non-vascular cell types in the lungs. However, upregulation of MAO-A could not be confirmed in whole lung lysates from PAH patients or rats with SuHx-induced PAH, nor in isolated MVECs and PAECs derived from PAH patient lungs. This study is the first to show increased MAO-A activity in the pulmonary vessels in experimental PAH. However, we were not able to perform activity measurements in human lungs because no cryosection samples were available. Therefore, the role of MAO-A in human PAH remains uncertain, and further studies are needed to investigate the relevance of MAO-A inhibition as a therapeutic target.

### MAO-A inhibitor as treatment for experimentally induced PH.

In PAH, increased ROS production has been found to be one of the stimuli responsible for pulmonary vascular remodelling, through EC dysfunction and SMC proliferation (29). Due to the intense crosstalk between different ROS sources in the cell, inhibition of a single ROS source can abolish oxidative stress, which make MAOs promising treatment targets for diseases related to oxidative injury (30, 31).

Increased MAO-A in diseased vessels can impair vasorelaxation by increasing ROS production, and inhibiting MAO-A can reduce ROS formation, increase cyclic guanosine monophosphate levels and restore vasorelaxation (25-27). More interestingly, increased MAO-A can induce proliferation in SMCs by increasing ROS production, which is a key feature of pulmonary vascular remodelling in PAH (13, 32). Based on those evidences, here we chose to test an irreversible MAO-A inhibitor clorgyline on SuHx induced PAH rat model, which can selectively inhibit MAO-A activity at a low concentration (6). As expected, we found that clorgyline reduced MAO-A activity in the lungs and RVs in the rats, and partly reversed established PAH in SuHx rats as shown by reduced RVSP, RV afterload and TPR. Moreover, clorgyline is beneficial to the RV as shown by reduced RV stiffness, improved RV relaxation and reversed RV hypertrophy in SuHx rats.

Further histology analysis revealed that clorgyline reversed pulmonary vascular remodelling, in particular the intima layer remodelling, indicating the role of MAO-A in EC function in PAH. It is further supported by our finding that clorgyline reduced proliferation in the intima layer of the pulmonary vasculatures. Moreover, we found that clorgyline reduced pulmonary vascular oxidative stress *in vivo* as shown by decreased 8-OHdG level. Our results on the intima layer of the vessels are in line with previous findings of reduced H<sub>2</sub>O<sub>2</sub> production in the endothelium *ex vivo* upon clorgyline administration (26, 27). As such, the role of H<sub>2</sub>O<sub>2</sub> as a stimulus for EC proliferation was confirmed (33).

Though it was shown by a previous study that clorgyline reduced proliferation in rabbit femoral SMCs and human PSMCs, in this study no difference was observed in the media layer remodelling after clorgyline treatment, neither in the media layer proliferation (13, 34). This might be due to the short period of the treatment. In addition to increased ROS production, it has to be noticed that increased MAO-A can also produce aldehyde, which is toxic for the biological system and associated with oxidative stress (35). Therefore, aldehyde could be also involved in the mechanisms underlying the effects of clorgyline treatment.

### **MAO-A up-regulation in the RV in PAH**

Here we find for the first time that MAO-A expression and activity is upregulated in the RV in experimental PAH and RV failure (SuHx and PTB). This finding is in line with a previous study reporting that MAO-A activity is up-regulated in the RV wall and isolated papillary muscles of monocrotaline (MCT) induced PH rats (36). The up-regulation of MAO-A in cardiomyocytes can be explained by the hyperactivation of SNS and renin angiotensin-aldosterone system (RAAS), as revealed by several studies on experimentally induced LV failure models (15, 37). Similarly, in PAH patients and experimentally induced PH, hyperactivation of SNS and RAAS has also been observed (38, 39). NE, as a main substrate of MAO-A, was found to be

increased in the plasma of PAH patients with end-stage heart failure, and it is correlated with pulmonary artery pressure, cardiac index and pulmonary vascular resistance in PAH patients (14, 40, 41). Moreover, NE was found to induce a rise in MAO-A expression with markedly increased ROS production in cardiomyocytes (15).

Here we compared RV MAO-A level of end-stage PAH patients with MI (outside the RV) patients and were unable to confirm the strong upregulation of MAO-A as observed in the animal models. Several factors may have contributed to the apparent discrepancy between the animal and human data. Firstly, we used autopsy tissue from patients, which represents end-stage RV failure, whereas the SuHx and PTB rats all survived until the end of the experiment and thus represent less severe RV failure. Secondly, limitations in tissue harvesting protocols, variable intervals between time of death and autopsy, and prolonged storage of human samples at  $-80^{\circ}\text{C}$  may have affected MAO-A levels in autopsy specimens. Moreover, in rodent hearts MAO-A is expressed much more than MAO-B, whereas in the human heart MAO-A and -B are equally active (8, 42). Therefore, the relative role of cardiac MAO-A could be different in humans and rats. Further research into the contribution of both MAO-A and -B and their interactions should reveal their relative importance in humans.

### **MAO-A inhibitor as treatment on the RV in PAH**

In PAH, the survival is determined by the condition of the RV rather than the degree of pulmonary vascular resistance (43). Therefore, it is important for drugs used in the treatment of PAH to be beneficial or at least non-toxic to the RV. Multiple studies highlighted MAO-A as an important source of ROS in the myocardium (15-17). Both pharmacological and genetic inhibition of MAO-A was found to be beneficial in various experimental heart failure, including those based on ischemia/reperfusion injury (16, 17), LV pressure overload (15, 18) and diabetes (19, 20). More interestingly, it was shown that clorgyline can decrease the basal rate of oxygen consumption of RV papillary muscles in MCT induced PH rats (36). At the other end of the scale, cardiac-specific MAO-A overexpression enhanced  $\text{H}_2\text{O}_2$  formation leading to cardiomyocyte necrosis and ventricular failure with mitochondrial impairment (18). In this study, we found that clorgyline is beneficial to the RV in SuHx-PAH rats, by reducing stiffness, improving relaxation and reducing hypertrophy. Though fibrosis and apoptosis are closely related to oxidative stress, here we did not find any effect of clorgyline on SuHx RV fibrosis or apoptosis, which could be due to the short treatment duration of 2 weeks.

A previous study showed that LV hypertrophy was exacerbated in MAO-A knockout mice subjected to transverse aortic constriction (TAC) due to hyperactivation of 5-HT<sub>2A</sub> receptors (44). Therefore, despite the improved RV function found in the

SuHx-PAH model, it is crucial to confirm the safety of MAO-A inhibitor on the RV. Here we treated PTB rats with clorgyline to investigate the direct effect on the RV. Unlike the results on SuHx-PAH or TAC model, we did not observe any beneficial or detrimental effects of clorgyline on the RV. Therefore, the beneficial effects of clorgyline on the RV of SuHx rats can be mainly due to reduced RV afterload, and possibly reduced RV oxidative stress. A previous study revealed that RV oxidative stress is largely increased in SuHx RV but unchanged in PTB (45), which may explain the negative findings on RV fibrosis and apoptosis, which are closely related to oxidative stress. Besides the different responses to pressure overload between RV and LV (46), it has to be noted that the starting time point of the drug administration in this study is different from the studies on TAC model. In this reversal study, clorgyline treatment started two weeks after PTB surgery, when the rats showed signs of RV dysfunction, while clorgyline was given to the TAC mice directly after TAC surgery as prevention.

### Limitations

Clorgyline is no longer used in the clinic due to the "cheese-effect", which can cause hypertensive crises after ingestion of food rich in tyramine (6). Although it limits the direct translation to the clinic, we believe it is justified for this proof of principle study, as clorgyline is a specific and selective MAO-A inhibitor. The introduction of a new generation of reversible MAO-A inhibitors can avoid the adverse cheese effect. Therefore, it is worth for future research to test those clinically approved new generation MAO-A inhibitors in combination with other PAH drugs, as well as the development of lung-specific delivery methods to achieve efficiency at low drug concentration.

The use of human samples obtained at autopsy clearly has limitations. The duration of storage of the cardiac samples ranged between 2-12 years at -80°C before analysis of MAO-A activity and expression. Also, the exact times between death and autopsy are unknown. However, MAO-A expression and activity is closely regulated by neurohormonal activity which is known to be increased in PAH. Therefore, the present results on the inhibition of MAO-A activity may still be of clinical significance in PAH patients.

The present study used two animal models. The SuHx rat model was used to investigate the effect of MAO-A inhibition on the pulmonary vasculature, and the PTB rat model to study the effect of MAO-A inhibition on RV failure. We believe that a treatment study with MCT rats may not add much valuable information, since the SuHx model provides a much better representation of vascular findings in human PAH.

## Conclusion

In conclusion, MAO-A is increased locally in the pulmonary vasculatures of PAH patients and in the pulmonary vasculature and RV of experimentally induced PH models. Treatment with MAO-A inhibitor clorgyline can partly reverse RV afterload and pulmonary vascular remodelling in established experimental PH by reducing pulmonary vascular proliferation and oxidative stress. Importantly, while it has no direct effect on cardiac function, it is beneficial to the RV by reducing RV afterload. Collectively, MAO-A seems to be involved in pulmonary vascular remodelling and further investigations should reveal the relevance of MAO-A in different stages of human PAH.

## Acknowledgements

The authors wish to thank Peter ten Dijke for his input and discussion.

HJB, AVN and FSdM were supported by the Netherlands CardioVascular Research Initiative: The Dutch Heart Foundation, Dutch Federation of University Medical Centres, the Netherlands Organization for Health Research and Development, and the Royal Netherlands Academy of Sciences (CVON-2012-08 PHAEDRA, CVON-2018-29 PHAEDRA-IMPACT, CVON-2017-10 Dolphin-Genesis). HJB and AVN were supported by research grants from Actelion, GSK and Ferrer (Therabel). EP, XS, AVN and FSdM were further supported by The Netherlands Organization for Scientific Research (NWO-VICI: 918.16.610, NWO-VIDI: 917.18.338). FSdM was supported by the Dutch Heart Foundation Dekker senior post-doc grant (2018T059).

## References

1. Rubin LJ. Primary pulmonary hypertension. *N Engl J Med* 1997; 336: 111-117.
2. Lajoie AC, Lauziere G, Lega JC, Lacasse Y, Martin S, Simard S, Bonnet S, Provencher S. Combination therapy versus monotherapy for pulmonary arterial hypertension: a meta-analysis. *Lancet Respir Med* 2016; 4: 291-305.
3. Fulton DJR, Li X, Bordan Z, Haigh S, Bentley A, Chen F, Barman SA. Reactive Oxygen and Nitrogen Species in the Development of Pulmonary Hypertension. *Antioxidants (Basel)* 2017; 6.
4. Kaludercic N, Mialet-Perez J, Paolocci N, Parini A, Di Lisa F. Monoamine oxidases as sources of oxidants in the heart. *J Mol Cell Cardiol* 2014; 73: 34-42.
5. Deshwal S, Di Sante M, Di Lisa F, Kaludercic N. Emerging role of monoamine oxidase as a therapeutic target for cardiovascular disease. *Curr Opin Pharmacol* 2017; 33: 64-69.
6. Youdim MB, Edmondson D, Tipton KF. The therapeutic potential of monoamine oxidase inhibitors. *Nat Rev Neurosci* 2006; 7: 295-309.
7. Holschneider DP, Kumazawa T, Chen K, Shih JC. Tissue-specific effects of estrogen on monoamine oxidase A and B in the rat. *Life Sci* 1998; 63: 155-160.
8. Sivasubramaniam SD, Finch CC, Rodriguez MJ, Mahy N, Billett EE. A comparative study of the expression of monoamine oxidase-A and -B mRNA and protein in non-CNS human tissues. *Cell Tissue Res* 2003; 313: 291-300.
9. MacLean MMR. The serotonin hypothesis in pulmonary hypertension revisited: targets for novel therapies (2017 Grover Conference Series). *Pulm Circ* 2018; 8: 2045894018759125.
10. Kereveur A, Callebert J, Humbert M, Herve P, Simonneau G, Launay JM, Drouet L. High plasma serotonin levels in primary pulmonary hypertension. Effect of long-term epoprostenol (prostacyclin) therapy. *Arterioscler Thromb Vasc Biol* 2000; 20: 2233-2239.
11. Eddahibi S, Guignabert C, Barlier-Mur AM, Dewachter L, Fadel E, Dartevielle P, Humbert M, Simonneau G, Hanoun N, Saurini F, Hamon M, Adnot S. Cross talk between endothelial and smooth muscle cells in pulmonary hypertension: critical role for serotonin-induced smooth muscle hyperplasia. *Circulation* 2006; 113: 1857-1864.
12. Lighezan R, Sturza A, Duicu OM, Ceausu RA, Vaduva A, Gaspar M, Feier H, Vaida M, Ivan V, Lighezan D, Muntean DM, Mornos C. Monoamine oxidase inhibition improves vascular function in mammary arteries from nondiabetic and diabetic patients with coronary heart disease. *Can J Physiol Pharmacol* 2016; 94: 1040-1047.
13. Coatrieux C, Sanson M, Negre-Salvayre A, Parini A, Hannun Y, Itohara S, Salvayre R, Auge N. MAO-A-induced mitogenic signaling is mediated by reactive oxygen species, MMP-2, and the sphingolipid pathway. *Free Radic Biol Med* 2007; 43: 80-89.
14. Mak S, Witte KK, Al-Hesayen A, Granton JJ, Parker JD. Cardiac sympathetic activation in patients with pulmonary arterial hypertension. *Am J Physiol Regul Integr Comp Physiol* 2012; 302: R1153-1157.
15. Kaludercic N, Takimoto E, Nagayama T, Feng N, Lai EW, Bedja D, Chen K, Gabrielson KL, Blakely RD, Shih JC, Pacak K, Kass DA, Di Lisa F, Paolocci N. Monoamine oxidase A-mediated enhanced catabolism of norepinephrine contributes to adverse remodeling and pump failure in hearts with pressure overload. *Circ Res* 2010; 106: 193-202.

## CHAPTER 5

16. Bianchi P, Kunduzova O, Masini E, Cambon C, Bani D, Raimondi L, Seguelas MH, Nistri S, Colucci W, Leducq N, Parini A. Oxidative stress by monoamine oxidase mediates receptor-independent cardiomyocyte apoptosis by serotonin and postischemic myocardial injury. *Circulation* 2005; 112: 3297-3305.
17. Pchejetski D, Kunduzova O, Dayon A, Calise D, Seguelas MH, Leducq N, Seif I, Parini A, Cuvillier O. Oxidative stress-dependent sphingosine kinase-1 inhibition mediates monoamine oxidase A-associated cardiac cell apoptosis. *Circ Res* 2007; 100: 41-49.
18. Villeneuve C, Guilbeau-Frugier C, Sicard P, Lairez O, Ordener C, Duparc T, De Paulis D, Couderc B, Spreux-Varoquaux O, Tortosa F, Garnier A, Knauf C, Valet P, Borchi E, Nediani C, Gharib A, Ovize M, Delisle MB, Parini A, Mialet-Perez J. p53-PGC-1 $\alpha$  pathway mediates oxidative mitochondrial damage and cardiomyocyte necrosis induced by monoamine oxidase-A upregulation: role in chronic left ventricular dysfunction in mice. *Antioxid Redox Signal* 2013; 18: 5-18.
19. Umbarkar P, Singh S, Arkat S, Bodhankar SL, Lohidasan S, Sitasawad SL. Monoamine oxidase-A is an important source of oxidative stress and promotes cardiac dysfunction, apoptosis, and fibrosis in diabetic cardiomyopathy. *Free Radic Biol Med* 2015; 87: 263-273.
20. Deshwal S, Forkink M, Hu CH, Buonincontri G, Antonucci S, Di Sante M, Murphy MP, Paolucci N, Mochly-Rosen D, Krieg T, Di Lisa F, Kaludercic N. Monoamine oxidase-dependent endoplasmic reticulum-mitochondria dysfunction and mast cell degranulation lead to adverse cardiac remodeling in diabetes. *Cell Death Differ* 2018; 25: 1671-1685.
21. Kurakula K, Sun XQ, Happe C, da Silva Goncalves Bos D, Szulcek R, Schaliij I, Wiesmeijer KC, Lodder K, Tu L, Guignabert C, de Vries CJM, de Man FS, Vonk Noordegraaf A, Ten Dijke P, Goumans MJ, Bogaard HJ. Prevention of progression of pulmonary hypertension by the Nur77 agonist 6-mercaptopurine: role of BMP signalling. *Eur Respir J* 2019; 54.
22. Andersen S, Axelsen JB, Ringgaard S, Nyengaard JR, Hyldebrandt JA, Bogaard HJ, de Man FS, Nielsen-Kudsk JE, Andersen A. Effects of combined angiotensin II receptor antagonism and neprilysin inhibition in experimental pulmonary hypertension and right ventricular failure. *Int J Cardiol* 2019; 293: 203-210.
23. Gouma E, Simos Y, Verginadis I, Lykoudis E, Evangelou A, Karkabounas S. A simple procedure for estimation of total body surface area and determination of a new value of Meeh's constant in rats. *Lab Anim* 2012; 46: 40-45.
24. Hauptmann N, Grimsby J, Shih JC, Cadenas E. The metabolism of tyramine by monoamine oxidase A/B causes oxidative damage to mitochondrial DNA. *Arch Biochem Biophys* 1996; 335: 295-304.
25. Poon CC, Seto SW, Au AL, Zhang Q, Li RW, Lee WY, Leung GP, Kong SK, Yeung JH, Ngai SM, Ho HP, Lee SM, Chan SW, Kwan YW. Mitochondrial monoamine oxidase-A-mediated hydrogen peroxide generation enhances 5-hydroxytryptamine-induced contraction of rat basilar artery. *Br J Pharmacol* 2010; 161: 1086-1098.
26. Sturza A, Leisegang MS, Babelova A, Schroder K, Benkhoff S, Loot AE, Fleming I, Schulz R, Muntean DM, Brandes RP. Monoamine oxidases are mediators of endothelial dysfunction in the mouse aorta. *Hypertension* 2013; 62: 140-146.
27. Sturza A, Duicu OM, Vaduva A, Danila MD, Noveanu L, Varro A, Muntean DM. Monoamine oxidases are novel sources of cardiovascular oxidative stress in experimental diabetes. *Can J Physiol Pharmacol* 2015; 93: 555-561.

28. Hervé P LJ, Scrobobaci ML, Brenot F, Simonneau G, Petitpretz P, Poubreau P, Cerrina J, Duroux P, Drouet L. Increased plasma serotonin in primary pulmonary hypertension. *Am J Med* 1995; 99: 249-254.
29. Aggarwal S, Gross CM, Sharma S, Fineman JR, Black SM. Reactive oxygen species in pulmonary vascular remodeling. *Compr Physiol* 2013; 3: 1011-1034.
30. Kaludercic N, Carpi A, Menabo R, Di Lisa F, Paolocci N. Monoamine oxidases (MAO) in the pathogenesis of heart failure and ischemia/reperfusion injury. *Biochim Biophys Acta* 2011; 1813: 1323-1332.
31. Duicu OM, Lighezan R, Sturza A, Ceausu RA, Borza C, Vaduva A, Noveanu L, Gaspar M, Ionac A, Feier H, Muntean DM, Mornos C. Monoamine Oxidases as Potential Contributors to Oxidative Stress in Diabetes: Time for a Study in Patients Undergoing Heart Surgery. *Biomed Res Int* 2015; 2015: 515437.
32. Toshner M, Voswinckel R, Southwood M, Al-Lamki R, Howard LS, Marchesan D, Yang J, Suntharalingam J, Soon E, Exley A, Stewart S, Hecker M, Zhu Z, Gehling U, Seeger W, Pepke-Zaba J, Morrell NW. Evidence of dysfunction of endothelial progenitors in pulmonary arterial hypertension. *Am J Respir Crit Care Med* 2009; 180: 780-787.
33. Porter KM, Kang BY, Adesina SE, Murphy TC, Hart CM, Sutliff RL. Chronic hypoxia promotes pulmonary artery endothelial cell proliferation through H<sub>2</sub>O<sub>2</sub>-induced 5-lipoxygenase. *PLoS One* 2014; 9: e98532.
34. Lawrie A, Spiekerkoetter E, Martinez EC, Ambartsumian N, Sheward WJ, MacLean MR, Harmar AJ, Schmidt AM, Lukanidin E, Rabinovitch M. Interdependent serotonin transporter and receptor pathways regulate S100A4/Mts1, a gene associated with pulmonary vascular disease. *Circ Res* 2005; 97: 227-235.
35. Chen CH, Budas GR, Churchill EN, Disatnik MH, Hurley TD, Mochly-Rosen D. Activation of aldehyde dehydrogenase-2 reduces ischemic damage to the heart. *Science* 2008; 321: 1493-1495.
36. van Eif VW, Bogaards SJ, van der Laarse WJ. Intrinsic cardiac adrenergic (ICA) cell density and MAO-A activity in failing rat hearts. *J Muscle Res Cell Motil* 2014; 35: 47-53.
37. Raasch W BT, Gieselberg A, Dendorfer A, Dominiak P. Angiotensin I-converting enzyme inhibition increases cardiac catecholamine content and reduces monoamine oxidase activity via an angiotensin type 1 receptor-mediated mechanism. *J Pharmacol Exp Ther* 2002; 300: 428-434.
38. Ciarka A, Doan V, Velez-Roa S, Naeije R, van de Borne P. Prognostic significance of sympathetic nervous system activation in pulmonary arterial hypertension. *Am J Respir Crit Care Med* 2010; 181: 1269-1275.
39. Piao L, Fang YH, Parikh KS, Ryan JJ, D'Souza KM, Theccanat T, Toth PT, Pogoriler J, Paul J, Blaxall BC, Akhter SA, Archer SL. GRK2-mediated inhibition of adrenergic and dopaminergic signaling in right ventricular hypertrophy: therapeutic implications in pulmonary hypertension. *Circulation* 2012; 126: 2859-2869.
40. Nootens M, Kaufmann E, Rector T, Toher C, Judd D, Francis GS, Rich S. Neurohormonal activation in patients with right ventricular failure from pulmonary hypertension: Relation to hemodynamic variables and endothelin levels. *Journal of the American College of Cardiology* 1995; 26: 1581-1585.
41. Nagaya N, Nishikimi T, Uematsu M, Satoh T, Kyotani S, Sakamaki F, Kakishita M, Fukushima K, Okano Y, Nakanishi N, Miyatake K, Kangawa K. Plasma brain natriuretic peptide as a prognostic indicator in patients with primary pulmonary hypertension. *Circulation* 2000; 102: 865-870.

## CHAPTER 5

42. Saura J, Kettler R, Da Prada M, Richards JG. Quantitative enzyme radioautography with 3H-Ro 41-1049 and 3H-Ro 19-6327 in vitro: localization and abundance of MAO-A and MAO-B in rat CNS, peripheral organs, and human brain. *J Neurosci* 1992; 12: 1977-1999.
43. Mauritz GJ, Kind T, Marcus JT, Bogaard HJ, van de Veerdonk M, Postmus PE, Boonstra A, Westerhof N, Vonk-Noordegraaf A. Progressive changes in right ventricular geometric shortening and long-term survival in pulmonary arterial hypertension. *Chest* 2012; 141: 935-943.
44. Lairez O, Calise D, Bianchi P, Ordener C, Spreux-Varoquaux O, Guilbeau-Frugier C, Escourrou G, Seif I, Roncalli J, Pizzinat N, Galinier M, Parini A, Mialet-Perez J. Genetic deletion of MAO-A promotes serotonin-dependent ventricular hypertrophy by pressure overload. *J Mol Cell Cardiol* 2009; 46: 587-595.
45. Bogaard HJ, Natarajan R, Henderson SC, Long CS, Kraskauskas D, Smithson L, Ockaili R, McCord JM, Voelkel NF. Chronic pulmonary artery pressure elevation is insufficient to explain right heart failure. *Circulation* 2009; 120: 1951-1960.
46. Zungu-Edmondson M, Suzuki YJ. Differential stress response mechanisms in right and left ventricles. *J Rare Dis Res Treat* 2016; 1: 39-45.

## Supplementary materials

Supplementary methods can be found at <https://www-atsjournals-org.vu-nl.idm.oclc.org/doi/suppl/10.1165/rcmb.2020-01050C>

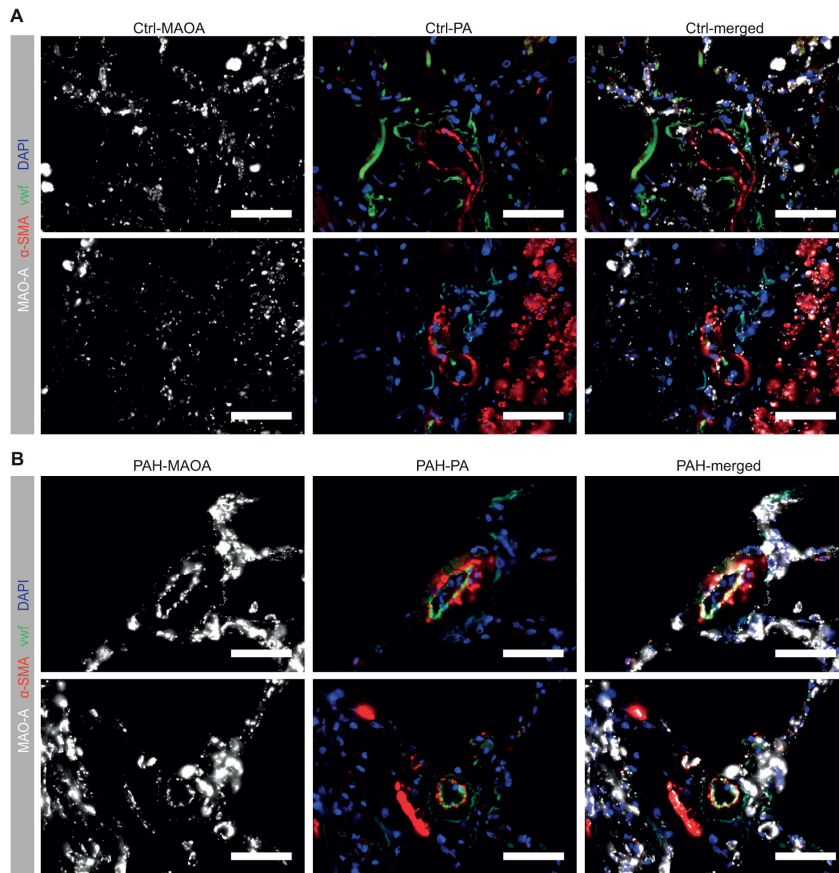


Figure E1 – **Representative images of MAO-A immunofluorescence staining in human lungs.** Representative lung immunofluorescence staining for MAO-A of ctrl donors (A) and end stage PAH patients (B).  $\alpha$ -SM (red), vWF (green) and DAPI (blue) were co-stained with MAO-A (white). Scale bar 50  $\mu$ m

CHAPTER 5

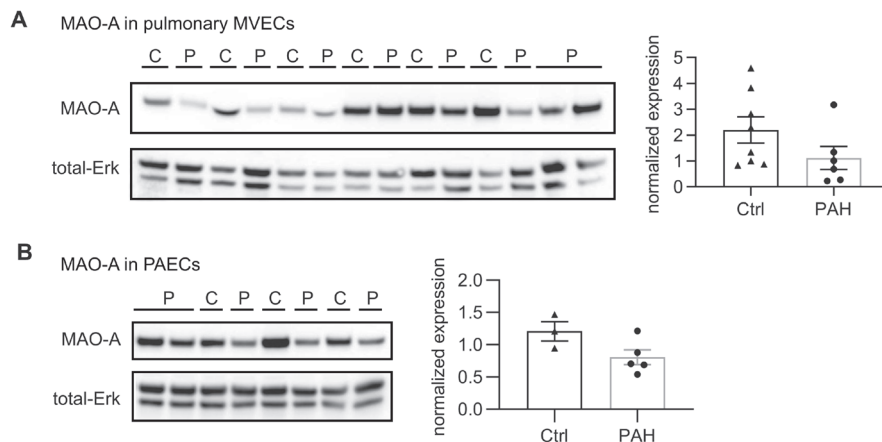
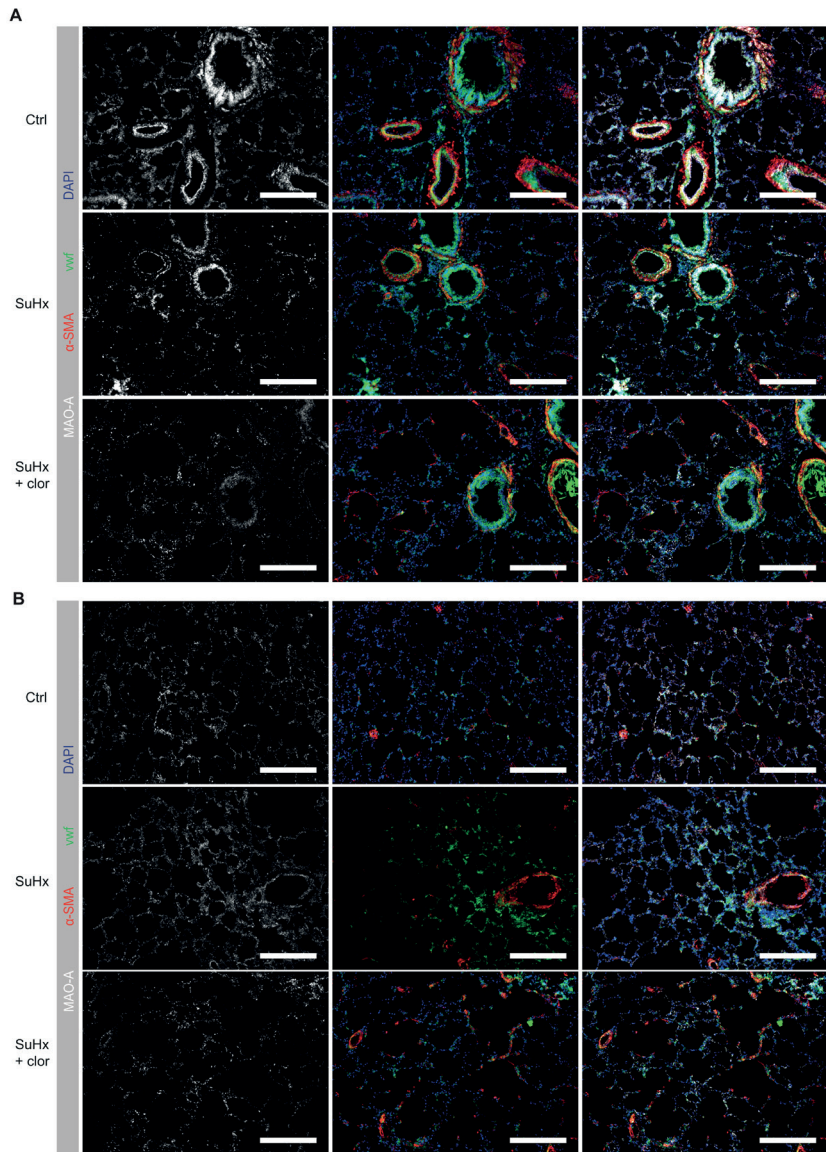


Figure E2 – **MAO-A expression in ECs of PAH patients.** Western blot analysis shows no difference in MAO-A expression in pulmonary MVECs (A) or PAECs (B) between non-PAH and PAH patients, with total-Erk as loading control. (A) Ctrl: n = 8, PAH: n = 6. (B) Ctrl: n = 3, PAH: n = 5. All data are presented as mean  $\pm$  SEM. Unpaired t-test



5

Figure E3 – **MAO-A expression on whole lung tissue.** Representative lung immunofluorescence staining for MAO-A of ctrl rats, SuHx rats, and SuHx rats with clorgyline treatment (A,B).  $\alpha$ -SM (red), vwF (green) and DAPI (blue) were co-stained with MAO-A (white). Scale bar 200  $\mu$ m.

CHAPTER 5

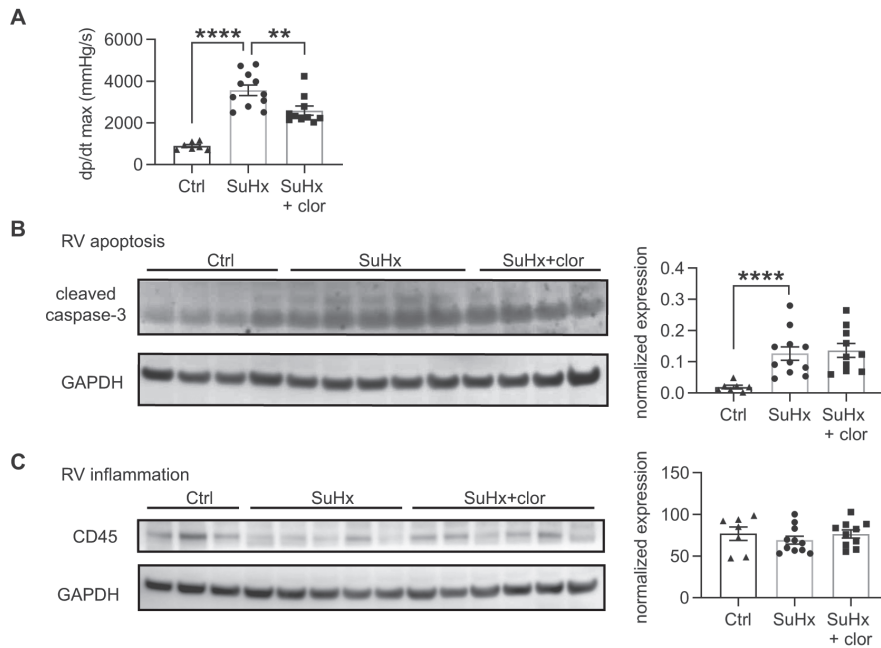


Figure E4 – **Cloglyline treatment on SuHx-PAH rats.** (A) Pressure-volume analysis shows decreased dp/dt max. ctrl: n = 7, SuHx: n = 11, SuHx+clor: n = 10. (B) Western blot analysis on the RV shows no difference in apoptosis between the groups. n = 7, SuHx: n = 11, SuHx+clor: n = 10. (C) Western blot analysis on the RV shows no difference in inflammation between the groups. n = 7, SuHx: n = 11, SuHx+clor: n = 10. All data are presented as mean  $\pm$  SEM; One-way ANOVA followed by Bonferroni posthoc comparison between ctrl and SuHx, SuHx and SuHx+clor. \*\*  $p < 0,01$ .

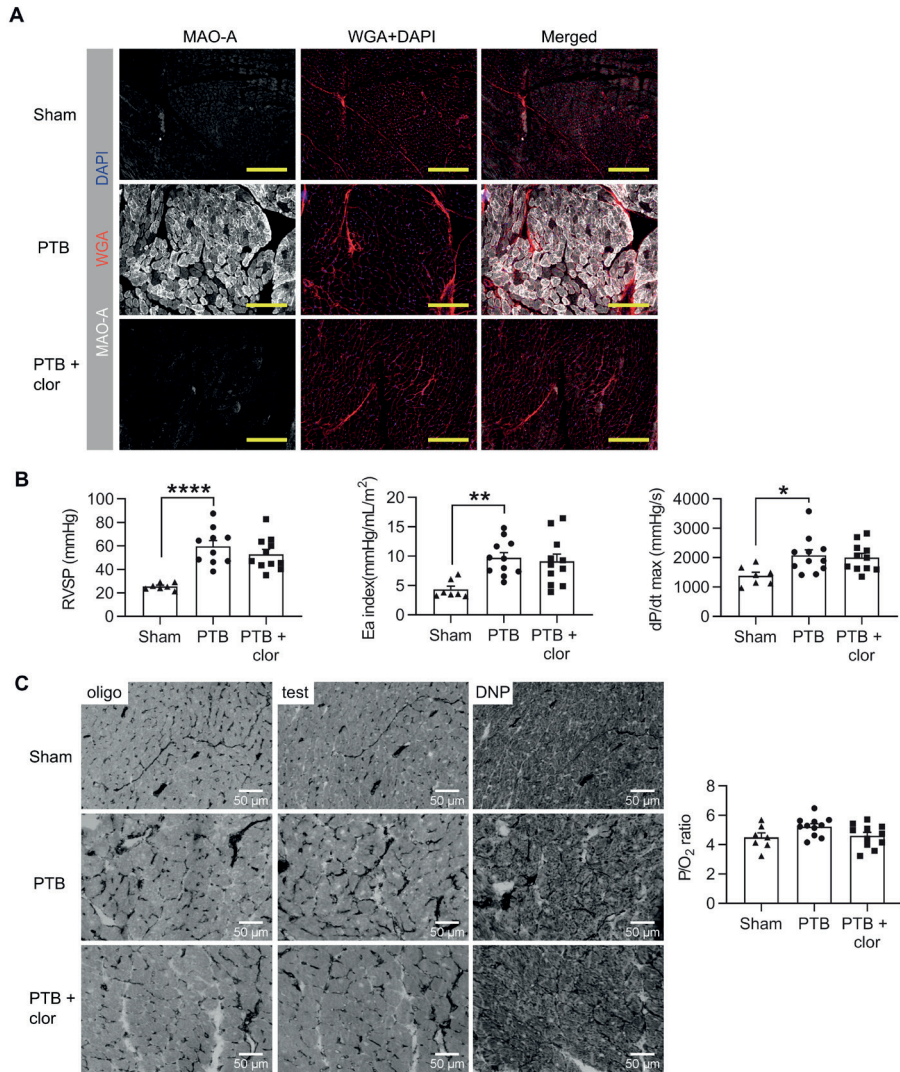
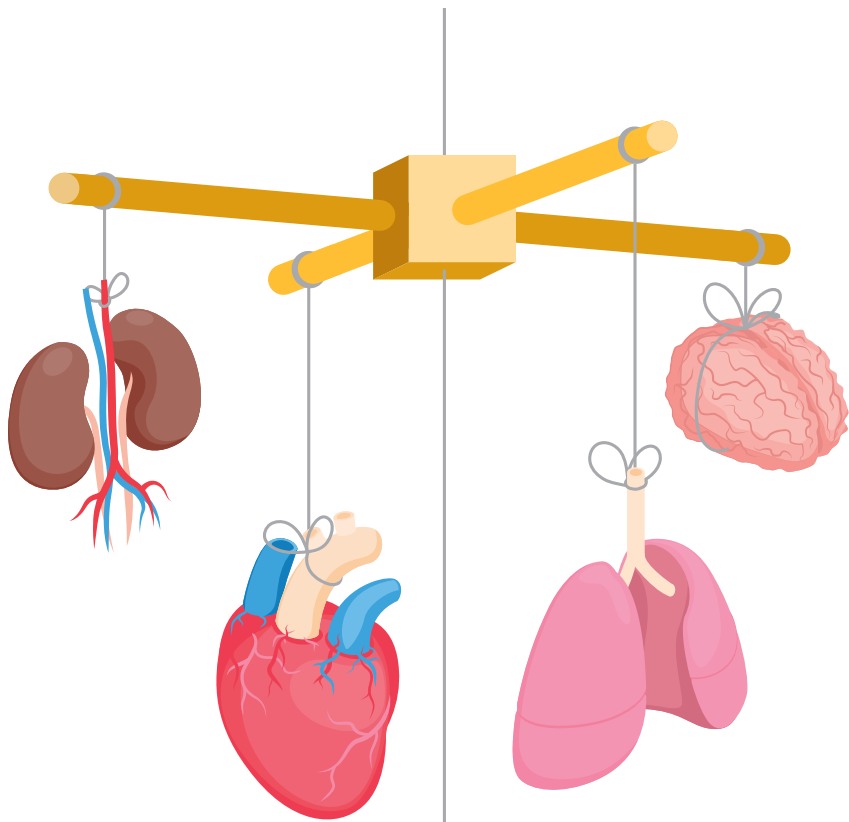


Figure E5 – Clorgyline treatment on PTB rats. (A) Representative RV immunofluorescence staining for MAO-A of Sham, PTB, and PTB rats with clorgyline treatment. WGA (red) and DAPI (blue) were co-stained with MAO-A (white). Scale bar 200  $\mu$ m. (B) Pressure-volume analysis shows increased RVSP, Ea index and dp/dt max in PTB rats, and clorgyline had no effect on those parameters. RVSP, Sham: n = 7, PTB: n = 10, PTB+clor: n = 11. Ea index and dp/dt max, Sham: n = 7, PTB: n = 11, PTB+clor: n = 11. (C) Mitochondrial efficiency was assessed by measuring the background, actual and maximal mitochondrial ATPase activity in serial cryosections of the RV, of which P/O<sub>2</sub> ratio was estimated. Scale bar 50  $\mu$ m. With the theoretical maximal P/O<sub>2</sub> being 6.3, all groups were in the normal range with no difference between the groups. Sham: n = 7, PTB: n = 11, PTB+clor: n = 11. All data are presented as mean  $\pm$  SEM; One-way ANOVA followed by Bonferroni posthoc comparison between ctrl and PTB, PTB and PTB+clor. SDH = succinate dehydrogenase.



6

# **BISOPROLOL AND/OR HYPEROXIC BREATHING DO NOT REDUCE HYPERVENTILATION IN PULMONARY ARTERIAL HYPERTENSION PATIENTS**

---

**Eva L. Peters\***, Jasmijn S.J.A. van Campen\*, Herman Groepenhoff, Frances S. de Man, Anton Vonk Noordegraaf, Harm Jan Bogaard

\*First authors contributed equally

*Submitted to Pulmonary Circulation, 2021.*

**To the editor:**

Pulmonary arterial hypertension (PAH) is a rare but severe disease, characterized by obstructive remodelling of pulmonary arteries and leading to right ventricular failure [1]. PAH is incurable and treatment options are limited. The main symptoms of PAH are (exertional) dyspnoea, impaired exercise performance and reduced quality of life [2].

PAH patients often present with an increased minute volume (VE) at rest (i.e., hyperventilation) and a steeper slope of ventilation relative to carbon dioxide production ( $VE/VCO_2$ ) during exercise [3–5]. Hyperventilation in PAH is related to disease severity [3, 5, 6] and is associated with hypocapnia, a strong and independent prognostic value for survival [7]. In addition, it may further exaggerate the feelings of dyspnoea. The mechanisms underlying hyperventilation in PAH are poorly understood, but include increased dead space ventilation and, possibly, autonomic imbalance and hypoxemia leading to alveolar hyperventilation [6, 8–10]. We hypothesized that lowering sympathetic activity and/or acute hyperoxic breathing will reduce hyperventilation. We took advantage of the bisoprolol trial in PAH [11] to investigate whether long-term beta blocker treatment or acute hyperoxic breathing, known to reduce sympathetic activity [10], lowers ventilation in PAH patients.

Informed consent was obtained from all patients and a Data Safety Monitoring Board (DSMB) was appointed. The trial was registered at [clinicaltrials.gov](http://clinicaltrials.gov) before recruitment was initiated (Clinicaltrials.gov NCT01246037, EudraCT 2010-020424-21). The study design and in- and exclusion criteria and the cardiopulmonary exercise testing (CPET) protocol have been described in detail elsewhere [11]. In short, all idiopathic PAH patients above 18 years of age and in New York Heart Association (NYHA) class II and III were screened for eligibility. Patients received 6 months of bisoprolol and placebo treatment in a cross-over manner, in random order. At baseline, before cross-over, and at the end of the study patients underwent CPET, arterial blood gas (ABG) analysis and ventilatory measurements. ABG was taken from the radial artery after at least ten minutes of supine rest. Ventilatory measurements were performed in absolute resting condition, in a supine position in a quiet room. After breathing room-air for at least ten minutes, minute ventilation (VE), tidal volume (VT), respiratory rate (RR) and end-tidal CO<sub>2</sub> ( $P_{ET}CO_2$ ) were measured breath-by-breath using a metabolic cart (Vmax Encore 21-1, Yorba Linda, USA) and analysed as 20 seconds averages. Oxygen saturation (SaO<sub>2</sub>) was measured by pulse-oximetry (9600, Nonin, Plymouth, USA) and heart rate by electrocardiography (Eagle 4000, Marquette). After ten minutes, the inspired oxygen fraction (FiO<sub>2</sub>) was changed. Measurements were performed with an FiO<sub>2</sub> of 21% and 40%, in random order, both for 10 minutes. Blinding codes were

broken on the last day of the third admission or at early termination of the study. However, all data were analysed in a blinded fashion. Statistics were performed using GraphPad Prism 7. Two-way repeated measures ANOVA was used to test for the effects of bisoprolol at baseline and after treatment, and to test the effects of hyperoxic breathing both after placebo and bisoprolol treatment.  $p < 0.05$  was considered statistically significant. Continuous variables are presented as mean  $\pm$  standard deviation (SD).

18 patients were enrolled into the study from February 2011 until January 2014 of whom 17 underwent CPET and ventilatory measurements at baseline. 15 out of 17 patients received placebo for the full six months during the placebo arm of the study. In the bisoprolol arm of this study, 16 patients received bisoprolol for 6 months [11]. As such, a complete paired set of data is available from 15 patients.

As a reflection of our general PAH population, NYHA class II and III were equally represented, mean age was  $46 \pm 14$  years and there was a strong female predominance (only one male patient was included). Average mean arterial pressure (mPAP) was  $48 \pm 11$  mmHg and 6-minute walking distance  $468 \pm 84$ m. Results of CPET, ABG and ventilatory measurements at baseline and after placebo and bisoprolol treatment are shown in table 1. Baseline measurements showed a high minute ventilation, and a low  $P_{\text{etCO}_2}$  and  $P_{\text{aCO}_2}$ . There were no signs of metabolic alkalosis.

The reached dosage of bisoprolol ( $4.5 \pm 3.3$  mg on average) was associated with a reduction in heart rate of 12 bpm ( $p=0.004$ ) at rest in normoxia, suggesting decreased sympathetic nerve activity. However, minute ventilation, tidal volume or respiratory rate were unchanged. No changes in  $P_{\text{etCO}_2}$  or  $P_{\text{aCO}_2}$  were observed, indicating an unchanged ventilation and perfusion. At baseline,  $VE/VCO_2$  slope was elevated ( $43.3 \pm 10.8$ ), indicating reduced ventilatory efficiency during exercise. Bisoprolol did not reduce heart rate at the start of CPET or at maximum exercise. Neither ventilatory efficiency,  $VE_{\text{peak}}$ ,  $RR_{\text{peak}}$ ,  $VT_{\text{peak}}$  or  $P_{\text{ETCO}_2}$  were changed after bisoprolol treatment.

Ten minutes of hyperoxic breathing with  $FiO_2 = 40\%$  significantly increased  $SaO_2$  with 3.9% ( $p=0.0012$ ) and decreased heart rate with 3.6 bpm ( $p=0.0044$ ). However, no effect was found on ventilation as reflected by  $VE$ ,  $RR$ ,  $VT$  and  $P_{\text{ETCO}_2}$ . In addition, no interaction-effect between bisoprolol treatment and hyperoxic breathing at rest was found for any of the outcome variables, indicating no cumulative or opposing effects of bisoprolol and hyperoxic breathing.

## CHAPTER 6

Collectively, our results show that ventilation at rest is not affected by bisoprolol or hyperoxic breathing, either alone or in combination. Furthermore, bisoprolol did not improve ventilatory inefficiency during exercise. The reductions in heart rate following bisoprolol treatment and hyperoxic breathing strongly suggest decreased SNS activity.

Limitations of the present study are the small sample size and the wide range of bisoprolol doses in our patients. We did not directly measure sympathetic nerve activity or chemoreceptor activity, and therefore cannot prove or exclude the role of the sympathetic nervous system in hyperventilation in PAH. The lack of effect in the current study may thus be related to the relatively low dose of bisoprolol, the type of beta blocker [12], or the level and short duration of hyperoxia. However, oxygen has also central effects on respiratory centres in the brain stem, possibly via ROS signalling, which causes long-lasting increases in ventilation [13]. Whilst the use of this effect is unknown, it may have masked the initial reduction in ventilation due to peripheral chemoreceptor silencing. Alternatively, other factors may drive ventilation in PAH, including mechanical forces in the pulmonary circulation, low work rate lactic acidosis, hyperkalaemia and altered central regulation of breathing [5, 14, 15]. Given the strong prognostic value of  $VE/VCO_2$  and hypocapnia, unravelling the aetiology of hyperventilation in PAH may help to improve treatment and thereby enhance survival and quality of life.

Table 1 – **Effects of bisoprolol and hyperoxic breathing on ventilation at rest and during exercise.** AT = anaerobic threshold, HR = heart rate, VE = total minute ventilation, RR = respiratory rate, VT = tidal volume,  $P_{ET}CO_2$  = end-tidal partial pressure of  $CO_2$ ,  $SaO_2$  = oxygen saturation,  $FiO_2$  = inspired fraction of oxygen.

	(Mean ± SD)	Baseline (n=17)	Placebo (n=16)	Bisoprolol (n=16)	Effect of bisoprolol (p-value)	Effect of hyperoxia (p-value)	Interaction bisoprolol-hyperoxia (p-value)
	<b>Work (watt)</b>	66±30	59±34	67±31	0.2914		
	<b>VO<sub>2</sub>AT (L/min)</b>	0.70±0.20	0.64±0.24	0.65±0.20	0.5194		
	<b>VO<sub>2</sub>max (L/min)</b>	1.01±0.34	0.95±0.41	0.98±0.34	0.5200		
<b>CPET</b>	<b>VO<sub>2</sub>/kg (mL/kg/min)</b>	15.2±4.6	13.8±5.2	14.6±4.5	0.9337		
	<b>HR start (bpm)</b>	80±14	76±13	74±18	0.8204		
	<b>HR max (bpm)</b>	138±21	124±26	123±27	0.9279		

Bisoprolol and/or hyperoxic breathing do not reduce hyperventilation in PAH patients

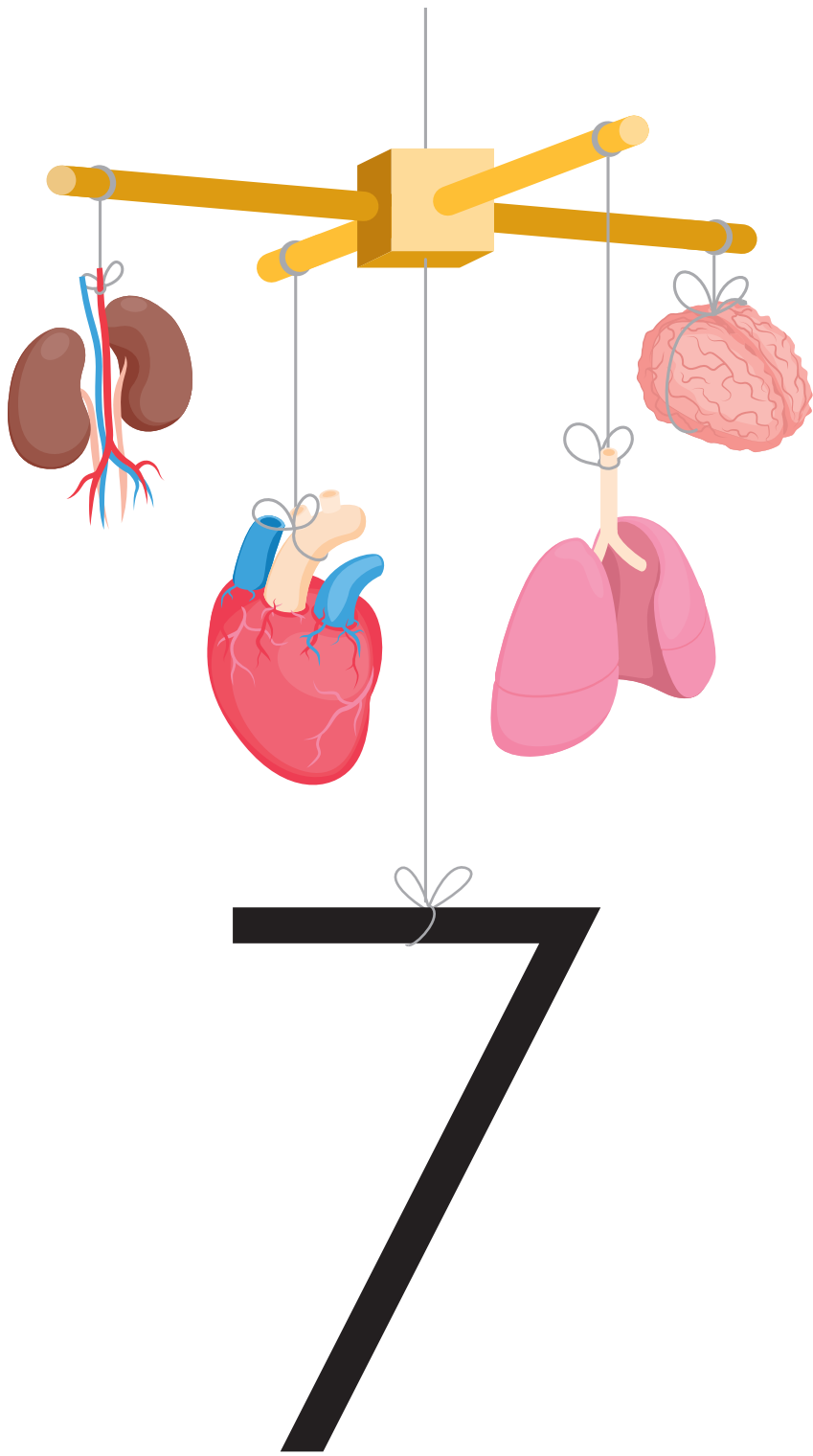
	(Mean ± SD)	Baseline (n=17)	Placebo (n=16)	Bisoprolol (n=16)	Effect of bisoprolol (p-value)	Effect of hyperoxia (p-value)	Interaction bisoprolol-hyperoxia (p-value)
CPET	O <sub>2</sub> pulse (mL/beat)	7.2±1.7	7.6±2.7	7.9±2.1	0.6477		
	VE <sub>peak</sub> (L/min)	54.2±24.0	48.1±28.0	49.4±16.7	0.9444		
	RR <sub>peak</sub> (min <sup>-1</sup> )	38±18	35±20	36±10	0.8462		
	VT <sub>peak</sub> (l)	1.4±0.4	1.4±0.4	1.4±0.3	0.2105		
	VE/VCO <sub>2</sub> slope	42.4±11.0	42.1±11.5	39.8±11.0	0.8425		
ABG	PaCO <sub>2</sub> (mmHg)	32.3±4.7	32.2±0.8	32.8±3.1	0.5737		
	PaO <sub>2</sub> (mmHg)	73.5±21.5	67.2±13.0	71.3±15.8	>0.9999		
Vent FiO <sub>2</sub> 21%	VT (l)	0.8±0.2	0.7±0.2	0.8±0.2	0.0149*		
	VE (L/min)	11.0±3.0	10.9±2.1	10.7±2.8	0.1751		
	RR (breaths/min)	14.5±3.1	15.8±3.0	15.1±4.1	0.2784		
	P <sub>ET</sub> CO <sub>2</sub> (kPa)	3.6±0.6	3.7±0.6	3.7±0.4	0.4822		
	SaO <sub>2</sub> (%)	93.0±5.7	92.4±5.2	92.0±7.0	0.3458		
	HR (bpm)	78±12	78±13	66±13	<0.0001*		
Vent FiO <sub>2</sub> 40%	VT (l)	0.8±0.2	0.8±0.2	0.8±0.2	0.0149*	0.4726	0.1634
	VE (L/min)	11.2±2.7	11.0±2.4	11.3±2.6	0.1751	0.2742	0.1518
	RR (breaths/min)	14.7±3.4	16.3±2.9	15.4±4.2	0.2784	0.6032	0.4689
	P <sub>ET</sub> CO <sub>2</sub> (kPa)	3.6±0.6	3.7±0.6	3.7±0.5	0.4822	0.2418	0.7034
	SaO <sub>2</sub> (%)	96.9±4.4	96.1±4.9	96.1±6.4	0.3458	0.0012*	0.8132
	HR (bpm)	74±12	75±13	64±13	<0.0001*	0.0044*	0.2906

## Acknowledgements

This research was financially supported by ZonMW (95110079). HJB, AVN and FSdM were supported by the Netherlands CardioVascular Research Initiative: the Dutch Heart Foundation, Dutch Federation of University Medical Centres, the Netherlands Organization for Health Research and Development, and the Royal Netherlands Academy of Sciences (CVON-2012-08 PHAEDRA, CVON-2018-29 PHAEDRA-IMPACT, CVON-2017-10 Dolphin-Genesis). HJB and AVN were supported by research grants from Actelion, GSK and Ferrer (Therabel). EP, AVN and FSdM were further supported by The Netherlands Organization for Scientific Research (NWO-VICI: 918.16.610, NWO-VIDI: 917.18.338).

## References

1. Galiè N, Humbert M, Vachiery J-L, Gibbs S, Lang I, Torbicki A, Simonneau G, Peacock A, Vonk Noordegraaf A, Beghetti M, Ghofrani A, Sanchez MAG, Hansmann G, Klepetko W, Lancellotti P, Matucci M, McDonagh T, Pierard LA, Trindade PT, Zompatorie M, Hoeper M. 2015 ESC/EAS Guidelines for the diagnosis and treatment of pulmonary hypertension. *Ration. Pharmacother. Cardiol.* 2016; 12: 79–86.
2. Sajkov D, Petrovsky N, Palange P. Management of dyspnea in advanced pulmonary arterial hypertension. *Curr. Opin. Support. Palliat. Care* 2010; 4: 76–84.
3. Sun XG, Hansen JE, Oudiz RJ, Wasserman K. Exercise pathophysiology in patients with primary pulmonary hypertension. *Circulation* 2001; 104: 429–435.
4. Wensel R, Opitz CF, Anker SD, Winkler J, Höffken G, Kleber FX, Sharma R, Hummel M, Hetzer R, Ewert R. Assessment of survival in patients with primary pulmonary hypertension: Importance of cardiopulmonary exercise testing. *Circulation* 2002; 106: 319–324.
5. Yasunobu Y, Oudiz RJ, Sun XG, Hansen JE, Wasserman K. End-tidal Pco<sub>2</sub> abnormality and exercise limitation in patients with primary pulmonary hypertension. *Chest* 2005; 127: 1637–1646.
6. Dimopoulos S, Anastasiou-Nana M, Katsaros F, Papazachou O, Tzanas G, Gerovasili V, Pozios H, Roussos C, Nanas J, Nanas S. Impairment of autonomic nervous system activity in patients with pulmonary arterial hypertension: a case control study. *J. Card. Fail.* 2009; 15: 882–889.
7. Hoeper MM, Pletz MW, Golpon H, Welte T. Prognostic value of blood gas analyses in patients with idiopathic pulmonary arterial hypertension. *Eur. Respir. J.* 2007; 29: 944–950.
8. Naeije R, Van de Borne P. Clinical relevance of autonomic nervous system disturbances in pulmonary arterial hypertension. *Eur. Respir. J.* 2009; 34: 792–794.
9. Farina S, Bruno N, Agalbato C, Contini M, Cassandro R, Elia D, Harari S, Agostoni P. Physiological insights of exercise hyperventilation in arterial and chronic thromboembolic pulmonary hypertension. *Int. J. Cardiol.* 2018; 259: 178–182.
10. Velez-Roa S, Ciarka A, Najem B, Vachiery JL, Naeije R, Van De Borne P. Increased sympathetic nerve activity in pulmonary artery hypertension. *Circulation* 2004; 110: 1308–1312.
11. Van Campen JSJA, De Boer K, Van De Veerdonk MC, Van Der Bruggen CEE, Allaart CP, Raijmakers PG, Heymans MW, Marcus JT, Harms HJ, Handoko ML, De Man FS, Noordegraaf AV, Bogaard HJ. Bisoprolol in idiopathic pulmonary arterial hypertension: An explorative study. *Eur. Respir. J.* 2016; 48: 787–796.
12. Contini M, Apostolo A, Cattadori G, Paolillo S, Iorio A, Bertella E, Salvioni E, Alimento M, Farina S, Palermo P, Loguercio M, Mantegazza V, Karsten M, Sciomer S, Magri D, Fiorentini C, Agostoni P. Multiparametric comparison of CARvedilol, vs. NEbivololol, vs. Bisoprolol in moderate heart failure: The CARNEBI trial. *Int. J. Cardiol.* 2013; 168: 2134–2140.
13. Dean JB, Mulkey DK, Henderson RA, Potter SJ, Putnam RW. Hyperoxia, reactive oxygen species, and hyperventilation: Oxygen sensitivity of brain stem neurons. *J. Appl. Physiol.* 2004; 96 p. 784–791.
14. Guyenet PG, Bayliss DA. Neural Control of Breathing and CO<sub>2</sub> Homeostasis. *Neuron* 2015; 87 p. 946–961.
15. Reybrouck T, Mertens L, Schulze-Neick I, Austenat I, Eyskens B, Dumoulin M, Gewillig M. Ventilatory inefficiency for carbon dioxide during exercise in patients with pulmonary hypertension. *Clin. Physiol.* 1998; 18: 337–344.



# NEUROHORMONAL MODULATION IN PULMONARY ARTERIAL HYPERTENSION

---

**Eva L. Peters**, Harm Jan Bogaard, Anton Vonk Noordegraaf, Frances S. de Man

*European Respiratory Journal, 2021. In press.*

## **Abstract**

Pulmonary hypertension is a fatal condition of elevated pulmonary pressures, complicated by right heart failure. Pulmonary hypertension appears in various forms; one of those is pulmonary arterial hypertension (PAH) and is particularly characterized by progressive remodelling and obstruction of the smaller pulmonary vessels. Neurohormonal imbalance in these patients is associated with worse prognosis and survival. In this back-to-basics review on neurohormonal modulation in PAH, we provide an overview of the pharmacological and non-pharmacological strategies that have been tested preclinically and clinically. The benefit of neurohormonal modulation strategies in PAH patients has been limited by lack of insight in how the neurohormonal system is changed throughout the disease and difficulties in translation from animal models to human trials. We propose that longitudinal and individual assessments of neurohormonal status are required to improve timing and specificity of neurohormonal modulation strategies. Ongoing developments in imaging techniques such as positron emission tomography (PET) may become helpful to determine neurohormonal status in PAH patients in different disease stages and optimize individual treatment responses.

## Introduction

Pulmonary hypertension is a fatal condition of elevated pulmonary pressures, complicated by right ventricular failure. Pulmonary hypertension is classified into five groups. Group one is pulmonary arterial hypertension (PAH) and is characterized by progressive remodelling and obstruction of the smaller pulmonary vessels [1]. The resulting decrease in arterial diameter can increase blood pressure in the pulmonary circulation up to five times the normal pressure [2]. The pulmonary circulation then changes from a low- into a high-pressure circulation, placing an increased load on the thin-walled right ventricle (RV). This eventually leads to RV failure and death [3, 4]. There is currently no cure for PAH and treatment options are limited.

One of the disease modifiers in all forms of pulmonary hypertension, is neurohormonal imbalance, which has repeatedly been associated with poor clinical outcome and survival in patients [5–7]. Therefore, many pharmacological and non-pharmacological interventions on the neurohormonal system have been investigated in preclinical and few clinical studies [8]. Nevertheless, translation from preclinical to clinical studies is difficult and is often lacking.

Two recent reviews extensively described molecular pathways underlying the detrimental effects of neurohormonal activation [9] and pharmacological or invasive strategies targeting the neurohormonal system in PAH [8]. We wish to extend on this topic, and thereby provide future directions for research into the neurohormonal system in PAH. In this back-to-basics article, we will therefore 1) recapitulate how the neurohormonal system ensures cardiovascular homeostasis; 2) describe how the neurohormonal system is changed in human PAH, both systemically and locally; 3) discuss how neurohormonal changes impact the progression of PAH and right heart failure; 4) give a comprehensive overview of the preclinical and clinical studies that intervene on the neurohormonal system in PAH.

Of note, neurohormonal changes likely play a role in all forms of pulmonary hypertension. Because most clinical data have been collected here, we focus in our review on PAH. Moreover, other forms of pulmonary hypertension are characterized by frequent co-morbidities (e.g. left heart failure or additional pulmonary diseases), complicating the view on the neurohormonal system. The neurohormonal changes and effects of interventions described hereafter are therefore focused on evidence obtained in PAH patients.

## Back to basics

An important function of the neurohormonal system is to maintain cardiovascular homeostasis. Two pillars of the neurohormonal system are the autonomic nervous system (ANS) and the renin-angiotensin-aldosterone system (RAAS). The different components and functions of both systems are depicted in figure 1.

The ANS can be subdivided into two divisions with opposite actions: the sympathetic and parasympathetic nervous system (SNS and PNS, respectively), as shown in figure 1a. The SNS possesses adrenergic synapses and is generally activated under (physiological) stress to prepare the body for action, while the PNS has cholinergic synapses and prevails during rest. However, both systems are continuously active at basal levels and the net physiological effect depends on the balance between SNS and PNS activity.

The ANS ensures short-term control of cardiovascular homeostasis. Blood pressure and arterial CO<sub>2</sub> levels are continuously monitored by baro- and chemoreceptors in the aortic arch and carotid sinus. When arterial blood pressure is falling, baroreceptors are inactivated and baroreceptor-controlled inhibition of SNS is relieved. Meanwhile, PNS activity is suppressed, striking the balance towards the SNS. The SNS is also activated when rising CO<sub>2</sub> levels in the blood are being detected by chemoreceptors.

SNS activation then causes release of noradrenaline from synapses directly onto cardiac myocytes and blood vessels. In addition, sympathetic nerves stimulate synthesis and release from the adrenal gland of adrenaline and noradrenaline [10] that reach the heart and lungs via the bloodstream. (Nor)adrenaline then binds to the  $\alpha$ - and  $\beta$ -adrenoreceptors ( $\beta$ -ARs). Increased signalling via ARs and reduced signalling from the parasympathetic nicotinic and muscarinic acetylcholine receptors (nAChR and mAChR) result in a net increase in the rate and force of myocardial contraction. In addition, stimulation of  $\alpha$ -ARs that are highly expressed in the vasculature causes vasoconstriction, so that arterial pressure is restored.

Like the ANS, the RAAS is subdivided in two counteractive divisions: the classical and alternative RAAS system, as shown in figure 1b. The classical RAAS has been known for a long time and involves angiotensin converting enzyme (ACE), angiotensin (Ang) II, Ang II type 1 receptor (AT<sub>1</sub>R), aldosterone and the mineralocorticoid receptor (MR). The alternative RAAS system is less well-studied and involves ACE2, Ang1-7, Ang1-9 and the MAS receptor.

## Neurohormonal modulation in pulmonary arterial hypertension

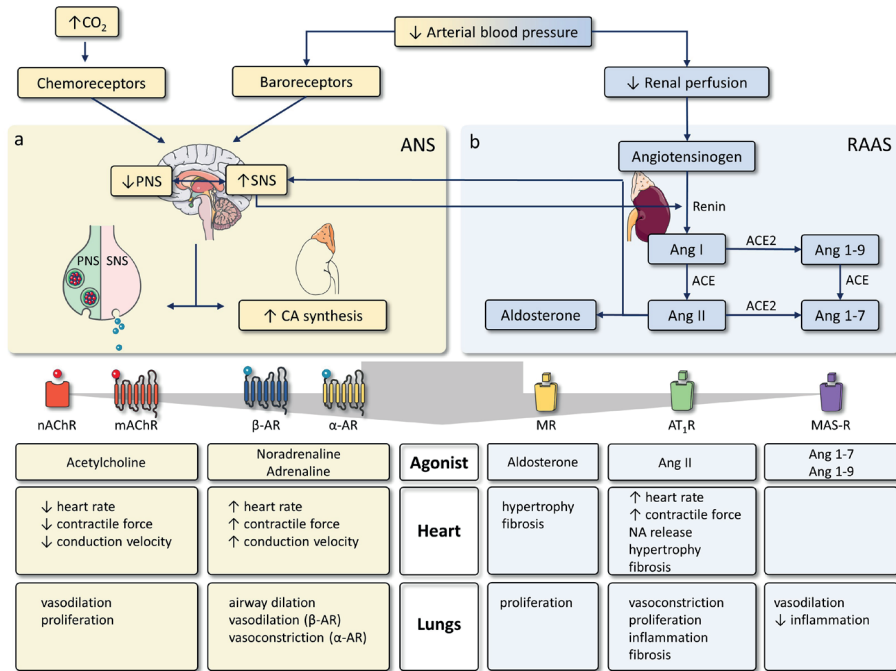


Figure 1 - **Short- and long-term control of blood pressure via neurohormonal signalling.** PNS = parasympathetic nervous system, SNS = sympathetic nervous system, CA = catecholamine, ANS = autonomic nervous system, nAChR = nicotinic acetylcholine receptor, mAChR = muscarinic acetylcholine receptor, AR = adrenergic receptor, Ang = angiotensin, ACE = angiotensin converting enzyme, RAAS = renin-angiotensin aldosterone system, AT<sub>1</sub>R = angiotensin II receptor type I, MR = mineralocorticoid receptor.

The RAAS ensures long-term control of blood pressure and volume. When arterial blood pressure drops, perfusion pressure of the kidney is reduced. As a consequence, renin is released from the kidney into the blood and facilitates the conversion of angiotensinogen to angiotensin I (Ang I). The latter is further converted to Ang II by ACE in the lungs [11]. Ang II acts as a strong vasoconstrictor via the AT<sub>1</sub>R but can also increase the rate and force of myocardial contractility [12]. Furthermore, Ang II promotes aldosterone release from the adrenal glands via the MR to induce sodium and water retention in the kidneys and increase blood volume. However, aldosterone also directly acts on the heart, leading to cardiac hypertrophy and fibrosis [13]. These effects of aldosterone in the heart are independent from the increase in blood pressure. In the (pulmonary) vasculature, pathological levels of aldosterone are associated with oxidative stress and vascular inflammation [13].

In the opposing alternative RAAS pathway, Ang I is converted into Ang1-9 while Ang II is converted to Ang1-7, both by ACE2. Ang1-7 and Ang1-9 largely oppose the vascular effects of the classical RAAS pathway via the MAS receptor [14, 15]. Direct effects of Ang1-7 and Ang1-9 in the heart are unknown.

### **Neurohormonal systems interfere systemically and locally**

The ANS and RAAS do not operate in isolation. Several interactions have been demonstrated, both centrally and locally, and mostly studied in chronic heart failure patients or experimental heart failure. Interactions at the system level include SNS-induced renin release from the kidneys [16, 17] and central actions of Ang II in the brain. For example, it was shown that inhibition of classical RAAS signalling by ACE inhibitors or AT<sub>1</sub>R blockers increases PNS activity [18] and reduces SNS activity [19]. The latter happens also when AT<sub>1</sub>R blockade is applied to the brain only [20], suggesting that Ang II directly acts on the central nervous system. Furthermore, Ang II enhances chemoreceptor activation [21, 22] and inhibits baroreceptor reflex control of heart rate [20, 23], both leading to increased SNS activity. By contrast, SNS activity can be reduced by the alternative RAAS pathway via inhibition of noradrenaline release in the hypothalamus [24].

Interactions between the ANS and RAAS occur locally as well. For instance, Ang II increases adrenergic signalling by potentiating the release of noradrenaline from sympathetic nerve terminals [20] and inhibits cardiac noradrenaline re-uptake [25]. In addition, gene expression of the AT<sub>1</sub>R in the heart is regulated by Ang II and the  $\beta_1$ AR [26, 27], suggesting that the balance of local SNS and classical RAAS determines gene expression of the AT<sub>1</sub>R in the heart. Also in the pulmonary vasculature, cross-talk between  $\beta$ -AR and RAAS signalling has been described [6].

### **Systemic and local changes in the neurohormonal system in PAH patients**

#### **Systemic changes in the autonomic nervous system**

PAH has repeatedly been associated with a systemic increase in SNS activity. SNS activity, directly measured via muscle sympathetic nerve activity (or MSNA) in a peripheral nerve, was increased in PAH patients [28, 29]. In addition, plasma levels of (nor)adrenaline were increased in PAH patients in most [30–33], but not all studies [34].

The SNS and PNS are connected in such a way, that increasing SNS activity will cause decreased PNS activity. PNS activity can be indirectly assessed by indices of heart rate variability and heart rate recovery after exercise. As expected, both heart rate variability indices for PNS activity [28, 35, 36] and heart rate recovery [37, 38] were found to be reduced in PAH patients. The autonomic imbalance towards SNS activity and away from PNS activity is related to a reduced exercise capacity [39, 40], worse New York Heart Association (NYHA) functional class [29, 41] and an increased mortality in PAH [30, 32].

### Local changes in the autonomic nervous system

In PAH, the SNS is not only systemically activated, but also locally in the myocardium [33, 35, 42]. Important triggers for SNS activation are atrial and ventricular stretch:  $\beta$ -AR expression is downregulated specifically in the right ventricle but not in the left ventricle in PAH patients [43], and was related to ventricular wall stress [44]. The role of atrial stretch on SNS activation was shown in studies investigating balloon atrial septostomy. Although, atrial septostomy was not designed to interfere with the neurohormonal system, it partially reduced muscle sympathetic nerve activity [45]. This reduction in muscle sympathetic nerve activity was related to the reduction in atrial pressure, suggesting that atrial stretch plays an additional role in SNS activation [45].

The acute increases in SNS are important to enhance the rate and force of cardiac contraction and thus to enable the RV to cope with the enhanced load. However, sustained cardiac SNS activation causes selective downregulation of  $\beta_1$ ARs and uncoupling of the remaining  $\beta$ -ARs from downstream signalling [43]. Reduced  $\beta$ -AR expression and signalling impairs RV function in at least two ways. First, although contractility (end-systolic elastance,  $E_{es}$ ) and force generating capacity of RV cardiomyocytes are enhanced in PAH-patients [3], the loss of  $\beta$ -AR signalling reduces the RV contractile reserve [43, 46]. Loss of contractile reserve results in arterio-ventricular uncoupling and acute RV dilatation during exercise [47], and is associated with lower exercise capacity and reduced survival [48]. Second, reduced  $\beta$ -AR expression also plays an important role in impaired diastolic function in PAH. One of the downstream targets of the  $\beta$ -AR is protein kinase A (PKA), which regulates cardiomyocyte stiffness via phosphorylation of the giant sarcomeric protein titin [49]. Thus, reduced  $\beta$ -AR expression results in reduced PKA activity and PKA-mediated phosphorylation of titin, thereby increasing the stiffness of the RV cardiomyocytes [50]. In experimental PAH, sustained adrenergic activation has further been linked to cardiac hypertrophy, fibrosis, apoptosis and reduced capillary density [51, 52].

## CHAPTER 7

Sustained adrenergic activation is also implicated in pulmonary vascular remodelling. Impaired  $\beta$ -AR signalling causes loss of nitric oxide production by pulmonary artery (PA) endothelial cells, resulting in pulmonary vasoconstriction [6]. This is further enhanced by direct adrenergic stimulation of PA smooth muscle cells and collectively leads to chronic pulmonary vasoconstriction [6]. Moreover, continuous adrenergic stimulation causes PA smooth muscle cell hypertrophy and proliferation [53, 54].

As opposed to what is known about local changes in the SNS, changes in counteractive PNS signalling have been reported in the RV in only one study so far. Da Silva Gonçalves Bos *et al.* showed that nAChR expression is increased in the RV of PAH patients at end-stage, and that there is likely reduced degradation of acetylcholine by acetylcholinesterase in the synaptic cleft [36]. If, and how the PNS is changed specifically in the lungs is largely unknown.

### **Systemic changes in the Renin-Angiotensin-Aldosterone system**

Imbalances in RAAS activation have been described in PAH as well. Plasma levels of Ang I and II are increased in PAH compared to healthy controls [55, 56]. However, Ang I and II levels are increased only in progressive PAH but not in stable PAH and are associated with disease progression and mortality [57]. Plasma aldosterone concentrations are higher in PAH patients than in controls with unexplained dyspnoea but without PAH [58]. In a subgroup of treatment naïve patients from this study, aldosterone levels correlated positively with pulmonary vascular resistance and negatively with cardiac output [58]. However, in a larger cohort of PAH patients, aldosterone concentration was not directly associated with cardiac output, 6-minute walking distance (6MWD) or survival [59].

In addition to classical RAAS activation, alternative RAAS activation may be reduced in PAH. Decreased plasma levels of Ang 1-7 and 1-9 in patients were reported in one study [56], while unchanged Ang 1-7 levels were reported in another study [55]. In the latter study, a higher Ang II/Ang1-7 ratio indicated reduced conversion from Ang II to Ang 1-7 by ACE2 [55]. Plasma concentrations of ACE2 are not lower in PAH patients compared to controls, but it was suggested that auto-antibodies may reduce ACE2 activity [56]. Collectively, the balance within the RAAS seems to be in favour of classical RAAS activation, which is associated with worse disease progression and survival.

### Local changes in the Renin-Angiotensin-Aldosterone system

In addition to systemic changes in classical RAAS signalling in PAH patients, local changes have been reported as well. The conversion from Ang I to Ang II by ACE happens predominantly in the lungs, where an overall decrease in pulmonary ACE activity was found [60]. This decrease however, may be partly because of a reduced endothelial surface area. By contrast, ACE activity was increased in isolated PA endothelial cells from PAH patients [57] and ACE expression was upregulated in smaller pulmonary vessels (intra-acinar arteries to capillaries) [61] and plexiform lesions [61, 62] of PAH patients. These findings implicate that the formation of Ang II is increased locally in the PAH pulmonary vasculature. In addition, distal pulmonary arteries from PAH patients have increased  $AT_1R$  expression [57]. Sustained Ang II exposure causes hypertrophy and proliferation of isolated patient PA smooth muscle cells via  $AT_1R$  signalling [57] and has been linked to vascular inflammation and fibrosis, and impaired endothelial function [12].

In addition, local aldosterone synthesis is possible in the pulmonary vasculature [63]. Changes in aldosterone levels or MR expression in the PAH lung have not been described. However, in experimental PAH and in isolated human PA smooth muscle cells and PA endothelial cells aldosterone has been associated with increased vascular remodelling [63–65].

Sustained classical RAAS activity has also unfavourable effects on the heart, including cardiomyocyte hypertrophy, fibrosis and conduction system disturbances [12]. The human heart possesses a local RAAS system, independent from but related to the circulating RAAS system [66]. Only one study was reported on local changes in RAAS activity in the heart in PAH. As opposed to the lungs,  $AT_1R$  expression was found to be decreased in the RV, despite increased ACE expression and Ang II formation [67]. Local changes in cardiac aldosterone signalling have not been described in PAH.

Little is known about local changes in alternative RAAS activity. With renewed interest in ACE2, the entry point for the SARS-CoV-2 virus, it was recently shown that mRNA of the soluble but not the membrane bound ACE2 is increased in explanted PAH lungs [68]. Although upregulated ACE2 can be considered beneficial in PAH, the implications of this shift towards soluble ACE2 for PAH patients are unknown. In the heart, ACE2 activity may be increased, as shown by increased formation of Ang1-7 from Ang II [69].

## Neurohormonal modulation strategies in PAH

From the foregoing, it becomes clear that the neurohormonal system in PAH is out of balance both systemically and locally. Imbalances at both levels are associated with worse disease progression, survival or cardiac and vascular remodelling. Although increased SNS and classical RAAS activity are required to maintain cardiovascular homeostasis in case cardiac output drops, it is thought that chronic activation of SNS and RAAS eventually become maladaptive. This may lead to a vicious circle of further cardiac deterioration and increased neurohormonal balance, exacerbated by progressive pulmonary vascular remodelling. Therefore, the neurohormonal systems have been the target of several experimental treatments. Treatment strategies can be divided into pharmacological and non-pharmacological approaches. An overview of both treatment strategies on the ANS and RAAS is given in figure 2 and 3 respectively.

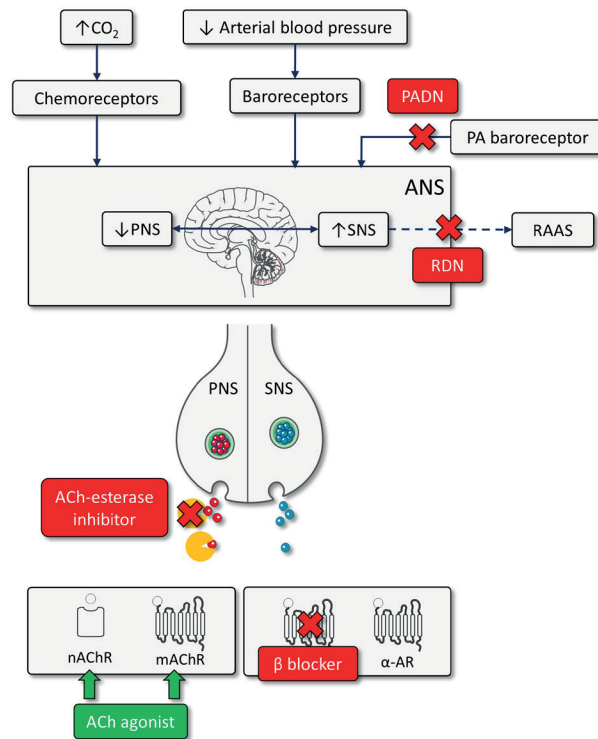


Figure 2 - **Targets of pharmacological and surgical interventions on the autonomic nervous system.** PA = pulmonary artery, PADN = pulmonary artery denervation, PNS = parasympathetic nervous system, SNS = sympathetic nervous system, CA = catecholamine, ANS = autonomic nervous system, ACh = acetylcholine, nAChR = nicotinic acetylcholine receptor, mAChR = muscarinic acetylcholine receptor, AR = adrenergic receptor, RDN = renal denervation.

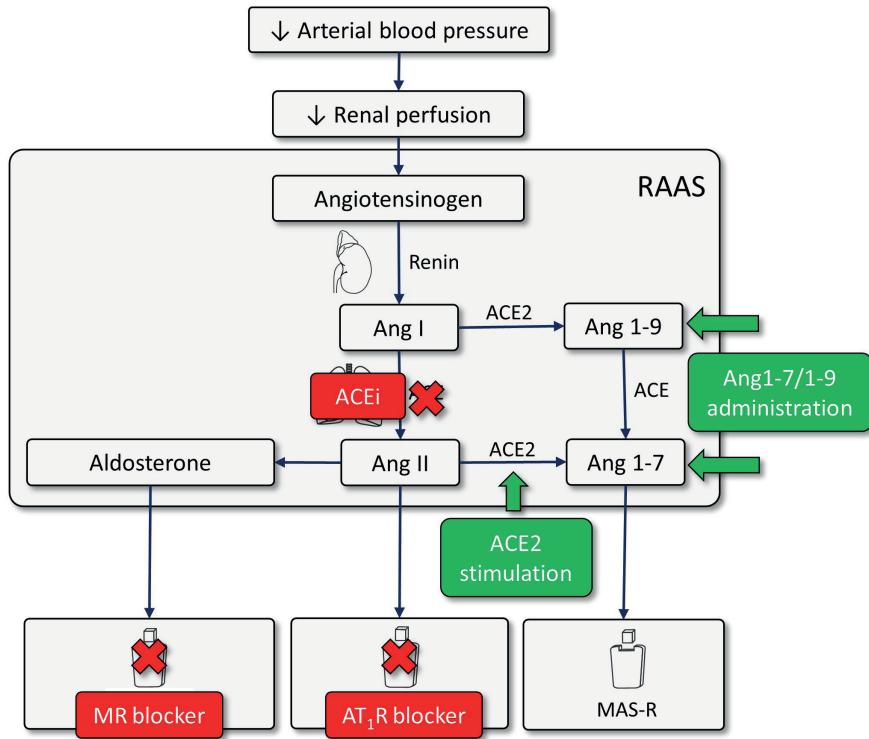


Figure 3 – Targets of pharmacological and surgical interventions on the renin-angiotensin-aldosterone system. ACE = angiotensin converting enzyme, ACEi = angiotensin converting enzyme inhibitor, MR = mineralocorticoid receptor, AT<sub>1</sub>R = angiotensin II receptor type 1

### Pharmacological treatments

The effects of pharmacological treatments seizing on the different neurohormonal systems are summarized in Table 1. Below, we will discuss the few approaches that have been tested in patients.

## CHAPTER 7

Table 1 - **The effect of pharmacological treatments targeted at different neurohormonal signalling pathways in preclinical and clinical studies.** ↑ Increased, = Unchanged, ↓ Decreased. SNS = sympathetic nervous system, PNS = parasympathetic nervous system, RAAS = renin-angiotensin-aldosterone system, mPAP = mean pulmonary artery pressure, PVR = pulmonary vascular resistance, ACE = angiotensin converting enzyme, AT<sub>1</sub> = Angiotensin II-receptor type 1, MR = mineralocorticoid receptor.

Target system	Treatment strategy	Preclinical	Clinical
SNS	β-blockers	Survival: ↑ [70] Disease progression: ↓ [71–73] Exercise capacity: ↑ [51] Cardiac function: ↑ [51, 73, 74], = [75] Cardiac remodelling: ↓ [51, 76], = [75] Vascular remodelling: ↓ [74, 77, 78], = [51]	Exercise capacity: = [79–81] Cardiac function: ↑ [79], ↓ [80]
PNS	Acetylcholinesterase inhibition	Disease progression: ↓ [36] Cardiac function: ↑ [36] Cardiac remodelling: ↓ [36] Vascular remodelling: ↓ [36]	
	Cholinergic agonists	Cardiac remodelling: ↓ [82] Vascular remodelling: ↓ [82]	
Classical RAAS	ACE inhibition	Disease progression: ↓ [83, 84], Cardiac function: ↓ [85], ↑ [84] Cardiac remodelling: ↓ [86–88], = [89] Vascular remodelling: ↓ [83–90], = [89]	Exercise capacity: = [91–93] Cardiac function: = [92, 93] mPAP/PVR: = [91, 92] (mPAP&PVR), ↓ [93] (mPAP)
	AT <sub>1</sub> blockers	Survival: ↑ [94] Disease progression: ↓ [57] Cardiac function: = [75] Cardiac remodelling: ↓ [95–97], = [75, 94, 98] Vascular remodelling: ↓ [57, 75, 96, 97], = [98, 99]	Exercise capacity: ↑ [100], = [101] Quality of life: = [101] mPAP/PVR: ↓ [100] (mPAP on echo)
	MR antagonists	Cardiac function: [102–104*] Cardiac remodelling: ↓ [63, 65, 103], [102, 104*] Vascular remodelling: ↓ [63, 65, 102, 103, 105, 106], [65] *combined with losartan	Exercise capacity: [107, 108] Cardiac function: [107] mPAP: [107]
Alternative RAAS	ACE2 activation	Disease progression: ↓ [109, 110] Cardiac function: ↑ [109, 110] Cardiac remodelling: ↓ [111, 110, 112] Vascular remodelling: ↓ [109–113]	Cardiac function: ↑ [55]
	Ang1-7 administration	Cardiac function: ↑ [110] Cardiac remodelling: ↓ [110, 114], = [115] Vascular remodelling: ↓ [110, 114], = [115]	
	Combined ACE2 and Ang1-7 administration	Cardiac function: ↑ [110], = [116] Cardiac remodelling: ↓ [116] [110] Vascular remodelling: ↓ [116] [110]	
	Ang1-9 administration	Cardiac remodelling: ↓ [14] Vascular remodelling: ↓ [14]	

$\beta$ -blockers target the SNS and are the cornerstone of treatment of left ventricular failure, but current guidelines advise against the use of  $\beta$ -blockers in PAH [2]. A small pilot study demonstrated the safety of the non-selective  $\beta$ -blocker carvedilol [79] in patients. However, in a bigger randomized controlled trial RV function and 6MWD did not improve with carvedilol [81], despite lower resting heart rate and increased  $\beta$ -AR expression. To prevent possible peripheral vasodilation and blunted exercise-induced skeletal muscle blood flow, the  $\beta_1$ AR selective  $\beta$ -blocker bisoprolol was tested. In this study, a drop in cardiac index observed caused concern that cardiac function actually deteriorated [80]. Although no other indicators of progressive heart failure were seen, the lack of improvements in cardiac function and 6MWD gave no indication to prescribe bisoprolol to PAH patients. Genetic variation in the  $\beta_1$ AR can cause hypersensitivity to carvedilol but insensitivity to metoprolol and bisoprolol [117] and may cause different individual responses to  $\beta$ -blockers.

Pharmacological interventions on the classical RAAS include ACE inhibition,  $AT_1$  blockade and MR antagonists. Clinical studies on ACE inhibition in pulmonary hypertension stem from the 1980s, when it was observed that captopril reduced both systemic- and pulmonary vascular resistance in congestive heart failure [118]. Two early studies indicated that captopril reduced systemic- but not pulmonary vascular resistance in PAH [91, 118]. By contrast, a significant decrease in pulmonary vascular resistance was found by Ikram *et al.* after only four days of captopril [93]. In this small study of five patients, the two youngest patients showed clinical improvements during three weeks of maintenance treatment. Collectively, these very small studies do not indicate a role for ACE inhibition by captopril in the treatment of PAH. In fact, the systemic vasodilatory effects of ACE inhibitors may exaggerate SNS and classical RAAS activities. While no further trials have been conducted, ACE inhibition may still have benefit in subgroups of patients.

$AT_1$  blockade has not been tested clinically in PAH. Instead, two clinical studies investigated the use of losartan in pulmonary hypertension (PH) secondary to chronic obstructive pulmonary disease (COPD) [101] and in PH secondary to lung disease or left ventricular failure [100]. Beneficial effects of losartan were observed after 8 weeks of treatment, including reduced mean pulmonary arterial pressure (mPAP) and increased exercise capacity [100]. However, in PH secondary to COPD losartan caused an early trend towards improvements in cardiac function and exercise capacity that was not maintained throughout 12 months of treatment [101]. Thus,  $AT_1$  blockade by losartan may have short-term but not long-term effects in PH patients.

## CHAPTER 7

Because of their diuretic action, MR antagonists are used to manage symptoms of RV failure in PAH. However, MR antagonists may have additional effects on the heart and lungs. Two studies investigated the use of the MR antagonist spironolactone in PAH. A retrospective analysis of patients using spironolactone while being enrolled in the ARIES-1 and -2 trial for the endothelin-receptor antagonist ambrisentan [119] revealed that spironolactone use enhanced the benefits of ambrisentan on 6MWD and the severity of PAH [108]. However, patients using spironolactone had generally more severe PAH at baseline. Therefore, in these patients the therapeutic potential of ambrisentan may have been higher, which would falsely suggest an effect of spironolactone. The use of spironolactone alone has recently been studied in 42 group I PAH patients, 19 of whom with idiopathic PAH [107]. Although no effects of spironolactone were found on markers of fibrosis, exercise capacity, disease progression or cardiac function, the use of spironolactone was safe and well-tolerated. An ongoing clinical trial (NCT01712620) aims to determine the clinical potential of spironolactone with longer treatment duration and earlier initiation.

Activating the counteractive alternative RAAS, instead of lowering classical RAAS activity, may also help to restore the balance within the RAAS. We are only beginning to recognize the role of the alternative RAAS system in the development of PAH. Therefore, to date only one clinical pilot study exists, investigating the effects of recombinant human ACE2 administration in five patients with either idiopathic PAH or hereditary PAH [55]. Importantly, no safety concerns were raised and ACE2 was well tolerated. In addition, short-term improvements in pulmonary haemodynamics and inflammatory status were observed, paving the way for additional trials into ACE2 administration.

### **Non-pharmacological treatments**

The results from preclinical and clinical studies into non-pharmacological strategies for neurohormonal modulation are summarized in Table 2. Only pulmonary artery denervation (PADN) has been studied in PAH patients.

Table 2 - **The effect of non-pharmacological treatments targeted at different neurohormonal signalling pathways in preclinical and clinical studies.** ↑ *Increased*, = *Unchanged*, ↓ *Decreased*. SNS = *sympathetic nervous system*, PNS = *parasympathetic nervous system*, RAAS = *renin-angiotensin-aldosterone system*, mPAP = *mean pulmonary artery pressure*, PVR = *pulmonary vascular resistance*, NA = *not available*

Target system	Treatment strategy	Preclinical	Clinical
SNS	Renal denervation	Survival: ↑ [120] Disease progression: ↓ [121] Cardiac function: ↑ [121, 122] Cardiac remodelling: ↓ [120–122] Vascular remodelling: ↓ [120–122]	
	Pulmonary artery denervation	Disease progression: ↓ [123] Exercise capacity: ↑ [123] Cardiac function: = [124], ↑ [123, 125–127] Cardiac remodelling: ↓ [123, 126, 127], = [124] Vascular remodelling: ↓ [123, 127, 128], = [124]	Survival: = [129] Disease progression: ↓ [129, 130] Exercise capacity: ↑ [129–132] Cardiac function: ↑ [129, 131, 132] mPAP/PVR: ↓ [129–132]
	Transection of the cervical sympathetic trunk	Cardiac function: ↑ [133] Cardiac remodelling: ↓ [133] Vascular remodelling: ↓ [133]	
PNS	Vagal nerve stimulation	Survival: ↑ [52] Cardiac function: ↑ [52] Cardiac remodelling: ↓ [52] Vascular remodelling: ↓ [52]	
Classical RAAS	N/A	N/A	
Alternative RAAS	N/A	N/A	

Pulmonary artery baroreceptor activation reflexively causes pulmonary vasoconstriction [134, 135], probably via adrenergic nerves [136]. This provides the rationale for PADN as a way to reverse pulmonary vasoconstriction. Indeed, an acute drop in mPAP was observed in 13 PAH patients who underwent PADN [129]. This reduction in mPAP was maintained during three months of follow-up, even while patients were completely withdrawn from PAH medication. In addition, progressive improvement in haemodynamics, 6MWD and clinical status were shown 6 months post-PADN. These improvements were maintained after up to one year of follow-up [131]. The improvements in hemodynamic status and 6MWD were recently confirmed in a multi-centre open label trial, although the benefit in that study was less dramatic [130]. Importantly, Rothman *et al.* showed

highly variable individual responses in patients who underwent PADN. While mPAP and pulmonary vascular resistance were reduced on average, in three patients the pulmonary vascular resistance actually increased [130]. Interestingly, however, no acute reductions in mPAP were observed in this study or in another case report [132], suggesting that mechanisms apart from relieving the reflexive vasoconstriction may play a role.

One such mechanism may be a general reduction in SNS activity. Stretch of the PA baroreceptors contributes to increased muscle sympathetic nerve activity in healthy individuals [137]. It is likely that this is the case in PAH patients too, given the extreme increase in PA pressure. In addition, PA baroreceptor stimulation increases the arterial baroreceptor setpoint and threshold [138], causing inactivation of arterial baroreceptors and thus increased SNS activity. However, heart rate at four- or six-months follow-up post PADN remained constant [130], suggesting that SNS activity was not reduced after the procedure.

### **Limitations for the use of neurohormonal modulation strategies in the clinic**

So far, we have described systemic and local neurohormonal imbalance in PAH patients and strategies to restore them. Translational difficulties and lack of mechanistic insight in the development of neurohormonal imbalance in PAH patients have limited the use of neurohormonal modulation therapies.

Three quarters of all studies described in this review were performed in various animal models of PAH, mostly rat, mouse and pig. However, promising results from  $\beta$ -blockers or ACE inhibitors seen in animal studies have not been translated to human trials. Obviously, the usefulness of these animal models can be disputed. First, commonly used rodent models resemble PAH in some but not all aspects. Experimental PAH usually develops over the course of several weeks instead of years as is the case in human PAH. This potentially limits the development of compensatory mechanisms [139]. Second, clinical studies have always been conducted against a background of PAH-specific therapy, while animals received the study medication only.

Clinical studies into neurohormonal modulation in PAH come with their own limitations. Importantly, the therapeutic window for any treatment is small in end-stage PAH, and thus early intervention is usually advocated for [140]. However, it should be emphasized that neurohormonal changes are not solely maladaptive. In fact, acute changes in neurohormonal activity are vital in the maintenance of cardiovascular homeostasis and thus, countering the neurohormonal systems may

at times be detrimental. At some point in the progression of PAH, the persistent neurohormonal activation becomes maladaptive. During this phase neurohormonal modulation may be beneficial. Longitudinal data on neurohormonal changes in either right- or left ventricular failure is scarce. In chronic congestive heart failure progressive increases in plasma levels of noradrenaline and renin have been described [141], suggesting progressive neurohormonal imbalance. In addition, levels of noradrenaline, Ang II and aldosterone that are found in failing hearts have been shown to exert deleterious effects on the heart and vasculature, as reviewed elsewhere [142], suggesting dose dependent effects of neurohormones. Thus, there seems to be an optimal treatment window to target the neurohormonal system, somewhere between the acute activation and chronic activation at pathologic levels. It is therefore pivotal to obtain longitudinal data of neurohormonal activity, in combination with hemodynamic and RV functional data.

Two important limitations have to be addressed that impede studies into neurohormonal changes over time. First, human tissue for investigation is hardly available and only from end-stage PAH. Therefore, it is less suitable to study longitudinal changes. Second, PAH is a rare disease and most clinical studies were able to include a few dozens of patients at best. This makes it difficult to reach sufficient statistical power, let alone to test subgroups of patients or different drug dosages and timing. The low number of patients is an important difference with studies into neurohormonal modulation in LV failure, where neurohormonal modulation strategies have been implemented despite similar lack of insight into neurohormonal changes over time. This affects clinical studies in two ways: first, in LV failure large cohorts of patients can be retrospectively analysed to identify factors that contribute to better or worse efficacy of neurohormonal modulation strategies. This is impossible in PAH. Second, small clinical studies with broad inclusion criteria did hardly show beneficial effects of neurohormonal modulation in PAH so far. Failure to enrol large numbers of patients requires diligent patient selection to prove smaller, yet clinically significant treatment effects.

Both the availability of human tissue for investigation and the limited numbers of patients in clinical trials will not change. Longitudinal assessment of neurohormonal changes could tell when and where neurohormonal derailment becomes evident in the course of the disease, and thereby help to select patients for specific neurohormonal modulation strategies. In addition, it will tell whether neurohormonal modulation strategies are timely and targeted as they are intended. Therefore, we advocate for the development, validation and use of non- and minimally invasive tools to monitor neurohormonal changes in PAH. In the following section, we will discuss possible tools, in different stages of development, that may help to improve our understanding of the neurohormonal changes in pulmonary hypertension.

## Strategies for longitudinal assessment of neurohormonal changes in PAH

The gold standard to measure autonomic activity is to directly measure (para) sympathetic nerve trafficking by muscle microneurography, usually in a superficial skeletal muscle. Alternatively, determination of regional noradrenaline spillover allows for an organ-specific determination of SNS activation. Using microdialysis, local acetylcholine concentrations can be determined to measure PNS activity [143]. However, these measurements are all highly invasive and as such do not lend themselves for repeated testing. Instead, plasma (nor)adrenaline levels have been used to study SNS activation but are not a reliable marker [29]. Alternatively,  $\beta$ -AR density in peripheral blood cells may serve as a marker of SNS (over-)activation [144]. Traditionally, determination of  $\beta$ -AR density relied on time consuming ligand binding assays. However, flow cytometric quantification of  $\beta$ -AR density was described recently [145] allowing for easy, high-throughput testing. Using this technique, it was shown that  $\beta$ -AR density is lower in blood cells in PAH patients compared to healthy controls [146] and is dose-dependently increased by the  $\beta$ -blocker carvedilol [81]. The changes in peripheral blood cells thus seem to mimic the changes seen in the heart. Further studies are needed to validate the use of flow cytometric quantification of  $\beta$ -AR expression as a marker of SNS in PAH patients.

Measuring PNS activity via plasma acetylcholine concentrations is not feasible due to high rates of degradation and clearance in the synaptic cleft [143]. Instead, plasma acetylcholinesterase activity may potentially serve as a biomarker for decreased PNS activity [147] but requires validation in PAH patients.

Non-invasive indirect measures for PNS and SNS activities have been drawn from ECG parameters. There is natural variation in the time between consecutive heart beats, called heart rate variability. When expressed in the frequency-domain, high-, low- and very-low frequency (HF, LF, VLF respectively) spectral power can be distinguished [148]. The LF/HF ratio is commonly used to determine sympatho-vagal balance, assuming that LF power is generated by the SNS while HF power is generated by the PNS. However, this assumption does not hold true [148]. Not surprisingly therefore, most studies do not find correlations between the LF/HF ratio and direct measures of SNS and PNS activities [143]. This is especially true in PAH where an inverse relation between LF/HF ratio and muscle sympathetic nerve activity has been observed [28]. Furthermore, proper measurement and analysis of heart rate variability variables outside standardized laboratory settings is complicated [143]. Nevertheless, improved methods for derivation of heartbeat-derived autonomic measures have been described [149] and the emergence of wearable devices, such as smartwatches and activity trackers, allows for ambulatory recordings in realistic settings.

Another non-invasive way to determine specifically PNS function is to measure heart rate recovery after maximal exercise. Heart rate recovery was shown to be reduced in PAH patients and was related to chronotropic incompetence and clinical worsening [36–38, 150, 151]. Heart rate recovery could easily and routinely be assessed by cardiopulmonary exercise testing (CPET). Even easier, however, would be the use of heart rate recovery after the 6-minute walking test, which is performed more frequently in the clinic. It was shown in heart failure patients, that the predictive value of heart rate recovery to predict survival is independent of whether the test is performed at maximal or sub-maximal intensity [152]. In PAH patients, it was shown that heart rate recovery after a 6-minute walking test was even more predictive for clinical worsening than the 6MWD itself [38]. However, a direct comparison for the use of heart rate recovery from the 6-minute walking test or maximal CPET has neither been made in heart failure, nor in PAH patients. One study showed that PAH patients exhibit relatively higher aerobic capacity during the 6-minute walking test compared to CPET, despite lower heart rate, but did not compare the use of heart rate recovery as a marker for PNS activity [153]. It is worth investigating further whether these non-invasive measurements, potentially easily derived from ambulatory measurements or simple tests, could help to determine and monitor autonomic status in PAH patients.

Neurohormonal changes can also be studied using imaging techniques. Positron emission tomography (PET) may become an additional powerful tool to study neurohormonal activation in a clinical setting. Many PET tracers have now become available to study different aspects of the ANS, including presynaptic neurotransmitter recycling,  $\beta$ -AR density, PNS terminal nerves and mAChR expression [154].

PET tracers also exist to study RAAS activity, via ACE- and AT<sub>1</sub>R expression [60, 155]. As ACE tracers usually accumulate in organs with high ACE expression, they are especially suitable to visualize ACE activity in the lungs [155]. Less tissue specific, but much quicker and cheaper, is the assessment of plasma levels and activity of the several RAAS components. As already mentioned, plasma levels of Ang I and II are increased in progressive but not in stable PAH [57]. In addition, plasma renin levels are an independent predictor of mortality in PAH [156].

Collectively, ongoing developments in heart rate variability algorithms and imaging techniques hold promise for the measurement and separation of neurohormonal activities. Together with plasma levels and CPET, they may provide tools for longitudinal assessment of the neurohormonal system and to study the interrelation between local neurohormonal systems in different organs.

## Conclusion

It is now clear that neurohormonal imbalance is involved in the development and progression of PAH. However, the neurohormonal system is vital for cardiovascular homeostasis. Thus, for successful clinical implementation, the timing and specificity of neurohormonal interventions needs to be improved. Because the number of patients available for clinical trials limit the use of subgroups, longitudinal assessment of neurohormonal activity is required. Non-invasive techniques such as imaging techniques may help to identify which patients may benefit from neurohormonal modulation, and at which phase of disease progression.

## Acknowledgements

The authors would like to thank Dr. Denielli da Silva Gonçalves Bos for discussion. HJB, AVN and FSdM were supported by the Netherlands CardioVascular Research Initiative: the Dutch Heart Foundation, Dutch Federation of University Medical Centres, the Netherlands Organization for Health Research and Development, and the Royal Netherlands Academy of Sciences (CVON-2012-08 PHAEDRA, CVON-2018-29 PHAEDRA-IMPACT, CVON-2017-10 Dolphin-Genesis). HJB and AVN were supported by research grants from Actelion, GSK and Ferrer (Therabel). ELP, AVN and FSdM were further supported by The Netherlands Organization for Scientific Research (NWO-VICI: 918.16.610, NWO-VIDI: 917.18.338). FSdM was supported by the Dutch Heart Foundation Dekker senior post-doc grant (2018T059).

## References

1. Farber HW, Loscalzo J. Pulmonary arterial hypertension. *N Engl J Med* 2004; 351: 1655–1665.
2. Trisvetova EL, Gubkin S V. 2015 ESC/EAS Guidelines for the diagnosis and treatment of pulmonary hypertension. *Eur. Heart J.* 2016; 37: 67–119.
3. Vonk Noordegraaf A, Westerhof BE, Westerhof N. The Relationship Between the Right Ventricle and its Load in Pulmonary Hypertension. *J. Am. Coll. Cardiol.* 2017; 69: 236–243.
4. Vonk Noordegraaf A, Haddad F, Chin KM, Forfia PR, Kawut SM, Lumens J, Naeije R, Newman J, Oudiz RJ, Provencher S, Torbicki A, Voelkel NF, Hassoun PM. Right heart adaptation to pulmonary arterial hypertension: Physiology and pathobiology. *J. Am. Coll. Cardiol.* 2013; 62: D22–D33.
5. De Man FS, Handoko ML, Guignabert C, Bogaard HJ, Vonk Noordegraaf A. Neurohormonal axis in patients with pulmonary arterial hypertension: Friend or foe? *Am. J. Respir. Crit. Care Med.* 2013; 187: 14–19.
6. Maron BA, Leopold JA. Emerging Concepts in the Molecular Basis of Pulmonary Arterial Hypertension: Part II: Neurohormonal Signaling Contributes to the Pulmonary Vascular and Right Ventricular Pathophenotype of Pulmonary Arterial Hypertension. *Circulation* 2015; 131: 2079–2091.
7. Vaillancourt M, Chia P, Sarji S, Nguyen J, Hoftman N, Ruffenach G, Eghbali M, Mahajan A, Umar S. Autonomic nervous system involvement in pulmonary arterial hypertension. *Respir. Res.* 2017; 18: 1–15.
8. Garcia-Lunar I, Pereda D, Ibanez B, Garcia-Álvarez A. Neurohormonal Modulation as a Therapeutic Target in Pulmonary Hypertension. *Cells* 2020; 9: 2521.
9. Maron BA, Leopold JA, Hemnes AR. Metabolic syndrome, neurohumoral modulation, and pulmonary arterial hypertension. *Br. J. Pharmacol.* 2020; 177: 1457–1471.
10. Rhoades RA, Tanner GA. *Medical Physiology*. First edit. 1995.
11. Ng KKF, Vane JR. Conversion of angiotensin I to angiotensin II. *Nature* 1967; 216: 762–766.
12. Mehta PK, Griendling KK. Angiotensin II cell signaling: Physiological and pathological effects in the cardiovascular system. *Am. J. Physiol. - Cell Physiol.* 2007; 292: C82–C97.
13. Hermidorff MM, de Assis LVM, Isoldi MC. Genomic and rapid effects of aldosterone: what we know and do not know thus far. *Heart Fail. Rev.* 2017; 22: 65–89.
14. Cha SA, Park BM, Kim SH. Angiotensin-(1-9) ameliorates pulmonary arterial hypertension via angiotensin type II receptor. *Korean J. Physiol. Pharmacol.* 2018; 22: 447–456.
15. Kostenis E, Milligan G, Christopoulos A, Sanchez-Ferrer CF, Heringer-Walther S, Sexton PM, Gemhardt F, Kellett E, Martini L, Vanderheyden P, Schultheiss HP, Walther T. G-protein-coupled receptor Mas is a physiological antagonist of the angiotensin II type 1 receptor. *Circulation* 2005; 111: 1806–1813.
16. Stella A, Zanchetti A. Functional role of renal afferents. *Physiol. Rev.* 1991; 71: 659–682.
17. Fong MW, Shavelle D, Weaver FA, Nadim MK. Renal denervation in heart failure. *Curr. Hypertens. Rep.* 2015; 17: 1–7.
18. Binkley PF, Haas GJ, Starling RC, Nunziata E, Hatton PA, Leier C V., Cody RJ. Sustained augmentation of parasympathetic tone with angiotensin-converting enzyme inhibition in patients with congestive heart failure. *J. Am. Coll. Cardiol.* 1993; 21: 655–661.

## CHAPTER 7

19. Schlaich MP, Sobotka PA, Krum H, Lambert E, Esler MD. Renal Sympathetic-Nerve Ablation for Uncontrolled Hypertension. *N. Engl. J. Med.* 2009; 361: 932–934.
20. Wang Y, Seto SW, Gollidge J. Angiotensin II, Sympathetic nerve activity and chronic heart failure. *Heart Fail. Rev.* 2014; 19: 187–198.
21. Schultz HD, Li YL, Ding Y. Arterial chemoreceptors and sympathetic nerve activity: Implications for hypertension and heart failure. *Hypertension* 2007; 50: 6–13.
22. Allen AM. Angiotensin AT1 receptor-mediated excitation of rat carotid body chemoreceptor afferent activity. *J. Physiol.* 1998; 510: 773–781.
23. Goldsmith SR. Interactions between the sympathetic nervous system and the RAAS in heart failure. *Curr. Heart Fail. Rep.* 2004; 1: 45–50.
24. Gironacci MM, Valera MS, Yujnovsky I, Peña C. Angiotensin-(1-7) inhibitory mechanism of norepinephrine release in hypertensive rats. *Hypertension* 2004; 44: 783–787.
25. Raasch W, Betge S, Dendorfer A, Bartels T, Dominiak P. Angiotensin converting enzyme inhibition improves cardiac neuronal uptake of noradrenaline in spontaneously hypertensive rats. *J. Hypertens.* 2001; 19: 1827–1833.
26. Katoh M, Egashira K, Takeshita A. Cardiac angiotensin II receptors are downregulated by chronic angiotensin II infusion in rats. *Jpn. J. Pharmacol.* 2000; 84: 75–77.
27. Dockstader K, Nunley K, Karimpour-Fard A, Medway A, Nelson P, Refidaff C, Liggett SB, Bristow MR, Sucharov CC. Temporal analysis of mRNA and miRNA expression in transgenic mice overexpressing Arg- and Gly389 polymorphic variants of the  $\beta$ 1-adrenergic receptor. *Physiol. Genomics* 2011; 43: 1294–1306.
28. McGowan CL, Swiston JS, Notarius CF, Mak S, Morris BL, Picton PE, Granton JT, Floras JS. Discordance between microneurographic and heart-rate spectral indices of sympathetic activity in pulmonary arterial hypertension. *Heart* 2009; 95: 754–758.
29. Velez-Roa S, Ciarka A, Najem B, Vachiere J-L, Naeije R, Van de Borne P. Increased sympathetic nerve activity in pulmonary artery hypertension. *Circulation* 2004; 110: 1308–1312.
30. Nagaya N, Nishikimi T, Uematsu M, Satoh T, Kyotani S, Sakamaki F, Kakishita M, Fukushima K, Okano Y, Nakanishi N, Miyatake K, Kangawa K. Plasma Brain Natriuretic Peptide as a Prognostic Indicator in Patients with Primary Pulmonary Hypertension. *Circulation* 2000; 102: 865–870.
31. Miyamoto S, Nagaya N, Satoh T, Kyotani S, Sakamaki F, Fujita M, Nakanishi N, Miyatake K. Clinical correlates and prognostic significance of six-minute walk test in patients with primary pulmonary hypertension. Comparison with cardiopulmonary exercise testing. *Am. J. Respir. Crit. Care Med.* 2000; 161: 487–492.
32. Nootens M, Kaufmann E, Rector T, Toher C, Judd D, Francis GS, Rich S. Neurohormonal activation in patients with right ventricular failure from pulmonary hypertension: relation to hemodynamic variables and endothelin levels. *J. Am. Coll. Cardiol.* 1995; 26: 1581–1585.
33. Mak S, Witte KK, Al-Hesayen A, Granton JJ, Parker JD. Cardiac sympathetic activation in patients with pulmonary arterial hypertension. *Am. J. Physiol. - Regul. Integr. Comp. Physiol.* 2012; 302: 1153–1157.
34. Richards AM, Ikram H, Crozier IG, Nicholls MG, Jans S. Ambulatory pulmonary arterial pressure in primary pulmonary hypertension: variability, relation to systemic arterial pressure, and plasma catecholamines. *Br. Heart J.* 1990; 63: 103–108.

35. Wensel R, Jilek C, Dörr M, Francis DP, Stadler H, Lange T, Blumberg F, Opitz C, Pfeifer M, Ewert R, Opitz C, Pfeifer M, Ewert R. Impaired cardiac autonomic control relates to disease severity in pulmonary hypertension. *Eur. Respir. J.* 2009; 34: 895–901.
36. Da Silva Gonçalves Bos D, Van der Bruggen CEE, Kurakula K, Sun X-Q, Casali KR, Casali AG, Rol N, Szulcek R, Dos Remedios C, Guignabert C, Tu L, Dorfmüller P, Humbert M, Wijnker PJM, Kuster DWD, Van der Velden J, Goumans M-J, Bogaard H-J, Vonk Noordegraaf A, De Man FS, Handoko ML. Contribution of Impaired Parasympathetic Activity to Right Ventricular Dysfunction and Pulmonary Vascular Remodeling in Pulmonary Arterial Hypertension. *Circulation* 2018; 137: 910–924.
37. Dimopoulos S, Anastasiou-Nana M, Katsaros F, Papazachou O, Tzani G, Gerovasili V, Pozios H, Roussos C, Nanas J, Nanas S. Impairment of autonomic nervous system activity in patients with pulmonary arterial hypertension: a case control study. *J. Card. Fail.* 2009; 15: 882–889.
38. Minai OA, Gudavalli R, Mummadi S, Liu X, McCarthy K, Dweik RA. Heart rate recovery predicts clinical worsening in patients with pulmonary arterial hypertension. *Am. J. Respir. Crit. Care Med.* 2012; 185: 400–408.
39. Billings CG, Hurdman JA, Condliffe R, Elliot CA, Smith IA, Austin M, Armstrong IJ, Hamilton N, Charalampopoulos A, Sabroe I, Swift AJ, Rothman AM, Wild JM, Lawrie A, Waterhouse JC, Kiely DG. Incremental shuttle walk test distance and autonomic dysfunction predict survival in pulmonary arterial hypertension. *J. Hear. Lung Transplant.* 2017; 36: 871–879.
40. Ciarka A, Doan V, Velez-Roa S, Naeije R, Van de Borne P. Prognostic significance of sympathetic nervous system activation in pulmonary arterial hypertension. *Am. J. Respir. Crit. Care Med.* 2010; 181: 1269–1275.
41. Bienias P, Ciurzynski M, Kostrubiec M, Rymarczyk Z, Kurzyrna M, Korczak DD, Roik M, Torbicki A, Fijalkowska A, Pruszczyk P. Functional class and type of pulmonary hypertension determinate severity. *Acta Cardiol.* 2015; 70: 286–286.
42. Mercurio V, Pellegrino T, Bosso G, Campi G, Parrella P, Piscopo V, Tocchetti CG, Hassoun P, Petretta M, Cuocolo A, Bonaduce D. EXPRESS: Cardiac Sympathetic Dysfunction in Pulmonary Arterial Hypertension: Lesson from Left-sided Heart Failure. *Pulm. Circ.* 2019; 9: 2045894019868620.
43. Bristow MR, Minobe W, Rasmussen R, Larrabee P, Skerl L, Klein JW, Anderson FL, Murray J, Mestroni L, Karwande S V. Beta-adrenergic neuroeffector abnormalities in the failing human heart are produced by local rather than systemic mechanisms. *J. Clin. Invest.* 1992; 89: 803–815.
44. Rijnierse MT, Groeneveldt JA, Van Campen JSJA, De Boer K, Van der Bruggen CEEE, Harms HJ, Raijmakers PG, Lammertsma AA, Knaapen P, Bogaard HJ, Westerhof BE, Vonk Noordegraaf A, Allaart CP, DeMan F. Bisoprolol therapy does not reduce right ventricular sympathetic activity in pulmonary arterial hypertension patients. *Pulm. Circ.* 2019; 9: 1–9.
45. Ciarka A, Vachiéry J-LL, Houssière A, Gujic M, Stoupe E, Velez-Roa S, Naeije R, Van de Borne P. Atrial septostomy decreases sympathetic overactivity in pulmonary arterial hypertension. *Chest* 2007; 131: 1831–1837.
46. Sharma T, Lau EMT, Choudhary P, Torzillo PJ, Munoz PA, Simmons LR, Naeije R, Celermajor DS. Dobutamine stress for evaluation of right ventricular reserve in pulmonary arterial hypertension. *Eur. Respir. J.* 2015; 45: 700–708.
47. Hsu S, Houston BA, Tampakakis E, Bacher AC, Rhodes PS, Mathai SC, Damico RL, Kolb TM, Hummers LK, Shah AA, McMahan Z, Corona-Villalobos CP, Zimmerman SL, Wigley FM, Hassoun PM, Kass DA, Tedford RJ. Right ventricular functional reserve in pulmonary arterial hypertension. *Circulation* 2016; 133: 2413–2422.

## CHAPTER 7

48. Grünig E, Tiede H, Enyimayew EO, Ehlken N, Seyfarth HJ, Bossone E, D'Andrea A, Naeije R, Olschewski H, Ulrich S, Nagel C, Halank M, Fischer C. Assessment and prognostic relevance of right ventricular contractile reserve in patients with severe pulmonary hypertension. *Circulation* 2013; 128: 2005–2015.
49. Krüger M, Linke WA. Protein kinase-A phosphorylates titin in human heart muscle and reduces myofibrillar passive tension. *J. Muscle Res. Cell Motil.* 2006; 27: 435–444.
50. Rain S, Andersen S, Najafi A, Schultz JG, Da Silva Gonçalves Bós D, Handoko ML, Bogaard HJ, Vonk Noordegraaf A, Andersen A, Van der Velden J, Ottenheijm CAC, De Man FS. Right ventricular myocardial stiffness in experimental pulmonary arterial hypertension. *Circ. Hear. Fail.* 2016; 9: e002636.
51. Bogaard HJ, Natarajan R, Mizuno S, Abbate A, Chang PJ, Chau VQ, Hoke NN, Kraskauskas D, Kasper M, Salloum FN, Voelkel NF. Adrenergic receptor blockade reverses right heart remodeling and dysfunction in pulmonary hypertensive rats. *Am. J. Respir. Crit. Care Med.* 2010; 182: 652–660.
52. Yoshida K, Saku K, Kamada K, Abe K, Tanaka-Ishikawa M, Tohyama T, Nishikawa T, Kishi T, Sunagawa K, Tsutsui H. Electrical Vagal Nerve Stimulation Ameliorates Pulmonary Vascular Remodeling and Improves Survival in Rats With Severe Pulmonary Arterial Hypertension. *JACC. Basic to Transl. Sci.* 2018; 3: 657–671.
53. Luo J, Gu Y, Liu P, Jiang X, Yu W, Ye P, Chao Y, Yang H, Zhu L, Zhou L, Chen S. Berberine attenuates pulmonary arterial hypertension via protein phosphatase 2A signaling pathway both in vivo and in vitro. *J. Cell. Physiol.* 2018; 233: 9750–9762.
54. Luo Q, Wang X, Liu R, Qiao H, Wang P, Jiang C, Zhang Q, Cao Y, Yu H, Qu L. alpha1A-adrenoceptor is involved in norepinephrine-induced proliferation of pulmonary artery smooth muscle cells via CaMKII signaling. *J. Cell. Biochem.* 2019; 120: 9345–9355.
55. Hemnes AR, Rathinasabapathy A, Austin EA, Brittain EL, Carrier EJ, Chen X, Fessel JP, Fike CD, Fong P, Fortune N, Gerszten RE, Johnson JA, Kaplowitz M, Newman JH, Piana R, Pugh ME, Rice TW, Robbins IM, Wheeler L, Yu C, Loyd JE, West J. A potential therapeutic role for angiotensin-converting enzyme 2 in human pulmonary arterial hypertension. *Eur. Respir. J.* 2018; 51.
56. Sandoval J, Del Valle-Mondragón L, Masso F, Zayas N, Pulido T, Teijeiro R, Gonzalez-Pacheco H, Olmedo-Ocampo R, Sisniega C, Paez-Arenas A, Pastelin-Hernandez G, Gomez-Arroyo J, Voelkel NF. Angiotensin converting enzyme 2 and angiotensin (1-7) axis in pulmonary arterial hypertension. *Eur. Respir. J.* 2020; 56.
57. De Man FS, Tu L, Handoko ML, Rain S, Ruiter G, François C, Schalij I, Dorfmueller P, Simonneau G, Fadel E, Perros F, Boonstra A, Postmus PE, Van der Velden J, Vonk Noordegraaf A, Humbert M, Eddahibi S, Guignabert C. Dysregulated renin-angiotensin-aldosterone system contributes to pulmonary arterial hypertension. *Am. J. Respir. Crit. Care Med.* 2012; 186: 780–789.
58. Maron BA, Opotowsky AR, Landzberg MJ, Loscalzo J, Waxman AB, Leopold JA. Plasma aldosterone levels are elevated in patients with pulmonary arterial hypertension in the absence of left ventricular heart failure: A pilot study. *Eur. J. Heart Fail.* 2013; 15: 277–283.
59. Safdar Z, Thakur A, Singh S, Ji Y, Guffey D, Minard CG, Entman ML. Circulating Aldosterone Levels and Disease Severity in Pulmonary Arterial Hypertension HHS Public Access. *J Pulm Respir Med* 2015; 5.
60. Qing F, McCarthy TJ, Markham J, Schuster DP. Pulmonary angiotensin-converting enzyme (ACE) binding and inhibition in humans: A positron emission tomography study. *Am. J. Respir. Crit. Care Med.* 2000; 161: 2019–2025.

61. Orte C, Polak JM, Haworth SG, Yacoub MH, Morrell NW. Expression of pulmonary vascular angiotensin-converting enzyme in primary and secondary plexiform pulmonary hypertension. *J. Pathol.* 2000; 192: 379–384.
62. Schuster DP, Crouch EC, Parks WC, Johnson T, Botney MD. Angiotensin converting enzyme expression in primary pulmonary hypertension. *Am. J. Respir. Crit. Care Med.* 1996; 154: 1087–1091.
63. Maron BA, Zhang YY, White K, Chan SY, Handy DE, Mahoney CE, Loscalzo J, Leopold JA. Aldosterone inactivates the endothelin-B receptor via a cysteinyl thiol redox switch to decrease pulmonary endothelial nitric oxide levels and modulate pulmonary arterial hypertension. *Circulation* 2012; 126: 963–974.
64. Yamanaka R, Otsuka F, Nakamura K, Yamashita M, Otani H, Takeda M, Matsumoto Y, Kusano KF, Ito H, Makino H. Involvement of the bone morphogenetic protein system in endothelin- and aldosterone-induced cell proliferation of pulmonary arterial smooth muscle cells isolated from human patients with pulmonary arterial hypertension. *Hypertens. Res.* 2010; 33: 435–445.
65. Preston IR, Sagliani KD, Warburton RR, Hill NS, Fanburg BL, Jaffe IZ. Mineralocorticoid receptor antagonism attenuates experimental pulmonary hypertension. *Am J Physiol Lung Cell Mol Physiol* 2013; 304: L678–L688.
66. Neri Sernerri GG, Boddi M, Coppo M, Chechi T, Zarone N, Moira M, Poggese L, Margheri M, Simonetti I. Evidence for the existence of a functional cardiac renin-angiotensin system in humans. *Circulation* 1996; 94: 1886–1893.
67. Zisman LS, Asano K, Dutcher DL, Ferdensi A, Robertson AD, Jenkin M, Bush EW, Bohlmeyer T, Perryman MB, Bristow MR. Differential Regulation of Cardiac Angiotensin Converting Enzyme Binding Sites and AT1 Receptor Density in the Failing Human Heart. *Circulation* 1998; 98: 1735–1741.
68. Pérez-Vizcaíno F. Lung ACE2 and ADAM17 in pulmonary arterial hypertension: Implications for COVID-19? *J. Hear. Lung Transplant.* 2020; 39: 1167–1169.
69. Zisman LS, Keller RS, Weaver B, Lin Q, Speth R, Bristow MR, Canver CC. Increased angiotensin-(1-7)-forming activity in failing human heart ventricles: Evidence for upregulation of the angiotensin-converting enzyme homologue ACE2. *Circulation* 2003; 108: 1707–1712.
70. Usui S, Yao A, Hatano M, Kohmoto O, Takahashi T, Nagai R, Kinugawa K. Upregulated neurohumoral factors are associated with left ventricular remodeling and poor prognosis in rats with monocrotaline-induced pulmonary arterial hypertension. *Circ. J.* 2006; 70: 1208–1215.
71. Ishikawa M, Sato N, Asai K, Takano T, Mizuno K. Effects of a pure alpha/beta-adrenergic receptor blocker on monocrotaline-induced pulmonary arterial hypertension with right ventricular hypertrophy in rats. *Circ. J.* 2009; 73: 2337–2341.
72. De Man FS, Handoko ML, Van Ballegoij JJMM, Schalij I, Bogaards SJPP, Postmus PE, Van der Velden J, Westerhof N, Paulus WJ, Vonk Noordegraaf A. Bisoprolol delays progression towards right heart failure in experimental pulmonary hypertension. *Circ. Hear. Fail.* 2012; 5: 97–105.
73. Fowler ED, Drinkhill MJ, Norman R, Pervolaraki E, Stones R, Steer E, Benoist D, Steele DS, Calaghan SC, White E. Beta1-adrenoceptor antagonist, metoprolol attenuates cardiac myocyte Ca<sup>2+</sup> handling dysfunction in rats with pulmonary artery hypertension. *J. Mol. Cell. Cardiol.* 2018; 120: 74–83.
74. Perros F, Ranchoux B, Izikki M, Bentebbal S, Happé C, Antigny F, Jourdon P, Dorfmueller P, Lecerf F, Fadel E, Simonneau G, Humbert M, Bogaard HJ, Eddahibi S. Nebivolol for improving endothelial dysfunction, pulmonary vascular remodeling, and right heart function in pulmonary hypertension. *J. Am. Coll. Cardiol.* 2015; 65: 668–680.

## CHAPTER 7

75. Andersen S, Schultz JG, Andersen A, Ringgaard S, Nielsen JM, Holmboe S, Vildbrad MD, De Man FS, Bogaard HJ, Vonk Noordegraaf A, Nielsen-Kudsk JE. Effects of bisoprolol and losartan treatment in the hypertrophic and failing right heart. *J. Card. Fail.* 2014; 20: 864–873.
76. Lima-Seolin BG de, Colombo R, Bonetto JHP, Teixeira RB, Donatti LM, Casali KR, Godoy AEG, Litvin IE, Schenkel PC, Rosa Araujo AS da, Belló-Klein A, de Lima-Seolin BG, Colombo R, Bonetto JHP, Teixeira RB, Donatti LM, Casali KR, Godoy AEG, Litvin IE, Schenkel PC, da Rosa Araujo AS, Belló-Klein A. Bucindolol improves right ventricle function in rats with pulmonary arterial hypertension through the reversal of autonomic imbalance. *Eur. J. Pharmacol.* 2017; 798: 57–65.
77. De Lima-Seolin BG, Hennemann MM, Fernandes RO, Colombo R, Bonetto JHP, Teixeira RB, Khaper N, Godoy AEG, Litvin IE, Sander da Rosa Araujo A, Schenkel PC, Belló-Klein A. Bucindolol attenuates the vascular remodeling of pulmonary arteries by modulating the expression of the endothelin-1 A receptor in rats with pulmonary arterial hypertension. *Biomed. Pharmacother.* 2018; 99: 704–714.
78. Fujio H, Nakamura K, Matsubara H, Kusano KF, Miyaji K, Nagase S, Ikeda T, Ogawa A, Ohta-Ogo K, Miura D, Miura A, Miyazaki M, Date H, Ohe T. Carvedilol inhibits proliferation of cultured pulmonary artery smooth muscle cells of patients with idiopathic pulmonary arterial hypertension. *J. Cardiovasc. Pharmacol.* 2006; 47: 250–255.
79. Grinnan D, Bogaard HJ, Grizzard J, Van Tassell B, Abbate A, DeWilde C, Priday A, Voelkel NF. Treatment of group I pulmonary arterial hypertension with carvedilol is safe. *Am. J. Respir. Crit. Care Med.* 2014; 189: 1562–1564.
80. Van Campen JSJA, De Boer K, Van de Veerdonk MC, Van der Bruggen CEE, Allaart CP, Rajmakers PG, Heymans MW, Marcus JT, Harms HJ, Handoko ML, De Man FS, Vonk Noordegraaf A, Bogaard H-J. Bisoprolol in idiopathic pulmonary arterial hypertension: an explorative study. *Eur. Respir. J.* 2016; 48: 787–796.
81. Farha S, Saygin D, Park MM, Cheong HI, Asosingh K, Comhair SA, Stephens OR, Roach EC, Sharp J, Highland KB, DiFilippo FP, Neumann DR, Tang WHW, Erzurum SC. Pulmonary arterial hypertension treatment with carvedilol for heart failure: a randomized controlled trial. *JCI insight* 2017; 2.
82. Deng Y, Guo SL, Wei B, Gao XC, Zhou YC, Li JQ. Activation of nicotinic acetylcholine  $\alpha 7$  receptor attenuates progression of monocrotaline-induced pulmonary hypertension in rats by downregulating the NLRP3 inflammasome. *Front. Pharmacol.* 2019; 10: 128.
83. Nong Z, Stassen J-M, Moons L, Collen D, Janssens S. Inhibition of Tissue Angiotensin-Converting Enzyme With Quinapril Reduces Hypoxic Pulmonary Hypertension and Pulmonary Vascular Remodeling. *Circulation* 1996; 94: 1941–1947.
84. Ortiz LA, Champion HC, Lasky JA, Gambelli F, Gozal E, Hoyle GW, Beasley MB, Hyman AL, Friedman M, Kadowitz PJ. Enalapril protects mice from pulmonary hypertension by inhibiting TNF-mediated activation of NF- $\kappa$ B and AP-1. *Am. J. Physiol. - Lung Cell. Mol. Physiol.* 2002; 282: L1209–L1221.
85. Abraham WT, Reynolds M V, Gottschall B, Badesch DB, Wynne KM, Groves BM, Lowes BD, Bristow MR, Benjamin Perryman M, Voelkel NF. Importance of Angiotensin-Converting Enzyme in Pulmonary Hypertension. *Cardiology* 1995; 86: 9–15.
86. Morrell NW, Atochina EN, Morris KG, Danilov SM, Stenmark KR. Angiotensin converting enzyme expression is increased in small pulmonary arteries of rats with hypoxia-induced pulmonary hypertension. *J. Clin. Invest.* 1995; 96: 1823–1833.

87. Kanno S, Wu YJL, Lee PC, Billiar TR, Ho C. Angiotensin-converting enzyme inhibitor preserves p21 and endothelial nitric oxide synthase expression in monocrotaline-induced pulmonary arterial hypertension in rats. *Circulation* 2001; 104: 945–950.
88. Okada K, Bernstein ML, Zhang W, Schuster DP, Botney MD. Angiotensin-converting enzyme inhibition delays pulmonary vascular neointimal formation. *Am. J. Respir. Crit. Care Med.* 1998; 158: 939–950.
89. Van Suylen RJ, Smits JFM, Daemen MJAP. Pulmonary artery remodeling differs in hypoxia- and monocrotaline-induced pulmonary hypertension. *Am. J. Respir. Crit. Care Med.* 1998; 157: 1423–1428.
90. Baybutt R, Herndon B, Umbehr J, Mein J, Xue Y, Reppert S, Van Dillen C, Kamal R, Halder A, Molteni A. Effects on Cytokines and Histology by Treatment with the Ace Inhibitor Captopril and the Antioxidant Retinoic Acid in the Monocrotaline Model of Experimentally Induced Lung Fibrosis. *Curr. Pharm. Des.* 2007; 13: 1327–1333.
91. Rich S, Martinez J, Lam W, Rosen KM. Captopril as treatment for patients with pulmonary hypertension. Problem of variability in assessing chronic drug treatment. *Br. Heart J.* 1982; 48: 272–277.
92. Leier C V, Bambach B, Nelson S. Captopril in primary pulmonary hypertension. *Clin. Res.* 1981; 29.
93. Ikram H, Maslowski AH, Nicholls MG, Espiner EA, Hull FT. Haemodynamic and hormonal effects of captopril in primary pulmonary hypertension. *Br. Heart J.* 1982; 48: 541–545.
94. Usui S, Yao A, Hatano M, Kohmoto O, Takahashi T, Nagai R, Kinugawa K. Upregulated neurohumoral factors are associated with left ventricular remodeling and poor prognosis in rats with monocrotaline-induced pulmonary arterial hypertension. *Circ. J.* 2006; 70: 1208–1215.
95. Nakamoto T, Harasawa H, Akimoto K, Hirata H, Kaneko H, Kaneko N, Sorimachi K. Effects of olmesartan medoxomil as an angiotensin II-receptor blocker in chronic hypoxic rats. *Eur. J. Pharmacol.* 2005; 528: 43–51.
96. Xie L, Lin P, Xie H, Xu C. Effects of atorvastatin and losartan on monocrotaline-induced pulmonary artery remodeling in rats. *Clin. Exp. Hypertens.* 2010; 32: 547–554.
97. Lu Y, Guo H, Sun Y, Pan X, Dong J, Gao D, Chen W, Xu Y, Xu D. Valsartan attenuates pulmonary hypertension via suppression of mitogen activated protein kinase signaling and matrix metalloproteinase expression in rodents. *Mol. Med. Rep.* 2017; 16: 1360–1368.
98. Tanabe Y, Morikawa Y, Kato T, Kanai S, Watakabe T, Nishijima A, Iwata H, Isobe K, Ishizaki M, Nakayama K. Effects of olmesartan, an AT1 receptor antagonist, on hypoxia-induced activation of ERK1/2 and pro-inflammatory signals in the mouse lung. *Naunyn. Schmiedeberg's. Arch. Pharmacol.* 2006; 374: 235–248.
99. Clements RT, Vang A, Fernandez-Nicolas A, Kue NR, Mancini TJ, Morrison AR, Mallem K, McCullough DJ, Choudhary G. Treatment of Pulmonary Hypertension with Angiotensin II Receptor Blocker and Nephilysin Inhibitor Sacubitril/Valsartan. *Circ. Hear. Fail.* 2019; 12.
100. Bozbaş ŞS, Bozbaş H, Atar A, Ulubay G, Eyüboğlu FÖ. Comparative effects of losartan and nifedipine therapy on exercise capacity, Doppler echocardiographic parameters and endothelin levels in patients with secondary pulmonary hypertension. *Anatol. J. Cardiol.* 2010; 10: 43–49.

## CHAPTER 7

101. Morrell NW, Higham MA, Phillips PG, Shakur BH, Robinson PJ, Beddoes RJ. Pilot study of losartan for pulmonary hypertension in chronic obstructive pulmonary disease. *Respir. Res.* 2005; 6: 88.
102. Boehm M, Arnold N, Braithwaite A, Pickworth J, Lu C, Novoyatleva T, Kiely DG, Grimminger F, Ghofrani HA, Weissmann N, Seeger W, Lawrie A, Schermuly RT, Kojonazarov B. Eplerenone attenuates pathological pulmonary vascular rather than right ventricular remodeling in pulmonary arterial hypertension. *BMC Pulm. Med.* 2018; 18.
103. Maron BA, Oldham WM, Chan SY, Vargas SO, Arons E, Zhang YY, Loscalzo J, Leopold JA. Upregulation of steroidogenic acute regulatory protein by hypoxia stimulates aldosterone synthesis in pulmonary artery endothelial cells to promote pulmonary vascular fibrosis. *Circulation* 2014; 130: 168–179.
104. Borgdorff MA, Bartelds B, Dickinson MG, Steendijk P, Berger RMF. A cornerstone of heart failure treatment is not effective in experimental right ventricular failure. *Int. J. Cardiol.* 2013; 169: 183–189.
105. Aghamohammadzadeh R, Zhang YY, Stephens TE, Arons E, Zaman P, Polach KJ, Matar M, Yung LM, Yu PB, Bowman FP, Opatowsky AR, Waxman AB, Loscalzo J, Leopold JA, Maron BA. Up-regulation of the mammalian target of rapamycin complex 1 subunit Raptor by aldosterone induces abnormal pulmonary artery smooth muscle cell survival patterns to promote pulmonary arterial hypertension. *FASEB J.* 2016; 30: 2511–2527.
106. Wang Y, Zhong B, Wu Q, Tong J, Zhu T, Zhang M. Effect of aldosterone on senescence and proliferation inhibition of endothelial progenitor cells induced by sirtuin 1 (SIRT1) in pulmonary arterial hypertension. *Med. Sci. Monit.* 2020; 26.
107. Safdar Z, Frost A, Basant A, Deswal A, O'Brian Smith E, Entman M. Spironolactone in pulmonary arterial hypertension: results of a cross-over study. *Pulm. Circ.* 2020; 10.
108. Maron BA, Waxman AB, Opatowsky AR, Gillies H, Blair C, Aghamohammadzadeh R, Loscalzo J, Leopold JA. Effectiveness of spironolactone plus ambrisentan for treatment of pulmonary arterial hypertension (from the [ARIES] Study 1 and 2 Trials). *Am. J. Cardiol.* 2013; 112: 720–725.
109. Shenoy V, Gjymishka A, Jarajapu YP, Qi Y, Afzal A, Rigatto K, Ferreira AJ, Fraga-Silva RA, Kearns P, Douglas JY, Agarwal D, Mubarak KK, Bradford C, Kennedy WR, Jun JY, Rathinasabapathy A, Bruce E, Gupta D, Cardounel AJ, Mocco J, Patel JM, Francis J, Grant MB, Katovich MJ, Raizada MK. Diminazene attenuates pulmonary hypertension and improves angiogenic progenitor cell functions in experimental models. *Am. J. Respir. Crit. Care Med.* 2013; 187: 648–657.
110. Shenoy V, Kwon KC, Rathinasabapathy A, Lin S, Jin G, Song C, Shil P, Nair A, Qi Y, Li Q, Francis J, Katovich MJ, Daniell H, Raizada MK. Oral delivery of angiotensin-converting enzyme 2 and angiotensin-(1-7) bioencapsulated in plant cells attenuates pulmonary hypertension. *Hypertension* 2014; 64: 1248–1259.
111. Yamazato Y, Ferreira AJ, Hong KH, Sriramula S, Francis J, Yamazato M, Yuan L, Bradford CN, Shenoy V, Oh SP, Katovich MJ, Raizada MK. Prevention of pulmonary hypertension by angiotensin-converting enzyme 2 gene transfer. *Hypertension* 2009; 54: 365–371.
112. Ferreira AJ, Shenoy V, Yamazato Y, Sriramula S, Francis J, Yuan L, Castellano RK, Ostrov DA, Oh SP, Katovich MJ, Raizada MK. Evidence for angiotensin-converting enzyme 2 as a therapeutic target for the prevention of pulmonary hypertension. *Am. J. Respir. Crit. Care Med.* 2009; 179: 1048–1054.
113. Li G, Zhang H, Zhao L, Zhang Y, Yan D, Liu Y. Angiotensin-converting enzyme 2 activation ameliorates pulmonary endothelial dysfunction in rats with pulmonary arterial hypertension

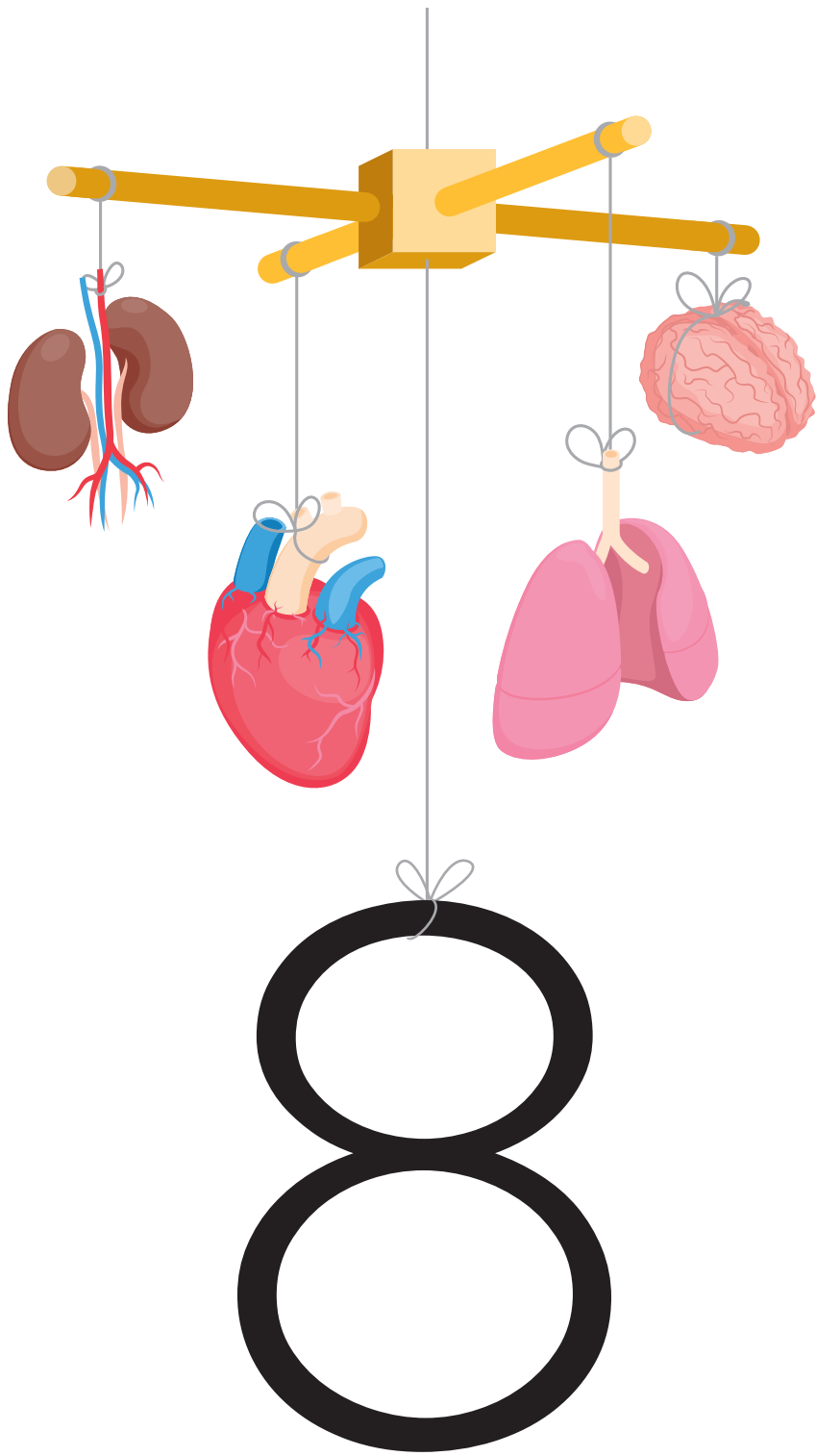
through mediating phosphorylation of endothelial nitric oxide synthase. *J. Am. Soc. Hypertens.* 2017; 11: 842–852.

114. Chen L, Xiao J, Li Y, Ma H. Ang(1-7) might prevent the development of monocrotaline induced pulmonary arterial hypertension in rats. *Eur Rev Med Pharmacol Sci* 2011; 15: 1–7.
115. Breitling S, Krauszman A, Parihar R, Walther T, Friedberg MK, Kuebler WM. Dose-dependent, therapeutic potential of angiotensin-(1–7) for the treatment of pulmonary arterial hypertension. *Pulm. Circ.* 2015; 5: 649–657.
116. Daniell H, Mangu V, Yakubov B, Park J, Habibi P, Shi Y, Gonnella PA, Fisher A, Cook T, Zeng L, Kawut SM, Lahm T. Investigational new drug enabling angiotensin oral-delivery studies to attenuate pulmonary hypertension. *Biomaterials* 2020; 233: 119750.
117. Rochais F, Vilardaga JP, Nikolaev VO, Bünemann M, Lohse MJ, Engelhardt S. Real-time optical recording of  $\beta$ 1-adrenergic receptor activation reveals supersensitivity of the Arg389 variant to carvedilol. *J. Clin. Invest.* 2007; 117: 229–235.
118. Leier C V, Bambach B, Nelson S, Bambach D, Nelson S, Hermiller JB, Huss P, Magorien RD, Unverferth D V. Captopril in primary pulmonary hypertension. *Clin. Res.* 1981; 29.
119. Galiè N, Olschewski H, Oudiz RJ, Torres F, Frost A, Ghofrani HA, Badesch DB, McGoon MD, McLaughlin V V., Roecker EB, Gerber MJ, Dufton C, Wiens BL, Rubin LJ. Ambrisentan for the treatment of pulmonary arterial hypertension: Results of the ambrisentan in pulmonary arterial hypertension, randomized, double-Blind, placebo-controlled, multicenter, efficacy (ARIES) study 1 and 2. *Circulation* 2008; 117: 3010–3019.
120. Liu Q, Song J, Lu D, Geng J, Jiang Z, Wang K, Zhang B, Shan Q. Effects of renal denervation on monocrotaline induced pulmonary remodeling. *Oncotarget* 2017; 8: 46846–46855.
121. Da Silva Gonçalves Bos D, Happé C, Schalij I, Pijacka W, Paton JFR, Guignabert C, Tu L, Thuillet R, Bogaard HJ, Van Rossum AC, Vonk Noordegraaf A, De Man FS, Handoko ML. Renal Denervation Reduces Pulmonary Vascular Remodeling and Right Ventricular Diastolic Stiffness in Experimental Pulmonary Hypertension. *JACC Basic to Transl. Sci.* 2017; 2: 22–35.
122. Qingyan Z, Xuejun J, Yanhong T, Zixuan D, Xiaozhan W, Xule W, Zongwen G, Wei H, Shengbo Y, Congxin H. Beneficial Effects of Renal Denervation on Pulmonary Vascular Remodeling in Experimental Pulmonary Artery Hypertension. *Rev. Esp. Cardiol. (Engl. Ed.)* 2015; 68: 562–570.
123. Huang Y, Liu YW, Pan HZ, Zhang XL, Li J, Xiang L, Meng J, Wang PH, Yang J, Jing ZC, Zhang H. Transthoracic Pulmonary Artery Denervation for Pulmonary Arterial Hypertension. *Arterioscler. Thromb. Vasc. Biol.* 2019; 39: 704–718.
124. Garcia-Lunar I, Pereda D, Santiago E, Solanes N, Nuche J, Ascaso M, Bobi J, Sierra F, Dantas AP, Galán C, San Antonio R, Sánchez-Quintana D, Sánchez-González J, Barberá JA, Rigol M, Fuster V, Ibáñez B, Sabaté M, García-Álvarez A. Effect of pulmonary artery denervation in postcapillary pulmonary hypertension: results of a randomized controlled translational study. *Basic Res. Cardiol.* 2019; 114.
125. Rothman AMK, Arnold ND, Chang W, Watson O, Swift AJ, Condliffe R, Elliot CA, Kiely DG, Suvarna SK, Gunn J, Lawrie A. Pulmonary Artery Denervation Reduces Pulmonary Artery Pressure and Induces Histological Changes in an Acute Porcine Model of Pulmonary Hypertension. *Circ. Cardiovasc. Interv.* 2015; 8.
126. Zhou L, Zhang J, Jiang X-M, Xie D-J, Wang J-S, Li L, Li B, Wang Z-M, Rothman AMK, Lawrie A, Chen S-L. Pulmonary Artery Denervation Attenuates Pulmonary Arterial Remodeling in Dogs With Pulmonary Arterial Hypertension Induced by Dehydrogenized Monocrotaline. *JACC. Cardiovasc. Interv.* 2015; 8: 2013–2023.

## CHAPTER 7

127. Zhang H, Yu W, Zhang J, Xie D, Gu Y, Ye P, Chen SL. Pulmonary artery denervation improves hemodynamics and cardiac function in pulmonary hypertension secondary to heart failure. *Pulm. Circ.* 2019; 9.
128. Liu C, Jiang X-M, Zhang J, Li B, Li J, Xie D-J, Hu Z-Y. Pulmonary artery denervation improves pulmonary arterial hypertension induced right ventricular dysfunction by modulating the local renin-angiotensin-aldosterone system. *BMC Cardiovasc. Disord.* 2016; 16: 192.
129. Chen S-L, Zhang F-F, Xu J, Xie D-J, Zhou L, Nguyen T, Stone GW. Pulmonary artery denervation to treat pulmonary arterial hypertension: the single-center, prospective, first-in-man PADN-1 study (first-in-man pulmonary artery denervation for treatment of pulmonary artery hypertension). *J. Am. Coll. Cardiol.* 2013; 62: 1092-1100.
130. Rothman AMK, Vachieri JL, Howard LS, Mikhail GW, Lang IM, Jonas M, Kiely DG, Shav D, Shabtay O, Avriel A, Lewis GD, Rosenzweig EB, Kirtane AJ, Kim NH, Mahmud E, McLaughlain V V., Chetcuti S, Leon MB, Ben-Yehuda O, Rubin LJ. Intravascular Ultrasound Pulmonary Artery Denervation to Treat Pulmonary Arterial Hypertension (TROPHY1): Multicenter, Early Feasibility Study. *JACC Cardiovasc. Interv.* 2020; 13: 989-999.
131. Chen SL, Xie DJ, Zhang J, Zhou L, Rothman AMK, Stone GW, Hoepfer MM, Galiè N, Chen SL, Zhang H, Xie DJ, Zhang J, Zhou L, Rothman AMK, Stone GW. Hemodynamic, Functional, and Clinical Responses to Pulmonary Artery Denervation in Patients with Pulmonary Arterial Hypertension of Different Causes: Phase II Results from the Pulmonary Artery Denervation-1 Study. *Circ. Cardiovasc. Interv.* 2015; 8: e002837.
132. Fujisawa T, Kataoka M, Kawakami T, Isobe S, Nakajima K, Kunitomi A, Kashimura S, Katsumata Y, Nishiyama T, Kimura T, Nishiyama N, Aizawa Y, Murata M, Fukuda K, Takatsuki S. Pulmonary Artery Denervation by Determining Targeted Ablation Sites for Treatment of Pulmonary Arterial Hypertension. *Circ. Cardiovasc. Interv.* 2017; 10.
133. Zhao Y, Xiang R, Peng X, Dong Q, Li D, Yu G, Xiao L, Qin S, Huang W. Transection of the cervical sympathetic trunk inhibits the progression of pulmonary arterial hypertension via ERK-1/2 Signalling. *Respir. Res.* 2019; 20: 121.
134. Osorio J, Russek M. Reflex changes on the pulmonary and systemic pressures elicited by stimulation of baroreceptors in the pulmonary artery. *Circ. Res.* 1962; 10: 664-667.
135. Juratsch CE, Emmanouilides GC, Thibeault DW, Baylen BG, Jengo JA, Laks MM. Pulmonary arterial hypertension induced by distention of the main pulmonary artery in conscious newborn, young, and adult sheep. *Pediatr. Res.* 1980; 14: 1332-1338.
136. Juratsch CE, Jengo JA, Castagna J, Laks MM. Experimental pulmonary hypertension produced by surgical and chemical denervation of the pulmonary vasculature. *Chest* 1980; 77: 525-530.
137. Simpson LL, Meah VL, Steele A, Thapamagar S, Gasho C, Anholm JD, Drane AL, Dawkins TG, Busch SA, Oliver SJ, Lawley JS, Tymko MM, Ainslie PN, Steinback CD, Stembridge M, Moore JP. Evidence for a physiological role of pulmonary arterial baroreceptors in sympathetic neural activation in healthy humans. *J. Physiol.* 2020; 598: 955-965.
138. Moore JP, Hainsworth R, Drinkhill MJ. Reflexes from pulmonary arterial baroreceptors in dogs: Interaction with carotid sinus baroreceptors. *J. Physiol.* 2011; 589: 4041-4052.
139. Ryan J, Bloch K, Archer SL. Rodent models of pulmonary hypertension: Harmonisation with the world health organisation's categorisation of human PH. *Int. J. Clin. Pract.* 2011; 65: 15-34.
140. Rafikova O, Al Ghouleh I, Rafikov R. Focus on Early Events: Pathogenesis of Pulmonary Arterial Hypertension Development. *Antioxidants Redox Signal.* 2019. p. 933-953.

141. Francis GS, Rector TS, Cohn JN. Sequential neurohumoral measurements in patients with congestive heart failure. *Am. Heart J.* 1988; 116: 1464–1468.
142. Hartupée J, Mann DL. Neurohormonal activation in heart failure with reduced ejection fraction. *Nat. Rev. Cardiol.* 2016. p. 30–38.
143. De Geus E, Van Lien R, Neijts M, Willemsen G. Genetics of Autonomic Nervous System Activity. *Oxford Handb. Mol. Psychol.* 2009. p. 357–390.
144. Brodde OE, Kretsch R, Ikezono K, Zerkowski HR, Reidemeister JC. Human  $\beta$ -adrenoceptors: Relation of myocardial and lymphocyte  $\beta$ -adrenoceptor density. *Science (80-. ).* 1986; 231: 1584–1585.
145. Saygin D, Wanner N, Rose JA, Naga Prasad S V., Tang WHW, Erzurum S, Asosingh K. Relative quantification of beta-adrenergic receptor in peripheral blood cells using flow cytometry. *Cytom. Part A* 2018. p. 563–570.
146. Rose JA, Wanner N, Cheong HI, Queisser K, Barrett P, Park M, Hite C, Naga Prasad S V., Erzurum S, Asosingh K. Flow cytometric quantification of peripheral blood cell  $\beta$ -adrenergic receptor density and urinary endothelial cell-derived microparticles in pulmonary arterial hypertension. *PLoS One* 2016; 11: 156940.
147. Brzezinski RY, Fisher E, Cohen N, Zwang E, Shefer G, Stern N, Zeltser D, Shapira I, Berliner S, Rogowski O, Shenhar-Tsarfaty S. Total serum cholinesterase activity predicts hemodynamic changes during exercise and associates with cardiac troponin detection in a sex-dependent manner. *Mol. Med.* 2018; 24.
148. Shaffer F, Ginsberg JP. An Overview of Heart Rate Variability Metrics and Norms. *Front. Public Heal.* 2017; 5: 258.
149. Valenza G, Citi L, Saul JP, Barbieri R. Measures of sympathetic and parasympathetic autonomic outflow from heartbeat dynamics. *J. Appl. Physiol.* 2018; 125: 19–39.
150. Parrella P, Campi G, Rodolico A, Mancini A, Franco R, Bruno D, Cuomo A, Tocchetti G, Petretta M, Bonaduce D, Mercurio V. Parasympathetic activity in pulmonary arterial hypertension: could a simple measure do the trick? *Eur. Respir. J.* 2018; 52: PA3324.
151. Wu C, Guo J, Liu H, Pudasaini B, Yang W, Zhao Q, Wang L, Liu J. The Correlation of Decreased Heart Rate Recovery and Chronotropic Incompetence with Exercise Capacity in Idiopathic Pulmonary Arterial Hypertension Patients. *Biomed Res. Int.* 2017; 2017.
152. Cahalin LP, Forman DE, Chase P, Guazzi M, Myers J, Bensimhon D, Peberdy MA, Ashley E, West E, Arena R. The prognostic significance of heart rate recovery is not dependent upon maximal effort in patients with heart failure. *Int. J. Cardiol.* 2013; 168: 1496–1501.
153. Deboeck G, Niset G, Vachier JL, Moraine JJ, Naeije R. Physiological response to the six-minute walk test in pulmonary arterial hypertension. *Eur. Respir. J.* 2005; 26: 667–672.
154. Boutagy NE, Sinusas AJ. Recent Advances and Clinical Applications of PET Cardiac Autonomic Nervous System Imaging. *Curr. Cardiol. Rep.* 2017; 19: 1–13.
155. Chen X, Werner RA, Javadi MS, Maya Y, Decker M, Lapa C, Herrmann K, Higuchi T. Radionuclide imaging of neurohormonal system of the heart. *Theranostics* 2015; 5: 545–558.
156. Plácido R, Cortez-Dias N, Robalo Martins S, Almeida AG, Calisto C, Gonçalves S, Sadoune M, Nunes Diogo A, Mebazaa A, Pinto FJ. Prognostic stratification in pulmonary hypertension: A multi-biomarker approach. *Rev. Port. Cardiol. (English Ed.)* 2017; 36: 111–125.



## **DISCUSSION AND FUTURE PERSPECTIVES**

---

Idiopathic pulmonary arterial hypertension (iPAH) is a rare, and severe, pulmonary vascular disease. Narrowing of the vascular lumen leads to right ventricular (RV) overload and ultimately RV failure. The continuous pressure overload on the RV induces a vicious circle of tissue hypoxia, altered metabolism, neurohormonal activation and further deterioration of RV function. We explored three possible strategies to slow down the vicious circle of RV deterioration and eventually RV failure in iPAH: improvement of oxygen supply (**Chapter 2 and 3**), reduction of oxygen demand (**Chapter 4 and 5**), and restoration of the neurohormonal balance (**Chapter 6 and 7**).

### Oxygen supply

In **chapter 2**, we investigated the regulation of myoglobin expression in the hypertrophied RV in the monocrotaline (MCT) model of PH. While total oxidative capacity, and thus oxygen demand, increased in the MCT rats, myoglobin (Mb) mRNA expression did not. Yet, the absolute amount of Mb protein increased, indicating increased translation. The minimal extracellular oxygen tension needed to prevent hypoxic cell cores when mitochondria are maximally active ( $PO_2$ crit) was calculated to be almost twice as high in the MCT animals compared to control. This indicates that the increase in Mb protein expression was just enough to compensate for the increase in cell size but not for the increased oxygen demand. Therefore, a mismatch between oxygen supply and demand arises during the development of RV hypertrophy. In an earlier study, Mb concentration protein expression was unchanged in stable PH, but reduced in progressive PH. Moreover, Mb mRNA expression per nucleus was upregulated in stable PH but not in progressive PH [1]. These findings together show that failure to upregulate Mb mRNA expression eventually leads to reduced functional Mb concentration in hypertrophied cardiomyocytes which may contribute to RV failure.

A reduction in Mb concentration has also been observed in human end-stage PAH [1], indicating the clinical relevance of these findings. At the time of diagnosis, most PAH patients have already developed severe RV hypertrophy. Future studies should therefore determine whether increasing Mb expression at late(r) stages of the disease will be sufficient to prevent cardiac hypoxia and RV failure. For this purpose, the pulmonary trunk banding (PTB) model of PH may provide a useful tool, as the degree of hypertrophy can be relatively well-controlled and banding could even be reversed [2, 3].

As much as there seems to be room for improvement, upregulating cardiac Mb expression seems difficult. Previous studies suggested that the combination of hypoxia with fatty acid supplementation may increase Mb expression [4, 5]. In **chapter 3**, we applied different levels of hypoxia in combination with fatty acid

supplementation to cultured skeletal muscle myotubes. In addition, we applied insulin-like growth factor (IGF)-1 to induce hypertrophy. We showed that IGF-1 can partly prevent hypoxia-induced atrophy but also inhibits Mb expression, which complicates combining hypertrophy and increasing Mb expression. Importantly, IGF-1 expression is upregulated in the RV both in the MCT and PTB rat models of PH [6–8], and thus may contribute to the lack of increase in Mb expression. In young mice, inhibition of the IGF-1 receptor attenuated RV hypertrophy and improved RV function [6]. Future studies should address the questions whether the effects of IGF-1 inhibition are partly caused by increased Mb expression and whether this could be a viable strategy to improve RV function in PAH. As IGF-1 is involved in a wide variety of signalling functions in almost every cell type, cardiac specific regulation of IGF-1 may be required and may not be without side-effects.

We were unable to induce Mb expression by fatty acid supplementation, unlike previous studies [4, 5]. Differences in timing and the relatively short duration of the supplementation may explain the discrepancy. Moreover, the regulation of Mb expression seems complex and is under regulation of several transcription factors [9] and additionally modulated by iron [10], calcium [9], thyroid hormone [11], reactive oxygen species (ROS) [4] and vascular endothelial growth factor (VEGF) [12]. Our finding that VEGF mRNA expression was reduced following lipid supplementation may partly explain the lack of effect on Mb expression. It is also a somewhat worrisome finding in the context of oxygen supply, as VEGF is an important driver of angiogenesis. Even if fatty acid supplementation in a different study design would upregulate Mb expression, its effect on VEGF levels and possibly on angiogenesis should be considered.

Other strategies to improve myocardial oxygen supply may include iron supplementation and stimulation of cardiac angiogenesis. Iron is an important co-factor for both Mb and haemoglobin (Hb) and as such important for oxygen supply. Iron deficiency is common in iPAH patients [13] while intravenous iron supplementation increased skeletal muscle Mb levels in iron deficient PAH patients [10]. Nevertheless, it did not change submaximal exercise capacity or RV function at rest, and it is unknown whether cardiac Mb was increased as well. In line with these findings, a recent randomized clinical trial reported the safety and efficacy of parenteral iron supplementation to restore iron levels, but showed no effect on exercise performance nor on cardiac function [14]. Despite impaired iron absorption in PAH patients [13], another clinical trial showed that oral ferric maltol can increase six-minute walking distance (6MWD) and decrease RV dimensions [15]. Collectively, iron supplementation may improve exercise capacity, but has unclear effects on cardiac myoglobin expression and RV function in PAH. All three reported clinical studies included iron deficient patients only. However, as they used different measures to define iron deficiency, they cannot be readily compared.

Uniform patient selection and combined analysis of trials as done by Howard *et al.* [14] may help to further reveal the potential of iron supplementation in PAH. In addition, for the purpose of increasing Mb expression, iron supplementation may be combined with other possible strategies to increase its expression.

Stimulation of angiogenesis may be another way to improve oxygen supply in the RV. In several animal models, capillary density sets apart adaptive from maladaptive cardiac hypertrophy and therefore seems to be an attractive therapeutic target. Several angiogenic stimulators exist, including VEGF, hypoxia-inducible factor (HIF)-1 $\alpha$  and HIF-2 $\alpha$ , apelin and miRNAs [16]. Multiple clinical trials in heart failure have investigated gene therapy delivery of VEGF but with unsatisfactory results [17]. An important hurdle for gene therapy is the difficulty of safe and efficacious delivery, preferentially in low doses. VEGF is also an additional major regulator of endothelial cell function and is highly expressed in plexiform lesions in the lungs of PAH patients [16]. This raises concerns regarding the safety and feasibility of gene therapy-induced angiogenesis in PAH. The potential and limitations of proangiogenic interventions in PAH are extensively reviewed elsewhere [16]. However, stimulation of angiogenesis in the RV is currently far from clinical application and may have severe side-effects in the pulmonary vasculature.

In conclusion, we showed that experimental PH is associated with failure to induce Mb mRNA expression. Supplementation with fatty acids, in combination with hypoxia and IGF-1 stimulation did not increase Mb expression. Nevertheless, we believe Mb is an important target for improving oxygen supply. The effects of iron supplementation on cardiac function and myoglobin expression are unclear and seem less beneficial than hoped for. Moreover, the safety and feasibility of proangiogenic strategies in the RV is unclear and not ready for clinical implementation yet. In addition, Mb has other functions (e.g., scavenging of ROS, NO production [18], regulation of lipid metabolism [19]) which may be of importance to cardiac adaptation in PAH as well. In depth research is needed to unravel the complex regulation of myoglobin expression during hypertrophy and hypoxia, for which cell culture models may provide a useful initial step. Although far from clinical application, it allows for relatively high-throughput screening for modulators of Mb expression under different conditions.

### Oxygen demand

In chapters 4 and 5, we investigated the possibilities of reducing oxygen demand. In **chapter 4**, we were able to quantify a histochemical determination to estimate mitochondrial efficiency *ex vivo* in small amounts of tissue. Using this technique, we observed a heterogeneous reduction in RV mitochondrial efficiency in experimental PH, possibly underlying the reported reductions in mechanical

efficiency in rats and PAH patients [20, 21]. However, in an MCT model comparable to ours, mitochondrial oxygen consumption was decreased in the failing RV [22]. The latter seems paradoxical in the light of reduced mitochondrial efficiency but seems to represent mitochondrial dysfunction [22].

Animal studies and indirect measures of mitochondrial dysfunction in human have shown mitochondrial hyperpolarization [23], increased complex II activity [24] and structural and functional abnormalities [25]. Surprisingly, a comparison between mitochondrial function in human remodelled RV and non-remodelled left ventricle (LV) of PH patients at the time of heart-lung transplant, revealed that despite differences in substrate handling, mitochondria from the RV were tightly coupled due to *less* proton leak [26]. There was, however, an impairment in the electron transport chain (ETC) or oxidative phosphorylation (OXPHOS) limiting complex I respiration [26]. A common limitation in such patient studies is the limited availability of samples and the lack of true healthy control samples, as was the case in this study as well (n=4, of which only one patient was iPAH). Therefore, RV samples had to be compared to samples from 'non-remodelled' LV samples from the same patients. The need for freshly isolated mitochondria to determine respiratory function further adds to the difficulty of obtaining such samples. Our method can take away at least this latter limitation, as frozen tissue can be used. Future studies could then include more samples and confirm the validity of comparing mitochondrial function in the remodelled RV to non-remodelled LV

The reduction in mitochondrial efficiency in our study was related to the fatty acid content of the inner mitochondrial membrane (IMM) (i.e., membrane stability). Loss of membrane stability causes proton leak and loss of the proton gradient across the IMM, and therefore inefficient ATP production. Basal proton leak largely depends on the fatty acid composition of the IMM [27] but is generally small compared to the total proton leak [28]. Although we showed a relation between fatty acid content of the IMM and mitochondrial efficiency, an important question is therefore to what extent basal proton leak contributes to reduced mitochondrial efficiency. In addition, the non-linearity of this relation suggests that other factors play a role. Basal proton conductance is largely related to the abundance of adenine nucleotide translocase (ANT) [28]. In addition, uncoupling proteins (UCPs) can facilitate proton transport across the IMM to regulate ROS levels [29, 30]. To our knowledge, no studies exist on ANT expression either in rat or human PH. However, ANT mRNA expression is increased after aortic banding and subsequent LV remodelling in rats [31], suggesting a response to pressure overload. UCP2 mRNA expression is upregulated in the RV of mice that underwent PTB, while genetic deletion of UCP2 protected against pressure-induced RV failure [32]. Although promising, targeting UCP2 may have adverse effects in the pulmonary vasculature, as UCP2 silencing in the lungs contributed to proliferation and remodelling, thereby inducing mild PH [32].

Collectively, using quantitative histochemistry we showed reduced mitochondrial efficiency, related to the fatty acid composition of the IMM. Although mitochondrial efficiency can be severely hampered, the contribution of IMM stability, ANT and UCPs to proton leak in PAH is unknown. Before even aiming to enhance mitochondrial efficiency via one of these targets, their roles should be investigated into more detail, especially because targeting the mitochondria may have effects in the lungs too. An important question in this regard is whether mitochondrial dysfunction is a consequence of or actually *drives* RV failure.

In **chapter 5**, we studied the role of monoamine oxidase (MAO)-A, a potential major source of ROS, and large consumer of oxygen in experimental PH. We observed that MAO-A inhibition by clorgyline reduced RV afterload and pulmonary vascular remodelling in a Sugen-Hypoxia model of PH, through reduced vascular proliferation and oxidative stress. However, using a PTB model of PH, we observed no direct effects of MAO-A inhibition on the RV, despite strong upregulation of MAO-A. Treatments targeting vascular remodelling should be beneficial or at least non-toxic to the RV. In that light, our findings of reduced vascular remodelling with no toxicity to the RV are encouraging. However, they are not in line with previous findings in the overloaded LV [33] and somewhat surprising, given the major upregulation of MAO-A expression with pressure overload. Two explanations may be explored: the RV may respond differently to MAO-A upregulation and inhibition which would confirm previously reported differences between the RV and LV in ROS production and antioxidant defence [34]. Alternatively, the timing for MAO-A inhibition may be of importance. Studies on MAO-A inhibition in LV failure have often started inhibition simultaneously with induction of pressure overload, whereas we started clorgyline treatment in established RV overload. This suggests that MAO-A inhibition may be preventive of cardiac failure but not able to reverse it. The latter would mean a clear limitation for the translation to the clinic, as the treatment window in PAH is small and advanced RV remodelling is present already at the time of diagnosis. In addition, we did not find increased MAO-A expression in the RV of PAH patients when compared to relatively healthy LV tissue of myocardial infarction patients, possibly limiting the clinical relevance. Both isoforms of MAO, A and B, are expressed in the human heart and both show detrimental cardiac effects when overexpressed in mice [33, 35]. Therefore, the role of MAO-B in the RV needs further attention. Unfortunately, we were unable to directly measure oxygen consumption of MAO-A in the RV and could not confirm the effects of MAO-A inhibition on oxygen consumption [36]. Thus, the contribution of MAO-A to mechanical inefficiency remains to be determined.

Altogether, mitochondrial efficiency and MAO-A may both contribute to enhanced oxygen demand in the RV, although little is known about their contributions to

eventual RV failure and the underlying mechanisms. Both may provide interesting treatment targets, but the relevance of these targets requires confirmation in human studies as well as mechanistic studies. The use of biobanks and proper conservation of scarce and unique human tissues would be of immense help. In addition, the validity of less-ideal control samples should be determined for the purpose of the different studies.

## The neurohormonal balance

The regulation of cardiovascular homeostasis is largely under control of the autonomic nervous system (ANS) and renin-angiotensin-aldosterone system (RAAS). In iPAH, there is neurohormonal imbalance both in the ANS and RAAS. Chronic overactivation of the sympathetic nervous system (SNS) is thought to underly hyperventilation, which is common among iPAH patients and associated with worse prognosis. Therefore, in **chapter 6**, we studied the effect of two relatively simple interventions that lower SNS activity on ventilation in iPAH patients. Although both long-term beta blocker treatment and short-term hyperoxic breathing reduced heart rate, indicating reduced sympathetic activation, we did not see any effect on ventilation, neither at rest nor during exercise. Our results did not allow for further investigation on the mechanisms of hyperventilation. Among the possible mechanisms are increased chemosensitivity [37], local mechanical forces in the pulmonary artery [38, 39], low work rate lactic acidosis [40], hyperkalaemia [41] and reduced peripheral blood supply [42]. Thus, hyperventilation in PAH may be multifactorial. We showed that interfering on the SNS did not alter ventilation, although adaptations on our protocol are worth investigating. Other possible causes of hyperventilation as mentioned above are difficult if not impossible to intervene on. In this light, exercise may be an important strategy. In CHF patients, exercise training restored autonomic balance and lowered HR, while reducing also  $VE/VCO_2$  by unknown mechanisms [43].

Finally, in **chapter 7** we reviewed the neurohormonal system in iPAH in more detail, as well as the interventions on it that have been tested clinically and preclinically. Despite the promising results in some studies, the small number of patients limits the confirmation by larger clinical trials. In addition, retrospective analysis to identify differences between responders and non-responders is difficult and patient tissue for research is scarce. Therefore, we argue for a more personalised approach and better insight into the neurohormonal changes over the course of the disease.

### Translation to the clinic

Collectively, this thesis showed that Mb expression, mitochondrial function, ROS formation and neurohormonal balance may provide treatment targets in PAH. However, most of these studies have been done in rat models of PAH which makes translation to the clinic still a long way. In chapter 7 we discussed the limitations of these preclinical models in the context of neurohormonal modulation. In general, the commonly used rodent models of PAH resemble human PAH all in different aspects, but never fully. Particularly the quick progression of RV overload and the lack of background therapy in these models distinguish them from human PAH. Thus, it is important to verify the significance of our findings in humans.

Yet, research in human PAH is difficult. As mentioned, the number of patients is relatively small and therefore does not allow for large clinical trials and retrospective analyses between responders and non-responders. In addition, RV tissue is only available from autopsy or from explanted hearts and thus always represents end-stage heart failure. We argued that longitudinal assessment of neurohormonal changes will help identify patients that will possibly benefit from a certain treatment. This not only applies to studies into neurohormonal modulation but to virtually all areas. In this light, developments in engineered heart tissue and the use of isolated and cultured pulmonary artery endothelial cells and smooth muscle cells will hopefully allow for more personalized approaches in the future. Until then, it is important to make use of the different animal models as well as the non- and minimally invasive strategies to monitor changes in patients over time.

Several additional factors may be considered when designing translational studies: first, studying drugs that are already clinically used may accelerate their way to the clinic for PAH. When choosing from different compounds for the same target, this should be taken into account. Second, as mentioned before, each animal model has its own similarities and differences with human PAH. Therefore, choosing the right animal model for the right purpose improves the translatability of the results. Third, to optimize clinical studies, selecting patients more likely to respond to a particular treatment (e.g., because of high/low baseline values or certain genetic traits) may help to personalize treatments and prove their potential.

### Targeting the vicious circle as a whole

Now that we discussed the strategies to interfere with oxygen supply, oxygen demand and the neurohormonal system in PAH, the obvious question arises which path to follow. However, as the ultimate cause of RV failure in PAH is unknown, it is impossible to prioritise one mechanism over the other when developing new treatments. It is conceivable that there is not one single strategy that will prevent

or slow the development of RV failure. In addition, there are pathophysiological mechanisms in the RV besides oxygen supply and demand and neurohormonal imbalance. Those include diastolic impairment due to sarcomeric stiffening of RV cardiomyocytes, impaired contraction and relaxation because of RV fibrosis, and a shift from mitochondrial glucose oxidation to aerobic glycolysis (the Warburg effect) causing lactate accumulation and reduced energy production. As such, future studies may want to target the vicious circle of RV failure as a whole. Thereto, the role of exercise programs seems promising.

Evidence for a supplementary role of exercise to standard pharmacological therapies is emerging [44]. A 15-week low dose exercise program in PAH and chronic thrombo-embolic PH (CTEPH) patients showed improved peak  $\text{VO}_2$ , indicating improved oxidative metabolism [45]. Moreover, improvements in cardiac index at rest and during exercise, exercise capacity and quality of life were reported [45]. An improvement in peak  $\text{VO}_2$  was also recently observed in the largest multi-centre study on exercise in PAH so far [46]. A clinical trial is currently under way to further investigate the effects of exercise specifically on the RV (NCT04224012). Nevertheless, the molecular mechanisms underlying the positive effects of exercise in PAH patients are largely unknown. Animal studies on this topic show adaptations related to  $\text{H}_2\text{O}_2$  concentration, apoptotic signalling, (mitochondrial) oxidative stress, cardiac remodelling, neurohumoral activation, metabolism and inflammation [47]. Studying the molecular changes underlying beneficial effects of exercise programs also in patients will help to optimize exercise programs.

To conclude, Mb expression, mitochondrial inefficiency, MAO-A activity and neurohormonal imbalance may serve as therapeutic targets. As it is likely that none of these mechanisms on its own causes the development and progression of RV failure, it is of importance to improve them all. Exercise can impact a wide variety of signalling pathways and mechanisms underlying the symptoms in PAH and may therefore be an ideal addition to pharmacological treatment, and can help to target the vicious circle of RV failure as a whole.

## References

1. Ruiter G, Wong YY, de Man FS, Handoko ML, Jaspers RT, Postmus PE, Westerhof N, Niessen HWM, van der Laarse WJ, Vonk-Noordegraaf A. Right ventricular oxygen supply parameters are decreased in human and experimental pulmonary hypertension. *J. Hear. Lung Transplant.* 2013; 32: 231–240.
2. Andersen S, Schultz JG, Holmboe S, Axelsen JB, Hansen MS, Lyhne MD, Nielsen-Kudsk JE, Andersen A. A Pulmonary Trunk Banding Model of Pressure Overload Induced Right Ventricular Hypertrophy and Failure. *J. Vis. Exp.* 2018; : 3–9.
3. Boehm M, Tian X, Mao Y, Ichimura K, Dufva MJ, Ali K, Prosseda SD, Shi Y, Kuramoto K, Reddy S, Kheyfets VO, Metzger RJ, Spiekerkoetter E. Delineating the molecular and histological events that govern right ventricular recovery using a novel mouse model of pulmonary artery de-banding. *Cardiovasc. Res.* 2020; 116: 1700–1709.
4. Schlater AE, De Miranda MA, Frye MA, Trumble SJ, Kanatous SB. Changing the paradigm for myoglobin: a novel link between lipids and myoglobin. *J. Appl. Physiol.* 2014; 117: 307–315.
5. De Miranda MA, Schlater AE, Green TL, Kanatous SB. In the face of hypoxia: Myoglobin increases in response to hypoxic conditions and lipid supplementation in cultured Weddell seal skeletal muscle cells. *J. Exp. Biol.* 2012; 215: 806–813.
6. Shi L, Kojonazarov B, Elgheznawy A, Popp R, Dahal BK, Böhm M, Pullamsetti SS, Ghofrani HA, Gödecke A, Jungmann A, Katus HA, Müller OJ, Schermuly RT, Fisslthaler B, Seeger W, Fleming I. MiR-223-IGF-1R signalling in hypoxia- and load-induced right-ventricular failure: A novel therapeutic approach. *Cardiovasc. Res.* 2016; 111: 184–193.
7. Connolly M, Garfield BE, Crosby A, Morrell NW, Wort SJ, Kemp PR. miR-322-5p targets IGF-1 and is suppressed in the heart of rats with pulmonary hypertension. *FEBS Open Bio* 2018; 8: 339–348.
8. Peters EL, Offringa C, Kos D, van der Laarse WJ, Jaspers RT. Regulation of myoglobin in hypertrophied rat cardiomyocytes in experimental pulmonary hypertension. *PLugers Arch. Eur. J. Physiol.* 2016; : 1–11.
9. Kanatous SB, Mammen PPA. Regulation of myoglobin expression. *J. Exp. Biol.* 2010; 213: 2741–2747.
10. Ruiter G, Manders E, Happé CM, Schalij I, Groepenhoff H, Howard LS, Wilkins MR, Bogaard HJ, Westerhof N, van der Laarse WJ, de Man FS, Vonk-Noordegraaf A. Intravenous iron therapy in patients with idiopathic pulmonary arterial hypertension and iron deficiency. *Pulm. Circ.* 2015; 5: 466–472.
11. Giannocco G, Dossantos RA, Nunes MT. Thyroid hormone stimulates myoglobin gene expression in rat cardiac muscle. *Mol. Cell. Endocrinol.* 2004; 226: 19–26.
12. Van Weel V, Deckers MML, Grimbergen JM, Van Leuven KJM, Lardenoye JWHP, Schlingemann RO, Van Nieuw Amerongen GP, Van Bockel JH, Van Hinsbergh VWM, Quax PHA. Vascular endothelial growth factor overexpression in ischemic skeletal muscle enhances myoglobin expression in vivo. *Circ. Res.* 2004; 95: 58–66.
13. Ruiter G, Lankhorst S, Boonstra A, Postmus PE, Zweegman S, Westerhof N, Van Der Laarse WJ, Vonk-Noordegraaf A. Iron deficiency is common in idiopathic pulmonary arterial hypertension. *Eur. Respir. J.* 2011; 37: 1386–1391.
14. Howard LSGE, He J, Watson GMJ, Huang L, Wharton J, Luo Q, Kiely DG, Condliffe R, Pepke-

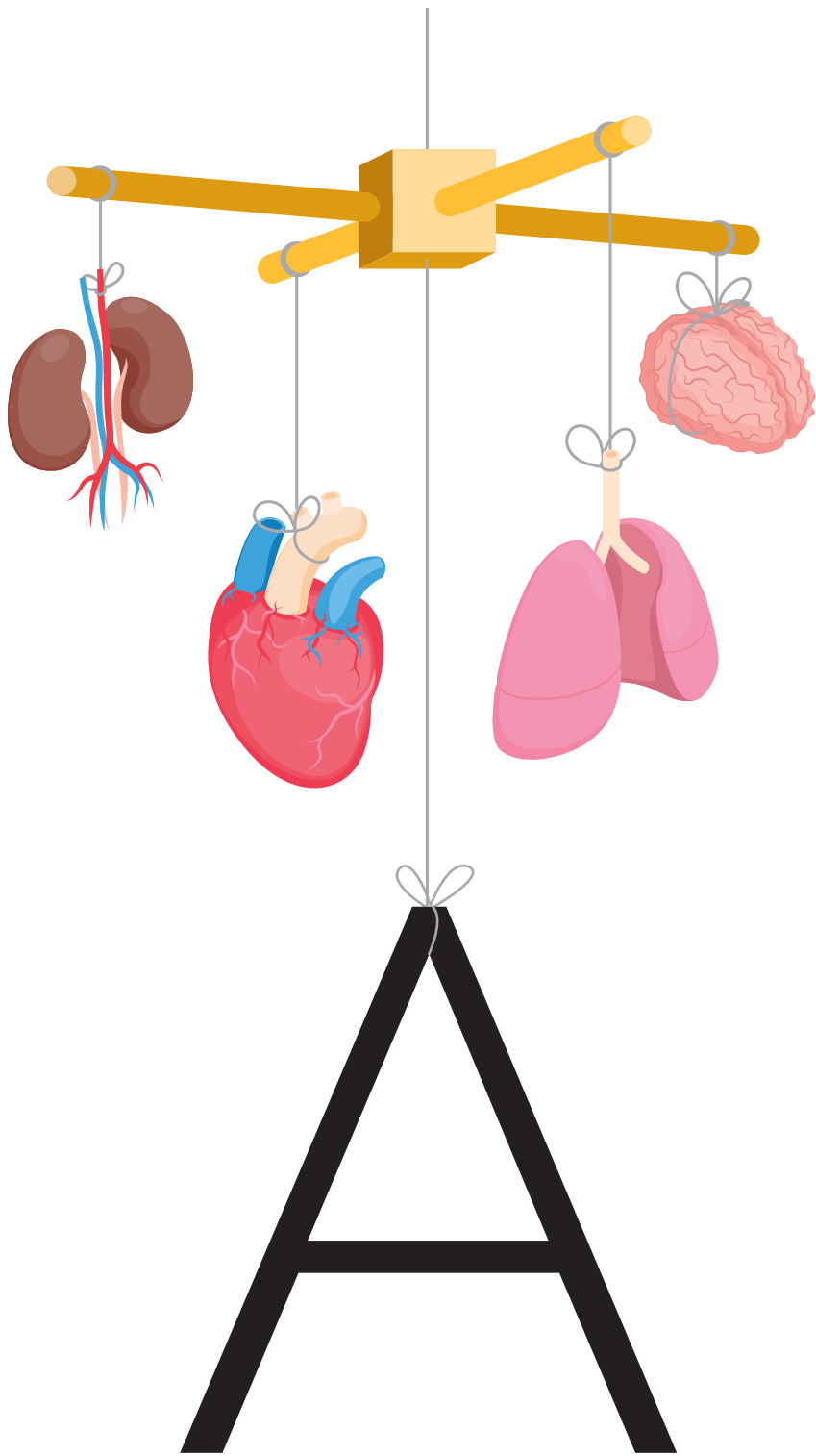
Zaba J, Morrell NW, Sheares KK, Ulrich A, Quan R, Zhao Z, Jing X, An C, Liu Z, Xiong C, Robbins PA, Dawes T, de Marvao A, Rhodes CJ, Richter MJ, Gall H, Ghofrani HA, Zhao L, Huson L, Wilkins MR. Supplementation with Iron in Pulmonary Arterial Hypertension: Two Randomized Crossover Trials. *Ann. Am. Thorac. Soc.* 2021; .

15. Olsson KM, Fuge J, Brod T, Kamp JC, Schmitto J, Kempf T, Bauersachs J, Hoeper MM. Oral iron supplementation with ferric maltol in patients with pulmonary hypertension. *Eur. Respir. J.* 2020;56.
16. Frump AL, Bonnet S, de Jesus Perez VA, Lahm T. Emerging role of angiogenesis in adaptive and maladaptive right ventricular remodeling in pulmonary hypertension. *Am. J. Physiol. - Lung Cell. Mol. Physiol.* 2018;314 p. L443–L460.
17. Cannatà A, Ali H, Sinagra G, Giacca M. Gene Therapy for the Heart Lessons Learned and Future Perspectives. *Circ. Res.* 2020;126 p. 1394–1414.
18. Garry DJ, Kanatous SB, Mammen PPA. Emerging roles for myoglobin in the heart. *Trends Cardiovasc. Med.* 2003;13 p. 111–116.
19. Jue T, Simond G, Wright TJ, Shih L, Chung Y, Sriram R, Kreutzer U, Davis RW. Effect of fatty acid interaction on myoglobin oxygen affinity and triglyceride metabolism. *J. Physiol. Biochem.* 2016; 73: 359–370.
20. Wong YY, Handoko ML, Mouchaers KTB, de Man FS, Vonk-Noordegraaf A, Van der Laarse WJ, Man FS de, Vonk Noordegraaf A, Van der Laarse WJ. Reduced mechanical efficiency of rat papillary muscle related to degree of hypertrophy of cardiomyocytes. *Am. J. Physiol. Heart Circ. Physiol.* 2010; 298: H1190-7.
21. Wong YY, Ruiter G, Lubberink M, Raijmakers PG, Knaapen P, Marcus JT, Boonstra A, Lammertsma AA, Westerhof N, van der Laarse WJ, Vonk-Noordegraaf A. Right Ventricular Failure in Idiopathic Pulmonary Arterial Hypertension Is Associated With Inefficient Myocardial Oxygen Utilization. *Circ Hear. Fail* 2011; 4: 700–706.
22. Balestra GM, Mik EG, Eerbeek O, Specht PAC, van der Laarse WJ, Zuurbier CJ. Increased in vivo mitochondrial oxygenation with right ventricular failure induced by pulmonary arterial hypertension: Mitochondrial inhibition as driver of cardiac failure? *Respir. Res.* 2015; 16.
23. Nagendran J, Gurtu V, Fu DZ, Dyck JRB, Haromy A, Ross DB, Rebeyka IM, Michelakis ED. A dynamic and chamber-specific mitochondrial remodeling in right ventricular hypertrophy can be therapeutically targeted. *J. Thorac. Cardiovasc. Surg.* 2008; 136: 168-178.e3.
24. Redout EM, Wagner MJ, Zuidwijk MJ, Boer C, Musters RJP, van Hardeveld C, Paulus WJ, Simonides WS. Right-ventricular failure is associated with increased mitochondrial complex II activity and production of reactive oxygen species. *Cardiovasc. Res.* 2007; 75: 770–781.
25. Ryan JJ, Archer SL. The right ventricle in pulmonary arterial hypertension: Disorders of metabolism, angiogenesis and adrenergic signaling in right ventricular failure. *Circ. Res.* 2014; 115: 176–188.
26. Gupte AA, Cordero-Reyes AM, Youker KA, Matsunami RK, Engler DA, Li S, Loebe M, Ashrith G, Torre-Amione G, Hamilton DJ. Differential Mitochondrial Function in Remodeled Right and Nonremodeled Left Ventricles in Pulmonary Hypertension. *J. Card. Fail.* 2016; 22: 73–81.
27. Brookes PS, Buckingham JA, Tenreiro AM, Hulbert AJ, Brand MD. The Proton Permeability of the Inner Membrane of Liver Mitochondria from Ectothermic and Endothermic Vertebrates and from Obese Rats: Correlations with Standard Metabolic Rate and Phospholipid Fatty Acid Composition. *Comp. Biochem. Physiol. - B Biochem. Mol. Biol.* 1998; 119: 325–334.

## CHAPTER 8

28. Cheng J, Nanayakkara G, Shao Y, Cueto R, Wang L, Yang WY, Tian Y, Wang H, Yang X. Mitochondrial proton leak plays a critical role in pathogenesis of cardiovascular diseases. *Adv. Exp. Med. Biol.* 2017;982 p. 359–370.
29. Vidal-Puig AJ, Grujic D, Zhang CY, Hagen T, Boss O, Ido Y, Szczepanik A, Wade J, Mootha V, Cortright R, Muoio DM, Lowell BB. Energy metabolism in uncoupling protein 3 gene knockout mice. *J. Biol. Chem.* 2000; 275: 16258–16266.
30. Arsenijevic D, Onuma H, Pecqueur C, Raimbault S, Manning BS, Miroux B, Couplan E, Alves-Guerra MC, Gubern M, Surwit R, Bouillaud F, Richard D, Collins S, Ricquier D. Disruption of the uncoupling protein-2 gene in mice reveals a role in immunity and reactive oxygen species production. *Nat. Genet.* 2000; 26: 435–439.
31. Hang T, Huang Z, Jiang S, Gong J, Wang C, Xie D, Ren H. Apoptosis in Pressure Overload-Induced Cardiac Hypertrophy Is Mediated, in Part, by Adenine Nucleotide Translocator-1. 2006.
32. Esfandiary A, Kutsche HS, Schreckenber R, Weber M, Pak O, Kojonazarov B, Sydykov A, Hirschhäuser C, Wolf A, Haag D, Hecker M, Fink L, Seeger W, Ghofrani HA, Schermuly RT, Weißmann N, Schulz R, Rohrbach S, Li L, Sommer N, Schlüter KD. Protection against pressure overload-induced right heart failure by uncoupling protein 2 silencing. *Cardiovasc. Res.* 2019; 115: 1217–1227.
33. Kaludercic N, Takimoto E, Nagayama T, Feng N, Lai EW, Bedja D, Chen K, Gabrielson KL, Blakely RD, Shih JC, Pacak K, Kass DA, Di Lisa F, Paolocci N. Monoamine oxidase a-mediated enhanced catabolism of norepinephrine contributes to adverse remodeling and pump failure in hearts with pressure overload. *Circ. Res.* 2010; 106: 193–202.
34. Sommer N, Schulz R. Mitochondrial monoamine oxidase: Another player in pulmonary hypertension? *Am. J. Respir. Cell Mol. Biol.* 2021.64 p. 277–278.
35. Kaludercic N, Carpi A, Nagayama T, Sivakumaran V, Zhu G, Lai EW, Bedja D, De Mario A, Chen K, Gabrielson KL, Lindsey ML, Pacak K, Takimoto E, Shih JC, Kass DA, Di Lisa F, Paolocci N. Monoamine Oxidase b prompts mitochondrial and cardiac dysfunction in pressure overloaded hearts. *Antioxidants Redox Signal.* 2014; 20: 267–280.
36. Van Eif VWW, Bogaards SJP, Van der Laarse WJ. Intrinsic cardiac adrenergic (ICA) cell density and MAO-A activity in failing rat hearts. *J. Muscle Res. Cell Motil.* 2014; 35: 47–53.
37. Farina S, Bruno N, Agalbato C, Contini M, Cassandro R, Elia D, Harari S, Agostoni P. Physiological insights of exercise hyperventilation in arterial and chronic thromboembolic pulmonary hypertension. *Int. J. Cardiol.* 2018; 259: 178–182.
38. Reybrouck T, Mertens L, Schulze-Neick I, Austenat I, Eyskens B, Dumoulin M, Gewillig M. Ventilatory inefficiency for carbon dioxide during exercise in patients with pulmonary hypertension. *Clin. Physiol.* 1998; 18: 337–344.
39. Yasunobu Y, Oudiz RJ, Sun XG, Hansen JE, Wasserman K. End-tidal Pco<sub>2</sub> abnormality and exercise limitation in patients with primary pulmonary hypertension. *Chest* 2005; 127: 1637–1646.
40. Ting H, Sun XG, Chuang ML, Lewis DA, Hansen JE, Wasserman K. A noninvasive assessment of pulmonary perfusion abnormality in patients with primary pulmonary hypertension. *Chest* 2001; 119: 824–832.
41. Paterson DJ, Friedland JS, Bascom DA, Clement ID, Cunningham DA, Painter R, Robbins PA. Changes in arterial K<sup>+</sup> and ventilation during exercise in normal subjects and subjects with McArdle's syndrome. *J. Physiol.* 1990; 429: 339–348.

42. Ferreira EV, Ota-Arakaki JS, Ramos RP, Barbosa PB, Almeida M, Treptow EC, Valois FM, Nery LE, Neder JA. Optimizing the evaluation of excess exercise ventilation for prognosis assessment in pulmonary arterial hypertension. *Eur. J. Prev. Cardiol.* 2014; 21: 1409–1419.
43. Coats AJS, Adamopoulos S, Radaelli A, McCance A, Meyer TE, Bernardi L, Solda PL, Davey P, Ormerod O, Forfar C, Conway J, Sleight P. Controlled trial of physical training in chronic heart failure: Exercise performance, hemodynamics, ventilation, and autonomic function. *Circulation* 1992; 85: 2119–2131.
44. Vecchia LAD, Bussotti M. Exercise training in pulmonary arterial hypertension. *J. Thorac. Dis.* 2018.10 p. 508–521.
45. Ehlken N, Lichtblau M, Klose H, Weidenhammer J, Fischer C, Nechwatal R, Uiker S, Halank M, Olsson K, Seeger W, Gall H, Rosenkranz S, Wilkens H, Mertens D, Seyfarth HJ, Opitz C, Ulrich S, Egenlauf B, Grünig E. Exercise training improves peak oxygen consumption and haemodynamics in patients with severe pulmonary arterial hypertension and inoperable chronic thrombo-embolic pulmonary hypertension: A prospective, randomized, controlled trial. *Eur. Heart J.* 2016; 37: 35–44.
46. Grünig E, MacKenzie A, Peacock AJ, Eichstaedt CA, Benjamin N, Nechwatal R, Ulrich S, Saxer S, Bussotti M, Sommaruga M, Ghio S, Gumbiene L, Palevičiūtė E, Jurevičienė E, Cittadini A, Stanzola AA, Marra AM, Kovacs G, Olschewski H, Barberà J-A, Blanco I, Spruit MA, Franssen FME, Vonk Noordegraaf A, Reis A, Santos M, Viamonte SG, Demeyer H, Delcroix M, Bossone E, et al. Standardized exercise training is feasible, safe, and effective in pulmonary arterial and chronic thromboembolic pulmonary hypertension: results from a large European multicentre randomized controlled trial. *Eur. Heart J.* 2020; .
47. Nogueira-Ferreira R, Moreira-Gonçalves D, Santos M, Trindade F, Ferreira R, Henriques-Coelho T. Mechanisms underlying the impact of exercise training in pulmonary arterial hypertension. *Respir. Med.* 2018.134 p. 70–78.



# APPENDIX

---

Nederlandse samenvatting

List of publications

Dankwoord

Squaring the circle

## Nederlandse samenvatting

Idiopathische pulmonale arteriële hypertensie (iPAH) is een zeldzame en ernstige aandoening van de arteriën in de longen. Vernauwingen in het lumen van deze bloedvaten verhogen de druk op het rechterventrikel (RV) van het hart, wat uiteindelijk leidt tot rechter hartfalen. De chronische overbelasting van het RV zorgt voor een vicieuze cirkel van zuurstoftekort, veranderingen in het metabolisme, neurohormonale activatie en verdere verslechtering van de RV functie. In dit proefschrift hebben we drie strategieën onderzocht die kunnen bijdragen aan het doorbreken of vertragen van deze vicieuze cirkel in iPAH: het verbeteren van zuurstof toevoer (**hoofdstuk 2 en 3**), het verminderen van de vraag naar zuurstof (**hoofdstuk 4 en 5**), en het herstellen van de neurohormonale balans (**hoofdstuk 6 en 7**).

### Zuurstof toevoer

In **hoofdstuk 2** hebben we de regulatie van myoglobine (Mb) in het hypertrofe RV bestudeerd, in het monocrotaline (MCT) model voor pulmonale hypertensie. Hoewel de totale oxidatieve capaciteit en daarmee de vraag naar zuurstof toenam in de MCT ratten, was er geen toename van Mb mRNA expressie. De totale hoeveelheid Mb eiwit nam wel toe, wat wijst op verhoogde translatie. Echter, de minimale extracellulaire zuurstofspanning die nodig is om te voorkomen dat de kern van de cel hypoxisch wordt was twee keer hoger dan in gezonde dieren. Dus is de toename in Mb eiwitexpressie net groot genoeg om de hypertrofie te compenseren, maar niet voldoende om ook te voldoen aan de verhoogde vraag naar zuurstof. Daarmee ontstaat een *mismatch* in de vraag en aanbod om zuurstof.

Eerdere studies lieten zien dat een combinatie van hypoxie met vetzuursuppletie de expressie van Mb kan verhogen. In **hoofdstuk 3** hebben we daarom verschillende mate van hypoxie in combinatie met vetzuursuppletie toegepast op skeletspiercellen in kweek. Daarnaast hebben we *insulin-like growth factor* (IGF)-1 toegevoegd om hypertrofie te stimuleren. We vonden dat IGF-1 deels de atrofie veroorzaakt door hypoxie kan voorkomen, echter remt het ook de expressie van Mb. Dit mechanisme bemoeilijkt het combineren van hypertrofie en een toename in Mb expressie. In tegenstelling tot eerdere studies vonden we geen toename in Mb expressie door vetzuursuppletie, mogelijk door verschillen in timing en duur. Er zijn vele factoren die de expressie van Mb kunnen reguleren of beïnvloeden en dus als aanknopingspunt dienen voor verder studies om de expressie in het hart te kunnen verhogen.

## Zuurstofverbruik

In **hoofdstuk 4** en **5** hebben we gekeken naar de mogelijkheden om de vraag naar zuurstof te verlagen. In **hoofdstuk 4** beschrijven we een kwantitatieve histochemische methode om daarmee mitochondriële efficiëntie *ex vivo* te kunnen schatten. Het voordeel van deze methode is dat we slechts kleine stukjes bevroren weefsel nodig hebben. Dit vergroot de kans dat schaars weefsel gebruikt kan worden voor deze bepaling. Met behulp van deze techniek vonden we een heterogene afname in mitochondriële efficiëntie in de harten van MCT ratten. De efficiëntie in deze harten was gerelateerd aan de vetzuursamenstelling van de mitochondriële binnenmembraan, er daarmee aan stabiliteit van de membraan.

In **hoofdstuk 5** hebben we monoamine oxidase A (MAO-A) bestudeerd, een andere mogelijk grote bron van zuurstofverbruik en producent van vrije zuurstofradicalen (ROS). Inhibitie van MAO-A activiteit met clorgyline verminderde de vasculaire vernauwing, en daarmee de belasting op het RV in het Sugren-Hypoxie (SuHx) model van pulmonale hypertensie. Om de directe effecten van MAO-A inhibitie op het RV te bestuderen gebruikten we een model waarbij de longslagader vernauwd wordt door middel van een bandje (PTB model). Hoewel de expressie van MAO-A in dit model sterk was toegenomen, zagen we geen effect van MAO-A inhibitie met clorgyline. Bij patiënten zagen we alleen een toename van MAO-A expressie in de longen, maar niet in het RV. Studies naar MAO-A inhibitie in het linkerventrikel (LV) laten wel directe effecten op het hart zien, maar het is niet duidelijk of het RV anders reageert op MAO inhibitie dan het LV of dat verschillen in studie-opzet het verschil verklaren. Ook de rol van een andere vorm van MAO, MAO-B, in iPAH vereist verder onderzoek.

## De neurohormonale balans

Regulatie van bloeddruk, hartslag en ventilatie staat grotendeels onder controle van het autonome zenuwstelsel (ANS) en het renin-angiotensine aldosteron systeem (RAAS). In iPAH is er een chronische onbalans in beide systemen wat kan leiden tot verdere verslechtering van de hartfunctie. Chronische activatie van het sympathische zenuwstelsel is mogelijk ook één van de oorzaken van hyperventilatie, een veelvoorkomend verschijnsel in iPAH patiënten en een voorspeller voor een slechtere prognose. In **hoofdstuk 6** hebben we daarom gekeken naar de effecten van twee relatief simpele methodes om de sympathische activiteit te verlagen in iPAH patiënten. Zowel langdurig gebruik van bètablokkers als het kortdurend inademen van extra zuurstof leidden tot een verlaging van de hartslag, wat wijst op een vermindering van de sympathische activiteit. Desondanks zagen we geen enkel effect van deze interventies op de ventilatie in rust of tijdens inspanning. Hoewel eerdere studies een belangrijke rol van het sympathisch zenuwstelsel in het ontstaan van hyperventilatie

A

## APPENDIX

suggereerden, lijkt het er dus op dat ook andere mechanismen een rol kunnen spelen. De opzet van onze studie liet het niet toe deze mechanismen verder te onderzoeken. Daarnaast zijn deze andere mogelijke mechanismen veel moeilijker te beïnvloeden dan het sympathisch zenuwstelsel, en daarmee wellicht minder goed toepasbaar in de kliniek.

Ten slotte hebben we in **hoofdstuk 7** het neurohormonale systeem in iPAH in detail besproken alsook de interventies erop die in het lab en in klinische studies zijn getest. Hoewel er veelbelovende resultaten zijn, zijn grote klinische trials om deze te bevestigen vaak niet mogelijk door het kleine aantal PAH-patiënten. Hierdoor is het vaak ook niet mogelijk om retrospectieve analyses te doen en zo verschillen tussen *responders* en *non-responders* te ontdekken. Verder is weefsel van patiënten dat beschikbaar is voor onderzoek zeer schaars. Daarom pleitten we in dit hoofdstuk voor een meer persoonlijke aanpak en beter inzicht in de neurohormonale veranderingen over de tijd, in patiënten.

### Vertaling naar de kliniek

De meeste studies in dit proefschrift zijn gedaan in rat modellen van pulmonale hypertensie. Dit maakt dat er nog een lange weg is van het lab naar de behandeling van patiënten. De beschikbare diermodellen bootsen PAH allemaal deels na, maar komen nooit volledig overeen met PAH zoals het in de mens is. Vooral het snelle verloop van de RV overbelasting en het feit dat deze diermodellen geen behandelingen krijgen anders dan de geteste behandeling, is een groot verschil met het verloop van PAH en studies in patiënten. Het is daarom belangrijk dat onze bevindingen ook in patiënten geverifieerd worden.

Echter, onderzoek naar PAH in patiënten is lastig. Zoals eerder vermeld is het aantal patiënten te klein voor grote klinische studies of retrospectieve analyses. Bovendien is RV weefsel van patiënten alleen beschikbaar na autopsie of ten tijde van harttransplantatie, waardoor het altijd een weergave is van ernstig hartfalen. Ontwikkelingen in het gebruik van gekweekt hartweefsel en endotheel- en gladde spiercellen in kweek, kunnen hopelijk in de toekomst bijdragen aan een meer gepersonaliseerde behandeling. Tot die tijd is het belangrijk om de verschillende diermodellen voor verschillende vraagstellingen te gebruiken, en ook de niet-invasieve methoden om veranderingen in patiënten over de tijd te monitoren. Om resultaten van dierstudies goed te kunnen vertalen naar een klinische toepassing moet er rekening gehouden worden met of het medicijn mogelijk al gebruikt wordt voor een andere ziekte, de keuze voor het diermodel waarin het medicijn getest wordt en de selectie van patiënten voor klinische studies die op basis van (genetische) kenmerken een grotere kans hebben op een positieve uitkomst van de behandeling.

## Behandelen van de vicieuze cirkel als één geheel

Nu we de verschillende strategieën om in te grijpen op de zuurstof toevoer, het zuurstofverbruik en het neurohormonale systeem in PAH hebben besproken, rijst de vraag welk van deze strategieën moet worden toegepast. Echter, dé oorzaak van hartfalen in PAH is niet bekend en het is daarom onmogelijk te zeggen welk mechanisme de hoogste prioriteit zou moeten hebben in de behandeling. Het is zelfs goed denkbaar dat een enkele strategie niet voldoende is om het ontstaan van hartfalen te voorkomen of vertragen. Ook spelen nog andere mechanismen een rol in de ontwikkeling van hartfalen zoals toegenomen stijfheid van de sarcomeren, verstoorde contractie en relaxatie door fibrose, en een verschuiving naar aerobe glycolyse die zorgt voor lactaat ophoping en verminderde energieproductie. Toekomstige studies zouden daarom moeten proberen de vicieuze cirkel van RV falen als één geheel te behandelen. In dit licht zouden revalidatieprogramma's en training een belangrijke rol kunnen spelen.

Er is meer en meer bewijs dat fysieke activiteit en sport een waardevolle toevoeging kunnen zijn op bestaande farmacologische behandelingen. Studies hiernaar in patiënten laten vooral zien dat de maximale zuurstofopname, het inspanningsvermogen en de kwaliteit van leven verbeteren. De effecten van fysieke activiteit op het RV in patiënten worden op dit moment in meer detail onderzocht. Toch zijn de moleculaire effecten van fysieke activiteit in patiënten grotendeels onbekend. Dierstudies laten aanpassingen zien in ROS, celdood, mitochondriële stress, adaptaties in het hart, neurohormonale activatie, metabolisme en inflammatie. Door het effect van fysieke activiteit op deze mechanismen ook in patiënten te onderzoeken, kunnen trainingsprogramma's hierop aangepast worden om zo het effect te maximaliseren.

Concluderend kunnen we stellen dat Mb expressie, mitochondriële inefficiëntie, MAO-A activiteit en neurohormonale onbalans als aangrijpingspunt voor behandelingen kunnen dienen. Omdat waarschijnlijk geen van deze mechanismes op zichzelf de ontwikkeling en progressie van RV falen veroorzaakt, is het van belang de vicieuze cirkel van RV verslechtering en falen als geheel aan te pakken. Hiertoe kunnen sport en fysieke activiteit een belangrijke rol dienen.

A

## List of publications

Ballak SB, Jaspers RT, Deldicque L, Chalil S, **Peters EL**, de Haan A, Degens H. Blunted hypertrophic response in old mouse muscle is associated with a lower satellite cell density and is not alleviated by resveratrol. *Exp Gerontol*, 2015. 62: p.23-31.

**Peters EL**, Offringa C, Kos D, Van der Laarse WJ, Jaspers RT. Regulation of myoglobin in hypertrophied rat cardiomyocytes in experimental pulmonary hypertension. *Pflugers Arch*, 2016. 468(10): p.1697-707.

**Peters EL**, van der Linde SM, Vogel ISP, Haroon M, Offringa C, de Wit GMJ, Koolwijk P, van der Laarse WJ, Jaspers RT. IGF-1 Attenuates Hypoxia-Induced Atrophy but Inhibits Myoglobin Expression in C2C12 Skeletal Muscle Myotubes. *Int J Mol Sci*, 2017. 18(9): p.1889.

**Peters EL**, Comerford D, Vaz FM, van der Laarse WJ, Meijer and Vloedman's histochemical demonstration of mitochondrial coupling obeys Lambert-Beer's law in the myocardium. *Histochem Cell Biol*, 2019. 151(1): p.85-90.

Sun XQ, **Peters EL**, Schalij I, Axelsen JB, Andersen S, Kurakula K, Gomez-Puerto MC, Szulcek R, Pan X, da Silva Goncalves Bos D, Schiepers REJ, Andersen A, Goumans MJ, Vonk Noordegraaf A, van der Laarse WJ, de Man FS, Bogaard HJ. Increased MAO-A Activity Promotes Progression of Pulmonary Arterial Hypertension. *Am J Respir Cell Mol Biol*, 2021. 64(3): p.331-343.

**Peters EL**, Bogaard HJ, Noordegraaf AV, de Man FS. Neurohormonal modulation in pulmonary arterial hypertension. *Eur Respir*, 2021. *In press*.

## Dankwoord

Alleen mijn naam staat op dit boekje, maar het is allerminst het werk van mij alleen. Ik ben veel mensen dank verschuldigd: voor hun directe bijdragen, voor hun vertrouwen en voor hun steun in de afgelopen vier jaar. Het zal niet meevallen daar recht aan te doen in slechts een paar pagina's, desondanks een poging:

Prof. Vonk Noordegraaf, beste Anton. Vanaf het begin kreeg ik jouw vertrouwen en als ik het zelf even kwijtgeraakt was, dan vond jij het weer terug. Je enthousiasme en betrokkenheid maakten dat ik na elke bespreking weer met hernieuwde moed aan de slag ging. Op wonderbaarlijke wijze kun jij in nauwelijks een half uur met oprechte aandacht informeren naar iemand, een goed boek aanraden, een feitje over bijen meedelen, nieuwe resultaten bespreken, tot de kern van het onderzoek komen, vijf nieuwe hypothesen aandragen, drie nieuwe onderzoeksprojecten bedenken en dat alles met haast achteloos gemak. Ik hoop ooit tot een fractie van deze vermogens te komen. Je hebt me doen inzien hoezeer een promotietraject ook een kans is tot persoonlijke ontwikkeling en hebt me daartoe alle ruimte en middelen gegeven: zonder twijfel de meest waardevolle uitkomst van het deze hele promotie. Het was een voorrecht om onder jouw begeleiding te mogen promoveren. Dankjewel!

Prof. Bogaard, beste Harm Jan. Zag ik alles altijd maar zo positief als jij. De eerste, de honderdste, de miljoenste en de definitieve versie van een manuscript: naast je scherpe suggesties voor verbetering ben je altijd enthousiast en positief. Een overstroming van het ziekenhuis of de covid-pandemie zie jij gewoon als een beetje reuring. Heel fijn om zo iemand erbij te hebben als het even tegenzit, en wellicht kan ik iets van deze kalmte met mee meenemen. Daarnaast heb ik genoten van je openheid, je humor en je verwondering over de stand van de technologie (wie had gedacht dat we ooit e-mails klaar konden zetten om automatisch op een later tijdstip te versturen?).

Dr. Handoko – de Man, beste Frances. Dankjewel dat je het stokje over wilde nemen van Willem en halverwege mijn promotie bent ingestapt. Wel honderd versies van het MAO-A manuscript en het review heb je gelezen en keer op keer voorzien van commentaar om het te verbeteren. En als je één ding zeker weet bij jouw suggesties, dan is het dat een onderzoek of manuscript er beter van wordt. Als jij een idee hebt, verdedig je dat vurig en als jij een studie begint kun je er zeker van zijn dat het linksom of rechtsom uiteindelijk uitgevoerd wordt. Ik neem graag wat van die doortastendheid en doelgerichtheid over!

A

## APPENDIX

Een kleine desillusie was het wel, toen ik me realiseerde dat ik met mijn onderzoek PH niet zou gaan genezen. Maar ik heb me erbij neergelegd. wetende dat ik jullie geoliede team van bevlogen artsen en onderzoekers anders werkloos zou maken.

Bernadette en Wouter, wat fantastisch dat jullie mijn paranimf willen zijn. Met twee van die lieve, slimme vrienden naast me moet het wel goedkomen! Wouter, ik heb tijdens onze boswandelingetjes al zoveel verteld over mijn onderzoeken, ik neem aan dat ik inhoudelijke vragen aan jou kan doorspelen.

I also want to sincerely thank the reading committee, for the time and attention that they have devoted to reading and discussing with me the work in this thesis.

Beste Willem, al tijdens mijn masterstage heb ik heel wat uren doorgebracht in jouw kamer. Altijd nam je uitgebreid de tijd om mee te denken en me weer op weg te helpen en mede door jouw vertrouwen kon ik aan deze promotie beginnen. Hoewel de zuurstofmetingen helaas niet gelukt zijn, en me soms ook de nodige frustraties hebben bezorgd, vind ik het een eer om met jouw unieke opstelling gewerkt te mogen hebben. Ik zal zo nu en dan terugdenken aan je nauwkeurigheid en bedachtzaamheid als ik weer eens te ongeduldig ben.

Sun, my MAO-A partner in crime! I really enjoyed working together with you. Thank you for coming to Aarhus with me in an old car full of white powders (all salts, we promise!). We spent some long days in the basement of the hospital but stayed fit with the scientific 7-minutes workout and parkruns (sorry for saying there is no way to get lost there, you proved me wrong). The Tupperware party was unforgettable! You are always happy and willing to help everyone, even if that means unexpectedly being with me in the UPC until 22.00 o'clock. Thank you so much! It was an honour to be your paranymp and I am sure you will do a fantastic postdoc in Canada. Hope to see you again after we both returned to Amsterdam!

Stine, Julie and Asger, thank you for having us in Aarhus and the great help with the experiments! We had the best experience we could wish for, both scientifically and personally. Thanks also to all other staff at the Institute of Clinical Medicine for taking care of our animals and helping us out a lot of times. Julie, we cannot thank you enough for doing well over 30 PTB procedures for us! How cool that you started your PhD now. I am sure you will do great!

Xue, de enige die mag lachen om mijn mislukte blotjes en gelukkig altijd bereid te helpen ze beter te krijgen. Het was tof om samen de schrijfcursus te doen, met jou te sparren, te vragen, te klagen (bijna nooit hoor) en elkaar te motiveren. Ik heb je echt zien groeien als onderzoeker en ik spreek je wel weer als je over een tijdje

toch professor bent geworden: misschien zoek je dan nog een technician.

Ingrid, geen dierexperiment zonder jou. Op en neer naar Aarhus om ons op weg te helpen met de experimenten, of over de telefoon helpen het UPC in alle haast om te bouwen voor de genterapie dieren, niks is te gek. Dank voor al je hulp en flexibiliteit! Bedankt ook aan alle medewerkers van het UPC die zich altijd weer inspinnen om elk experiment zo goed mogelijk te ondersteunen.

Also, many thanks to all other pulmonology colleagues. Rowan en Pan, meer dan eens mijn redding in het lab! Joanne, Natalia, Aida, Liza, Chermaine, Kim, Samara, Jessie, Jeroen, Azar, Fjodor, Keimei, Jurjan, Robert, Denielli, Anna, Mo, Josien, Taka, Jelco and Berend, thank you for all the discussions during the meetings and for the fun Christmas events! Natalia en Liza, Madrid was een stuk leuker met jullie! Chermaine, voor Kerst kregen we van Anton jouw boek. Als preklinisch onderzoeker kreeg ik hiermee voor het eerst pas echt een goed beeld wat PH voor een patiënt inhoudt, en dat is helaas geen pretje. Wel gaf het me extra motivatie voor het onderzoek in het lab, waarbij de patiënt soms ver weg lijkt. Eindeloos veel bewondering heb ik voor hoe jij jouw ervaringen gebruikt in je eigen onderzoek! Ik hoop dat er veel moois uit gaat komen.

Roy en Ting, het was me een genoegen jullie te mogen begeleiden tijdens jullie bachelor-stages. Jullie hebben veel werk verzet en ook niet onbelangrijk: hielden mij scherp met jullie vragen. Ik vond het leuk jullie in amper vier maanden grote stappen vooruit te zien maken, en ben benieuwd wat de onderzoeks-toekomst jullie gaat brengen.

Werken op twee afdelingen betekent ook twee keer zoveel leuke collega's! Jolanda, Coen, Ed, Reinier, Diederik, Josine, Sylvia en Max, bedankt voor de sportieve tegenstand als ook de waardevolle adviezen, soms gevraagd en soms zomaar gekregen. Diederik, de mailtjes ter aankondiging van de vrijdagmiddag meeting waren elke week een zeer gewaardeerd kunststukje. Coen, dankjewel voor je vertrouwen in mij en Stefan om ons samen naar Tucson te sturen! Ik hoop maar dat die nieuwe labmanager daar een beetje oké is ;-).

Irma, Anny, Constance, Aimée, en in het bijzonder Ella, bedankt voor de secretariële ondersteuning vanuit beide afdelingen en voor het altijd weer vinden van een gaatje in alle agenda's. Van toegangspassen tot facturen en van declaraties tot bestellingen, jullie lijken overal het antwoord op te weten! Zonder jullie zouden we het gebouw nog niet eens inkomen.

Duncan, bedankt voor je inzet en betrokkenheid bij de zuurstofopstelling. Uit onze mix van MS-DOS computers, analoge schrijvers en moderne technologie

## APPENDIX

(Windows XP) wist jij alle relevante data te verkrijgen die ik nodig had voor de analyse. Zonder dat zat ik nu waarschijnlijk nog steeds op de grond de hokjes op het meterslange grafiekpapier te tellen.

Flex-werkplekken are famous for their undesirability. After two months of walking around with my papers on several floors each morning, I landed happily in room 12W28. Martijn, Marloes, Denise, Larissa, Xu, Elisa, Kennedy, Riccardo, and Hua, thank you for all the help, the fun, the shared food, the peanut butter smells and what more. Long after we all have left the office, only the famous quote of Larissa will remain on our klagmuur: experiments you can repeat, but not the party!

Van klagmuur naar klimmuur. Bedankt Louise, Maike, Larissa, Jeroen, Edgar, Pedro, Wout, Rowan en Stefan, voor vele gezellige avonden en het samen puzzelen op een route. Jammer dat het met team blue nog niks is geworden maar dat komt nog wel. Tot die tijd: just hang!

Maike, Larissa, Pedro, Tatjana and Laura. When I started working, I did not drink coffee at all and the coffee machines in O2 also did not give me any reason to start doing so. But much can change in four years! Celebrations, frustrations, and everything in between, there was always a reason for a good cappuccino. Maybe, if the Science Café would not have closed during COVID, my thesis had been finished months earlier, who knows. Their logo is unmatched anyways.

Thank you also to all the other colleagues from physiology for a lot of fun during the past years. Be it Monday morning coffee, Wednesday afternoon drinks, TPO weekends, or labuitje, I feel blessed with so many nice colleagues!

The first time in my life that I left Europe, it was to the ISHR conference in Beijing and I have to admit that it was quite a culture shock! But it was fantastic to share this experience with you Maike, and with the good help of Jin, Hua, Pan and Sun we could not have been prepared more. Presenting at a conference while feeling upside down from the jetlag, being photographed as if we were monkeys in the zoo, walking the Chinese wall, the highspeed train to Shanghai, very interesting Google translate suggestions, the taxi ride when we missed the last metro and all the unknown food we ate: it is a pity that I do probably not remember even half of the crazy situations that we found ourselves in constantly. I never came home from a trip so exhausted from all the new impressions and laughter.

Richard, nadat je me enthousiast had gemaakt voor het spieronderzoek gaf je me de kans mijn eerste artikel te publiceren. Wie had gedacht dat dit uiteindelijk het eerste hoofdstuk van mijn proefschrift zou worden! Guus, Carla, Wendy en Gerard, bedankt voor jullie hulp tijdens mijn stages en daarmee ook bij de eerste

twee hoofdstukken. Mijn fijne tijd in het myolab heeft zeker bijgedragen aan mijn plezier in onderzoek doen. Sander en Anouk, helaas spreek ik jullie niet zo vaak maar gelukkig hebben we aan een half woord ook genoeg. Ik hoop onze onderzoeksgebieden nog eens in één publicatie te kunnen bundelen!

Soms heb je iemand nodig die jou niet kent, maar die je met een frisse blik weer de goede kant op kan sturen. Manon Stockmann, ik ken weinig mensen die zo goed zonder oordeel kunnen vragen en luisteren. Het was fijn om soms even hardop te denken, de zaken vanuit een ander perspectief te kunnen bekijken of juist met een concreet plan weer op weg te gaan. Op het moment dat de finish misschien wel het verste weg leek, heb je me een paar belangrijke duwtjes in de goede richting kunnen geven, bedankt!

Stilzitten is niet één van mijn kwaliteiten, maar gelukkig weet ik jullie altijd gek genoeg voor mijn gekste plannen: Sven-Yvo, Wessel, Luuk, Dennis, Niels en Maartje. Twee Alpen op één dag op fietsen, NH100 op de mountainbike, koffierondjes, of op avontuur over het natuurrijks: net zo vaak komt het stomme idee niet eens van mij. Ik zie jullie in Salt Lake en vergeet mijn schaatsen niet! Hierbij hoort natuurlijk ook de rest van onze trainingsgroep. Wat fantastisch dat ik nog steeds bij de jeugd mag trainen, hoewel ik daar natuurlijk ook nog perfect tussen pas, al zeg ik het zelf. Niets fijners dan alle ongein op de ijsbaan, wielervedbaan of tijdens de landtraining met jullie. Gerrit, een speciale vermelding voor jou. Jouw urenlange workshop trainingsleer, verspreid over meerdere jaren Sauerland, heeft in ieder geval bij mij de interesse voor de ATP-synthese gewekt. De rest was toen denk ik al in slaap gevallen.

Bernadette en Jelle, team raketje forever! Ik ben super trots dat jullie mijn vrienden zijn en wat een geluk dat jullie nu met eentje meer zijn. Met jullie op vakantie naar Italië, op de fiets naar Parijs, en heel veel Sauerland weekendjes bij Leo en Els: van avonturen met jullie krijg ik altijd wel enige vorm van spierpijn en is het nog jaren nagenieten!

Bram en de Purmerend Killers, ook op de skeelerbaan heb ik de nodige energie achter kunnen laten (en misschien ook wat stukjes knie en ellenboog). Het zal niet meevallen een goede vervanging te vinden voor Gladys corner, maar met al dat woestijnzand in m'n lagers zal ik wel lekker sterk worden.

Mijn trouwste BRC-vrienden! Bij jullie kan ik terecht met al mijn tegenslagen en successen. Juul, het was heerlijk om een jaartje met jou een huis te delen en van dichtbij te zien hoe groep 3 leert lezen en schrijven. Jij houdt ons bij elkaar! Lorraine, mijn favoriete thuiswerk-collega, wat was het fijn om het PhD leven met jou te kunnen delen. Als het met mijn boekje zelfs goed is gekomen, komt het

## APPENDIX

met jouwe zeker goed. Anne-Marijn, mijn overbuurmeisje voor altijd. Ik ken jou al mijn hele leven, en dat wil ik graag zo houden! Misschien weer eens een museum beginnen samen? Kim, kon ik in groep 4 nog bij je afkijken met rekenen, was het even wennen dat ik het vanaf mijn master zonder jou moest doen. Jij bent de allertrouwste persoon die ik ken. Blijf vooral trouw aan jezelf! Shahira, ik ben soms jaloers op mensen die zo duidelijk voor ogen hebben wat ze willen bereiken. Jij hebt keihard gewerkt om je dromen waar te maken en nu ben je arts. Ik ben super trots!

Veel dank ook aan beide kanten van de familie voor jullie oprechte belangstelling en support, al hadden jullie misschien soms geen idee wat ik allemaal uitspookte. Christine, so far the only PhD in my family, thank you for supporting me through the first steps in science, and for proofreading my first ever manuscript. What a pleasant surprise to meet you at the ERS congress in Madrid! Elma en Emma, wat fantastisch dat ik het rijtje Dr. E. Peters-en compleet mag maken. En dan natuurlijk ook al mijn andere lieve neven en nichten: mooi om te zien hoe ieder zijn eigen weg gaat zonder elkaar uit het oog te verliezen. Ik hoop jullie snel weer allemaal bij elkaar te zien!

Simon en Elsbeth, en Thomas en Robyn, ik heb het maar getroffen met zulke schoonfamilie. Vanaf dag één voelde ik me welkom bij jullie. Bedankt voor jullie interesse en steun.

Hugo, mijn persoonlijke ICT-helppdesk op afstand. Ik had eigenlijk gehoopt dat ik jou kon inzetten om met AI nog veel meer uit mijn data te halen, maar het is er vooralsnog niet van gekomen. Nu zal ik wel de hoofdprijs moeten betalen om je als duurbetaalde consultant in te huren, de volgende keer dat ik opeens al mijn bestanden kwijt ben of mijn bitcoins wil verkopen. Hopelijk neem je ook dollars aan. Konden we vroeger aan tafel nog goede grappen maken, nu zijn jouw nerd-grappen mijn niveau ver voorbij. Ik ben super trots op je! Noor, bedankt dat ik eindelijk weet hoe een e-reader werkt en bedankt voor de gezelligheid tijdens de familie-weekenden. De apenheul blijft een hoogtepunt!

Lieve papa en mama! Als ik vroeger aan tafel een vraag stelde, kreeg ik altijd een beetje spijt als dan de encyclopedie of de Grote Bosatlas erbij gehaald werd. Dan wist ik al dat ik er weer niet met een kort of simpel antwoord vanaf ging komen. Jullie hebben mijn nieuwsgierigheid aangemoedigd en ondersteund, en ongetwijfeld is toch de basis gelegd in NEMO. Ik heb me altijd zowel vrij als gesteund gevoeld mijn eigen weg te kiezen, soms vastbesloten, meestal aarzelend, maar gelukkig vooralsnog zonder enige spijt. Bedankt!

Lieve Stefan, ik ben soms wat traag van begrip maar ik ben blij dat je hebt volgehouden. Jij krijgt me in actie en brengt me tot rust en laat me steeds weer dingen doen waarvan ik dacht dat ik ze niet kon. De Olympus beklimmen, kamperen op de mooiste plekken, of urenlang wegwerkzaamheden op de A9 bekijken, met jou is alles leuker. Gelukkig maar dat ik zelf niet ben bezweken aan hartfalen toen je midden in de nacht onaangekondigd mijn slaapkamer in Aarhus binnenviel. Saai is het in ieder geval nooit met jou en ik kan niet wachten op nog veel meer avonturen samen!

## **Squaring the circle**

Squaring the circle refers to an ancient geometric problem that encompasses constructing a square with the same area as a given circle, in a finite number of steps and only using a compass and a ruler. The problem was mathematically proven to be impossible but this has not prevented many people from spending years on it anyway. In literature, squaring the circle has therefore been used to express that something is deemed impossible. Circle-squarers are regarded unworldly dreamers, unaware of the mathematical impossibility of this problem.

Trying to find ways to slow down the vicious circle of right heart failure in pulmonary arterial hypertension, I have felt myself a circle-squarer from time to time. Nevertheless, hope should be drawn from the fact that several close approximations to squaring the circle have been made. Hopefully, one day we will also be able to square the vicious circle of right heart failure in pulmonary arterial hypertension, be it in close approximation.

A